Cyclical loading of electrospun scaffolds affects Mesenchymal stem cell response

LA Bosworth, SR Rathbone, S Downes, SH Cartmell

School of Materials, The University of Manchester, Oxford Road, Manchester, M13 9PL, UK

INTRODUCTION: In selected patients, the repair of injured tendons involves grafting autologous tendon tissue. This procedure is time consuming, increases patient morbidity and further increases the risk of infection. We have previously reported the use of electrospun poly(ε-caprolactone) scaffolds with geometries similar to that of native tendon tissue¹. Continuing our research with these scaffolds, we report the effects of cyclical loading on the response of seeded human Mesenchymal stem cells (hMSCs) after a 21-day period.

METHODS: Electrospun scaffolds were fabricated from a 10 %w/v solution of poly(εcaprolactone) (M_n 70,000-90,000 g/mol; Sigma) dissolved in 1,1,1,3,3,3-Hexafluoroisopropanol (HFIP; Sigma) and subjected to: voltage – 20 kV; flow-rate - 1 ml/hr; spinning distance – 20 cm; spin time – 15 mins. Aligned fibres were collected on a rotating mandrel (1 mm thick; 600 RPM). Fibres were cut into 5 cm lengths, submerged in distilled water and manually twisted to create 3D scaffolds (Ø ~200 µm). Scaffolds were sterilised in Ethanol (50 – 100 %v/v; Fisher), washed in phosphate buffer solution (Gibco) and submerged in MSC growth medium (PromoCell). Scaffolds were mounted into either custom-made frames or 6-well CellCrowns (Scaffdex) and seeded with bone marrow derived hMSCs (500,000 cells per scaffold; PromoCell) for 5 days in culture media at 37 °C, 5 % CO₂ (Fig. 1).



Fig. 1: Experimental set-up for (A) cyclic loading and (B) static conditions. Arrows indicate position of scaffold(s).

Frames were mounted within a BOSE biodynamic chamber (BD5110) with 225 N load cell and subjected to a tensile, sinusoidal loading pattern (5 % strain; 1 Hz for 1 hour per day). CellCrowns were held under static conditions within low binding well-plates. All scaffolds were fully submerged in culture media at 37 $^{\circ}$ C, 5 % CO₂ for 21 days.

Following 21 days, scaffolds were tensile tested to failure using an Instron with 10 N load cell. RT-PCR was used to quantify the level of gene

expression for 6 genes associated with tendons and 3 negative controls (Taqman Probes).

RESULTS: Cyclic loading of scaffolds yielded an increase in both Young's Modulus (+23 %) and tensile strength (+183 %) compared to static scaffolds (Fig. 2).

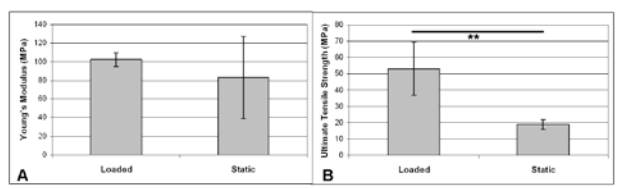


Fig. 2: (A) Young's Modulus and (B) Ultimate Tensile Strength for hMSC-seeded electrospun scaffolds (n=5) subjected to either cyclic loading or static conditions. (Data represented as mean \pm st. deviation; T-test - ** p < 0.01)

Genes associated with tendon repair were upregulated for scaffolds experiencing cyclical loading, particularly; Collagen Type 1 and 3 and Tenascin-C (Fig. 3).

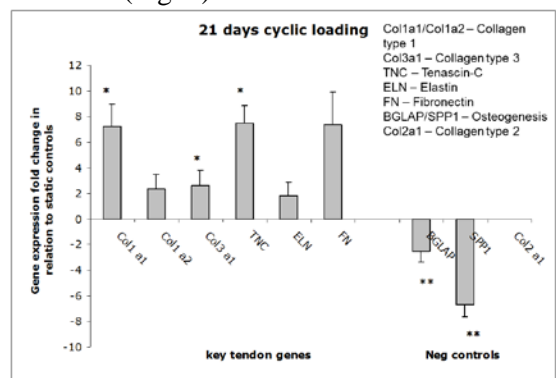


Fig. 3: Gene expression markers for scaffolds (n=4) subjected to cyclic loading compared to static culture. (Data represented as mean \pm st. deviation; T-test - ** p < 0.01, * p < 0.001)

DISCUSSION & CONCLUSIONS: 21-day cyclical loading of hMSC-seeded scaffolds, resulted in significant increases in tensile strength and up-regulation of tendon markers. This is a positive step towards better simulating and understanding *in vivo* conditions.

REFERENCES: ¹ LA. Bosworth and S. Downes, European Cells and Materials Vol. 22. Suppl. 2, 2011 (page 2).

ACKNOWLEDGEMENTS: Funded by the MRC-DPFS (grant code G1000788-98812).



Interactions between mesenchymal stem cells and nucleus pulposus cells: Implications for intervertebral disc regeneration

S Khan¹, SM Richardson¹, JA Hoyland ¹University of Manchester, Manchester, UK,

INTRODUCTION: Intervertebral disc (IVD) degeneration is a major cause of low back pain. Mesenchymal stem cells (MSCs) are a promising cell population for regeneration of the degenerate IVD. We have previously shown that direct cellcell interaction between MSCs and nucleus pulposus (NP) cells stimulates the differentiation of MSCs towards NP like cells and enhances matrix gene expression within NP cells^{1,2} suggesting restoration of a non-degenerate phenotype. However, these studies did not consider the harsh microenvironmental "niche" of the degenerate IVD characterized by reduced oxygen and nutrients³. Therefore the purpose of this study was to use an in vitro co-culture model system to investigate MSC: NP cell interactions under IVDlike microenvironmental niche (low oxygen and reduced serum) conditions.

METHODS: Human bone marrow MSCs (n=3) were fluorescently labelled and co-cultured with degenerate NP cells (n=5) in monolayer with cellcell contact at 50:50 ratio in either normoxia (20% O₂) supplemented with 10% fetal calf serum (FCS) or hypoxia (2% O₂) supplemented with 10% or 2% FCS for 7 days. Following co-culture, cells were separated using fluorescence activated cell sorting. Labelled MSCs and unlabelled NP cells were also cultured alone under identical conditions. QRT-PCR analysis of NP markers genes (Col II, SOX-9, ACAN, VCAN, PAX-1 and FOXF1) was performed to compare the effect of degenerate IVD-like microenvironmental conditions on alone and co-cultured cell phenotypes.

RESULTS: NP cells and MSCs cultured alone under IVD like microenvironment niche did not demonstrate phenotype changes. Following co-culture under hypoxia degenerate NP cells showed significant increases in VCAN and PAX-1 gene expression levels. Serum reduction under hypoxia significantly increased expression of all NP marker gene expression (Figure 1A). MSCs co-cultured with degenerate NP cells under hypoxia showed significant increases in ACAN and VCAN. Co-cultured MSCs under hypoxia with reduced serum demonstrated significant increases in expression of PAX-1 and FOXF1 (Figure 1B).

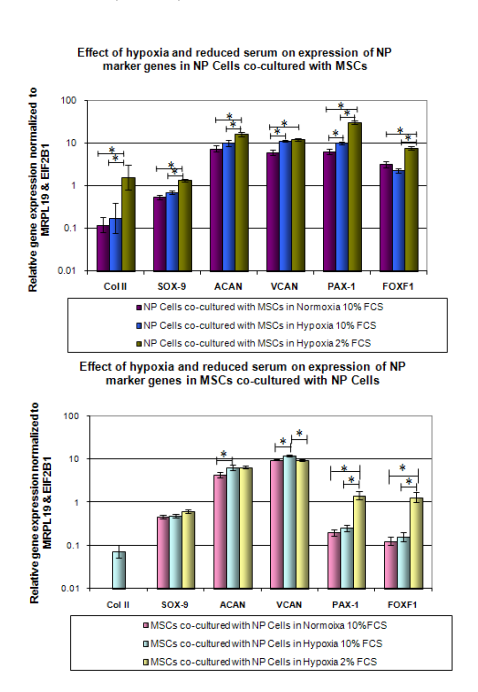


Figure 1: QRT-PCR analysis of NP markers genes in co-cultured NPCs (A) and MSCs (B).

DISCUSSION & CONCLUSIONS: The results demonstrate that IVD-like microenvironmental factors had minor effects on degenerate NP cell phenotype and MSC differentiation when cells were cultured alone. Importantly co-culture under conditions which mimic the IVD niche resulted in significant increases in NP marker gene expression in both NP cells and MSCs. This suggests that cellular communication between MSCs and NP cells under hypoxic and reduced serum may favour the release of bidirectional stimulatory signals that restore a more normal NP cell phenotype and initiate **MSCs** differentiation. This demonstrates that MSCs and NP cells are able to interact in an environment similar to that of the degenerate IVD "niche". Importantly it highlights the fact that model systems should mimic the in vivo situation as closely as possible to ensure that function appropriately will following implantation.

REFERENCES: ¹S.M. Richardson, R.V. Walker, S. Parker, et al (2006) *Stem Cells* **24**: 707-16. ²S. Strassburg, S.M. Richardson, A.J. Freemont, et al (2010) *Regenerative Medicine* **5**:701-11. ³W.E. Johnson, S. Stephan, S. Roberts (2008) *Arthritis Res Ther*, **10**:R46.



Testing and FEA modelling of a modified suture technique to accommodate a tissue engineered tendon *in vivo*

P Sawadkar¹, S Alexander¹ M Tolk³, L Bozec² and V Mudera¹

¹ Tissue Repair and Engineering Centre, UCL Stanmore Campus, London, ² UCL Eastman Dental Institute London, ³ UCL Department of Physics and Astronomy, London

INTRODUCTION: Tendon repair is surgically challenging as the tendon often retracts resulting in a gap between the torn end and its bony insertion. Tendon auto- or allografts are currently used to fill this deficit, but both are associated with potential complications. We have developed a highly reproducible, rapid process technique to manufacture compressed cell seeded type I collagen constructs to replace tendon grafts (1). However, the material properties of the engineered constructs are currently unsuitable to complete load bearing in vivo. A modified suture technique has been developed to withstand physiological loading and off load the artificial construct whilst integration occurs.

METHODS: Lapine tendons were used to test the strength of different suture techniques with different sizes of prolene sutures and tissue engineered collagen constructs in situ.

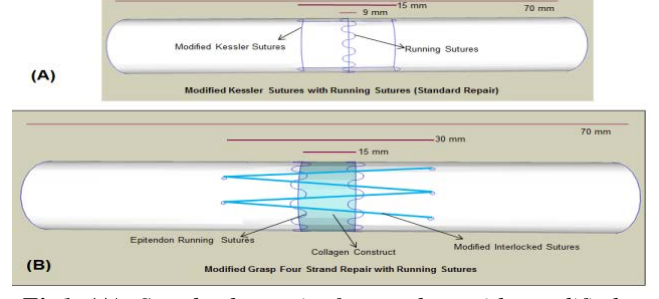


Fig1 (A) Standard repair for tendon with modified Kessler sutures, (B) Modified repair Grasp four strand sutures with tissue engineered collagen construct

The data was compared to standard modified Kessler suture using a standard tendon graft. Mechanical testing was carried out and a FEA stress distribution model constructed using COMSOL 3.5 software.

RESULTS: The break point for modified suture technique with tissue engineered collagen construct was significantly higher (50.62 ± 1.62 N) compared to standard modified Kessler suture [12.49±8.17N (p<0.05)]. In FEA modelling Van Mises stress

in the middle of the geometry, i.e. in the middle of the collagen

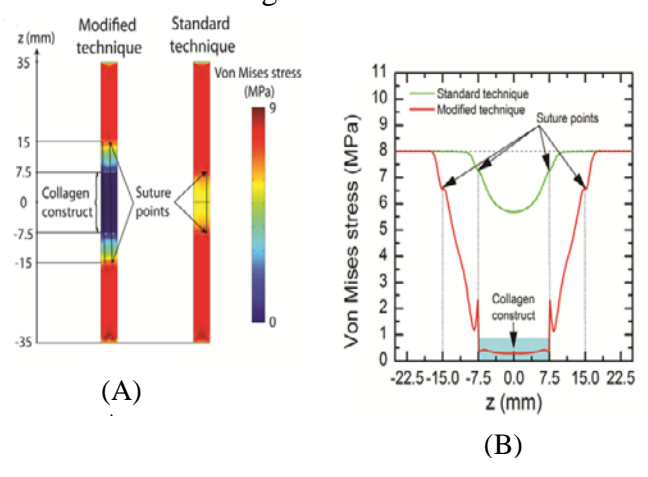


Fig2 Stress distribution finite element analysis model for modified suture technique and standard technique(A), Von Mises stress across suture points and collagen construct (B). construct (for the modified technique) or at the point of the running sutures (for the standard technique) are as follows (at a load of 8 10⁶ Pa): standard technique - 56 10⁵ Pa; modified technique - 2.8 10⁵ Pa. Hence, it is evident that, stress is 20 times less if the modified

DISCUSSION & CONCLUSIONS: Distributing suture tension further proximally and distally from the tendon ends increased the mechanical strength of the repairs. Using this proof of concept data, we will now test this modified suture technique in vivo to test integration and function in a lapine model.

technique is applied.

REFERENCE: 1.Mudera V, Morgan M, Cheema U, Nazhat S, Brown R. Ultra-rapid engineered collagen constructs tested in an in vivo nursery site. *J Tissue Eng Regen M*. 2007;1(3):192-8.

ACKNOWLEDGEMENT: I would like to thank government of India for funding this project.



Mononuclear cells enhance cell migration out of human articular cartilage

NM Hopper¹, J Wardale¹, N Rushton¹

¹ Orthopaedic Research Unit, University of Cambridge, Addenbrooke's Hospital, UK

INTRODUCTION: The belief that adult articular cartilage lacks progenitor cells has been challenged in the past few years with the hypothesis that a progenitor cell population might reside in the superficial zone of the cartilage. This study aimed to characterize the articular cartilage cell population and to compare two different cell isolation methods. In addition, a real-time cell analyzer was used to monitor cell migration from human cartilage tissue revealing the novel finding that peripheral blood mononucleated cells (PBMC) act as a chemoattractant for cartilage-derived cells.

METHODS: Human tissue was obtained from patients undergoing total joint replacement for full osteoarthritis with ethical consent (06/Q0108/213). Primary cell lines were derived from articular cartilage using Collagenase A (11088793001, Roche, Mannheim, Germany) digestion. Mononuclear cells were prepared from volunteers whole blood of healthy LymphoprepTM (Axis-Shield, Norway) gradient centrifugation. The cell surface antigen phenotype and protein expression of the primary cell lines were analysed with flow-cytometry and western blot, respectively. The xCELLigence System RTCA DP (Roche) was employed to assess the migration potential of chondrocytes and to compare the activity of chemoattractants.

RESULTS: Cells derived from a three hour Collagenase A digestion were 96.5 % positive for CD90 (Thy-1), a cell surface marker generally expressed on mesenchymal stem cells (Figure 1). However, the cell population migrating out from cartilage explants was only 0.025% positive for CD90. In addition, digested and migratory cell populations had markedly different protein expression profiles. Cell migration was studied with the addition of mononuclear cells (2.0×10^4) either in contact with the cartilage explant in the upper chamber (paracrine signaling model) or added as a chemoattractant in the lower chamber in the Boyden model (Figure 2). The results show that the control (1% FBS) was a strong attractant but the addition of mononuclear cells increased the cell migration rate by 40%.

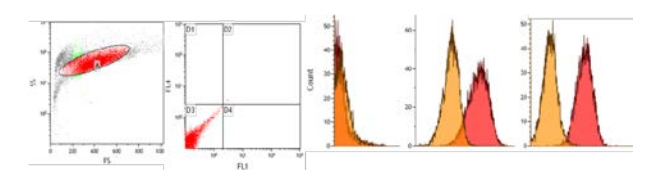


Fig. 1: Surface marker analysis of cartilagederived cells with flow-cytometry. In total 10,000 events were scored. Histograms and logarithmic dot scatter graphs showing cell distribution and gating. The graph on the far right shows the cell population positive for CD90 (96.5 %).

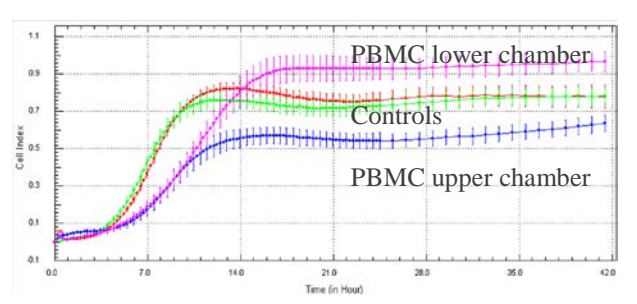


Fig. 2: Cell index presenting the cell migration from articular cartilage during the first 42 hours measured with xCELLigence (Roche) comparing the effect of adding PBMC to the upper chamber (combination) or lower chamber (directed chemotaxis towards chemoattractant).

DISCUSSION & CONCLUSIONS: In order to develop new therapies for the osteochondral niche it is essential to understand the underpinning biological mechanisms that control the fate of progenitor and other cell types homing to the tissue repair site. This study has established that the cell population that migrates out of adult cartilage explants is radically different to that released by enzymatic digestion. Cell migration studies established that PBMCs could activate and induce the cell migration out of cartilage tissue with a positive dose response.

ACKNOWLEDGEMENTS: Special thanks to Dr. Roger Brooks and Dr. Daniel Howard for excellent guidance and advice. Many thanks to the surgeons, theatre staff, patients and volunteers at the Addenbrooke's hospital for the tissue and blood samples.



Investigating the Effect of Plasma Polymers on Neuronal and Glial Cells

J.H.A. Bell & J.W. Haycock

Kroto Research Institute, Department of Materials Science and Engineering, University of Sheffield, UK.

INTRODUCTION: Materials used for peripheral nerve guide conduits should degrade at an appropriate rate. However, the maximum distance for re-innervation is limited at approximately 20mm. Improvements to this could be made in terms of materials that better support cell attachment and proliferation [1]. Coating existing FDA approved materials may be a way of increasing nerve regeneration across conduits. The aim of the present work involved plasma polymerisation of acrylic acid and maleic anhydride to investigate if these surface coatings improved the attachment, growth and neurite extension of primary rat dissociated dorsal root ganglion (DRG) cultures.

METHODS: X-ray photoelectron spectroscopy (XPS), time-of-flight - secondary-ion mass spectrometry (ToF-SIMS) and contact angle were used to confirm the presence of acid and anhydride groups after deposition. For biological evaluation, primary DRG were extracted from adult white wistar rats. A dissociation protocol similar to that specified in 3D Cell Culture Protocols [2] was used, with minor revisions. As well as the plasma polymers, for comparative purposes DRGs were also plated onto uncoated and laminin coated glass slides. After 4 days culture in Bottenstein and Sato medium with nerve growth factor supplement, DRGs were fixed and immunostained with; neural marker β-tubulin III with secondary antibody Texas Red, Schwann cell marker S100ß with FITC secondary antibody and DAPI, a nuclear stain that labels all cell types including 'contaminating' cells. Cells were then imaged using a Zeiss LSM510 META confocal microscope.

RESULTS: XPS, ToF-SIMS and contact angle measurements demonstrated that the desired chemical functionalities had been deposited on the Average fresh contact angle slips. measurements were 55° for acrylic acid and 52° for maleic anhydride. XPS demonstrated the presence of the desired chemical functionality, whilst ToF-SIMS confirmed that the plasma coated maleic had retained anhydride anhydride slides functionality. The dissociated DRG cultures on the plasma polymer coated glass slides clearly developed longer and more numerous neurite extensions compared to the native glass slides.

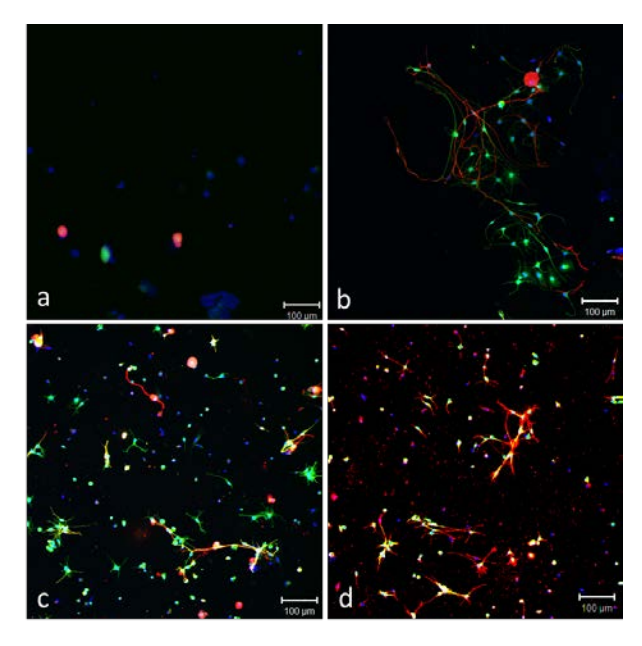


Figure. 1: Confocal laser micrographs of primary rat dorsal root ganglion cells grown on: a) glass, b) laminin, c) acrylic acid and d) maleic anhydride.

work demonstrates that surface chemistry clearly influences the growth and neurite formation of neuronal cells. Maleic anhydride and acrylic acid plasma polymer coatings look to be very promising coatings for nerve guide conduits, especially as the coating technique can potentially be applied to any material. The plasma coating process also sterilises all treated surfaces, another clear advantage. This work is being further investigated with established, FDA approved nerve guide conduit materials such as poly-caprolactone (PCL).

REFERENCES:

- 1. J.H.A.Bell, J.W. Haycock, (2012) *Tissue Eng Part B Rev* **18**:116-28.
- 2. P. Kingham et al (2011) *Methods Mol Biol* **695**:115-128.

ACKNOWLEDGEMENTS: The authors would like to thank the EPSRC for funding and Dr Claire Hurley for collecting the XPS and ToF-SIMS spectra.



The development of a 3D neuronal glial co-culture model using aligned electrospun polycaprolactone (PCL) microfibres scaffolds for peripheral nerve studies

MFB. Daud¹, KC. Pawar¹, F Claeyssens¹, AJ. Ryan², JW. Haycock¹

¹Department of Materials Science & Engineering, Kroto Research Institute, University of Sheffield, Sheffield, S3 7HQ, U.K. ^bDepartment of Chemistry, University of Sheffield, Sheffield, S3 7HF.

INTRODUCTION: Three-dimensional cell culture models are seeing a rapid rate of development, due to the need for conducting studies in a more relevant environment, in comparison to the two dimensional cell cultures. Such models hold considerable value for a breadth of studies including developmental biology, disease studies and the design of devices and scaffolds for peripheral nerve repair. The aim of the present study was to investigate the feasibility of aligned electrospun PCL microfibers scaffolds as substrate for 3D peripheral nerve model as well as the impact of fibre dimensions on the behavior of neuronal and Schwann cells.

METHODS: Electrospinning parameters were devised for systematically producing aligned polycaprolactone (PCL) fibres with specific diameters (1/5/8 µm). SEM was use to characterize fibre diameters and the orientation of fibres as a population when fabricated as mats. Neuronal and primary Schwann cell attachment and growth was investigated in vitro on aligned fibres. Neuronal and primary Schwann cell co-cultures and primary dorsal root ganglion explants on aligned fibres were conducted. Neurite extension, Schwann cell responses and neuronal/Schwann cell co-culture responses on aligned fibres were examined using 3D confocal microscopy and immunolabelling. Cell behaviour was also investigated in 2D on a range of materials for control purposes.

RESULTS: More than eighty percent of fibres measured varied within 4° for all three groups confirming that a high number of fibres were parallel to each other. Mean fibre diameter was 8.06 ± 0.07 µm for large fibres, 5.08 ± 0.13 µm for intermediate fibres, and $1.02 \pm 0.05 \mu m$ for small fibres. The longest neurite was measured on 8 µm fibre with a mean length of $142.36 \pm 13.69 \,\mu\text{m}$. On 5 μ m fibres, the mean length was 94 \pm 7.16 μ m, while the mean neurite length on 1 µm fibres was 61.83 ± 6.89 µm. The figures show that neuronal/Schwann cells co-culture was established on the fibres. Neurite growth and Schwann cell organization corresponded to the direction of fibre alignment (indicated by arrow in the figure). Dorsal root ganglion explants when grown on scaffolds showed both organised aligned neurite guidance and notably the co-localization of Schwann cells with neurites

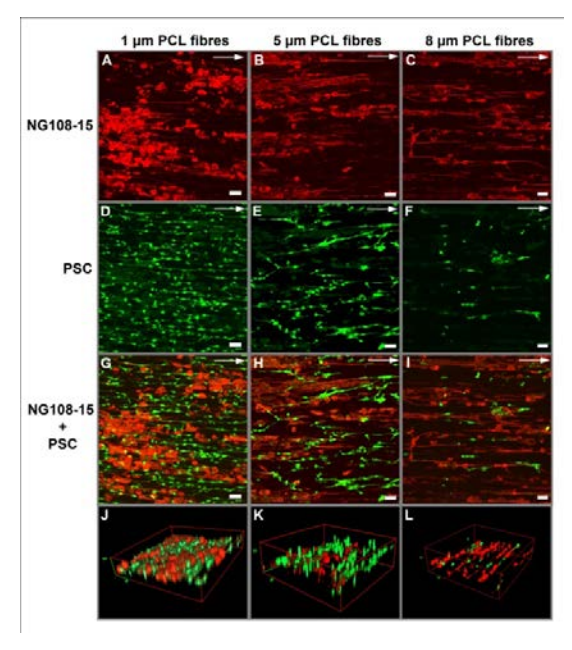


Figure 1: Images of β III tubulin labelled neurons and S100 labelled Schwann on aligned PCL fibres. J, K and L are 3D projected images of the co-cultures on the fibres.

DISCUSSION & CONCLUSIONS: In summary, the study shows that aligned electrospun PCL microfibers scaffolds can be used to construct an in vitro 3D peripheral nerve model containing neuroanl and glial cells. Scaffold dimensions impact on neuronal and glial cell response in respect of neurite outgrowth and Schwann cell phenotype and optimal dimensions hav ebeen defined. This work will go forward to the development of in vitro 3D culture model for peripheral nerve as an alternative to 2D culture models (and potentially animal studies) in areas of disease, disorder and toxicity studies.

REFERENCES: 1. Murray-Dunning (2011) Methods. Mol. Biol. 695, 155-166.

ACKNOWLEDGEMENTS: The authors are grateful to Majlis Amanah Rakyat (MARA) and the University of Kuala Lumpur for funding this work.



Injection of adipose derived stem cells after peripheral nerve injury: mechanisms and effects on regeneration

ML Vermeille^{1,2,3}, DF Kalbermatten^{2,3}, W Raffoul², M Wiberg^{1,4}, PJ Kingham¹

¹ Department of Integrative Medical Biology, Umeå University, Umeå, Sweden. ² Department of Plastic, Reconstructive and Aesthetic Surgery, University Hospital of Lausanne, Lausanne, Switzerland. ³ Department of Plastic, Reconstructive, and Aesthetic Surgery, University Hospital of Basel, Basel, Switzerland. ⁴ Department of Surgical & Perioperative Sciences, Umeå University, Umeå, Sweden.

INTRODUCTION: Functional recovery after repair of peripheral nerve injuries is far from optimal. Adipose-derived stem cells (ADSCs) are an easily accessible and promising cell source in regenerative medicine. We have previously shown that ADSCs enhance nerve regeneration [1] but the mechanisms involved remain unclear. We hypothesize that ADSCs promote regeneration by producing neurotrophic and angiogenic molecules and by modulating the Schwann cell and inflammatory cell reactions following nerve injury. In this study we investigated the effects of adipose derived stem cell transplantation by direct injection in the distal stump of the injured nerve.

METHODS: ADSCs were isolated from rat adipose tissue and expanded in vitro. Cultures were treated with a mixture of glial growth factors to differentiate the cells towards a Schwann cell-like phenotype (dADSCs) [2]. Primary Schwann cells (SC) were co-cultured with the stem cells or treated with stem cell conditioned media in vitro. The Alamar blue assay was used to assess SC proliferation and neurotrophic factors were determined using ELISAs. For in vivo experiments a rat sciatic nerve injury model was used and stem cells were injected into the distal nerve stump using a 27G needle. Either a transection and repair was performed or a gap injury of 1cm was bridged with a fibrin conduit. Nerve tissue was collected for Western blot analysis at 1 week and axon regeneration was determined at 3 weeks using βIII tubulin immunohistochemistry.

RESULTS: In vitro, adipose derived stem cells enhanced the proliferation of Schwann cells which was mediated by the release of soluble factors. Stem cells expressed high levels of VEGF and the dADSCs produced significantly more BDNF than undifferentiated cells. In vivo, elevated levels of BDNF and VEGF were observed in the animals treated with dADSCs. The inflammatory reaction (ED-1 positive macrophages) was more pronounced in animals treated with dADSCs.

Compared with nerve gap repair using empty fibrin conduits, injection of dADSCs in the distal nerve stump increased the number of axons entering the distal nerve 3 weeks after injury. Also there were more axons compared with repair using conduits containing transplanted stem cells.

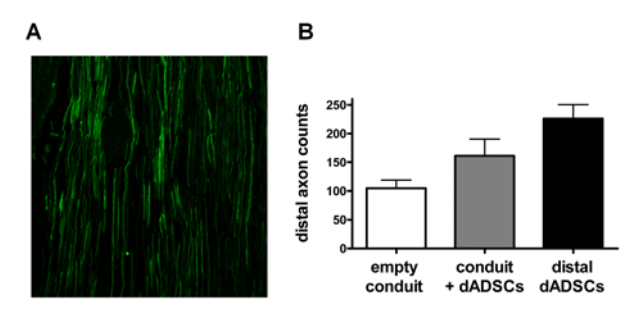


Fig. 1: (A) Immunostaining of β III tubulin positive axons in the distal nerve stump. (B) Quantification of axons regenerating across a 1cm gap injury and into the distal nerve stump.

DISCUSSION & CONCLUSIONS: ADSCs may promote nerve regeneration either directly by providing enhanced neurotrophic factor support or indirectly via effects on Schwann cell proliferation and the inflammatory reaction. Compared with transplantation in a nerve conduit, injection of differentiated ADSCs in the distal nerve stump appears to be more effective at enhancing axon regeneration.

REFERENCES: ¹ P.G. di Summa, D.F. Kalbermatten, E. Pralong, et al. (2011) *Neuroscience* **181:** 278-91 ² P.J. Kingham, D.F. Kalbermatten, D. Mahay, et al (2007) *Exp Neurol.* **207:** 267-74.

ACKNOWLEDGEMENTS: This study was supported by the Swedish Medical Research Council, European Union, Umeå University, County of Västerbotten, Åke Wibergs Stiftelse, Magnus Bergvalls Stiftelse, Clas Groschinskys Minnesfond, Gunvor and Josef Aner Foundation, SUVA and University of Lausanne FBM.



Amine functionalised nanodiamond as a neuronal cell substrate

AP Hopper ¹, F Claeyssens ¹

¹ Dept. of Materials Science & Engineering, The Kroto Research Institute, North Campus, University of Sheffield, Broad Lane, Sheffield, S3 7HO

INTRODUCTION: Normally, when culturing primary neuronal cells, prior deposition of an organic layer, normally composed of extracellular matrix proteins such as laminin, is a necessity to facilitate in vitro attachment and proliferation. However, such surfaces may pose problems for in vivo applications due to their animal derived origin. The availability detonation of nanodiamond, first produced four decades ago [1], may provide a viable alternative growth substrate. The unique combination of material characteristics (nanometre dimensions, spherical topography, biocompatibility electrical properties, functionalisation versatility) make it particularly well suited for the formation of in vivo electrically conductive neuronal interfaces in applications such as nerve guidance conduits. Such particles can be applied to surfaces by ultrasonication in a matter of minutes making the procedure quick and simple to undertake.

The aim of this study is to assess the suitability of amine functionalised nanodiamond particles for the coating of neural implants. Neuronal adhesion and cytocompatibility of nanodiamond substrates were assessed using NG108-15 neuroblastoma and primary rat Schwann cells.

METHODS: Glass cover slips (13mm) were coated with acrylic acid by plasma polymersiation (10 mins, 15W). Detonation nanodiamond was hydrogenated and the particles were then photochemically functionalised with trifluoroacetic acid protected 10-amino-dec-1-ene (TFAAD) $(\lambda = 254 \text{nm})$ for 4 hours and subsequently deprotected in acidified methanol over 24 hours. These particles were applied to plain and acrylic acid coated glass cover slips by ultrasonication for 10 mins. Neuronal NG108-15 cells were then cultured on these glass slides for up to 7 days in serum-free media whilst primary rat Schwann cells were cultured for a period of 3 weeks in their respective medium on either poly-L-lysine or nanodiamond surfaces. Cell morphology was analysed by fluorescence microscopy, labelling neuronal cells with Phallodin-FITC and DAPI. Primary Schwann cells were visualised by immunolabelling of S100.

RESULTS: MTT assays of NG108-15 cell growth on functionalised ND indicates that ND is capable

of sustaining neuronal cells, and that amine-functionalisation greatly improves neural adhesion and proliferation on these surfaces. Cell aspect ratio measurements indicate that neurite outgrowth is more prevalent in cultures grown on functionalised ND/acrylic acid coated glass. Furthermore, Atomic Force Microscopy (AFM) images illustrated the formation of a coherent nanodiamond coating upon the acrylic acid coated glass. Primary Schwann cells have also been successfully cultured upon the nanodiamond substrates over a period of 3 weeks.

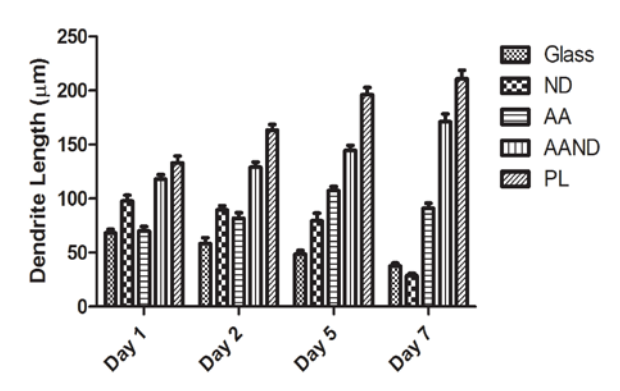


Fig. 1: Average length of neurites measured from NG108-15 neuroblastoma cells cultured on glass, 10-amino-dec-1-ene functionalised nanodiamond treated glass (ND), acrylic acid plasma polymer coated glass (AA), AA treated with amino-dec-1-ene functionalised nanodiamond (AAND) and poly-l-lysine coated tissue culture plastic (PL) over a period of 1,2,5 and 7 days.

DISCUSSION & CONCLUSIONS: Our data highlights that ND is a modifiable substrate suitable for culturing neuronal cells. Amine functionalisation enhances the proliferative capacity of NG108-15 cells and increased neurite outgrowth significantly. Acrylic acid surfaces ensure the amine coated ND adheres. The most optimal results were observed in samples cultured on acrylic acid coated glass layered with amine functionalised ND. Primary Schwann cells also were cultured with similar levels of success.

REFERENCES: ¹ A. Krueger et al. (2005) Unusually tight aggregation in detonation nanodiamond: identification and disintegration, Carbon 43(8):1722-30.

ACKNOWLEDGEMENTS: We are grateful to the EPSRC for funding this research.



Developing a 3D co-culture model to simulate perinatal hypoxic-ischaemic brain injury in preterm infants

ET Osei¹, L Evans¹, <u>JB Phillips</u>¹, <u>AJ Loughlin</u>¹

¹ <u>Faculty of Science</u>, The Open University, Milton Keynes, MK7 6AA

INTRODUCTION: Hypoxic-ischaemic cerebral injury in preterm infants at time of birth is a significant cause of childhood disability, in particular cerebral palsy. The major neuropathology is diffuse white matter injury attributed to selective loss of oligodendrocyte precursor cells (OPCs) and associated with glial cell activation [1]. Progress in developing therapeutic interventions is hampered by the lack of experimental models in which potential treatments can be tested and refined in a controlled and reliable manner. The aim here was to develop a novel 3D rat mixed glial cell culture system for rapid testing and refinement of potential therapeutic interventions for hypoxic-ischaemic injury in premature babies.

METHODS: Mixed glial cells (OPCs, microglia and astrocytes) were isolated from P1-P2 rat brain tissue and seeded within 2 mm deep collagen gels [2,3]. To simulate acute hypoxia-ischaemia, cultures under test were subjected to lowered oxygen levels (2% O₂, 7% CO₂, 91% N₂) and/or glucose-free medium for up to 24h. Live/dead staining using propidium iodide was combined with fluorescent labeling of O4, GFAP and ISL-B4 to determine the relative levels of cell death in OPCs, astrocytes and microglia respectively within the mixed population. Astrocyte reactivity was assessed using confocal microscopy and 3D image analysis to examine GFAP expression and morphological changes.

RESULTS: Treatment with low O₂ and/or glucose resulted in significant death of OPCs, with relative sparing of astrocytes and microglia (Fig 1). Astrocyte reactivity increased in all treatment conditions (Fig 2).

DISCUSSION & CONCLUSIONS: Exposure of the 3D mixed glial cultures to simulated hypoxia-ischaemia successfully modelled the selective OPC death and the astrocyte activation seen *in vivo* in brain injury associated with premature birth. This novel approach will provide a means to develop and refine new therapeutic interventions for perinatal brain injury in preterm babies.

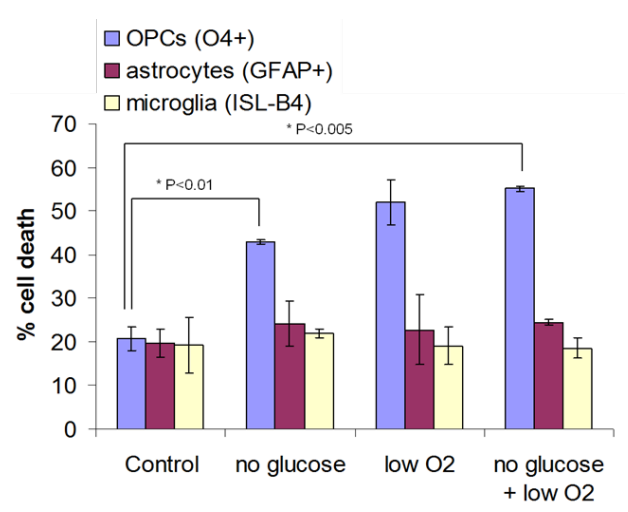


Fig. 1: Hypoxic-ischaemic conditions cause OPC death but do not affect survival of astrocytes and microglia.

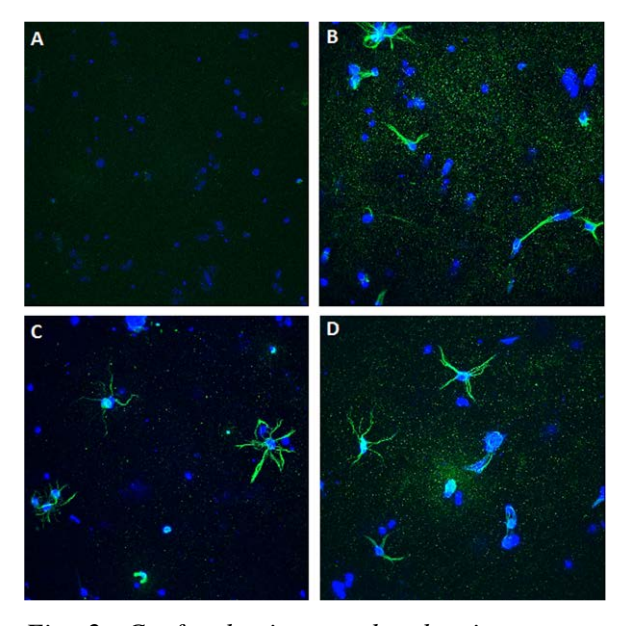


Fig. 2: Confocal micrographs showing astrocyte reactivity: (A) control, (B) no glucose, (C) low O_2 and (D) low glucose + low O_2 .

REFERENCES: ¹ R.D. Folkerth (2006) *Pediatr Devel Pathol* **9**:3-13. ² K.E. Wright et al (2009) *Br J Cancer* **101**:658-665. ³ E. East, J.P. Golding, and J.B. Phillips (2009) *J Tiss Eng Regen Med* **3**: 634-646.



Transplantation of human adipose derived stem cells reduces glial cell reactions after spinal cord injury in rats

MK Kolar^{1,2}, LN Novikova¹, M Wiberg^{1,2}, LN Novikov¹, PJ Kingham¹

¹Department of Integrative Medical Biology, Section of Anatomy, Umeå University, Umeå, Sweden ²Department of Surgical and Perioperative Sciences, Section for Hand and Plastic Surgery, Umeå University, Umeå, Sweden

INTRODUCTION: Spinal cord injuries occur at an incidence of between 12.1- 57.8 per million worldwide and of these, 40-60% of the injuries occur at the cervical level [1] leading to significant morbidity and mortality. Spinal cord injuries cause an inflammatory response that leads to scarring at the site of injury, preventing regrowth of axons through the injury site. Therefore, therapies which could reduce the glial cell reaction around the injury zone may help recovery following spinal cord injury. We have previously shown that transplantation of rat bone marrow stem cells into injured spinal cord have neuroprotective and growth promoting effects and attenuate astrocyte and microglial cell reactivity [2]. Compared with bone marrow stem cells, adipose derived stem cells (ASC) are harvested relatively more easily, found in higher abundance, and proliferate more readily [3]. Therefore, in this study we have investigated the effect of human ASC in our spinal cord injury model.

METHODS: Human ASC were isolated from abdominal fat tissue and expanded in vitro. Cultures were characterised using stem cell marker antibodies. RT-PCR was used to measure neurotrophic and angiogenic molecule expression. The ASC were injected in a rat spinal cord injury model. The spinal cord was transected through the lateral funiculus at the C3-C4 level unilaterally. Cells were injected 1mm cranial and caudal to the injury zone. Three weeks following injections, spinal cord tissue was harvested and analysed for human growth factor gene expression. At 8 weeks, tissue was harvested and the microglial and astrocyte cell reactions analysed by quantitative immunohistochemistry using OX-42 and GFAP antibodies respectively.

RESULTS: Human ASC were positive for the general mesenchymal stem cell markers CD29 and CD54 and expressed fibronectin and type I collagen. The cell cultures were negative for haematopoietic cell markers CD14 and CD45. The cells could be efficiently differentiated along bone and fat cell lineages. In vitro, the cells expressed NGF, BDNF, NT-3, VEGF, IGF-1 and angiopoietin genes. Importantly, human mRNA

transcripts were also detected in rats 3 weeks following spinal cord injury. At 8 weeks, analysis of immunohistochemistry showed a significant decrease in astrocytes and microglial cell reactivity in the rats injected with ASC.

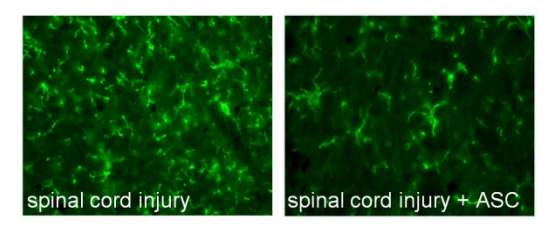


Fig. 1: OX-42 immunostaining for microglia at the C2 level showing a reduction of reactivity in the rats treated with ASC.

DISCUSSION & CONCLUSIONS: These preliminary results suggest that human adipose derived stem cells might provide some therapeutic effects following spinal cord injury. This needs to be further investigated with respect to effects on axonal regeneration and functional outcomes.

REFERENCES: ¹M.J. DeVivo (2012) Epidemiology of traumatic spinal cord injur: trends and future implications *Spinal Cord* 1-8. ² L.N. Novikova, M. Brohlin, P.J. Kingham, et al (2011) Neuroprotective and growth-promoting effects of bone marrow stromal cells after spinal cord injury in adult rats *Cytotherapy* **13**: 873-887. ³J.K. Fraser, I. Wulur, Z. Alfonso and M.H. Hedrick (2006) Fat tissue: an underappreciated source of stem cells for biotechnology *TRENDS in Biotechnology* **24**:150-155

ACKNOWLEDGEMENTS: This study was supported by the Swedish Medical Research Council, European Union, Umeå University, County of Västerbotten, Åke Wibergs Stiftelse, Magnus Bergvalls Stiftelse, Clas Groschinskys Minnesfond and the Gunvor and Josef Aner Foundation.



Development of synthetic scaffolds for delivering limbal epithelial cells to the cornea

<u>P Deshpande¹</u>, C Ramachandran², F Sefat¹, C Johnson¹, I Mariappan², D Balasubramanian², AJ Ryan³, G Vemuganti⁴, VS Sangwan², S MacNeil¹

¹Department of Material Sciences & Engineering, Kroto Research Institute, University of Sheffield, Sheffield, United Kingdom, ²Sudhakar and Sreekant Ravi Stem Cell Lab, L V Prasad Eye Institute, Kallam Anji Reddy Campus, L V Prasad Marg, Hyderabad, India, ³Department of Chemistry, University of Sheffield, Sheffield, United Kingdom, ⁴ School of Medical Sciences, University of Hyderabad, Hyderabad, India

INTRODUCTION: One of the many causes of loss of corneal transparency is limbal stem cell deficiency. Several procedures have developed to prevent blindness by transfer of cultured limbal cells often on an amniotic membrane. The results can be good but the transparency of the cornea is not completely regained and there is a small disease transmission risk in using human donor amniotic membrane. The aim of this project was to develop a synthetic delivery system for transferring limbal epithelial cells, both laboratory expanded and from limbal explants for treatment of limbal stem cell deficiency. The approach explored was the use of biodegradable 3D polymeric scaffolds as an alternative to the commonly used amniotic membrane.

METHODS: Poly (lactide-co-glycolide) 3D scaffolds were electrospun to produce scaffolds of 3 micron diameter fibres and 150 micron thickness and limbal explants/cells from both human and rabbit corneas were placed/seeded onto the scaffolds. After 2 weeks in culture the cells on the scaffolds were stained with ABCG2, P63 (putative stem cell markers), cytokeratin 3 (differentiation marker) and DAPI and examined using fluorescent, confocal microscopy and scanning electron microscopy.

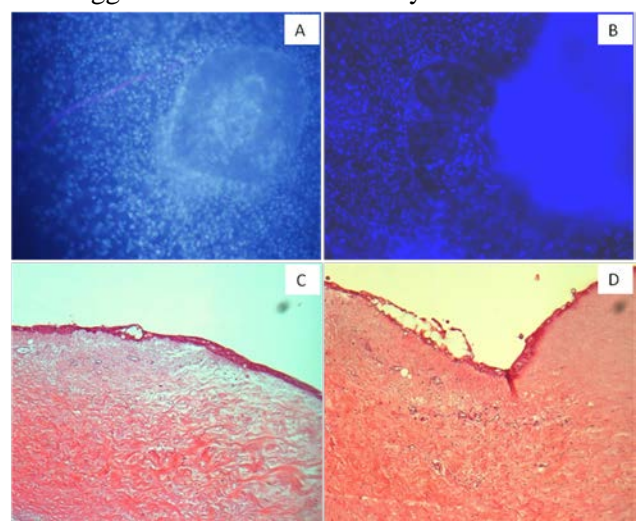
In addition cells were cultured on the scaffolds for one week and explants placed on the scaffolds after which they were placed either cell/explant side down or up on a cornea organ culture and either at an air-liquid interface or submerged for 4 weeks. The transfer of cultured cells from these scaffolds onto a rabbit cornea organ culture was assessed using histology, immunohistochemistry and scanning electron microscopy.

RESULTS: Scaffolds supported cultured cell growth and cell outgrowth from explants (Fig 1. a&b). Cells transferred from the scaffolds to a rabbit cornea ex vivo model forming a layer 2-3 cells thick after 4 weeks culture (Fig 1. c&d).

Scaffolds completely degraded within 6 weeksand degraded faster in the presence of cells.

Fig 1. Fluorescent images of human (A) and rabbit (B) cell outgrowth from explants onto scaffolds. Cells were stained with DAPI (blue). H&E of rabbit cornea organ cultures with cells transferred from scaffolds after 4 weeks in culture (C&D).

We suggest that this carrier may be used as an



alternative to the amniotic membrane in the treatment of limbal stem cell deficiency reducing the risk of disease transmission to the patient and providing a more reproducible and an off-the-shelf alternative to the amniotic membrane.

REFERENCES: Blackwood KA et al. (2008) *Biomaterials* 2008 29:3091-104, Deshpande P et al. (2010) *Regen Med.* 5:395-401.

ACKNOWLEDGEMENTS: This work was funded by the Wellcome Trust Affordable Healthcare for India.



Development of Tissue Engineered Stem Cell Niches for Corneal Repair

<u>I. Ortega ¹, P. Deshpande ¹, A. J. Ryan ², S. MacNeil ¹ and F. Claeyssens ¹</u>

¹ Biomaterials and Tissue Engineering Group, <u>Department of Materials Science and Engineering</u>, Kroto Research Institute, University of Sheffield, Sheffield, United Kingdom. ²<u>Department of Chemistry</u>, University of Sheffield, United Kingdom

INTRODUCTION: Corneal blindness occurs as a result of limbal epithelial cells (LEC) deficiency due to causes such as chemical burns, Aniridia, radiation or multiple surgeries. LEC are located in the limbus at the Palisades of Vogt in specific microenvironments or stem cell niches¹. In some cases of corneal disease limbus and niches are destroyed. In this situation cells from the conjunctiva migrate to the cornea producing scar tissue which reduces vision². Our aim is to develop an experimental model of the limbus in which to study LEC activity. Specifically, we are designing a corneal outer ring with micropockets to simulate LEC microenvironments. We hypothesise that the micropockets will aid in tissue regeneration by providing physical protection for LEC.

METHODS: Corneal outer rings were prepared by microstereolithography using PEG diacrylate (PEGDA) as a prepolymer and Camphorquinone as a photoinitiator. The microstructures were fabricated via blue laser irradiation (473 nm). The uncured polymer was washed out with isopropanol and then dried for subsequent sterilization.

PEGDA rings were biofunctionalised using biotinylated fibronectin and cell culture work was performed using rabbit limbal fibroblasts (RLF) and rabbit limbal epithelial cells (RLEC). The outer rings seeded with RLEC were placed on 3D wounded *in vitro* rabbit cornea models for 4-6 weeks and regeneration of the epithelium was studied using histology.

RESULTS: Artificial stem cell niches of sizes around 300 μm were successfully created and imaged using optical microscopy and SEM (fig.1 a, b). Cell attachment to micropockets was improved by biofunctionalising the basic PEG-structure with biotinylated fibronectin (not shown). RLF and RLEC were located in the PEGDA micropockets and imaged using fluorescence microscopy and SEM. H&E staining showed partial regeneration of the corneal epithelium demonstrating the migration of cells from the

PEGDA micropockets to the deliberately wounded cornea (fig 1 c, d).

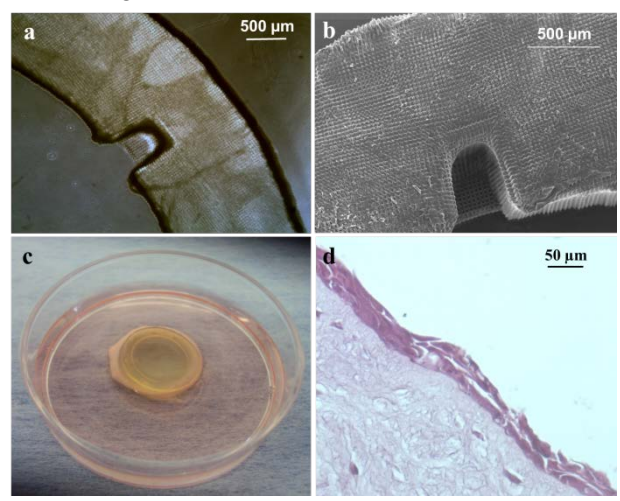


Fig. 1: Optical microscopy and SEM images of PEGDA micropockets (a, b). PEGDA outer ring on wounded cornea (c). H & E staining of wounded cornea after 6 weeks cultured with PEGDA ring loaded with RLEC (d).

DISCUSSION & **CONCLUSIONS:** Cells attached to these fibronectin coated rings were found inside the artificial niches. Preliminary data showed that RLEC migrated from the PEGDA micropockets to form a multilayered epithelium on the denuded rabbit corneas.

Future work will involve the development of an alternative biodegradable microstructured ring and the study of the behaviour of LEC inside the artificial niches in combination with stromal cells and ECM components.

REFERENCES: H S Dua, VA Shanmuganathan, et al. (2005) *Br J Ophthalmol* **89**:529-32. AJ Huang, SC Tseng (1991) *Invest Ophthalmol Vis Sci* **32**:96-105.

ACKNOWLEDGEMENTS: This work was supported by a Wellcome Trust Affordable Healthcare for India Award.



Time in organ culture storage has a detrimental effect on the survival of limbal cells.

SL Mason¹, SB Kaye², P Rooney³, E Austin³, CM Sheridan¹

¹University of Liverpool, Liverpool. ² St Paul's Eye Unit, Liverpool. ³NHS Blood and Transplant, Speke

INTRODUCTION: Limbal stem cells are a population of adult ocular stem cells found in the limbus; the transitional zone between the conjunctiva and cornea. These stem cells, found in the basal epithelial layer, proliferate in response to damage and migrate into the cornea where they differentiate into mature corneal epithelial cells to repopulate it. Limbal stem cell deficiency causes significant loss of vision. However, vision can be improved if cultured limbal cells are placed back into the deficient eye.

It has been suggested that limbal cultures could be initiated using rings left over from surgery instead of freshly donated eyes.² Corneas used for surgery can be stored in organ culture for up to 1 month before use, whereas eyes obtained from donors are placed into culture less than 48 hours post mortem.

Here we assess the effect of storage on the cells of the limbus.

METHODS:

The Limbus was dissected out and trimmed to a couple of mm in diameter. It was subsequently cut into 16 even sized pieces and exposed to 0.05% trypsin in 0.02% EDTA to dissociate the cells. Tissue was exposed to trypsin for four twenty minute intervals at 37°C. The cell suspension was removed and placed into medium with FCS to neutralise the action of the trypsin after each 20 min digestion. At the end of the full 80 min digestion the cells were pooled and centrifuged to form a pellet, resuspended and counted in 1:4 trypan blue to assess cell number and death. The age of the donors of fresh eyes was obtained to compare the effect of storage time to age.

RESULTS:

Cell numbers obtained from fresh limbus were 3.5 times as high as those obtained from corneal rings from surgery. Statistical analysis with ANOVA showed that this was significant at the 0.01 level. The percentage of dead cells after trypsinisation was also affected by storage time, with 1.7 times as many dead cells in cell samples from the stored corneas compared to the fresh. However, statistical

analysis with ANOVA showed that this was not significant at the 0.05 level.

For the fresh eyes there was a positive correlation between age and cell number of 0.5. The correlation between age and cell death was very weakly positive (0.07).

cell counts after trypsinisation

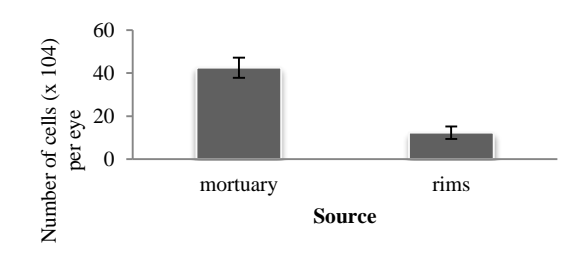


Fig. 1: Effect of storage on cell number after trypsinisation of limbus.

DISCUSSION & CONCLUSIONS:

Corneas are routinely stored for up to a month prior to their use during corneal transplant surgery, to allow the relevant tests to be carried out. Here we have shown that during this time the tissue degenerates so that fewer cells are present at the end of storage. The storage also appears to either kill some of the remaining cells or cause them to become more sensitive so that more die in the presence of trypsin.

Age of the donor did not appear to have a detrimental effect on the cells. Ages ranged from 36 to 91yrs.

REFERENCES:

¹ SH Dua and A Azuara-Blanco (2000) *Limbal stem cells of the corneal epithelium*. Survey of Ophthalmology, 44 (5) 415 -425. ² S.E.James, A. Rowe, L. Ilari, S. Daya, and R. Martin (2001) *The potential for eye bank limbal rings to generate cultured corneal epithelial allografts* Cornea, 20 (5): 488-494

ACKNOWLEDGEMENTS:

This project was funded by NHS Blood and Transplant



Stem cell generated angiogenic growth factor gradient: guiding endothelial cells

K Stamati, V Mudera, U Cheema

Tissue Repair and Engineering Centre, UCL Institute of Orthopaedics and Musculoskeletal Science, Stanmore campus, HA7 4LP, Middlesex UK

INTRODUCTION: Engineering vascular networks in vitro is critical for the long term success of engineered tissues. In vivo, endothelial cells are exposed to angiogenic growth factor gradients which influence cell migration and sprouting. In this study we aim to engineer and test the effect of a human bone marrow stem cell (hBMSC) generated angiogenic growth factor gradient, to which endothelial cells are exposed to, within a 3D environment. HBMSC seeded collagen spirals generate an oxygen gradient from the core (~35mmHg) to the outer surface (~100mmHg) of the constructs, similar to previous findings using human dermal fibroblasts^{1,2}, resulting in the up-regulation of a cascade of angiogenic growth factors.

METHODS: hBMSCs were seeded in compressed, spiralled, collagen constructs before being placed in hydrogels with human umbilical vein endothelial cells (hUVECs) (fig 1a). Immunofluorescence for CD31 was used to test endothelial cell morphology within different compartments of the hydrogels. ELISA was used to test VEGF levels within different spatial locations (spiral area (1), mid (2), distal (3) and medium) of the constructs (fig.1a).

RESULTS: Once the hBMSC seeded collagen spirals were placed in the hydrogels with the HUVECs the angiogenic growth factors were released as a gradient, with highest VEGF values in the HBMSC spiral area (~1600pg/ml), decreasing as the proximity to the depot increased (~1000pg/ml, 1cm away and ~900pg/ml 2cm away from the depot). In addition, endothelial cells fused to produce network like structures along the path of the angiogenic growth factor (fig 1b).

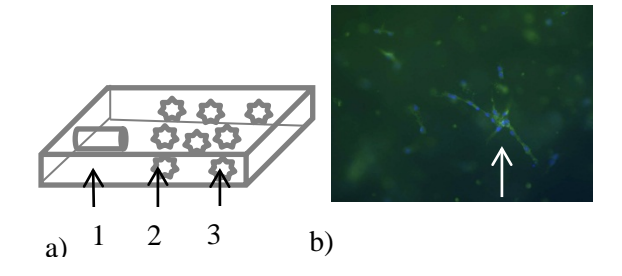


Fig 1: a) schematic representation of the 3D collagen hydrogel with the HBMSC spiral on one end, segregated by the HUVEC populated area. Numbers indicate the spiral, mid and distal segments of the gel. b) CD31 image of a network like structure (arrow) within the HUVEC seeded compartment.

DISCUSSION & CONCLUSIONS: In this study we have generated an angiogenic growth factor gradient, which we have shown to influence endothelial cell morphology within 3D collagen constructs. This was achieved through the use of hBMSCs, a cell type known to respond to cell generated hypoxia in 3D to upregulate angiogenic growth factors. We have therefore identified growth factor gradients as a critical parameter in affecting endothelial cell morphology in 3D collagen constructs.

REFERENCES: ¹U.Cheema, R.A.Brown, B.Alp, A.J.MacRobert (2008) Spatially defined oxygen gradients and vascular endothelial growth factor expression in an engineered 3D cell model. *Cell Mol.Life* Sci. **65**, 177-186. ²E. Hadjipanayi, U.Cheema, V. Mudera, D.Deng, W.Liu, R.A. Brown (2011) First implantable device for hypoxia mediated angiogenic induction J. Control Release **153** 217-224

ACKNOWLEDGEMENTS: Katerina Stamati is funded by the UCL Impact Studentship and Oxford Optronix. Umber Cheema is a BBSRC David Philips Fellow.



Neural differentiation of pluripotent stem cells is regulated by scaffold format.

E.G. Knight^{1,2}, S.A. Przyborski^{1,2}

¹ School of Biological Science, Durham University, South Road DH1 3LE UK
² Reinnervate Ltd, NETPark Incubator, Thomas Wright Way, Co. Durham, TS21 3FD UK

INTRODUCTION: Many Developmental processes rely on signalling between cells in three dimensions (3D) to determine cell fate. This has major relevance for stem cell biology as the objective is to reproduce developmental processes and engineer specific cell and tissue types *in vitro*.

Previously, a three-dimensional environment has been provided using cell aggregates. Aggregation of embryonal carcinoma (EC) cells promotes neural gene expression [1]. Culturing the pluripotent EC cell line TERA2.cl.SP12 on two dimensional (2D) tissue culture plastic, generates a limited yield of neuronal cells (~10-15%) [2]. However, a higher yield of neuronal cells can be achieved using a 3D aggregate culture system [3].

An increasing effort is focused on the development of new technologies to improve the conventional 2D culture environment. During this process we have identified that differences in scaffold presentation for 3D cell culture can help to maintain stem cell phenotype or promote differentiation.

METHODS: Using Alvetex[®], a commercial non-biodegradable porous polystyrene scaffold, we have established protocols for retinoid induced differentiation of TERA2.cl.SP12 cells in 3D.

Scaffolds fit into a standard well insert referred to as a closed wall insert. Alternatively they can be placed in a newly designed insert which allows diffusion of nutrients through the entire scaffold and the movement of media between the insert and the surrounding media reservoir (open wall insert).

Cells grown in Alvetex[®] can be processed for histology and immunostaining in a similar way to tissue samples [4]. Cells can also be removed from the scaffold for flow cytometric analysis.

RESULTS: Retinoid-induced differentiation allows cells to form complex 3D structures similar to tissues found in teratomas derived from these cells *in vivo*.

The two types of inserts cause difference in media quality. The closed wall insert allows waste products to build up inside the insert whereas an open wall insert allows a uniform distribution throughout the media.

This in turn leads to differences in cell distribution. The closed wall insert allows cells to migrate throughout the scaffold at a low cell density (Fig1A). Whereas open wall inserts allow a thick layer of densely-packed cells to survive at the surface of the scaffold (Fig.1B). This maintains a stem cell phenotype for longer in comparison to cells in the closed wall insert as demonstrated by Oct-4 staining (Figure 1C-D). Retinoid-treated cells in closed inserts display expression of neuronal differentiation marker, TUJ-1 whereas this is minimal in open wall cultures.

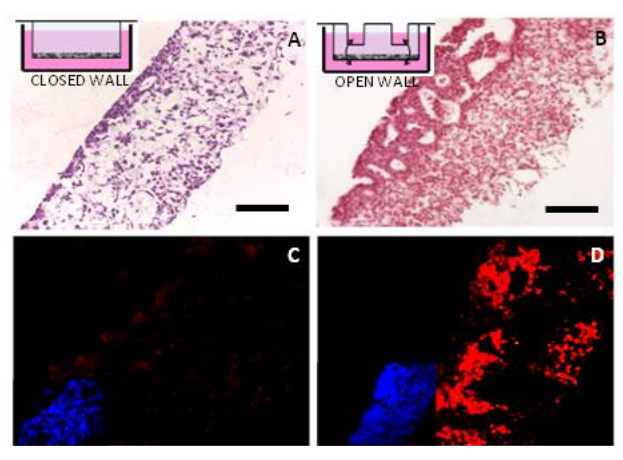


Fig. 1: Differentiation of cells within the scaffold in closed wall inserts (A,C) and open wall inserts (B,D). Cell distribution(A-B) and Oct-4 expression (C-D) at 7 days of RA-treatment differs between the two insert formats. Scale bar = $100\mu m$

DISCUSSION & CONCLUSIONS: The manner in which a scaffold is presented and used is critical to cell behaviour. Subtle differences in well insert design impact on media quality. Evidence suggests these differences can affect stem cell distribution and their differentiation.

REFERENCES: ¹Megiorni,F. et al (2005) **373** *Neurosci Lett;* ²Stewart,R. et al (2003) **21** *Stem Cells;* ³Horrocks,G.M. et al (2003) **304** *Biochem Bioph Res Co;* ⁴Knight,E. et al (2011) **695** *Methods Mol Biol.*

ACKNOWLEDGEMENTS: This research is funded by an MRC CASE studentship in collaboration with Reinnervate Ltd.



Immunological considerations of autologous stem cell transplantation following immuno-affinity separation

Matthew Fok¹, Nicholas Bryan¹, John Hunt¹

¹ <u>Clinical Engineering (UKCTE)</u>, University of Liverpool, Duncan, Building, Daulby Street, Liverpool, United Kingdom, L69 3GA

INTRODUCTION: Adult stem cells (ASCs) hold great promise for use as tools in regenerative medicine. ASCs are a rare cell, and for their potential to be realized, separation from the heterogeneous cellular milieu of primary human tissue is necessary. Typically separation strategies utilize immuno-afinity; the targeted capture of cells onto a surface or particle using an antibody specific to ASCs. It is inevitable that re-implanted cells will have non-host immunoglobulins (Ig) attached to their surface. This may potentiate an acute inflammatory response, beyond that of normal wound healing, through leukocyte Fc receptor stimulation.

Activated leukocytes produce reactive oxygen species (ROS) during acute inflammation, termed the respiratory burst¹. A well balanced ROS response is required to successfully heal tissue. Excessive ROS can substantially damage healthy native tissue and implanted cells. Recent evidence has shown ROS suppression in ASCs can potentially inhibit differentiation².

Thus it will be crucial to predict the inflammatory effects on the clinical efficacy of an ASC based implants populated with non-host Ig. This study investigated this *in vitro* using pholasin, a highly sensitive chemiluminescent ROS probe, as a predictor of an *in vivo* host response.

METHODS: Chemiluminescent detection of ROS was carried out under continuous luminometric recoding at 37°C. All experiments were performed using fresh healthy dilute human capillary blood (1:100) and pholasin, following manufacturers instructions (Knight Scientific, UK). The leukocyte stimulants fMLP and PMA were used to terminate the assay as internal controls.

10μL animal antibodies of varying class and isotype (IgG1, IgG2a, IgG2b, IgG3, IgM, and human IgG1 for control) (0.01mg/mL) were added to a white 96 well plate. Blood was immediately added to each well before luminescence was recorded continuously for 90 minutes. Opsonised hMSCs were added at a concentration of 1000 or 5000 cells per well +/- fresh diluted blood. Statistics were performed using student T test and Waller Duncan Ranking (P<0.05).

RESULTS: We observed striking inter-donor variations in ROS production in response to murine antibodies of varying class and isotype despite basal ROS production being statistically similar across 3 donors tested as measured in total relative light units (RLU) emitted (mean 3.2x10⁴ RLU, n=4, p<0.05). All three donors had statistically different ROS production when incubated with IgG2b, percentage decrease was seen in two donors (0.64% and 10.22%) and a percentage increase in one donor (15.13%). (p<0.05). This variation was not limited to IgG2b. A dramatic suppression in ROS production was observed from human leukocytes with the addition of mouse IgM (83% \pm 3.7) and rabbit IgG (81% \pm 0.74) (mean percentage decrease \pm SD, n=2donors, p***<0.005 vs. basal). The suppression achieved with mouse IgM could be reversed with the addition of CD105 mouse IgG (n=6).

A large respiratory burst and sustained level of ROS production was seen in hMSCs that increased with the number of cells per well (1000 or 5000 cells/well). Furthermore, the addition of CD105 IgG antibody, suppressed ROS production in hMSCs to that below basal levels of blood.

DISCUSSION: We observed inter-donor differences in ROS production in response to varying mouse antibody isotypes which has not been documented previously. This implies the efficacy of autologous cell implants may be optimized by tailoring the cell isolation protocol on an individual patient basis. Large ROS production in hMSCs was observed, that could be suppressed with antibodies directed against stem cells. Which are encouraging results in consideration of reimplantation, demonstrating excessive ROS can potentially be quenched by retention of Ig capture artifact. The results in leukocyte ROS production is likely to be facilitated through an Fc mediated response which we intend to dissected further to deduce the influence of specific subclasses of Fc receptors.

REFERENCES:

¹M Navarro, F Pu, J Hunt (2011) Experimental cell research **318**:361–70. ²K Yasunari, H Takashi, W Sang, et al (2011) Life Sciences **89**:250-258



Nanotopography-induced osteogenic differentiation of human embryonic stem cells and adult skeletal stem cells

E Kingham¹, N Gadegaard², MJ Dalby³, ROC Oreffo¹,

¹Bone & Joint Research Group, Centre for Human Development, Stem Cells and Regeneration Human Development and Health, Institute of Developmental Sciences, University of Southampton, UK, ²Division of Biomedical Engineering, School of Engineering, University of Glasgow ³Centre for Cell Engineering, Department of Electronics and Electrical Engineering, Rankine Building, University of Glasgow, UK.

INTRODUCTION: The efficient production of osteogenic cell types from adult and embryonic cells will be of significant medical and research benefit. Current differentiation protocols rely on chemical induction or genetic manipulation which increases the risks associated with transplantation. Previously, we reported that a square arrangement of nanopits can maintain the adult skeletal stem cell state¹ whilst displacement of this square arrangement induced osteogenic differentiation^{1,2}. These findings provide the possibility to produce patient-specific osteogenic cells from skeletal stem cells and to improve implant osseointegration using nanotopographical surfaces.

Here we describe the manipulation of embryonic stem cell differentiation using nanotopographical surfaces to induce mesodermal differentiation. In addition we have explored possible epigenetic mechanisms underlying nanotopographical regulation of adult skeletal stem cell fate and uncovered developmental epigenetic regulation of osteocalcin.

METHODS: Nanotopographical substrates displaying 120nm diameter nanopits arranged in square (centre-centre spacing of 300nm) and near square geometries (displaced by 50nm in x and y were implemented. Nanotopographical substrates were seeded with either HUES7 human embryonic stem cell (hESC) line or bone marrow isolated STRO+ adult skeletal stem cells from consenting patients undergoing routine hip replacement surgery. Typical culture media lacking differentiation inducing factors (e.g. ascorbate, dexamethasone) was used and the resulting cell types were characterised using immunofluorescent staining, qPCR and epigenetic techniques. Developmental stages were also represented using fetal femur derived cells.

RESULTS: hESCs differentiated on near square nanotopography substrates exhibited a down-regulation of hESC markers Nanog, OCT4, SOX2, TRA-1-60 and SSEA4, an up-regulation of adult skeletal stem cell-specific genes including STRO1

and CD44, and enhanced expression of osteogenic markers type I collagen, RUNX2 and osteonectin. While global methylation remained the same, changes in DNA methylation of promoter regions (osteocalcin, OCT4) were detected, furthermore methylation changes were akin these chemically-induced hESC differentiation. Following induction of differentiation formation of embryoid bodies, cells became less sensitive to nanotopographical cues.

Assessment of methylation within the promoter region of the osteogenic gene, osteocalcin revealed DNA methylation status to be dependent on the developmental stage of the cells. Significant demethylation was observed to occur between the fetal and adult stages.

In adult skeletal stem cells, chromatin accessibility within the osteocalcin promoter was enhanced following chemical or nanotopographical-induction and correlated with enhanced expression of osteocalcin.

DISCUSSION & CONCLUSIONS: Directed differentiation of embryonic and adult stem cells using nanotopographical cues provides a unique approach to overcome regenerative medical challenges with downstream applications in stem cell biology, small molecule screening and therapeutic use.

REFERENCES: ¹ M. Dalby, N. Gadegaard, R. Tare, et al (2007) *Nat Mater* **6**: 997-1003. ² R. J. McMurray, N. Gadegaard, P.M. Tsimbouri, et al (2011) *Nat Mater* **10**, 637-644.

ACKNOWLEDGEMENTS: Kate Murawski and Kate Wright are acknowledged for technical assistance. This research was funded by the BBSRC.



Mechanotransduction effects and Stem Cell Differentiation in Response to Bioactive Nanotopography

PM Tsimbouri¹, N Gadegaard², E Kingham³, ROC Oreffo³ & MJ Dalby¹

¹ Centre for Cell engineering, Faculty of Biological & Life Sciences, Joseph Black Bld, University of Glasgow, Glasgow G12 8QQ,UK, ² Centre for Cell engineering, Department of Electronics and Electrical Engineering, Rankine Bld, University of Glasgow, Glasgow G12 8QQ,UK, ³ Bone and Joint Research Group, University of Southampton, Southampton, SO16 6YD, UK

INTRODUCTION: A detailed examination of the effects of nanotopography on cell adhesion and morphology and the consequences of those changes in the nucleus and gene expression will be presented. This will help bring us a step closer to understanding, and even controlling, stem cell differentiation. This information will benefit materials scientists working on next-generation tissue engineering scaffolds.

METHODS: Stro-1-selected skeletal stem cells study early time-point were used to mechanotransductive events. Nanopits with a controlled degree of disorder, were compared to planar and ordered nanopit controls. These surfaces are known to change stem cell fate [1-2]. To examine mechano-transductive events, cell, nucleus and adhesion morphology has been quantified and phenotypic changes investigated. The organization of the interphase nucleus was investigated by lamin nucleoskeletal staining and chromosome mapping. Metabolomics were used to study changes on stem cell metabolism as a response to nanotopography.

RESULTS: We observed significant changes in cell adhesion, nucleus and lamin morphologies in response to the different surfaces. These changes relate to changes in packing of chromosome territories within the interphase nucleus. This leads to changes in transcription factor activity, phenotypical signalling and metabolism.

DISCUSSION & CONCLUSIONS:
Nanotopography is an excellent, non-invasive tool for studying cellular mechanotransduction, gene and protein expression patterns, through its effects on cell morphology. Different nanotopographies result in different morphological changes in the cyto- and nucleo-skeleton as well as the chromosomes. MSCs retained as stem cells can be differentiated and then dedifferentiated towards a stem cell state when cultured on different nanopatterns. Their metabolic profile (activity and percentage of unsaturated metabolites) closely reflects their phenotype. The use of bioinformatics

to fit metabolic data into pathway analysis resulted in the selection of ERK1/2 as a key canonical pathway of interest for MSC modulation amongst others; this was further supported by findings from pharmacological inhibition studies.

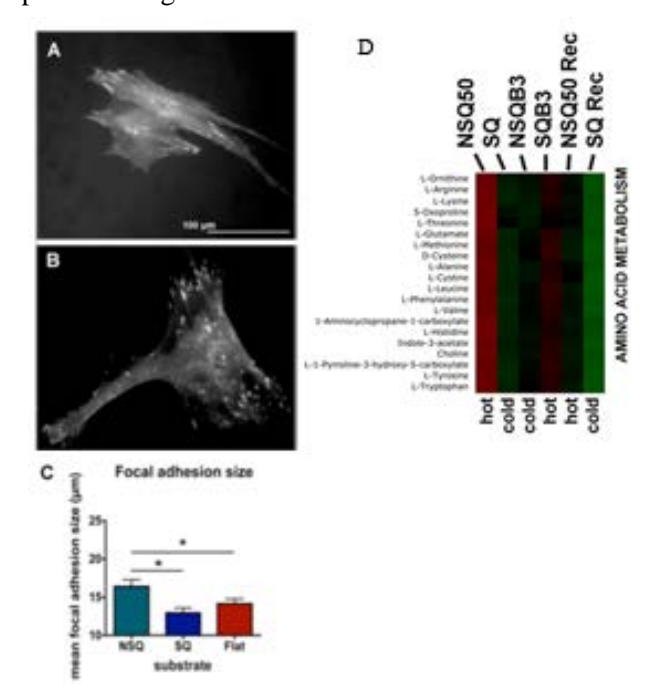


Fig1. Adhesion morphology on (A) NSQ50 and (B) SQ after 3 days of MSC culture. (A) on NSQ50, MSCs formed fewer (p<0.01) adhesions of greater size (p<0.05) that seen in cells on SQ or planar control. (B) MSCs on SQ, however, displayed similar numbers of similar sized adhesions to planar control (P>0.05). Results = mean \pm SD for at least 50 cells on n=3 material replicates, ANOVA *=p<0.05. (D) Metabolic data reflecting their phenotypic changes.

REFERENCES: 1) Dalby MJ, etal., (2007). The Control of Mesenchymal Stem Cell Differentiation Using Nanoscale Symmetry and Disorder. Nat Mat (doi:http://dx.doi.org/10.1038/nmat2013)
2) R J. McMurray, et al., (2011). Nanoscale surfaces for the long-term maintenance of MSC phenotype and multipotency .*Nature Materials*, DOI:10.1038/NMAT3058.

ACKNOWLEDGEMENTS: Project funding: BBSRC grant BBG0088681. We thank K. Muraski for providing the MSC cells.



Mononuclear cells for haematopoietic progenitor cell expansion as an approach to increase output for erythroid maturation

HT van Veen¹, F Pu¹ NP Rhodes¹, JA Hunt¹

¹UKCTE, Clinical Engineering, The Institute of Ageing and Chronic Disease, University of Liverpool, Liverpool, UK

INTRODUCTION: Published research provides evidence that peripheral blood mononuclear cells (PBMCs) will be advantageous for erythroid maturation compared with peripheral blood (PB) isolated CD34+ haematopoietic progenitor cells (HPCs). Van den Akker et al compared a mononuclear cell (MNC), CD34-, and a CD34+ cell population for *in vitro* erythroid expansion and found that the potential of CD34- cells outweighs the contribution of CD34+ cells^[1]. We have developed this further and analysed the expansion of CD34+ cells within a cultured population of PBMCs on a stromal layer to recreate a niche-like environment. Initial experiments have indicated large increases in CD34+ cell numbers from PBMCs (up to 340x). This approach will be utilised with umbilical cord blood MNCs (UBMCs) to compare HPC expansion potential and subsequently analyse efficiency in erythroid maturation. If successful, this should generate higher numbers erythrocytes (i.e. erythroid maturation) than has so far been achieved.

METHODS: MNCs were prepared of diluted PB samples on Histopaque-1077 (Sigma) at 2000rpm for 20 min. CD34+ cells were isolated using MACS Magnetic Bead Cell Separation technique (Miltenyi Biotec). Umbilical Cord Blood (UCB) CD34+ cells were kindly provided by Banc de Sang i Teixits (Barcelona, Spain) and Cell Biology Laboratory Germany). Cells were cultured up to 28 days in either P-medium: HPC Expansion Medium DFX supplemented with Cytokine Mix E (PromoCell), D-medium: basic medium designed by Douay et al. (2009)^[2] supplemented with SCF, TPO, and Flt3-L (each 50ng/mL), or I-medium: ISCOVE (BioChrom AG) supplemented with 5mM Glucose, 2mM Glutamine, 0.04mM Inositol, 10% Fetal Calf Serum and SCF, TPO, and Flt3-L (each 50ng/mL). Cells were cultured in 24 or 48 tissue culture well plates (Nunc) either with or without a stromal layer. Stromal cells were either isolated from fresh adipose tissue (AMSC) or purchased bone marrow stem cells (BMSC). Analysis was performed using FACS: cells were incubated with either FITC-

hCD34 antibodies or FITC Mouse Isotype IgG (negative) prior to analysis. Data was analysed using CellQuest software.

RESULTS: The PBMCs in a haematopoietic niche-like environment demonstrated an increase in the CD34+ populations, where CD34+ isolated cells only, lost their phenotype rapidly (Fig 1). UCB CD34+ in a similar setup did not lose their CD34+ phenotype (data not shown) as dramatically when compared to PB CD34+ isolated cells.

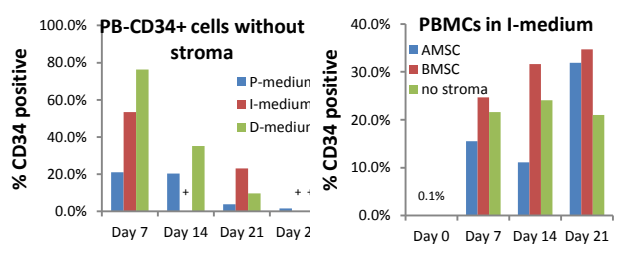


Fig. 1: PBMCs. (<u>Left:</u> CD34+ isolated cells lose their phenotype rapidly- +:No data available. <u>Right:</u> CD34+ cell population within MNCs increased rapidly on different stroma)

DISCUSSION **CONCLUSIONS:** potential of heterogeneous MNC populations for **HPC** expansion has been experimentally evidenced. The hypothesis that CD34+ HPC expansion will have better prospects in a niche-like environment has been demonstrated. combination of a stroma and a heterogeneous cell population will lead to higher HPC expansion potentials than is currently demonstrated³. Subsequently we are now using this knowledge to differentiate UBMCs for erythroid maturation. An increased efficiency of ex vivo haematopoiesis and subsequent erythroid maturation should lead to greater numbers of erythrocytes for clinical purposes.

REFERENCES: ¹ E. Van den Akker (2010) *Haematologica*, **95**: 1594. ² L. Douay (2009) *Stem Cells in Regenerative Medicine* **482**: 127. ³ A. Dahlberg (2011) *Blood*, **117**: 6083.

ACKNOWLEDGEMENTS: The Redontap Project (Framework 7).



Evaluation of a novel, rapid method to catch and release therapeutic numbers of viable adult stem cells from adipose

FC Lewis¹, N Bryan¹, D Bond², C Stanley², JA Hunt¹

¹ UKCTE, Clinical Engineering, The Institute of Ageing and Chronic Disease, University of Liverpool, Liverpool, L69 3GA, UK. ² Cellcap Technologies Ltd. The Greens Farm, Todmorden, U.K.

INTRODUCTION: Adult stem cells (ASCs) are a powerful candidate cell for regenerative medical applications due to their plasticity and presence in numerous tissue sources. Adipose contains a relatively high abundance of ASCs therefore, isolation and interrogation of the ASC component of adipose has become a fundamental research goal across the ASC research field. Isolating therapeutic doses (>10⁶) of ASCs is difficult and routine methods centered on small antibody labeled paramagnetic particles do not work well in primary tissues without extensive pre-processing. Additionally they can become internalised causing phenotypic alteration with potential immuocompromisation. Here we evaluate a new large, dense capture bead to isolate ASCs, which also permits cell release with minimal isolation artefacts.

METHODS: Adipose was isolated from 10 week old male and female Wistar rats and collagenase digested (90 minutes, 37°C, rolled). Capture beads (density 3.5 g/l, 50-200μm diameter, Cellcap Technologies Ltd, UK) populated with anti-CD90 antibody were combined with adipose (15mins, 4°C). Proceeding washing, capture beads were incubated with release buffer (15mins, RT) to elute captured cells.

RESULTS: Flow cytometric analysis of adipose stromal vascular fraction (SVF) validated CD90 as an optimal target for ASC isolation. Typically 5-10% of cells in rat white adipose were CD90⁺, which did not vary as a function of anatomical location, n=7 (Fig. 1).

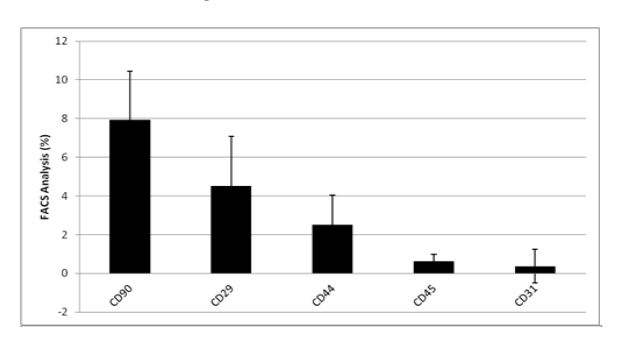


Fig. 1: Flow cytometric analysis of SVF confirms CD90⁺ population.

confirmed by positive qRT-PCR for the CD90 transcript (Fig. 2A). Using the release buffer captured cells could be recovered (Fig. 2B) and introduced into culture without internalisation of capture beads.

Beads allowed selective capture of CD90⁺ cells

depleting up to 80% of ASCs from primary

adipose. The phenotype of the isolated cells was

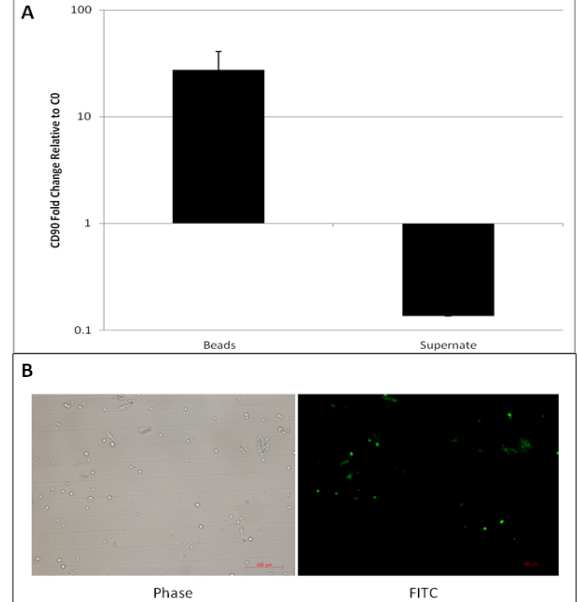


Fig. 2: (A) qRT-PCR analysis of CD90 fold change relative to unlabelled control. Error bars represent 1 standard deviation, n=3. (B) Fluorescent microscopic observation of released cells visualized by the presence of FITC CD90.

DISCUSSION & CONCLUSIONS: This study presents a novel cell selection strategy for ASCs. The technique can process large volumes of minimally processed crude tissue allowing capture and release of therapeutic numbers of ASCs, whilst avoiding internalisation. Also the ability to tailor this approach by simply varying the antibody used gives it a wide application across cell biology and biomedicine.

ACKNOWLEDGEMENTS: The authors wish to thank SPARK, UK for funding this research.



Optimisation of a 3D engineered skeletal muscle-motoneuron co-culture using fibrin-cast gels

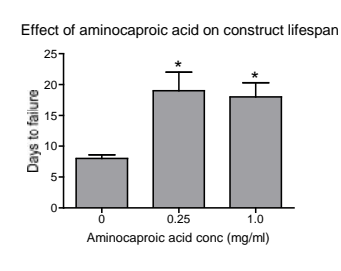
S.L. Passey¹, A.S.T Smith^{1,2}, N.R.W Martin¹, V. Mudera³, L. Greensmith², K. Baar⁴ and M.P. Lewis^{1,5}.

INTRODUCTION:. A number of in vitro engineered models of skeletal muscle have been described that demonstrate many structural, biochemical and physiological similarities to in vivo muscle. At present however there is no truly biomimetic in vitro model of skeletal muscle which takes into account neuromuscular interactions. Indeed an important aspect of in vivo muscle development and maintenance is the presence of a neuronal input via neuromuscular junctions (NMJs). Here we have increased the complexity of an existing 3D skeletal muscle model by introducing primary motoneurons with the aim of engineering a functional neuronal input.

METHODS: The fibrin gel model of skeletal muscle culture has been described elsewhere (1) which we have supplemented with aprotinin. Rat MDCs were isolated from the hind limbs of P1 Sprague-Dawley rat pups, and were seeded at 2 x 10⁵ cells per construct. In an attempt to increase construct longevity, the day following cell seeding the media was supplemented with 6-aminocaproic acid or maintained in standard growth media and cultured until the gels detached from the sutures. In co-culture experiments MDCs were cultured until confluent before the addition of MNs. Primary MNs were isolated from the ventral horn of spinal cords from Sprague-Dawley rat E14 embryos and plated at 50,000 cells per construct. Co-cultures were maintained for up to 7 days prior to processing for immunostaining or q-PCR.

RESULTS: Constructs seeded with primary rat detached from the sutures approximately 7 days in culture which prevented analysis of neuromuscular interactions. addition of 0.25mg/ml or 1 mg/ml 6-aminocaproic acid to the culture medium resulted in improved longevity of the constructs which allowed MN's to be successfully cultured in fibrin constructs (Figure 1A). Neither MDC nor MN survival was affected by the supplementation as determined by immunostaining cells of in monolayer. Colocalisation of the presynaptic protein Synaptic Vesicle Protein 2 (SV2) and the post-synaptic

Acetylcholine Receptor (AchR, visualized using α -bungarotoxin) was observed suggesting interaction between the MNs and the myotubes after both 7 and 10 days in co-culture (Figure 1B).



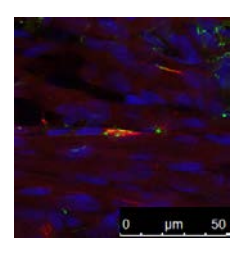


Figure 1. (A) Improved longevity of fibrin-cast skeletal muscle constructs (B) Colocalisation between presynaptic (SV2, green) and post-synaptic (BTX, red) markers in MN-Myotube co-cultures. Scale bar = $20\mu m$.

DISCUSSION & CONCLUSIONS: Inhibition of plasminogen activity via the addition of 6-aminocaproic acid allowed for longer-term culture of the MNs with the myotubes. Colocalisation of pre- and post-synaptic markers was observed indicating possible early interactions between the two cell types; representing the first step towards the formation of organized NMJs. Establishment of a 3D muscle-MN culture system will be of great benefit to the study of NMJ formation, maturation, and function and will reduce reliance on animal models for such studies.

REFERENCES: ¹ Rapid Formation of functional muscle in vitro using fibrin gels. Yen-Chih Huang, Robert G. Dennis, Lisa Larkin, and Keith Baar. J Appl. Physiol. 98:706-713, 2005.

ACKNOWLEGEMENTS: This work was supported by an NC3Rs project grant.



¹ Musculoskeletal Research Group, School of Sport, Health and Exercise Science, Loughborough University, Loughborough, SE11 3TU. ² The Sobell Department of Motor Neuroscience and Movement Disorders, UCL Institute of Neurology. ³ UCL Institute of Orthopaedics and Musculoskeletal Science, Stanmore. ⁴ Functional Molecular Biology Lab, UC Davis, California, USA. ⁵ UCL School of Life and Medical Sciences, London.

Regenerative cell injection in denervated muscle reduces atrophy and enhances recovery following nerve repair

D Schaakxs^{1,2}, DF Kalbermatten³, W Raffoul², M Wiberg^{1,4}, PJ Kingham¹

¹ Department of Integrative Medical Biology, Umeå University, Umeå, Sweden. ² Division of Plastic, Reconstructive & Aesthetic Surgery, CHUV, University Hospital of Lausanne, Lausanne, Switzerland. ³ Department of Plastic, Reconstructive and Aesthetic Surgery, University Hospital of Basel, Basel, Switzerland. ⁴ Department of Surgical & Perioperative Sciences, Umeå University, Umeå, Sweden

INTRODUCTION: Functional muscle recovery after a peripheral nerve injury is far from optimal due to atrophy of the muscle arising from prolonged denervation. We hypothesised that injecting regenerative cells in denervated muscle would reduce atrophy.

METHODS: A rat sciatic nerve lesion was performed and Schwann cells (SC) or adipose derived stem cells, untreated and induced to a "Schwann cell-like" phenotype (dASC) [1], were injected into the gastrocnemius muscles. Nerves were either repaired immediately or capped to prevent muscle reinnervation. One month later, functionality was measured using a walking track test [2] and muscle atrophy was assessed by examining muscle weight and histology.

RESULTS: In both experimental models (repair and capping of the nerve), cell injection groups displayed significantly higher muscle weight than the sham groups. Animals subjected to nerve injury followed by repair and injection of growth medium in the muscle showed greater than 60% weight reduction compared with the contra-lateral side. Injections of untreated ASC did not enhance muscle weights. However, significantly less muscle atrophy was observed in the dASC (p<0.01 for nerve repair, p<0.001 for capping of nerve) and in the SC groups (p<0.001 for nerve repair, p<0.001 for capping of nerve). Nerve repair also resulted in increased muscle weights compared with the no-repair groups. Histological (Fig. 1) and functional analysis confirmed these results. The repair sham group showed both fast and slow muscle fibers with less than 20% area size compared with the contra-lateral side. In animals treated with injections of dASC or Schwann cells there was a significant increase in muscle fiber size. The rats in the dASC and Schwann cell injection groups also showed significantly better functional results in the walking track test when compared with the sham group. The times required

for the rats to cross the ladder were reduced and there was an increased accuracy of foot placement.

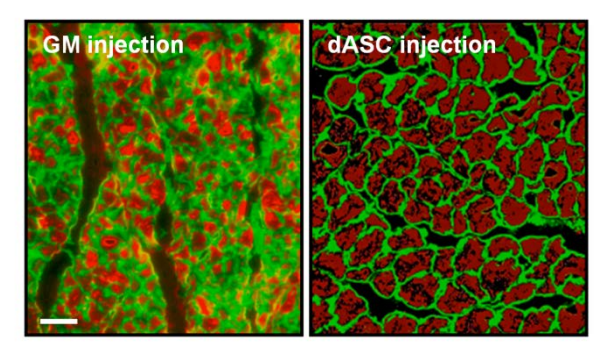


Fig. 1: Transverse sections of gastrocnemius muscle stained with laminin antibody (green) and fast myosin heavy chain protein antibody (red). Samples shown are from the operated side after one month survival time of animals from repair group which received injections of either growth medium (GM) alone or dASC.

DISCUSSION & CONCLUSIONS: Our results indicate that injecting stem cells or Schwann cells reduces muscle atrophy occurring as a result of denervation. Adipose derived stem cells appear to be a promising, clinically relevant cell population, for treatment of traumatic nerve injuries.

REFERENCES: ¹ P.J. Kingham, D.F. Kalbermatten, D. Mahay, et al (2007) *Exp Neurol.* **207:** 267-74. ² G.A. Metz, I.Q. Whishaw (2002) *J Neurosci. Meth.* **115:** 169-79

ACKNOWLEDGEMENTS: This study was supported by the Swedish Medical Research Council, European Union, Umeå University, County of Västerbotten, Åke Wibergs Stiftelse, Magnus Bergvalls Stiftelse, Clas Groschinskys Minnesfond, Gunvor and Josef Aner Foundation, SUVA and University of Lausanne FBM.



Identification and characterisation of multipotent PW1⁺ interstitial cells from porcine skeletal muscle

FC Lewis¹, BJ Henning¹, G Marazzi², D Sassoon², GM Ellison¹, B Nadal-Ginard¹

BioStem, Liverpool JMU, Liverpool, UK. ²Myology Group, INSERM, Paris, France

PW1^{pos}/Pax7^{neg} **INTRODUCTION:** muscle interstitial cells (PICs) are myogenic in vitro and efficiently contribute to skeletal muscle regeneration in vivo providing a promising candidate for skeletal muscle regeneration [1]. To conduct meaningful pre-clinical therapies for skeletal muscle we require a model which is more similar to humans than the currently available rodent models. The pig, because of its similarities in terms of tissue biology, size and physiology, has proven a useful large animal Here, we define new criteria for the isolation of PICs from porcine skeletal muscle, which represent a promising source of cells for pre-clinical assessment of skeletal regenerative therapies.

METHODS: PICs (PW1^{pos}/Pax7^{neg}) and Satellite cells (PW1^{pos}/Pax7^{pos}) were isolated by enzymatic digestion from the hindlimb skeletal muscle of mouse (21 days) and porcine (28 days). Satellite cells (CD56^{pos}) and PICs were purified using MACS technology (Miltenyi) according to expression of the cell surface markers, CD45^{neg}, and Sca-1^{pos} (mouse) or CD34^{pos} (porcine). PICs were characterised for stem cell surface marker and multipotency gene expression, clonogenicity, differentiation mvogenic potential developmental potential into multiple lineages, flow cytometry, cell culture, immunocytochemistry and qRT-PCR.

RESULTS: PICs showed high positivity for PW1 and negativity for CD45 and Pax7 (Fig. 1). They also expressed the pluripotent stemness markers Oct4 (99%), Sox2 (92%) and Nanog (93%). This phenotype distinguished them from both satellite and side population stem cells.

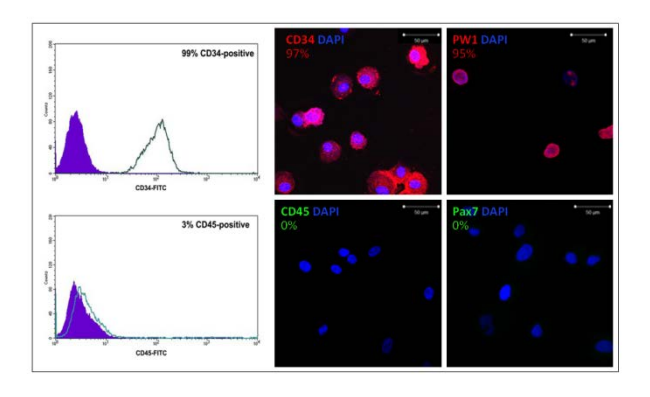


Fig. 1: Flow cytometric analysis and cytospin immunocytochemistry confirms isolation of CD34^{pos}/CD45^{neg} skeletal muscle porcine cells by MACS technology.

Porcine PICs demonstrate stem cell properties of clonogenicity (mouse 48±5%, porcine 50±10%), self-renewal and can be propagated and maintained in an undifferentiated, stable state in culture >40 passages. In addition, PICs demonstrate robust, bipotent myogenic potential acquiring both skeletal and smooth muscle phenotypes characterised by a significant upregulation of myosin heavy chain (24%) and smooth muscle actin (83%) respectively (Fig. 2).

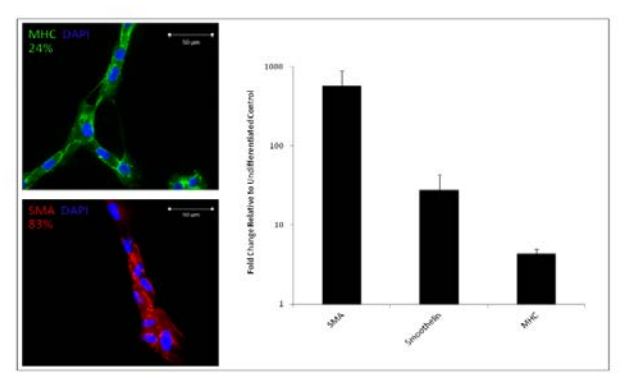


Fig. 2: Bi-potent myogenic potential of porcine PICs confirmed by immunocytochemistry and qRT-PCR analysis.

Furthermore, preliminary data suggests that PICs have a broad developmental plasticity and under proper culture conditions give rise to derivatives of all 3 germ layers.

DISCUSSION & CONCLUSIONS: Together these findings highlight PICs as a unique stem cell population with advantageous properties for use in tissue engineering and regenerative medicine.

REFERENCES: ¹ K.G. Mitchell, et al. (2010) Identification and characterisation of a non-satellite muscle resident progenitor during postnatal development. Nature Cell Biology 12(3):257-66

ACKNOWLEDGEMENTS: This work is funded by the FP7-Health – 2009 ENDOSTEM project.



In vitro measurement of material stimulated leukocyte reactive oxygen species (ROS) production as a predictor of the acute inflammatory reaction in vivo

N Bryan¹, H Ashwin², Y Bayon², S Wohlert², N. Smart³, JA Hunt¹

¹Clinical Engineering (UKCTE), University of Liverpool Institute of Ageing and Chronic Disease, Duncan Building, Daulby Street, Liverpool, UK. ²Covidien – Sofradim Production, 116 Avenue du Formans – BP132, F-01600 Trevoux, France. ³Exeter Health Science Research Unit, Royal Devon and Exeter Hospital, Barrack Road, Exeter, UK.

INTRODUCTION: All implanted materials are interrogated by leukocytes from the moment they enter the patient, these cells are critical in orchestrating inflammation through constructive wound healing phase. A balanced leukocyte response is pivotal to the efficacy of an implanted device, insufficient inflammation results in poor material integration, minimal tissue ingrowth and unsatisfactory mechanical stabilisation of the material in-situ. Contrary, excessive inflammation may induce catastrophic damage to otherwise healthy host tissue and accelerate the degradation profile of the implanted biomaterial. ROS are a key component of the leukocyte arsenal. These molecules act both inside and outside of the cell to perform antimicrobial and signalling roles, critical in successful wound healing, although if left unrestricted may be severely cytotoxic to healing tissue. In this study we utilised an in vitro chemiluminescent reporter system to quantify leukocyte ROS production in conjunction with a subset of biomaterials typically utilised in soft tissue repair. In this study a range of synthetic, allogenic and xenogenic (porcine) were compiled with controlled variation in their manufacturing processes in order to deduce the individual effects of components of the fabrication process on cell response. These materials were then implanted in vivo to validate the in vitro observations as a realtime predictor of *in vivo* acute inflammation.

METHODS: Synthetic materials; polypropylene, polyester-terephthalate polyglycolic acid varying in fibre number and arrangement. Tissue-based implants; human and porcine materials from dermis and small (SIS) submucosa varying intestinal decellularisation and cross linking chemistries. Materials were incubated under continuous luminescent recording with whole blood from healthy human donors of mixed gender (n=4), adjuvant K and pholasin, a chemiluminescent reporter molecule which emits measurable photons in the presence of ROS. In vivo; 6 week old, male wistar rats, 4 implants adjacent to dorso-lumbar musculature. Sacrifices performed at days 2,5,7,14&28. Explants characterised using histology & immunohistochemistry,

n=6/material/time point. Statistics; Waller-Duncan post hoc ranking

RESULTS: Quantification of leukocyte ROS allowed demonstration of the influence of discrete processing steps during material fabrication and preparation on down-stream inflammatory cell activation. From the tissuebased materials analysed SIS was a significantly more pro-inflammatory anatomical pre-origin compared to dermis (p>0.05). SDS was the most ROS stimulating decellularisation reagent. this experiment cross- linking using HDMI induced adverse ROS production vs a non-crosslinked equivalent. The synthetic materials demonstrated that polymer conformation was more determining in cell response than polymer composition. It was possible to show inter-donor variation in material/ROS which also varied as a function of time demonstrated using repeated blood collections from the same donor cohort over 1 month. In vivo these findings were validated histologically by characterising extensive populations of polymorphonuclear cells interrogating the SIS and SDS materials compared to the remainder of the materials in vivo as predicted from the in vitro platform..

DISCUSSION: In vitro chemiluminesence reporting of leukocyte ROS emission was demonstrated as a quantifiable prediction of biomaterial acute inflammatory dynamics. The technique showed discrete material processing variables modified leukocyte ROS response, the magnitude of which varied between individuals. A relevant rat model validated these findings which concluded the technique to be an acurate representation of in vivo consequence. This study has allowed the hypothesis of a personal medical approach to selection of a prosthesis on an invidual patient basis, maximising graft efficacy by screening a small blood sample against a palette of materials pre-surgery allowing the surgeon to select the material with the greatest potential for patient compliance.

ACKNOWLEDGEMENTS: The authors would like to thank Covidien for funding this research



Moving towards a 3D environment for in vitro studies: an alternative to animal studies in asthma research

G.E.Morris¹, A.J. Knox², J.W. Aylott³, A.M. Ghaemmaghami⁴, C.E.Brightling⁵, F.R.A.J. Rose¹

¹ Division of Drug Delivery and Tissue Engineering, School of Pharmacy, ² Division of Respiratory Medicine, School of Clinical Sciences, ³Laboratory of Biophysics and Surface Analysis, School of Pharmacy, ⁴ Immunology and Allergy, Faculty of Medicine and Health Sciences, all University of Nottingham,. ⁵ Institute of Lung Health, University of Leicester

INTRODUCTION: Studies into airway disease have historically been limited to whole animal in vivo or single cell-type in vitro studies. In asthma, mouse immunological studies have lead to our understanding of the Th2 paradigm¹. However, this reveals only a modest proportion of the human condition. Mice do not spontaneously develop asthma nor do their smooth muscle bundles exhibit mast cell infiltration, both important features in the human disease². In vitro primary cells studies provide insight into the underlying signaling mechanisms in airway disease, but tissue culturedplastic restricts cell growth to a 2D monolayer, far removed from in vivo conditions. Reliance on these traditional platforms is decreasing as current protocols (such as collagen gels and decellularised or electrospun matrices) provide a better 3D environment for cells to inhabit in vitro.

This project aims to provide a new diagnostic tool to aid our understanding of asthma and provide a viable alternative to animal usage in investigating airway disease. We are developing a novel immune-competent, self reporting, tissue engineered 3D model of a human airway bronchiole. This construct will be contained within a flow perfusion bioreactor system designed to allow real-time monitoring of the cells within the construct without disturbing the construct itself (see fig 1).

METHODS: The three main structural cells of the airway bronchiole (epithelial, fibroblast, and smooth muscle) will be sourced by bronchoscopy from both healthy and asthmatic patients. Using defined electrospinning parameters, individually tailored scaffolds have been created to support the growth of each cell type. Upon cell-confluency, the individual scaffolds are brought together to form a multilayered construct that is transferred to a flow perfusion bioreactor. By using interchangeable cell layers there is an opportunity to introduce primary immune cells into direct contact with the epithelial or airway smooth muscle layer.

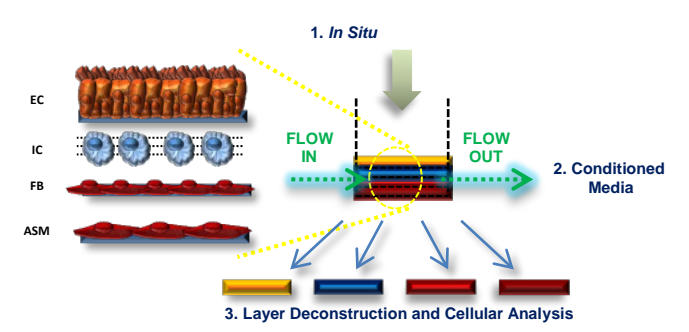


Fig. 1: Schematic of Bioreactor containing Multi-Layered Construct. Epithelial cells (EC), immune cells (IC), fibroblasts (FB), and airway smooth muscle (ASM) will be seeded onto individual scaffolds before assembly into a multi-layered construct that will be monitored insitu using both microscopy (1) and conditioned media released (2). After stimulation, construct can be deconstructed and undergo analysis (3)

RESULTS: Nanofibrous, microfibrous, and patterned polyethylene tetraphthalate (PET) electrospun scaffolds have been optimized for epithelial, fibroblast, and ASM cell growth respectively. Cells have been cultured both on their individual scaffolds and in coculture. Transfer of a complete construct to the flow perfusion bioreactor remains a current goal.

DISCUSSION & CONCLUSIONS: Initial findings suggest electrospun scaffolds provide a suitable environment for the multiple cell types to inhabit and a platform to investigate cell-type interactions. Stimulation with various respiratory agonists suggests interdependency between the various cell types that is not apparent when studying each cell type in isolation.

REFERENCES: ¹ T Mosmann (1986) Two types of murine helper T cell clone. *J Immunol* **136**: 2348-57

² S Holgate (2009) A new look at the pathogenesis of asthma. *Clin Science* **118**:439-50

ACKNOWLEDGMENTS: This work was funded by the National Centre for the Replacement, Refinement and Reduction of Animals in Research.



Biochemical changes caused by decellularization may compromise mechanical integrity of tracheal scaffolds

<u>L Partington</u>^{1,2}, <u>NJ Mordan</u>³, <u>J Knowles</u>^{3,4}, <u>MW Lowdell</u>², <u>M Birchall</u>^{5,6}, <u>I Wall</u>^{1,4}

¹<u>Dept. Biochemical Engineering</u>, UCL, UK. ²Dept. Haematology, UCL-RFH Medical School, UK. ³UCL Eastman Dental Institute, UK. ⁴WCU Dept. Nanobiomedicine, Dankook University, Korea. ⁵<u>UCL Ear Institute</u>, RNTNE Hospital, UK. ⁶Dept. Otolaryngology, UC Davies, USA.

INTRODUCTION: Tissue engineered airways have achieved success in clinic, but there remain concerns about short-term loss of biomechanical properties, necessitating a stent in several clinical cases. Desired outcomes of decellularization include retention of physical properties important for: cell attachment and vascularization (fibronectin and laminin); and biomechanical strength (type II collagen and glycosaminoglycans (GAGs)). Our aim was to assess whether structural changes take place in decellularized trachea that might affect biomechanical properties, leading to risk of stenosis.

METHODS: Tracheas were decellularized (DC) using a chemical-detergent method: 25 cycles of [4% sodium deoxycholate (4h); 2 kU/mL DNase in 1M NaCl (3h); PBS containing 1% antibiotic-antimycotic (17h)]. Native and time-matched non-decellularized PBS stored (NDC) tracheas were used as controls. Tissue sections were prepared for immunohistochemistry (IHC) and structural proteins were additionally quantified. Tensile testing was used to determine circumferential cartilage ring strength.

RESULTS: Decellularization removed most cells, but chondrocytes and DNA remained after 25 cycles (Fig 1). Fibronectin was retained in the lamina propria and laminin at basement membranes, but residual genetic material was bound to ECM fibers (Fig 2).

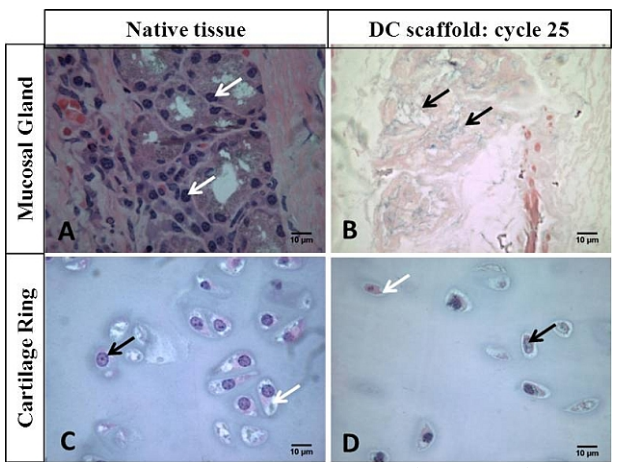


Fig. 1: H&E staining of native and DC trachea



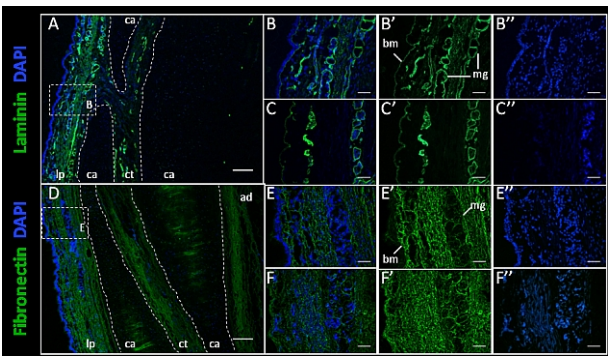


Fig.2: Laminin and fibronectin IHC in native (A,B,D,E) and DC(C,F) tracheas.

A decrease in GAG was observed in both DC and NDC tissue versus native trachea (P<0.01; Fig 3) but alcian blue indicted this was greater in DC tissue ($data\ not\ shown$). Type II collagen was decreased in DC versus NDC trachea (P<0.01; Fig 3), which was confirmed by IHC ($data\ not\ shown$).

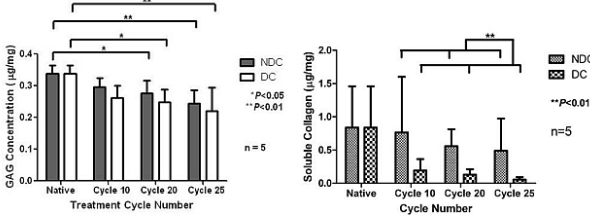


Fig.3: GAG and Collagen content.

Tensile strength declined throughout the process and significant decreased in DC traches compared.

Tensile strength declined throughout the process and significant decreased in DC tracheas compared to NDC tracheas.

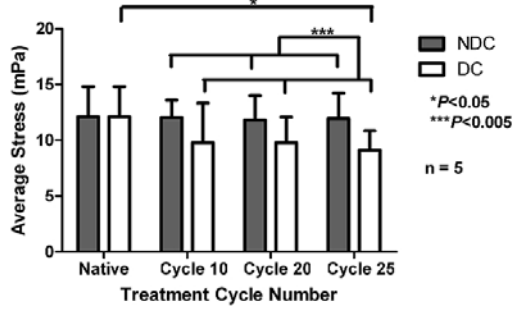


Fig.4: Tensile testing of cartilage ring strength.

DISCUSSION & CONCLUSIONS: Our data demonstrate that GAGs and type II collagen are significantly reduced and could compromise mechanical integrity of scaffolds. Overcoming this will be necessary to optimize clinical benefit.

ACKNOWLEDGEMENTS: EPSRC, UKSCF

Semi-quantitative method for collagen density analysis: use in rapid tissue fabrication

NS Tan, T Alekseeva, RA Brown

University College London, UCL Tissue Repair & Engineering Centre, Institute of Orthopaedics & Musculoskeletal Sciences, Stanmore Campus, London, HA7 4LP.

INTRODUCTION: Collagen is the most abundant protein in the body and plays key roles in providing structural support and in influencing cell behaviour. Plastic compression (PC) has been previously developed to engineer collagen into dense tissue-like constructs ¹. It is important to have a means for quantifying the collagen density at the cell scale in these constructs as it is likely to affect cell behaviour. Here we present a novel semi-quantitative method for analysing collagen density at the micro-scale.

METHODS: 4 variants of PC constructs were fabricated (*A* flat, unpatterned, *B* flat, unpatterned, with a linear density gradient, *C* embossed with round grooves, *D* embossed with rectangular grooves) ^{2, 3}, processed for histology and stained with sirius red (which has a high affinity for collagen fibres) and digital photographs were analysed using ImageJ (v1.45). Images were converted to greyscale and pixel intensities were measured in sequence using "line selections" across regions that were pre-determined to have collagen density changes. These measurements were then plotted against the position of the corresponding selection along the construct (Figure 1).

RESULTS: *A* showed no significant differences in collagen density along their lengths. *B* produced linear measured gradients. *C* showed a single peak with mean increase in density of $21.4\pm4\%$ over baseline. *D* had two peaks $(15.2\pm4\%)$ and $16.9\pm3\%$ located at the internal corners of each groove, all of which were statistically significantly different from the baseline density at p<0.05.

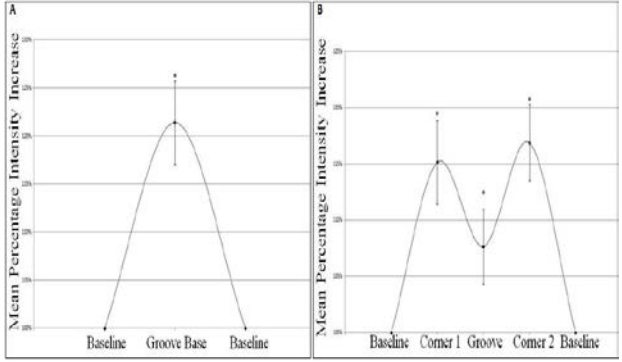


Figure 1 Graphs of the mean percentage increase

in intensity of grooved regions. A: The mean percentage intensity increase plot for round grooves (N=7). B: The mean percentage intensity increase plot for rectangular grooves (N=8). * P<0.05 Groove base compared to the baseline, corners compared to the baseline, and corners compared to the groove base.

DISCUSSION & CONCLUSIONS: Testing this novel method of analysis against an established model of density gradients in PC constructs validated the method. This method was able to semi-quantitatively measure the collagen density differences and allowed us to obtain collagen distribution profiles of constructs at the microscale which likely affects cell behaviour. In developing the method, we have gained insight into the mechanisms and dynamics of the plastic compression process.

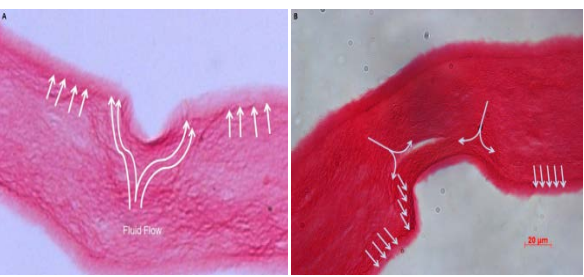


Figure 2 Collagen constructs embossed with round grooves (A) or rectangular grooves (B) stained with sirius red. Arrows indicate predicted direction of fluid flow.

REFERENCES: ¹Brown RA, Wiseman M, Chuo CB, Cheema U, Nazhat SN (2005). Adv Funct Mater **15:** 1762-1770. ² E Hadjipanayi, V Mudera and RA Brown (2009). Cell Motil. Cytoskeleton 66:121-128. ³ Alekseeva T., Hadjipanayi E., Abou Neel EA., Brown RA. 2012. Eur Cell Mater 28-40.

ACKNOWLEDGEMENTS: Funded by TSB-EPSRC (UK).



Decellularised bone gels – novel materials for bone regeneration

LJ White¹, MJ Sawkins ¹, SF Badylak², KM Shakesheff ¹

¹School of Pharmacy, University of Nottingham, UK ²McGowan Institute for Regenerative Medicine, University of Pittsburgh, USA

INTRODUCTION: Treatment of critical sized defects, such as bone tumour resections or non union fractures, remains a difficult and challenging problem. Current treatment options have limited effectiveness: use of autografts is restricted by the availability of bone graft and donor site morbidity whereas difficulties patient vascularisation and remodelling have contributed fracture and necrosis of allografts.[1] Extracellular matrix (ECM) scaffolds derived from decellularized tissues can provide templates for tissue repair and regeneration [2] as recently shown by the successful transplantation of a decellularized human trachea.[3] In this work, a novel ECM material was harvested from bovine bone and was subsequently pepsin digested to form an ECM gel.

METHODS: Bovine femurs, acquired from a specialist butcher, were cleaned, sorted into cancellous segments and immersed in Gentamicin (50 mg/ml, Invitrogen, UK) for 1 hour at 37°C. Segments were then fragmented using a Krups coffee grinder and subjected to in-house developed protocols for demineralisation and decellularization. pepsin digest and A solubilisation procedure was undertaken with the demineralised bone matrix (DBM) and decellularised bone (bECM) to form gels. Spectrophotometry was used to assess the gelation kinetics of DBM and bECM compared to collagen. Pre-gel solutions at 4°C were placed into a prewarmed spectrophotometer at 37°C, and the optical density at 405 nm was measured every 3 minutes until gelation was complete. The proliferation of human osetosarcoma cells on collagen, DBM and bECM gels was also assessed.

RESULTS: Histological evaluation showed that cellular fragments present in demineralised bone (DBM) were removed by the decellularisation process. Spectrophotometric data of gel formation revealed that gelation proceeded at different rates for the three different materials. Cellular proliferation on DBM and bECM gels was equivalent or greater to that observed on collagen gels.

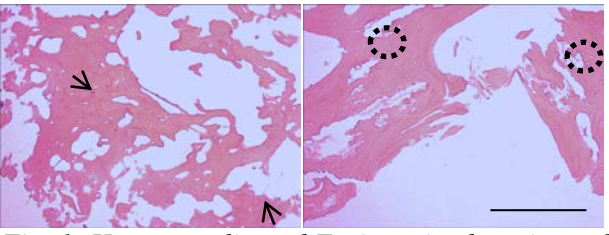


Fig. 1: Haematoxylin and Eosin stained sections of (A) DBM and (B) bECM material. Arrows indicate cell nuclei whilst dotted circles highlight the occurrence of empty pits. Representative images from triplicate histological sections are shown; scale bar: 125 µm.

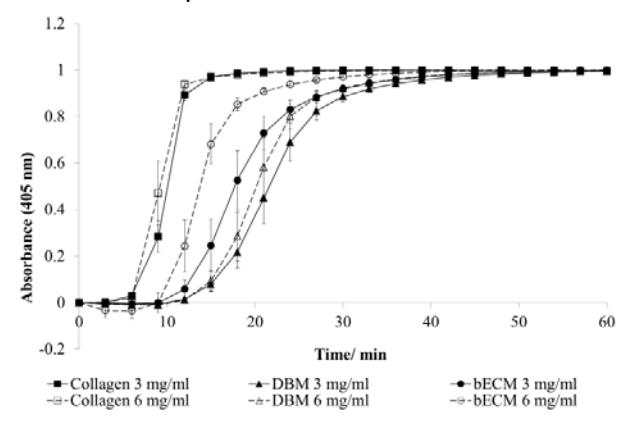


Fig. 2: Normalised absorbances at 405 nm for pregel solutions incubated at 37°C.

DISCUSSION & CONCLUSIONS: Gelation in all cases is expected to occur via collagen fibril formation; however the distinct gelation kinetics may suggest different formation mechanisms. In all cases higher concentration gels formed more quickly. Gels formed from novel bECM material have comparable gelation kinetics to collagen and are an innovative material for bone regeneration.

REFERENCES: ¹ J.D. Boerckel, Y. M. Kolambkar, K.M. Dupont et al (2011) *Biomaterials* **32**: 5241-5251. ² S.F. Badylak, D.O. Freytes, T.W. Gilbert (2009) *Acta Biomater* **5**:1 13. ³ P. Macchiarini, P. Jungebluth, T. Go et al (2008) *The Lancet* **372**:2023-30.

ACKNOWLEDGEMENTS: This work was supported by the Biotechnology and Biological Sciences Research Council (BBSRC), UK through a LoLa grant, Grant No. BB/G010617/1.



A novel dressing coated with self-assembled peptide for wound healing

R S Alazragi¹, R P W Davies¹, S Russell², A Aggeli¹.

¹Centre for Molecular Nanocience, School of Chemistry, University of Leeds. ² Centre for Technical Textiles, School of Design, University of Leeds.

INTRODUCTION: The ideal wound dressing should fulfill fast wound healing with minimal inconvenience to the patient¹. Frequent dressing damage the newly changes may epithelium. Another major problem is the uncontrolled release manner. If the release is fast, entire drug will be released before the infections are arrested and drug overdose toxicity might be occurred. If the release is delayed, the infections may further set in the wound². To overcome these limitations, in this project, cellulose wound dressing will be coated with pH-dependent behavior self-assembled peptide (OORFOWOFEOO). Its gel-fluid transition has been shown to be controlled by pH³. It forms monomeric peptide solutions at low pH and gel at high pH. When the coated sample placed on an open wound, the release of the peptide will be controlled by the pH of the wound.

METHODS: Monomer solution of P₁₁-8 plus fluorescence P₁₁-4 [ratio 1:60] was prepared using distilled water [pH 5.3]. A size of 0.5 x 0.5 cm square cellulose fabric was dipped overnight in the P₁₁-8 monomer solution to allow peptide monomers to deeply penetrate into the cellulose fabric. Then, the pH was increased to pH 10 (by adding NaOH) to trigger peptide self-assembly and to convert the fluid solution to gel. The sample was left in the gel overnight and then removed. Scanning electron microscope, SEM, attenuated total reflectance infrared, ATR-IR, and confocal laser scanning microscopy CLSM were employed to compare between the coated sample and uncoated one.

RESULTS: Cellulose fabric was submersed in a liquid P_{11} -8. The peptide P_{11} -8 self-assembled into a self-supporting gel triggered by the addition of NaOH, see Fig 1. The difference in morphology between the coated sample and the uncoated one is shown in Fig 2a & 2b. The uncoated sample has a smooth surface, while the coated one has a rough surface due to the presence of P_{11} -8 fibrils. *Fig 2D* shows green fluorescence comes from peptide coat which is absent in Fig 2C. Fig 3 shows a characteristic β-sheet IR spectrum (red) in the regions 1600-1700 cm⁻¹ and 3000-3500 cm⁻¹ which indicates that the cellulose sample is coated with

 P_{11} -8, while uncoated sample does not show β-sheet characteristic spectra (green).

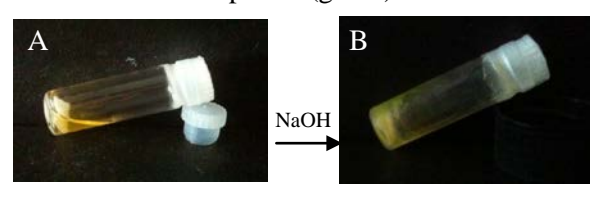


Fig. 1: a piece of cellulose in P_{11} -8 solution. A)at pH 5.3. B) at pH10.

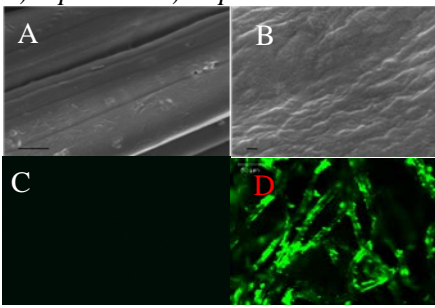


Fig. 2: A) SEM image of uncoated sample (scale $bar=1\mu m$); B) SEM image of P_{11} -8 coated sample (scale bar=100 nm); C) CLSM image of uncoated sample; D) CLSM image of coated.

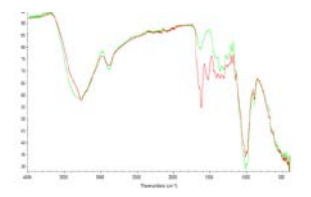


Fig. 3: IR spectrum for coated sample (red) and uncoated sample (green).

DISCUSSION & CONCLUSIONS: The results from all complementary techniques used show that the cellulose fabric is completely coated with P_{11} -8. Future studies will focus on biofunctionalisation of the cellulose sample coated with peptide.

REFERENCES: ¹J. S. Boateng, K. H. Matthews, H. N. E. Stevens and G. M. Eccleston, *Journal of pharmaceutical sciences*, 2008, **97**, 2892-2923. ².W. K. Loke, S. K. Lau, L. L. Yong, E. Khor and C. K. Sum, *Journal of Biomedical Materials Research*, 2000, **53**, 8-17. ³L. M. Carrick, A. Aggeli, N. Boden, J. Fisher, E. Ingham and T. A. Waigh, *Tetrahedron*, 2007, **63**, 7457-7467. **ACKNOWLEDGMENT:** This work is funded by the Saudi Arabian Cultural Bureau.



Galactosylated poly (ethylene glycol) as a scaffold for primary hepatocytes

C Hamilton¹, C J Henderson¹, R V Ulijn², M H Grant¹

¹Bioengineering Unit & ²Department of Pure and Applied Chemistry, <u>University of Strathclyde</u>, Glasgow

INTRODUCTION: Maintaining stable cultures of viable and metabolically active primary hepatocytes is a long standing problem¹. Synthetic biomaterials with tuneable chemical properties may provide a suitable platform for the culture of primary cells. Hepatocytes are capable of binding terminal galactose residues via the hepatocyte asialoglycoprotein receptor (ASGPr); targeting of this receptor may facilitate binding of cells, influence morphology and ultimately improve cellular function².

METHODS: Galactosamine coated poly (ethylene glycol) (PEG-Gal) surfaces were prepared using established methods³. Surfaces were characterised using a variety of techniques including water contact angle goniometry and atomic force microscopy. Primary hepatocytes were prepared as previously described by perfusion of rat liver with collagenase¹. Viability and function was determined using a combination of live/dead fluorescent staining; crystal violet staining and testosterone metabolism.

RESULTS: Water contact angle goniometry (Figure 1) was used to verify the addition of the galactosamine molecule; shown by the decrease in contact angle from sample 3 to 4.

Water Contact Angle

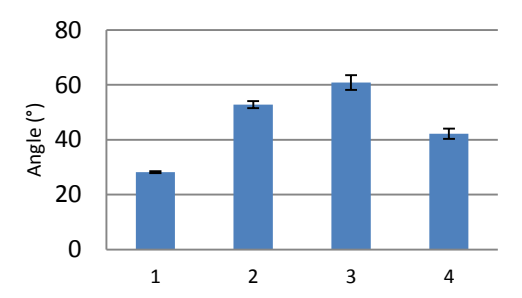


Fig. 1: Water contact angle goniometry; 1 – Clean Glass, 2 - (3-Glycidyloxypropyl)trimethoxysilane, 3 – Poly (ethylene glycol) and 4 – PEG-Gal. Values are presented as mean \pm SEM, n=15.

Live/Dead fluorescent staining (Figure 2) shows that cells cultured on collagen controls samples begin to exhibit changes in morphology after 4 days (which often signifies cell de-differentiation). Galactosamine coated samples however show

signs of cellular aggregation into spheroid-like structures.

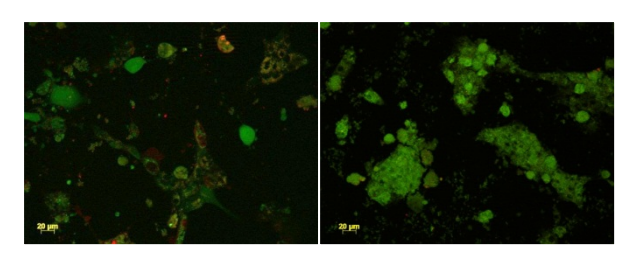


Fig. 2: Live/Dead fluorescent staining (Carboxyfluorescein diacetate and Propidium Iodide) at 4 days of A) collagen controls and B) PEG-Galactosamine.

Testosterone metabolism by cytochrome P450 (Figure 3) shows that galactosamine coated surfaces maintain metabolically active cells for up to 4 days; producing known metabolites in quantities similar to collagen controls.

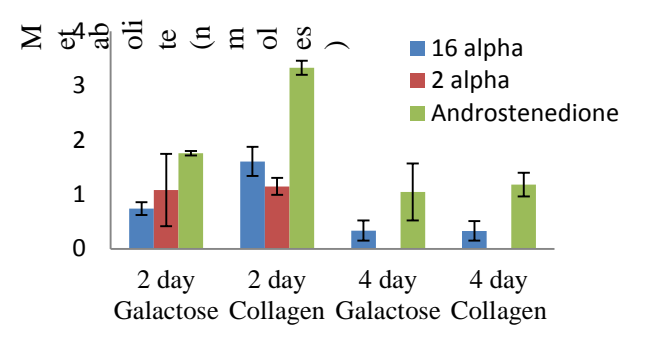


Fig. 3: Metabolism of testosterone by cytochrome P450 at 2 and 4 days on collagen controls and Galactosamine coated surfaces.

DISCUSSION & CONCLUSIONS:

Galactosamine coated surfaces may provide a suitable scaffold for the culture of primary hepatocytes. Cells remain stable up to 4 days in culture, show signs of spheroid formation and remain metabolically active for up to 4 days. Future work will involve subsequent surface modification to include the RGD peptide sequence to enhance cell adhesion and function.

REFERENCES:

¹Katarapoulou M, et al. *Human & Experimental Toxicology* (2003) **22**; 65 -71. ²Cho CS, et al. *Biomaterials* (2006) **27**; 576-585. ³Todd SJ, et al. *Langmuir* (2009) **25**; 7533–7539



Hydraulic and rheological evaluation of a Pneumatic Direct-write Bioprinter

Hongyi Yang, Emily Chruscikowski, Joel Segal, Svetan Ratchev*

Manufacturing Research Division, Faculty of Engineering, University of Nottingham, Nottingham

INTRODUCTION: Bio-printing is a new technology developed in recent years for the fabrication of tissue engineering constructs [1]. The performance of the bio-printing system significantly depends on various factors including the rheological properties of the materials used, the diameter of the printing nozzle, and the working pressure applied [2, 3]. To date the effects of these factors and the optimal combination of these effects in bio-printing applications have received insufficient attention.

METHODS: 3D direct-write bio-printing system was built, and the effects of the above factors in the bio-printing process are investigated. The developed bio-printing system (Fig 1) consists of a pneumatically actuated syringe pump installed on a 3D assembly platform (Klocke Nanotechnik, Germany). A disposable syringe loaded with hydrogel is connected to a pneumatic driving unit (UltimusTM I dispensing workstation, Nordson EFD, USA), which is able to produce a driving pressure in the range of 0-7bar. The syringe with a needle of internal diameter of either 150µm or 250µm is used as the printing nozzle. Hydrogels of required concentration were prepared by mixing Sodium alginate (Sigma, UK) powders with deionised water. The dispensing time is finely controlled. The flow rate and the rheological properties of hydrogels with different nozzle diameters and driving pressures are studied.

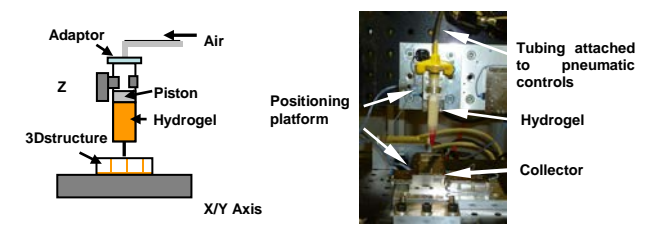


Fig. 1: (a) Schematic of the Pneumatic printing system, (b) Picture of the Pneumatic printing system.

RESULTS: Write speeds for Alginate solutions in a range of pressures through $150\mu m$ and $250\mu m$ nozzles are shown in Figure 2. To investigate the rheological properties of the hydrogel, the shear stress and the shear rate are calculated with the Ostwald-de Wale power law equations. The shear stress and shear rate in response to the different nozzle diameters, driving pressure and flow rate are given in Table 1.

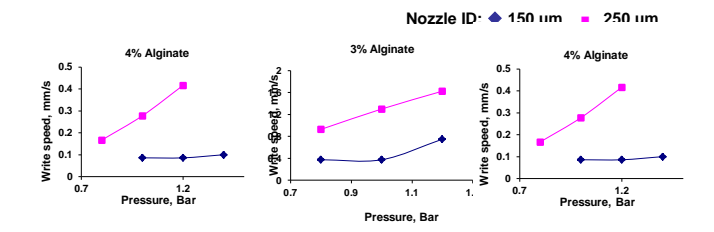


Fig. 2: Write speeds for Alginate Solutions in a range of pressures.

Table 1 Rheological properties of 4% Alginate under different extrusion conditions

Nozzle	Pressure	Flow	Shear	Shear	Viscosity
ID	(bar)	rate	stress	rate	$(Pa \cdot s)$
(mm)		(mm^3/s)	(Pa)	(s^{-1})	
0.15	1.0	0.00151	187.5	4.57	41.02
	1.2	0.00151	225	4.57	49.22
	1.4	0.00177	262.5	5.33	49.22
0.25	0.8	0.00818	250	5.33	46.88
	1.0	0.0136	312.5	8.89	35.15
	1.2	0.0204	375	13.33	28.12

DISCUSSION & CONCLUSIONS: This study investigated the hydrogel flow rate under different nozzle diameters and driving pressures, with shear stress, shear rate and material viscosity as derived indexes to further assist the determination of optimal process parameters in specific bio-printing processes. This for the first time provides a quantitative evaluation of the hydraulic response of the bio-printing system and the resultant material rheological properties in the system, which is essential for improvement of the productivity and the performance of the bio-printing system.

REFERENCES:

¹K. Jakab, C. Norotte, F. Marga, et al (2008) Biofab. 2: 1-14, (2010). ²J. Cheng, F. Lin, H. Liu, et al (2008) J Manuf. Sci. Eng. 130: 021014. ³B. Slaughter, S. Khurshid, O. Fisher, et al (2009) Adv. Mater. 21: 3307-29.

ACKNOWLEDGEMENTS: This project was supported by the Faculty of Engineering Research Placements Scheme of The University of Nottingham.



Rapid Micropatterning of Cell lines and Human Pluripotent Stem Cells on Elastomeric Membranes

Isha Paik¹, David J. Scurr², Bryan Morris³, Graham Hall⁴, Chris Denning⁵, Morgan R. Alexander², Kevin M. Shakesheff¹, **James E. Dixon¹**

Wolfson Centre for Stem Cells, Tissue Engineering, and Modelling (STEM), Centre of Biomolecular Sciences, School of Pharmacy¹, School of Clinical Science⁵. Laboratory of Biophysics and Surface Analysis, School of Pharmacy². Medical Engineering Unit, School of Biomedical Sciences³, University of Nottingham, Nottingham, UK. Tannlin Ltd., Newmoor Industrial Estate, Irvine, Ayrshire, UK⁴

INTRODUCTION: Tissue function during development and in regenerative medicine completely relies on correct cell organization and patterning at micro and macro scales. We describe a rapid method for patterning mammalian cells including human embryonic stemcells (HESCs) and induced pluripotent stem cells (iPSCs) on elastomeric membranes such that micron-scale control of cell position can be achieved over centimeter-length scales.

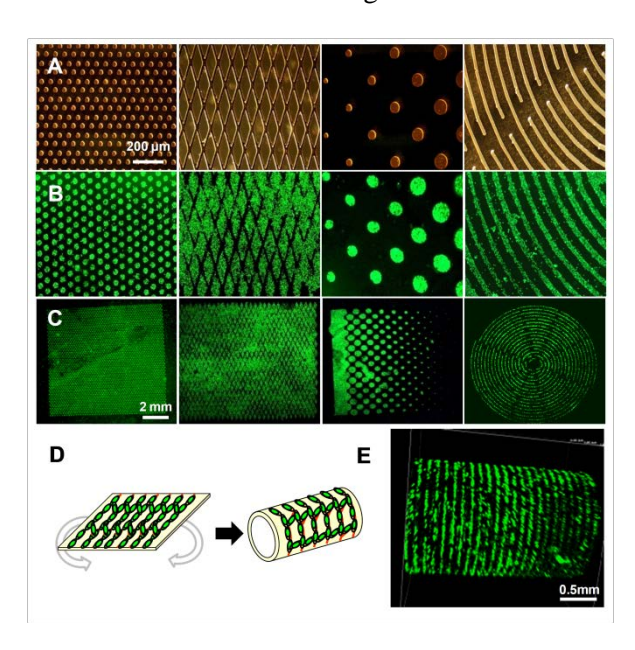


Figure 1..Micrographs showing A) microstencils with Complex pattern features. B) The corresponding eGFP labeled NIH-3T3 cell micropatterns on PDMS membranes. C) The entire cell micropattern.
D) PDMS sheets can be manually rolled to form tubes. E) Tubes remain patterned and cells remain viable.

METHODS: Our method employs surface engineering of hydrophobic polydimethylsiloxane (PDMS) membranes by plasma polymerization of allylamine. Deposition of plasma polymerized allylamine (ppAAm) using our methods may be spatially restricted using a micro-stencil leaving faithful hydrophilic ppAAm patterns. We employed airbrushing to create aerosols which deposit extracellular matrix

(ECM) proteins (such as fibronectin and MatrigelTM) onto the same ppAAm-rich regions.

RESULTS: Cell patterns were created with a variety of well characterized cell lines (e.g. NIH-3T3, C2C12, HL1, BJ6, HESC line HUES7, and HiPSC line IPS2). Individual and multiple cell line patterning was also achieved. Patterning remains faithful for several days and cells are viable and proliferate. To demonstrate the utility of our technique we have patterned cells in a variety of configurations (Figure 1).

DISCUSSION & CONCLUSIONS:

Using plasma deposition this method can convert a hydrophobic surface (such as elastic PDMS) by changing surface chemistry and aid the uniform adherence of specific sprayed ECM proteins to control cell attachment and spreading. Importantly we demonstrate the patterning of human pluripotent stem cells requiring a specific culture surface coating and that micropatterned PDMS sheets can be used to create three dimensional structures such as tubes.

These micropatterns remain faithful in the long term and can be complex as well as discontinuous, unlike those achieved by some lithography or printing techniques. Our method may be used to pattern other factors such as recombinant proteins, synthetic polymers, or peptides.

We believe this methodology should be utilized in future biomedical approaches and applications such as stem cell biology, cell-based biosensors, microarrays, drug delivery, and tissue engineering strategies for regenerative medicine.

REFERENCES: I. Paik, D.J. Scurr, B. Morris, G. Hall, C. Denning, M.R. Alexander, K.M. Shakesheff, J.E. Dixon. *BioTech. BioEng. In press.*

ACKNOWLEDGEMENTS: This work was funded by the BBSRC, ERC and Regentec.



Fabrication and degradation of fluorescently tagged 3D scaffolds

I Wimpenny, Y Yang, A J El Haj

ISTM, Keele Univisity, Stoke-on-Trent, UK.

INTRODUCTION: It is important to establish non-invasive tools to monitor both the structure and degradation of tissue engineering scaffolds. This can be achieved through tagging methods for biodegradable materials. Here we are developing a toolkit which will allow degradation of a 3D scaffold to be tracked using a model *in vitro* system and in the future, this can be correlated to *in vivo* observations, using similar fluorescently tagged materials.

METHODS:

Fabrication: 1% Chitosan (76% degree of deacetylation) 1% acetic acid/ethanol. The solution was cast into square molds and dried. The films were neutralised in ethanol/ 0.1M NaHCO₃ (60%/40%). Approximately 1.5cm² sections were cut from the film. The films were then tagged with isothiocyanate-based fluorescent markers. Amine groups were the target for covalent conjugation of isothiocyanate groups fluorescein of rhodamine (FITC and TRITC, respectively). The molar ratio of dye:amine groups for tagging was 1:500. Briefly, the mass of dye required was dissolved in DMSO, then mixed with 0.1M NaCO₃. The solution was then applied to the film, sealed in a container, protected from light and agitated for 12h. After this time, the solution was removed and the tagged films were rinsed in water. Samples were then immersed in 70% industrial methylated spirits to remove any un-bound FITC/TRITC. The washing process was repeated until no further release of fluorescence was detected. Tagged films were then dissolved in 1% acetic acid. Once dissolved, the solution was placed in a 2.5 mm Ø mold and frozen at -80°C. The sample was then placed in a freeze drier overnight. The intensity of fluorescence prior to contact with films was recorded using a synergy II plate reader at 485/520 ex/em for FITC and 528/590 ex/em for TRITC. The fluorescence was monitored prior post tagging and after subsequent washes. The scaffolds were observed by micro computed tomography (µCT) and confocal laser scanning microscopy (CLSM) to identify 3D characteristics of the material.

RESULTS: It was possible to fluorescently conjugate fluorescent markers to the amine groups of films. Subsequent washing revealed that un-

bound fluorescence could be removed rapidly (Figure 1).

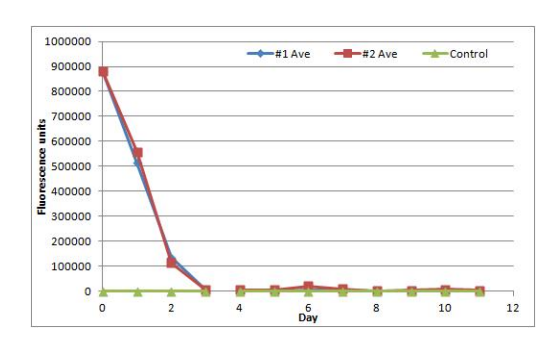


Fig. 1: Demonstration of fluorescence intensity prior to and after tagging of chitosan (0 and 1 day) and removal of unbound fluorescence.

Scaffolds could then be freeze dried and analysed by μCT to indicate the overall homogeneity and porosity of the scaffold. CLSM was also used to investigate the size and structure of the pores of the fluorescently tagged scaffold (Figure 2A & B, respectively).

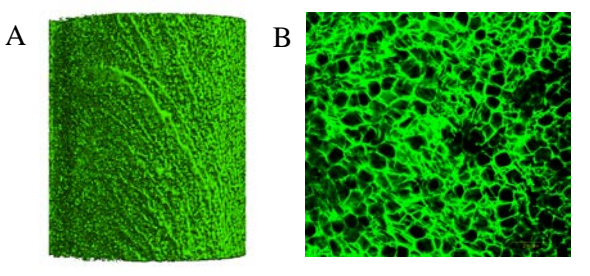


Fig. 2: μ CT rendering of a 3D, fluorescently tagged scaffold (A) and corresponding cross-sectional image obtained by CLSM (B).

DISCUSSION & CONCLUSIONS: It was possible to use chitosan as a model material to develop the potential toolkit for fluorescently tagged 3D scaffolds. Fluorescent materials can be monitored to correlate scaffold degradation and extracellular matrix metabolism over time.

REFERENCES:

Yang Y, Ahearne M, Wimpenny I et al (2010). Investigation of a tissue engineered tendon model by PS-OCT. *SPIE* 75660A-65

ACKNOWLEDGEMENTS: BioDesign EUFP7-NMP.20102.3-1; Grant: 262948.



Endothelial cell growth on novel biocompatible polymeric coatings, for potential use as cardiovascular stent coatings

C M Nickson¹, S Dixon², R L Williams³

¹ CI KTN, The Heath, Runcorn, Cheshire. ² Biomer Technology Ltd., Tudor Road, Manor Park, Runcorn, Cheshire. ³ Dept of Eye & Vision Science, Institute of Ageing & Chronic Disease, University of Liverpool.

INTRODUCTION: Biomer Technology Ltd (BTL) has developed a range of novel polymers that can be used to coat stents. The coating technology is based upon the ability of certain chemical groups to invoke positive, negative or neutral interactions at the biological interface. Discrete modification to the composition of these chemical groups is used to optimise the surface to enhance endothelial cell growth and inhibit in-stent restenosis.

The objective of this work is to assess the qualitative and quantitative performance, in terms of endothelial cell growth, of a range of novel polymeric biomaterials (provided by BTL) for potential use as stent coatings.

METHODS: Three BTL coatings were tested, BTL010008, BTL01015 and BTL01002, selected to highlight the range of polymers available. The compositional balance of the polymers under investigation is illustrated in the table below:

Property	Trend			
Charge	$BTL02 \Rightarrow BTL15 \Leftrightarrow BTL08$			
Charge density	$BTL02 \Rightarrow BTL08 \Rightarrow BTL15$			
Hydrophilicity	$BTL02 \Rightarrow BTL15 \Rightarrow BTL08$			
Mwt	$BTL02 \Rightarrow BTL08 \Leftrightarrow BTL15$			

Samples were supplied as 50% or 100% coated 13mm glass discs for qualitative and quantitative analysis respectively. *Two tests* in vitro were carried out on all the materials:

- 1. Direct Contact 5x10⁴ human aortic endothelial cells (HAECs), Promocell, were cultured directly onto polymer surfaces and incubated under standard conditions for 96h. The cells were fixed with 4% glutaraldehyde and stained with 0.04% methylene blue. Stained samples were imaged using an Axioplan II microscope (Carl Zeiss Ltd) to assess the growth of the cells on the polymer surface.
- Quantification 5x10⁴ HAECs were cultured directly onto the polymer surfaces and incubated under standard conditions for 24, 48, 72 and 96 hours. At each time point the cells were trypsinised and counted using a haemocytometer.

RESULTS: Figure 1 shows that over a 96h period endothelial cell growth on BTL01015 was greater than on glass control (BTL15 has 1.57x10⁵ cells and glass has 1.32 x10⁵ at 96h). The extent of cell coverage can be seen in Figure 2. Conversely cell growth on BTL01002 remains unchanged throughout 96h, being significantly less than that on the glass, highlighting the changes in cellular response that can be achieved through modification to the chemistry of the polymers. Interestingly results with vascular smooth muscle cells (not shown) mirrors the behavior of endothelial cells on BTL01002 but for all the polymers.

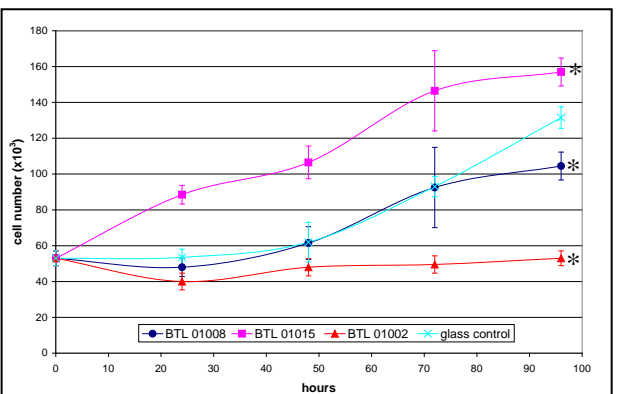


Figure 1: Growth curve of HAECs on BTL polymers and glass control. *Statistical significance $(P \le 0.05)$ vs. glass control

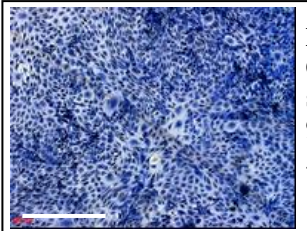


Figure 2: Cells growing on the surface of BTL01015 at 96h. Scale bar represents 500µm.

DISUSSION & CONCLUSIONS: Polymeric biomaterials can be modified to influence endothelial cell growth and achieve confluence. As a stent coating this could aid the formation of a natural endothelial lining within the artery reducing the risk of thrombosis and restenosis.

ACKNOWLEDGEMENTS: The authors would like to acknowledge Biomer Technology Ltd. and EPSRC for supporting this work.



Investigation of anti-inflammatory drug delivery from polymeric scaffolds using an *in vitro* bone inflammation model

L. E. Sidney^{1,2}, A. Abed², T. R. J. Heathman², C.V. Rahman¹, L. D. K. Buttery¹

¹Drug Delivery and Tissue Engineering, Department of Pharmacy, University of Nottingham, UK.

INTRODUCTION: Inflammation in bone diseases such as rheumatoid arthritis and nonunion fractures is usually controlled by systemic anti-inflammatory drug treatment that can produce major side-effects over time. Site-specific, local delivery of these drugs will allow a more efficacious dose to be delivered locally, while minimising systemic toxicity. Development of a basic in vitro model of osteochondral inflammation allows simple initial screening and monitoring of drug release from polymeric scaffolds. The proinflammatory cytokines interleukin-1β (IL-1β), tumour necrosis factor-α (TNF-α) and interferon-ν (IFN-y), can help create this model due to their association with the innate inflammatory response during tissue healing and control of bone tissue remodelling.1

METHODS: Novel sintered polymer scaffolds, prepared using a previously described² temperature sensitive poly(DL-lactic acid-co-glycolic acid)/poly(ethylene glycol) (PLGA/PEG) particles, were loaded with the anti-inflammatory drug diclofenac sodium (DS). Release of DS into phenol-red free αMEM was monitored by UV spectrophotometry at a wavelength of 276 nm.

A simple *in vitro* model of bone inflammation was created using primary mouse calvarial cells (mPCs) and the addition of proinflammatory cytokines IL-1 β (0.25 ng/mL), TNF- α (2.5 ng/mL) and IFN- γ (25 ng/mL) to the culture media. Monitoring of the effect of DS on this model was performed by live/dead staining alongside MTS viability, nitrite release and PGE₂ production.

RESULTS: Release of DS from the PLGA/PEG scaffolds was successful at different concentrations, up to 1000 μ g/scaffold (fig.1). All concentrations showed a similar release profile with a high burst within the first 24 hours with release slowing to around 1% per day from day 4. The effect of DS on the cell viability of the bone inflammation model is shown in figure 2A and B. Live/dead staining shows the presence of DS inhibits the drop in viability caused by presence of IL-1β, TNF-α and IFN-γ.

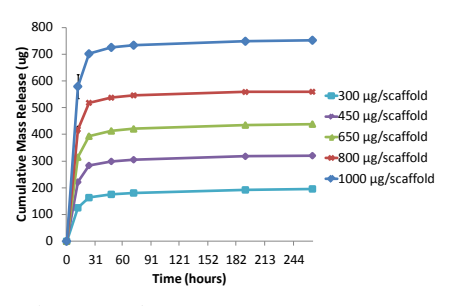


Fig. 1: Release of different concentrations of DS from PLGA/PEG scaffolds.

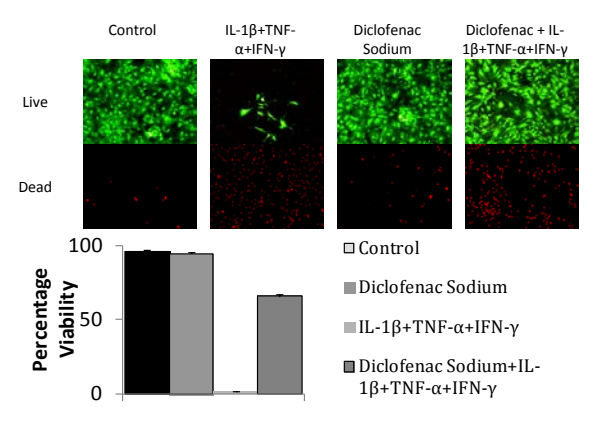


Fig. 2:Live/dead staining (above) and percentage viability analysis (below) showing effect of DS on proinflammatory cytokine stimulated mPCs.

DISCUSSION & **CONCLUSIONS:** The PLGA/PEG scaffolds have previously described as excellent candidates for bone repair due to mechanical properties and porous structure.⁴ The release of anti-inflammatory agents will enhance the properties of these scaffolds by mediating the inflammatory response caused by disease state or implantation of the scaffold. Diclofenac sodium has been used as a model anti-inflammatory drug that but this system could be adapted for many anti-inflammatory drugs. The inflammatory model allows testing of the efficacy of the drugs being released.

REFERENCES: ¹T.Skerry, (1994) *Eur. J. Clin. Nutr.* **48**, S190-S198. ²Hamilton *et al.*, (2010) *J. Pharm. Pharmacol.*, **62**, 1498-1499.

ACKNOWLEDGEMENTS: The authors would like to acknowledge EPSRC Doctoral Training Centre in Regenerative Medicine for funding.



²Doctoral Training Centre in Regenerative Medicine, Loughborough University, Keele University, University of Nottingham, UK.

Bioplotting of novel scaffold materials and complex constructs for osteochondral tissue engineering

MJ Sawkins^{1,2}, BN Brown², LJ Bonassar², FRAJ Rose¹ & KM Shakesheff¹

¹ Tissue Engineering Group, School of Pharmacy, University of Nottingham, UK
² Department of Biomedical Engineering, Sibley School of Mechanical & Aerospace Engineering, Cornell University, USA

INTRODUCTION: Scaffolds for tissue engineering are typically spatially homogenous in their properties, and uniformly seeded with cells. Increasingly it is believed that this approach may not be sufficiently complex for the repair of large defects encompassing multiple cell/tissue types.

Bioplotting is a rapid prototyping technology which can be used to fabricate spatially heterogeneous constructs by the extrusion of materials at ambient conditions. This allows live cells and labile therapeutic proteins to be processed with minimal loss of viability and functionality.

In this work the Fab@Home system¹ is utilised to deposit a thermoresponsive microparticulate polymer which can be sintered to form constructs suitable for bone repair². The production of multimaterial constructs incorporating cell-laden hydrogels is also considered.

METHODS: Thermoresponsive microparticles are produced via melt blending of poly(lactic-coglycolic acid) (PLGA) with poly(ethylene glycol) (PEG) and cryomilling. PLGA microspheres are produced via a W/O/W double emulsion technique.

Bioplotted constructs are produced from PLGA-PEG microparticles with or without PLGA microspheres and calcium-crosslinked alginate with or without cells. All constructs are sintered for 24 hours after production.

Sintered constructs are analysed via compression testing and scanning electron microscopy (SEM). Cell viability is assessed using live/dead (calcein AM/ethidium homodimer-1) staining.

RESULTS:

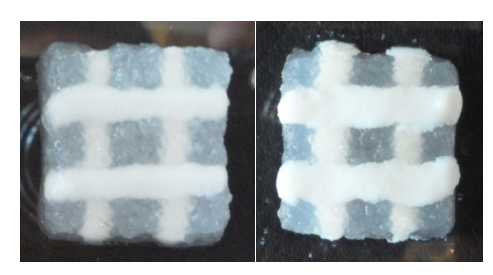


Fig. 1: Pre-/post-sinter (left/right) images of 15 x 15 mm scaffolds composed of PLGA-PEG microparticles and alginate hydrogel.



Compression testing shows a mean yield stress of 30 kPa for sintered PLGA-PEG constructs.

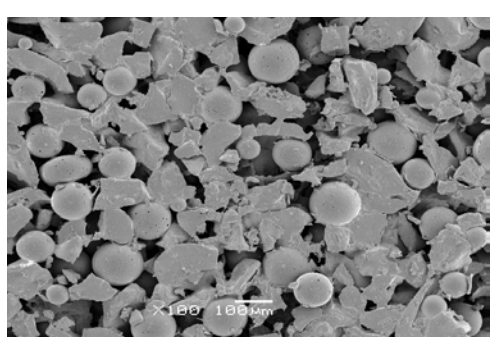


Fig. 2: Scanning electron micrograph showing the formation of adhesion bridges in a sintered PLGA-PEG microparticulate construct incorporating PLGA microspheres.

Live/dead staining of alginate-encapsulated cells indicates high levels of post-plotting viability – 78 \pm 9% for MC3T3-E1 murine pre-osteoblasts and 80 \pm 2% for bovine articular chondrocytes.

DISCUSSION & CONCLUSIONS: The Fab@Home system can be used to produce sintered constructs for tissue engineering from thermoresponsive PLGA-PEG microparticles. Further optimisation of this process is required to achieve optimal mechanical properties for bone repair whilst maintaining adequate flowability for bioplotting. Dual material constructs can be produced incorporating a cell-laden hydrogel phase which shows high post-print cell viability.

Preliminary results show simultaneous patterning of materials, cell populations and microsphere-encapsulated proteins during construct fabrication. Further work is required to optimise this complex patterning and ensure functionality and long-term retention of cell and protein patterns.

REFERENCES: ¹ E. Malone and H. Lipson (2007) *Rapid Prototyping J* **13**:245-55. ² L. Hamilton et al (2010) *J Pharm Pharmacol* **62**:1498-9.

ACKNOWLEDGEMENTS: The authors wish to thank Jeff Lipton and Carol Bayles for training and advice, and the ERC, EPSRC and Cornell University for funding.

Osteogenic differentiation of primary human Mesenchymal Stem Cells enhanced by capacitive electrical stimulation

R Balint¹, NJ Cassidy ², SH Cartmell¹

¹ Materials Science Centre, University of Manchester, Grosvenor Street, Manchester, M13 9PL, UK
² School of Physical and Geographical Sciences, William Smith Building, Keele University,
Staffordshire, ST5 5BG, UK

INTRODUCTION: Electric and electromagnetic stimulation is used to promote bone growth in several orthopaedic, dental and maxillofacial therapies, such as treating normal and non-union fractures, osteoporosis, osteoarthrosis, lumbar spine fusions and promoting the integration of implanted biomaterials. Furthermore, in vitro and in vivo experiments have demonstrated that this modality can enhance proliferation differentiation of various musculoskeletal cell lines. In our work we aim to develop Electrical Stimulation into an effective modality for Tissue Engineering, more specifically for the creation of bone implants.

METHODS: A capacitive bioreactor, designed and built by our group, was used to deliver electrical stimuli, to primary Mesenchymal Stem Cells cultures in osteogenic medium, with 15 V electrode potential. 3D computer models were created in the commercial software MATLAB and in COMSOL Multiphysics, to allow the calculation of the of the electrical field strength inside the bioreactor. Stimulation was delivered with 500 Hz frequency, and 1 and 1000 microsecond pulse width for 3h per day. Cell numbers were assessed with Picogreen assay, metabolism and viability with Alamar Blue, differentiation by Alkaline Phosphatase assay and the qRT-PCR of the bone related markers BMP-2 and ALPL at Day 4 (3 sessions of stimulation) and Day 7 (6 sessions).

RESULTS: According to our simulations the 15 V electrode potential produces an electrical field strength of approx. 0.2 V/mm. In 1 microsec pulse stimulated samples cell numbers were significantly lowered both at Day 4 (p<0.005) and Day 7 (p<0.005), but this coincided with a significant enhancement of cellular metabolism (p<0.005 and p<0.05) and alkaline phosphatase activity (p<0.005 and p<0.005). On the other hand, none of the assays showed a significant change in the behaviour of the cells with the 1000 microsec pulses. At Day 7 expression of the gene ALPL was increased 3 fold (p=0.04) with to 1 microsec pulse stimulation. The presence of BMP-2 was not detected in controls, but was detected in 1 microsec treated samples.

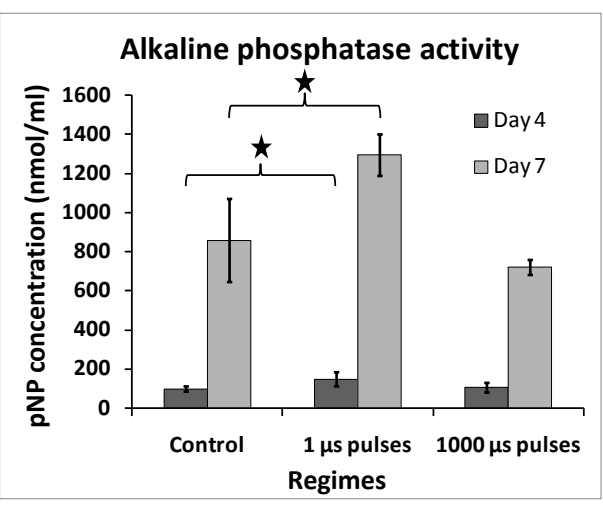


Fig. 1: Alkaline phosphatase activity of hMSCs after 3 and 6 sessions of electrical stimulation. 1 microsecond pulses significantly up-regulated alkaline phosphatase concentration as early as Day 4.

DISCUSSION & CONCLUSIONS: Capacitive stimulation with 1 microsecond pulses hastens the differentiation of hMSCs. osteogenic enhanced metabolic activity might allow the faster production of ECM proteins and quicker mineralisation. The up-regulation of bone ECM genes connected to this, can help in ensuring the commitment of the adult stem cells to the bone lineages. The fact that this happens as early as after just 3 sessions of stimulation shows the great potential that this modality has for bone Tissue Engineering. Capacitive electrical stimulation could allow the generation of better quality implants under shorter time spans. As the mechanisms behind these effects are still unknown. further investigations are necessary.

ACKNOWLEDGEMENTS: We would like to thank the EPSRC "Bridging the gap" and DTA awards, the BBSRC BB/F013892/1 grant, and the Orthopaedic Research UK Foundation for the financial support.



Expression of type VI collagen in bone and osteosarcoma cell lines indicates a role in the development of bone

PJM Wilson¹, JP Dillon¹, BW Wlodarski¹, WD Fraser², SC Wagstaff³, JA Gallagher¹

¹ Dept of Musculoskeletal Biology, Institute of Ageing and Chronic Disease, University of Liverpool, England. ² Faculty of Medicine and Health Sciences, University of East Anglia, England. ³ Bioinformatics and Systems Biology, Liverpool School of Tropical Medicine, England.

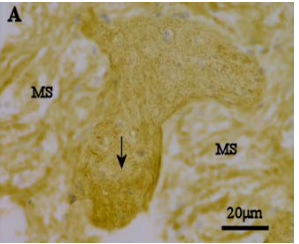
INTRODUCTION: In order to develop new biomarkers of skeletal development and turnover. we raised a panel of monoclonal antibodies against human bone cells. Antibody secreting clones were screened by immunochemistry initially targets were identified interesting immunoscreening of a cDNA expression library constructed in house. One antibody was found to recognise the alpha 3 chain of collagen VI, which is a microfibrillar forming protein that has ubiquitous distribution throughout connective tissue. (1) Collagen VI is expressed at a low level in articular cartilage but is switched on at an early stage of degeneration. Its expression pattern in bone has not been previously reported.

METHODS: Immunohistochemistry Frozen human bone at various stages of maturity were cut into 10μm thick sections, mounted onto slides and fixed in acetone. Sections were incubated with hybridoma supernatant, washed in PBS, incubated with secondary anti-mouse HRP conjugated antibody and developed using the FASTDAB substrate. Sections were counterstained with haematoxylin and dehydrated before being mounted in DPX.

Western blot Equal concentrations of protein extracts from human osteosarcoma cell lines, MG-63, TE85 and SaOS-2, were loaded on an SDS-PAGE gel. Samples prepared with reducing gel loading buffer and heat denature at 95°C for 5mins before separation on a 10% acrylamide gel. Transfer of protein to nitrocellulose membrane was achieved using the BioRad Mini Trans Blot System. The membrane was removed and used for immunodetection of antigen through ECL.

Quantitative-PCR of gene expression RNA was extracted from the osteosarcoma cell lines and reverse transcribed to cDNA from confluent cell cultures. To compare the rates of the genes relative expression, qPCR was performed and monitored using Bio-Rad iCycler iQ following the protocol recommended by the manufacturer. cDNA samples were analyzed for collagen VI $\alpha 3$, collagen 1 $\alpha 2$, alkaline phosphatase and the reference gene, β -actin. The relative rate expression for each gene was calculated using β -actin as a normalizer.

RESULTS: Collagen VI expression was observed in osteoblasts but not bone lining cells, traces around the pericellular area of osteocytes, abundant expression throughout immature but not mature osteoid and its prevalence in the marrow stroma of both immature and mature bone (Fig. 1). The absence in mature bone was not a result of masking by the mineral component of bone as the pattern of staining remained the same even after decalcification. COL6A3 had the expression in MG63, and the lowest in SaOS-2. Whereas for COL1A2 and ALP, the highest expression in SaOS-2, and the lowest in MG-63.



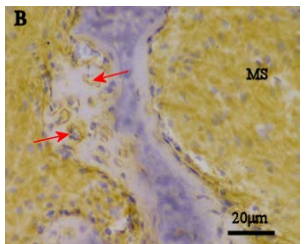


Fig. 1: Type VI collagen in osteoclastoma tissue – A)Strong expression is observed by brown staining in the immature osteoid (black arrow). B)From the same section of tissue in A, but of a different site, antigen is localised to the pericellular area of osteocytes (red arrows) and marrow stroma (MS).

DISCUSSION & **CONCLUSIONS**: The osteosarcoma cell lines represent osteoblast cells at different stages of maturation. The degree of their differentiation is associated with progressive changes in the expression of collagen VI, with the least well differentiated being positive and the most well differentiated being virtually negative for collagen VI expression.

Collagen VI through its array of cell and matrix molecule binding sites has a role in stabilising the extracellular matrix during development by providing the initial scaffolding upon which mineralisation takes place but is consequently removed as mineralisation proceeds.

REFERENCES: ¹ von der Mark H, Aumailley M, Wick G, Fleischmajer R, Timpl R (1984) Immunochemistry, genuine size and tissue localization of collagen VI. *Eur J Biochem* **142:**493-502.



Single and multiple surface chemical modifications applied to a 3D PLGA scaffold for mesenchymal stem cell differentiation *in vitro*.

SA Fawcett¹, L Hammilton² JM Curran¹, NP Rhodes¹,MR Alexander² K Shakesheff² and JA Hunt¹

Institue of Aging and Chronic disease, University of Liverpool. ² School of Pharmacy, Nottingham
University

INTRODUCTION: There is evidence in previous work [1][2][3][4] to support the hypothesis that chemical modifications of polymer and glass surfaces can directly influence mesenchymal stem cell fate. Here we apply similar chemistries by plasma polymerization to an injectable 3D PLGA system with potential for clinical application. The hypothesis of this study was that selective chemical modification applied by a novel plasma polymer deposition technique to a particulate based polymer system can discretely influence stem cell fate, in single and mixed modification cultures as there is evidence to suggest that -NH₂ can give an osteogenic response, -OH to a chondrogenic response and -CH₃ can maintain stem cell phenotype on a 2D surfaces.[1, 2]

METHODS: Closed chamber plasma [3][4] was used to deposit plasma polymerised allyl amine (ppAAm), allyl alcohol (ppAAl), hexane (ppHex) and acrylic acid (ppAAc) onto the surface 100-200µm diameter PLGA spheres. Spheres were mixed with PLGA-PEG adhesive in 1:3 ratio. The single modification powders were compacted into a modified 1ml syringe to a volume of 0.07mls. The dual modification scaffolds comprised of the particles used in volumes of 0.035mls of -OH and 0.035mls of -NH₂. The triple modification used 0.023mls volumes of -OH, -CH₃ and -NH₂ with 100ul of basal mesenchymal stem cell media (Lonza, UK), seeded with $5x10^5$ mesenchymal stem cells (Lonza UK) and scaffolds were allowed to cure at 37°C for 30 minutes. Scaffolds were ejected from the syringes, then cultured in basal mesenchymal stem cell media on a rocker plate at a pre-optimised speed for 7, 14 and 28 days, with 1ml of media added to each well every 4 days. A Histological study was conducted on the samples, using a range of staining procedures to identify mesenchymal stem cell differentiation. Sections were stained at 200µm intervals taken from the whole scaffold.

RESULTS: The histological examination of the allyl amine modified scaffolds showed positive Van Geison after 7 days, Von Kossa and Alizian red staining throughout the scaffold after 28 days. The histological examination of the ppAAl modified scaffold showed positive Van Geison, and Alcian blue staining throughout the scaffold at

14 days. The ppHex and ppAAc modified scaffolds did not differ from the untreated control, which showed no evidence of mesenchymal stem cell differentiation. The combined triple modification scaffold after 28 days in culture showed positive Alizian red staining located to one end of the scaffold and Alcian blue staining at the opposite end of the scaffold with positive Van Geison staining seen throughout the scaffolds.

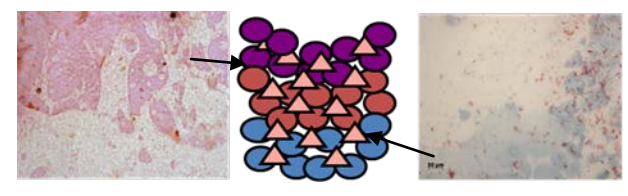


Fig. 1.Purple spheres indicate allyl amine treated spheres. Blue Spheres indicate allyl alcohol treated spheres and red spheres indicate hexane treated spheres, pink triangles indicate the PLGA adhesive. Left image shows positive Alizian red staining on top portion of section. Right image indicates positive Alcian blue in lower portion of section.

DISCUSSION & CONCLUSIONS: The results from the single modification scaffolds indicated that an osteogenic response in the form of mineralised matrix production was seen in the ppAAm scaffold at 28 days. The Alcian blue stain indicated GAG was present on the ppAAl treated scaffold at 14 days highlighting a chondrogenic response. The dual modification showed that the cells were capable of diversifying into separated populations by different surface chemistries on the scaffold, and the ppHex treated portion of the scaffold deters stem cell differentiation. technique could have implications osteochondral tissue engineering, and implies that modifications surface differentiation in the presence of conflicting cell signalling allowing separate populations form.[4]

REFERENCES: ¹ J.M.Curran et al (2005) Biomaterials **26:** 7057-7067 ² J.M.Curran et al (2006) Biomaterials 27 4783-4793, ³ E, Bible (2009) Biomaterials **30**:16 2985-94. ⁴ D.Bennoit et al (2008) Nature Materials. 7:10 816-823

ACKNOWLEDGEMENTS: With thanks to the EPSRC for funding the project.



Osteogenic nano- and multi-structured titania surfaces for orthopaedics

<u>LE</u> McNamara¹, T Sjöström⁴, K Seunarine¹, K Burgess², ROC Oreffo⁵, RM Dominic Meek³, B Su⁴, MJ Dalby¹

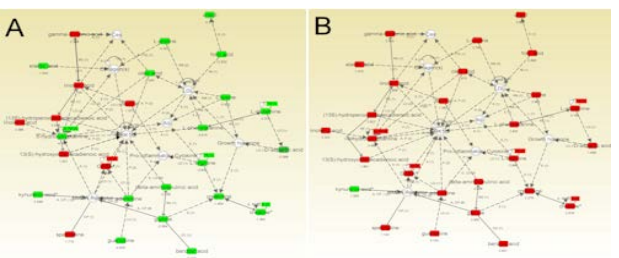
¹ Centre for Cell Engineering, ²ScotMet, University of Glasgow, ³Southern General Hospital, Glasgow, UK., ⁴School of Oral and Dental Science, University of Bristol, Bristol, UK. ⁵Bone and Joint Research Group, University of Southampton, Southampton, UK.

INTRODUCTION: Functionalisation of clinically relevant load-bearing materials (such as titanium, Ti) with defined osteogenic topographies would potential to improve have great osseointegration of orthopaedic implants. have previously demonstrated that 15 nm high Ti pillar-like features were osteogenic [1]. In this study, 8 nm high and 15 nm high Ti pillars and combined micro-nano Ti surfaces patterned with both micron-scale pits and 15 nm high pillars were examined for their osteoinductive capacity, and for evidence of direct cellular interactions with these extremely small features.

METHODS: Nanosurfaces were prepared by a block copolymer mask approach, and micron-scale pits were added by micromachining. Human mesenchymal stem cells (MSCs) were cultured for 3d on the nanosurfaces or planar control Ti substrates, for SEM and 3D SEM, and for 21d on the nano- and micro-nano combined surfaces for assessment of bone marker production by immunostaining. Metabolomic analysis was performed to identify differentially abundant metabolites, and data was analysed using Ingenuity Pathways Analysis (IPA).

RESULTS: The nanosurfaces, particularly the 15 nm pillars, were osteogenic, with increased production of the bone markers osteocalcin and osteopontin compared to the planar control. The metabolic profile of MSCs cultured on the 15 nm high pillars was markedly distinct from those on tissue culture plastic and the planar control Ti (Fig 1A, B). The combined micro-nano surface was also osteoinductive, as assessed by bone marker production. Most interestingly, cells could directly sense the 8 nm features using nanoscale membrane projections we have termed "nanopodia" (Fig 1C, inset), which were not present on unpatterned areas of the surface (Fig 1C, inset). On the 15 nm high pillars, there was also additional filopodial interaction.

DISCUSSION & CONCLUSIONS: MSCs were capable of direct interactions with nanofeatures as small as 8 nm high (previously the smallest features shown to engender direct cell interactions



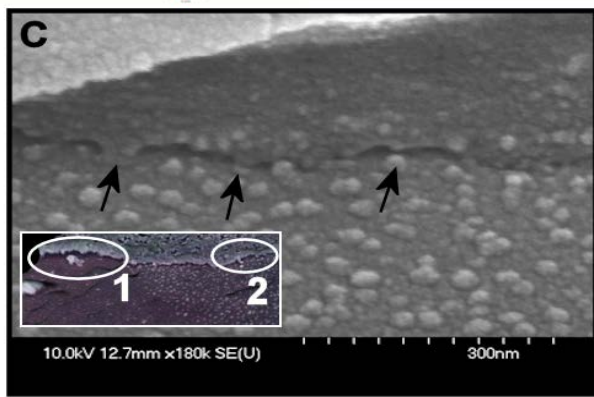


Fig.1: IPA network of metabolites up-regulated (red) and down-regulated (green) in MSCs on tissue culture plastic (A) and 15 nm high pillar-like features (B) versus planar Ti. Note the direct membrane interactions with the 8 nm pillars by SEM (arrows in C) and 3D SEM (C, inset – note nanopodia on the nanopatterned region (2), and absence of interactions on adjacent unpatterned region (1)). Fig1 A, B are modified from [3].

were 10 nm high [2]). The 15 nm high pillars were particularly osteogenic, and MSCs cultured on these surfaces were metabolically distinct. A combined surface with micron-scale pits and the 15 nm pillars was also osteoinductive, and shows promise as a surface for use in orthopaedics.

REFERENCES: ¹ L.E. McNamara, T. Sjöström, KE Burgess, et al (2011) *Biomaterials* **32**:7403-10. ²M.J Dalby, M.O Riehle, H Johnstone, et al (2004) *Cell Biology International* **28**: 229-246. ³L.E. McNamara, T. Sjöström, R. M. Dominic Meek, et al (in press) *J. R. Soc. Interface*.

ACKNOWLEDGEMENTS: The authors thank Kate Murawski for stem cell isolation, Peter Chung for assistance with 3D SEM, and all in CCE for helpful discussion.



Topographic regulation of primary cilia length and orientation in mesenchymal stem cells.

RJ McMurray¹, J Connelly², MM Knight¹

¹ Institute of Bioengineering, School of Engineering and Materials Science, Queen Mary University of London, London, UK ² Centre for Cutaneous Research, Barts and The London School of Medicine and Dentistry, London, UK

INTRODUCTION: Primary cilia are singular finger-like projections expressed by most mammalian cells upon entry into G0. The cilium has been shown to act as a hub for signalling pathways such as hedgehog and non-canonical Wnt^{1,2}. A role for primary cilia in directing the differentiation of mesenchymal stem cells (MSCs) has recently been demonstrated in response to chemical cues³. In addition there is increasing evidence for the role of the primary cilia in sensing other environmental cues. The purpose of this study was to test the hypothesis that surface topography, which regulates MSC differentiation, influences primary cilia structure and function.

METHODS: Grooved topographical surfaces were produced by hot embossing a quartz stamp into the polymer polycaprolactone (PCL) and then coating in fibronectin (10ug/ml) to promote even cell attachment. MSCs were cultured for 1 and 3 days in basal media (α -MEM + 10% FBS) followed by 24 hours culture in serum free media on either grooved (540nm deep) or planar surfaces. Cells were fixed and stained with acetylated α -tubulin to label the primary cilia which were visualised using confocal microscopy.

RESULTS: MSCs and their primary cilia were observed to orientate parallel to the grooves. In addition primary cilia length was found to be significantly different (p<0.005) between the two surfaces with mean lengths 3.1µm and 2.6µm for cells on grooved and planar surfaces respectively.

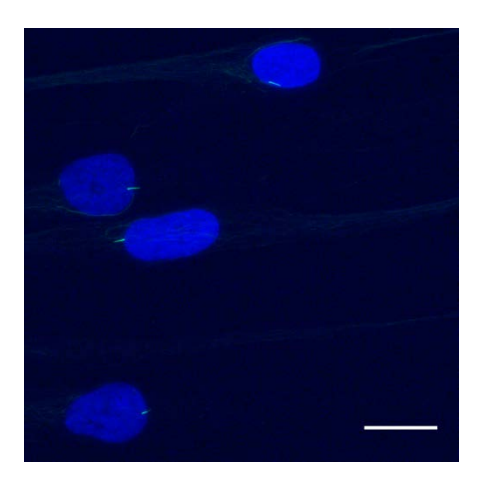


Fig. 1: MSCs cultured on grooved PCL. Primary cilia are seen to align along the grooves. Green = primary cilia and blue = nucleus. Scale bar = 20um.

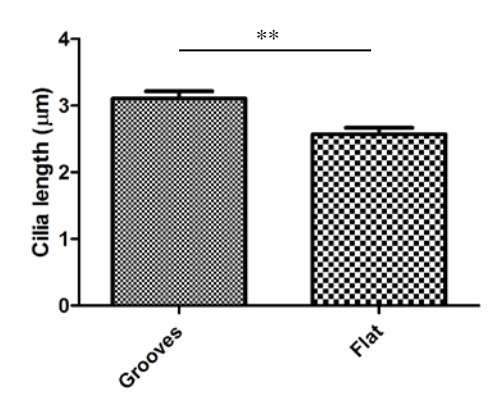


Fig. 2: Primary cilia length is found to be longer in MSCs cultured on grooved PCL when compared with MSCS cultured on flat PCL. P<0.005.

DISCUSSION & CONCLUSIONS: The mechanism for cilia alignment in response to topography is unclear but is unlikely to be mediated by alignment of the extracellular matrix as suggested in tissue. These changes in primary cilia structure may be involved in mediating stem cell differentiation and other changes in cell function associated with the topographical cues.

REFERENCES:

- 1 Lancaster *et al. Nat Cell Biol* **13**, 700-707, doi:ncb2259 [pii] 10.1038/ncb2259 (2011).
- 2 Tran *et al. Nat Genet* **40**, 403-410, doi:ng.105 [pii]10.1038/ng.105 (2008).
- 3 Tummala *et al. Cell Mol Bioeng* **3**, 207-212, doi:10.1007/s12195-010-0127-x (2010).

ACKNOWLEDGEMENTS: RJ McMurray is supported by the Wellcome Trust, UK. We thank Carol-Anne Smith for providing the surfaces.



The effects of elongation factor 1 alpha (eEF1A) on the organisation of actin and the mechanical properties of yeast cells

Annette Doyle ^{1,2}, Steven Crosby², David R. Burton¹, Francis Lilley², Mark Murphy^{1,2}

¹ General Engineering Research Institute (GERI), Liverpool John Moores University (LJMU), Liverpool. ² School of Pharmacy & Biomolecular Science, LJMU, Liverpool.

INTRODUCTION: Many diseases including cancer have been associated with mechanical weakness at both the tissue and cellular level. Therefore. understanding more mechanical properties of cells and how such properties alter with disease may help in the development of new treatments. At present little is about the fundamental mechanical properties of cells or what causes such mechanical weaknesses. The cytoskeleton plays a major role in providing the cell with mechanical integrity and it has been suggested that disruption of the normal disorganisation of the actin cytoskeleton contribute to cells becoming mechanically compromised.

Elongation factor 1 alpha (eEF1A) has been found to be over-expressed in certain cancers and is thought to affect actin organisation. This paper will present recent results which show that *in vitro*, eEF1A does bind and bundle F-actin. The paper will also introduce how atomic force microscopy can be used to investigate the mechanical properties of yeast strains having mutated forms of eEF1A.

METHODS: Actin (rabbit skeletal muscle) was purchased from Cytoskeleton Inc, UK. Purification of eEF1A from *S.cerevisiae* yeast strain MC213 (Sandbaken and Culbertson, 1988) was performed according to a scheme modified from Cavallius *et al.* (1997).

Atomic force microscopy (AFM) and confocal microscopy were used to obtain images of actin organisation both in the absence and presence eEF1A.

Mechanical properties of yeast cells were investigated by means of force-indentation experiments using AFM. The Hertz model was used to determine Young's modulus (E) while scanning electron microscopy (SEM) was used to investigate yeast cell morphology.

$$F = \frac{2}{\pi} \frac{E}{(1 - v^2)} \tan \alpha \delta^2 \tag{1}$$

RESULTS: Figure 1(A) & (B) show AFM images of F-actin polymerised in the absence & presence of eEF1A. As can be seen there is a clear difference with eEF1A promoting actin bundling.

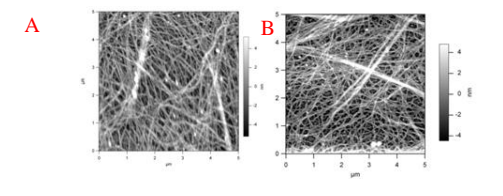


Fig. 1 AFM image of (A) actin polymerised in the absence of eEF1A and (B) in the presence of eEF1A.

Figure 2 shows an SEM image of a yeast cell highlighting how the force-indentation curves were taken on individual cells. Figure 3 shows a force-indentation-curve with the fitted Hertz model and the resultant value for Young's modulus.

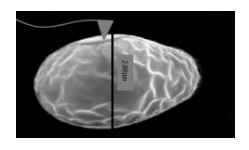


Fig. 2: SEM image of a yeast cell with cell size and AFM cantilever illustrating measurement of force indentation curves

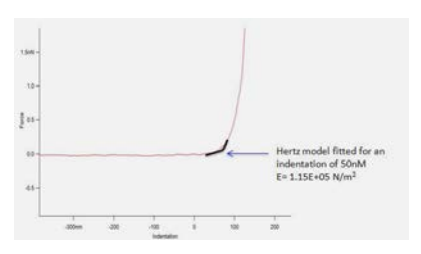


Fig. 3: Example force-indentation curve with the fitted Hertz model over 50nm indentation

DISCUSSION & CONCLUSIONS:

Using AFM it was shown that eEF1A binds & bundle F-actin. AFM force measurements on yeast strains having mutated forms were found to differ in their mechanical properties compared to the control.

REFERENCES:

Cavallius, J., Popkie, A.P., Merrick, W.C., 1997. Site-directed mutants of post translationally modified sites of yeast eEF1A using a shuttle vector containing a chromogenic switch. *Biochim. Biophys. Acta.* 1350, 345–358.

Sandbaken, M.G., Culbertson, M.R., 1988. Mutations in Elongation Factor EF-la affect the frequency of frame shifting and amino acid misincorporation *Saccharomyces cerevisiae*. *Genetics* 120, 923–934.



A novel method for isolation and release of autologous adult stem cells from primary tissue

Matthew Fok¹, Nicholas Bryan¹, John Hunt¹

¹ <u>Clinical Engineering (UKCTE)</u>, University of Liverpool, Duncan, Building, Daulby Street, Liverpool, United Kingdom, L69 3GA

INTRODUCTION: Autologous adult stem cell (ASC) transplants have been hindered through the inability to purify therapeutic numbers of cells, without in vitro expansion which is time consuming, expensive, and subjects cells to compounds of xenogeneic origin raising regulatory concerns regarding their re-implantation¹. Cell isolation can be achieved with excellent purity and yield through immunobead magnetic separation and has an extensive track record². However this method is inadequate for isolating cells from primary tissue. This is principally due to the physical properties of the small beads (50 nm to 4.7 µm diameter) used in these techniques, which impede their motility through primary tissue³. Coupled with this small isolation particles are typically internalized into cells which may destabilize their phenotype. Therefore prior to isolation, small bead technologies typically require multiple rounds of tissue processing before cell isolation. In this study we used large (50-100 µm), dense antibody labelled beads, with a novel capture and release method, to purify ASCs from primary tissue with a minimal ex vivo manipulation.

METHODS: Immunobeads were labelled with 10µL of CD90 antibody for 30mins in the conjugation buffer (buffer A) supplied (Cellcap Technologies, UK) at 4°C. Cells were incubated with CD90 antibody, in buffer A. Separation was achieved by mixing beads and cells and incubating with continuous agitation. Release of cells is accomplished with incubation of beads with supplied release buffer (buffer B). Unless stated otherwise all incubations were for 15mins at 4°C. Capture of cultured human mesenchymal stem cells (hMSCs, Lonza, UK)) from a co-culture of hMSCs and fresh human peripheral blood mononuclear cells (hPBMCs) was achieved using immunobead separation at a ratio of 250µL beads to 2x10⁶ cells. Purity of isolated populations was characterised by flow cytometry. Adipose-derived stem cells were isolated from collagenase (1mg/mL) digested (90 minutes, rolled 37°C) white adipose tissue, excised from the visceral and subcutaneous tissues of 12 week old male and female Wistar rats, using immunobead separation at a ratio of 250µL beads to 5x106 cells. Negative

depletion of CD90+ and CD44+ cells was characterised by flow cytometry.

Statistics were performed using students T-test (P<0.05).

RESULTS:

<u>Cultured cell separation</u>: Isolation of CD90+ hMSCs was achieved, with a depletion of 74% from a co-culture mix of hMSCs and hPBMCs using immunobead separation. (P<0.05 vs. control, n=3)

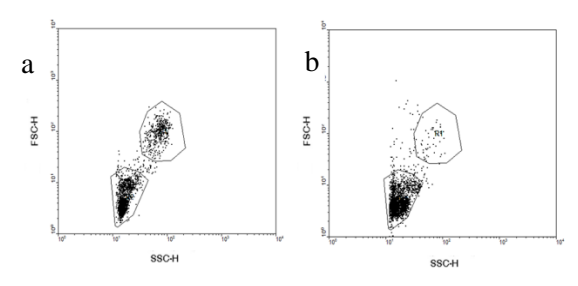


Fig. 1: Representative forward scatter/side scatter plot of a co-culture of hMSCs and human leukocytes a) before and b) after separation with CD90 labelled immunobeads showing ablation of the hMSC region after CD90 cell separation.

Primary tissue separation: A 43% depletion of CD90+ cells from primary rat adipose tissue was achieved with CD90 labelled immunobeads. A concurrent decrease of 35% in the hMSC marker CD44 was observed further confirming the removal of hMSCs. (P<0.05 vs. Control, n=3)

DISCUSSION & CONCLUSIONS: We show excellent initial results in validation of a novel method of MSC isolation from primary tissue, with simple translational potential into routine clinical practice. Proceeding experiments will focus on release and differentiation of captured cells utilizing the Cellcap release mechanism.

REFERENCES: ¹G Rena, X Chen, F Dong, et al (2011) Stem Cells Trans Med 1:51-58. ² S Miltenyi, W Müller, W Weichel, et al (1990) Cytometry 11:231-38. ³CC Berry, S Wells, S Charles, Biomaterials 25:5405-13



Viability of Porcine and Bovine Corneal Endothelium in Culture

T F Somerville, S Ahmad, S B Kaye, C M Sheridan and R M K Stewart

Department of Eye and Vision Science, University of Liverpool, UCD Building, Daulby Street, Liverpool L69 3GA, United Kingdom

INTRODUCTION: The corneal endothelium is required to maintain the optical clarity of the cornea and hence vision. Human corneas available for endothelium research are restricted in number and advancements in corneal graft transplantations are limited without representative animal models. Interspecies variation of animal corneas has been noted in a number of studies looking at various aspects of corneal transplantation such as cryopreservation and dextran sulphate [1, 2]. Porcine and bovine globes are often used in eye research because of their high availability and low cost and particularly in porcine; the apparent anatomical and physiological similarities to the human eye [3]. How appropriate these models are in representing human endothelium viability needs to be clarified further and optimized accordingly.

METHODS: Corneas were taken from human. porcine and bovine globes. Porcine and bovine globes were collected from local slaughterhouses within 24 hours of death. Experiments were carried out in triplicates. One human cornea was obtained from the mortuary at Royal Liverpool University Hospital at 8 hours post-mortem. Corneas were cultured in a standard medium (Dulbecco's Modified Eagle's Medium/Nutrient F-12 Ham with 10% fetal calf serum) at 37°C, 5% CO₂. Porcine corneas were additionally cultured in Opti-MEM-1, a selected medium found previously to improve the proliferation potential of porcine corneal endothelial cells [4]. Endothelial viability was assessed at 24 hour intervals by staining with 0.08% trypan blue solution for 10 minutes. Viability was expressed as a percentage of the area devoid of trypan blue staining as assessed using Image J.

RESULTS: Porcine and bovine endothelium viability decreased in comparison to human endothelium viability which remained at 95% over 5 days. Bovine endothelium viability in culture decreased at a faster rate than porcine endothelium (falling to 4% compared to 68% viability at 5 days). Opti-MEM-1 supported 36.4% less growth in the porcine model than standard media in this study.

The time taken between enucleation and corneal excision was shown to significantly decrease endothelium viability with greater effect in the porcine model (figure 1).

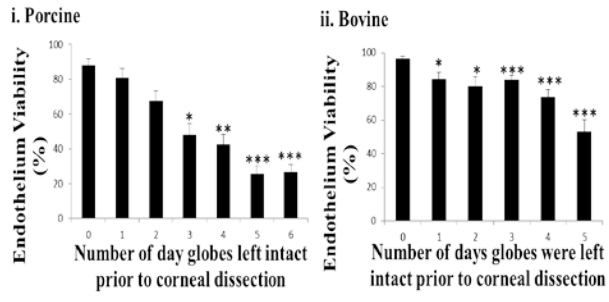


Figure 1: Decreasing viability of i) porcine and ii) bovine endothelium as the number of days the globes were left intact prior to corneal excision increases. T test analysis, *P < 0.05, **P < 0.01, ***P < 0.001.

DISCUSSION & CONCLUSIONS: The porcine model has most comparable viability to human endothelium ex vivo, although further optimization of culture conditions is needed to maximise this. Significantly less endothelial viability demonstrated in both porcine and bovine models with increasing time globes are left intact post enucleation and prior to corneal excision. This may have implications for eye bank practices; prompt corneal excision and culture could maximize the endothelial viability of donor corneas and thus reduce graft failure rates. Equivalent studies of human endothelial viability are thus warranted.

REFERENCES: ¹.Wusteman MC, Armitage WJ. Cryopreservation studies with porcine corneas. Current Eye Research, 1999. 19(3): p. 228-233. ². Ram JI. Dextran sulfate protects porcine but not bovine cultured endothelial cells from free radical injury. Canadian Journal of Veterinary Research, 2004. 67(2) ³.Proulx S. Methods being developed for preparation, delivery and transplantation of a tissue-engineered corneal endothelium. Experimental Eye Research, 2012. 95(1): p. 68-75. ⁴. Proulx S, Bourget JM. Optimization of culture conditions for porcine corneal endothelial cells. Molecular vision, 2007. 13: p. 524-33.



Development of platelet derived growth factor-ββ release PHBHHx nanoparticles to control differentiation of human mesenchymal stem cells

CL Dong¹, WR Webb¹, Q Peng⁴, JZ Tang³, NR Forsyth¹, GQ Chen², AJ El Haj¹

¹Institute of Science and Technology in Medicine, Keele University, Stoke on Trent, UK. ²Department of Biological Science and Biotechnology, Tsinghua University, Beijing, China. ³Department of Pharmacy, University of Wolverhampton, Wolverhampton, UK. ⁴West China School of Pharmacy, Sichuan University, Chengdu, China.

INTRODUCTION: Mesenchymal stem cells (MSCs) can differentiate into multiple lineages under controlled conditions. Growth factors have been shown to be powerful regulators of cell proliferation and differentiation[1]. Platelet derived growth factor (PDGF) in human serum is known to induce smooth muscle actin (SMA) expression in MSCs and promote smooth muscle differentiation [2]. Our overall aim is to design a PHBHHx release nanoparticle which will allow localized differentiation within a 3 D matrix. This report defines the range of concentration of PDGF-ββ which will promote a morphologic and phenotypic effect on hMSCs in monolayer which can be employed to develop a nanoparticle release strategy. Initial optimization and characterization of the nanoparticles has been carried out.

METHODS: Sub-confluent (90%) flasks hMSCs were trypsinised, then distributed into 6-well plates with the density of 3×10^4 cells per well. Media supplemented with PDGF-ββ at 0, 5, 10, and 25 ng/ml without nanoparticles was introduced. RNA lysates for RT-PCR and fixation of cells for immunocytochemistry were undertaken at regular time intervals (Days 0, 2, 5, 10, 15 and 20). PHBHHx nanoparticles were fabricated by a reverse micelle-solvent evaporation method, then measured by Zetasizer (*Malvern Ltd UK*).

RESULTS: RT-PCR results demonstrate smooth muscle actin gene (ACTA-2) expression is elevated in response to 10ng/ml PDGF-ββ (*Fig. 1*). Immunocytochemistry confirmed the RT-PCR result of smooth muscle actin expression (*Fig. 2*). The PHBHHx nanoparticles, observed by SEM, were mostly spherical in shape and well distributed

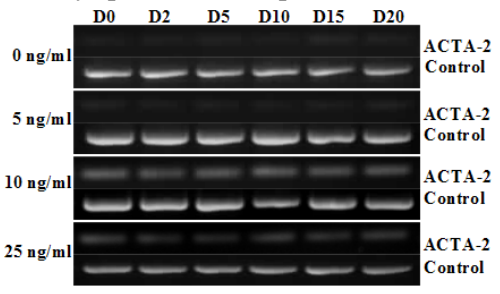


Figure 1. ACTA-2 gene expression from hMSCs incubated in different concentration PDGF-ββ (0, 5, 10 & 25ng/ml) medium. Control: ACTB

in size (*Fig. 3*). The lyophilization process did not lead to a significant change in mean particle size, polydispersity index (PDI), zeta potential (ZP) (*Table 1*).

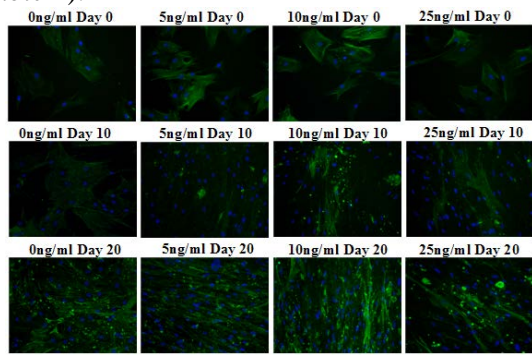


Figure 2. Immunological staining of MSCs incubated in 0, 5, 10, 25ng/ml PDGF- $\beta\beta$ media. Smooth muscle actin (green, 3s), DAPI (blue, 400ms). (20×)

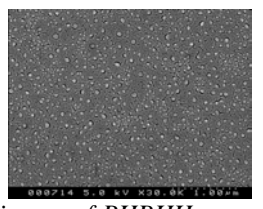


Figure 3. SEM image of PHBHHx nanoparticles. Scale bar: 1.00um; accelerating voltage: 5kV.

Table 1. Characterization of nanoparticles before and after lyophilized

sample	size (nm)	PDI	ZP(mV)
before lyo	138.4±2.1	0.184 ± 0.026	-21.8±2.6
after lyo	159.1±3.7	0.182 ± 0.013	-20.2 ± 1.8

Values are mean ± s.d. (n=6). Lyophilization: -80°C pre-freezing 12h, then lyophilization 24h.

DISCUSSION & CONCLUSIONS: Our results suggest an optimal concentration of 10 ng/ml PDGF-ββ without nanoparticles will induce a response in MSCs in vitro. Work on the parallel effects of PHBHHx nanoparticle released PDGF-BB on MSCs is in progress.

REFERENCES: ¹S Thomopoulos, R Das, ES Sakiyama, et al, 2010 *Annals of biomedical engineering* 38(2): 225-34. ² Ball S, Shuttleworth C, Kielty C. 2007 *J Cell Mol Med* 11, 1012-30.

ACKNOWLEDGEMENTS: Supported by the EU 7th Framework HYANJI Program.



Isolated human foetal femur cells maintain Stro-1 expression and differentiation potential over prolonged culture: a potential source of skeletal stem cells

D Gothard¹, J Kanczler¹, K Cheung¹ and ROC Oreffo¹

¹Bone and Joint Research Group, Human Development and Health, Institute of Developmental Sciences, Faculty of Medicine, University of Southampton, Southampton, SO16 6YD.

INTRODUCTION: Osteoporosis and osteoarthritis are a significant socio-economic burden in an increasingly aged population. Skeletal stem cells (SSCs) provide an ideal cell source for bone tissue engineering strategies to address this medical challenge. Adult SSCs enriched using the osteogenic cell marker Stro-1 lose expression and differentiation potential over prolonged in vitro culture ¹. This can result in limited expansion potential: an essential requirement for clinical translation. The present study investigated human foetal femurs as a new source of SSCs assessing their proliferative and differentiation potential in relation to bone tissue generation ^{2, 3}.

METHODS: Skeletal cells were regionally isolated from human foetal femurs as epiphyseal and diaphyseal populations (separated around the metaphysis) and characterised in 2D monolayer potential) (differentiation and 3D organotypic culture (tissue formation potential). Isolations were characterised by percentage alkaline phosphatase positive colony forming unitfibroblastic (ALP+ CFU-F) capacity and in vitro differentiation potential. Following in vitro characterisation Stro-1+ populations were found and isolated dependent on stage of development. Stro-1+ populations were assessed for expression, population doubling rate, ALP+ CFU-F capacity and tri-potentiality over passage by cytochemical analysis.

RESULTS: Epiphyseal and diaphyseal isolations generated distinct in vitro populations capable of chondrogenic and osteogenic differentiation. This was assessed using ALP+ CFU-F assay and expression analysis for osteochondral genes including ALP, CLEC3B, Col I, Col II DCN, LOXL4, OCN, ON, Runx2 and Sox9. 3D pellet culture exhibited unstructured tissue formation from both populations containing both cartilage and bone matrix. Stro-1+ populations were identified within the foetal femur dependent on stage of development and were largely restricted to These cells exhibited SSC diaphysis. characteristics including stro-1 expression on serial and tri-potentiality. Importantly, phenotype maintenance was observed to passage 6.

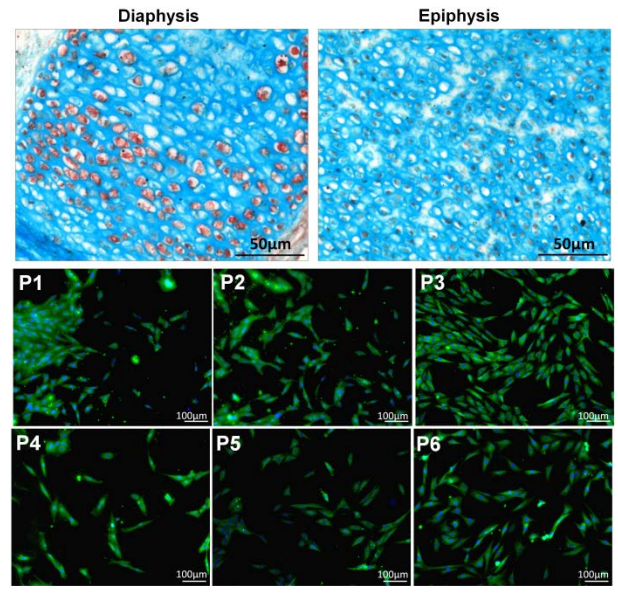


Figure 1: Stro-1+ SSCs located within the diaphysis of a human foetal femur, and phenotype stability over 6 passages in vitro.

DISCUSSION & CONCLUSIONS: Human foetal femurs present a unique source of SSCs for tissue engineering strategies. **Epiphyseal** populations provide a chondrogenic source and diaphyseal populations provide an osteogenic source. Interestingly, Stro-1+ SSCs enriched from foetal femurs exhibit comparable properties to adult human bone marrow isolated Stro-1+ populations. The major advantage of these foetal femur derived Stro-1+ cells is their expression maintenance over prolonged passage. Phenotype stability during in vitro expansion resolves ultimately, current supply issues when clinically translated.

REFERENCES: ¹ K. Schallmoser, *et al* (2010) *Haematologica* 95 (**6**) pp. 867-874. ² S. H. Mirmalek-Sani, *et al* (2006) *Stem Cells* 24 (**4**) pp. 1042-1053. ³ N. Krattinger, *et al* (2011) *European Cells and Materials* 21 pp. 46-58.

ACKNOWLEDGEMENTS: We are grateful to Prof Wilson for provision of foetal femur samples. This work was funded by the BBSRC (BB/GO10579/1).



variations in dental pulp progenitor cell ageing influence regenerative potential

A Alraies^{1,2}, RJ Waddington^{1,2}, R Moseley^{2,3} and AJ Sloan^{1,2}

¹Mineralised Tissue Group, Tissue Engineering & Reparative Dentistry; School of Dentistry, Cardiff University, UK; ²Cardiff Institute for Tissue Engineering and Repair, Cardiff University, UK; ³Wound Biology Group, Tissue Engineering & Reparative Dentistry; School of Dentistry, Cardiff University, UK.

INTRODUCTION: Exogenous adult stem cells offer significant potential in the development of cell-based therapies for clinical use. Dental pulp progenitor cells (DPPCs) are among many stem cell sources with potential therapeutic benefits. However, distinct DPPC subsets are suggested to exist within dental pulp, with contrasting proliferative/regenerative potential. This is a key consideration for the tissue engineering exploitation of DPPCs, in terms of the abilities of isolated clones to undergo sufficient in vitro expansion for therapeutic use before senescence, while maintaining their regenerative potential.

METHODS: DPPCs were isolated from the wisdom teeth of two patients, the pulps dissected cel1 suspensions obtained collagenase/dispase digestion. Individual clones were isolated by fibronectin adhesion¹. Clones (A31, A11 and B1) were maintained in the absence and presence of sub-lethal doses of hydrogen $(0-200 \mu M)$ peroxide throughout culture. Population doublings (PDs) were monitored, as was the expression of stem cell markers (CD105/CD90/CD73) by RT-PCR. Senescence was determined at <0.5PD/week and confirmed by senescence-associated-β-gal staining and telomere restriction fragment analysis. The abilities of each clone to undergo osteogenic, chondrogenic and adipogenic differentiation, were also assessed at early and late PDs.

RESULTS: Significant variations in clonal PDs and the onset of senescence were determined, with highly proliferative clones, such as A31, exhibiting greater proliferation (>100PDs) under normal and oxidative stress conditions, compared to low proliferative clones (<10PDs), such as A11 and B1. Although telomerase negative, highly proliferative clones possessed inherently longer telomeres (≈12-20kb) and maintained stem cell marker expression and osteogenic/chondrogenic differentiation for longer periods in culture. In contrast, low proliferative clones had shorter telomeres (<10kb), reduced stem cell marker expression and exhibited increased adipogenesis

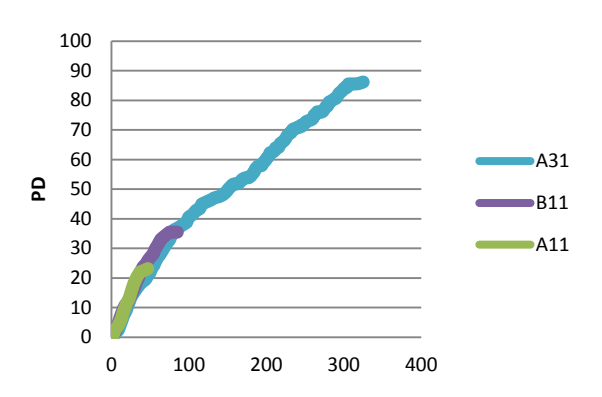


Fig. 1: Contrasting PDs between 3 DPPC clones, A31, A11 and B1.

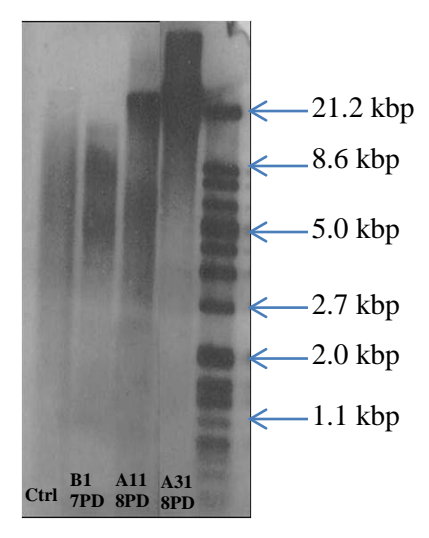


Fig. 2. Telomere length differences between 3 DPPC clones, A31, A11 and B1.

DISCUSSION & CONCLUSIONS: Results indicate that significant variations in the proliferative/differentiation capabilities of DPPC clones exist, partly explained by differences in telomere length and cellular ageing. Identification of clonal populations with different capacities for tissue repair provides the opportunity to develop screening strategies for the selective isolation of more efficacious DPPC clones for therapeutic use.

REFERENCES: ¹Waddington RJ, *et al.* (2008). *Cells Tiss. Organs* 189:268-74.

ACKNOWLEDGEMENTS: We acknowledge financial support from Albawani Company.



High-throughput skeletal stem cell separation using magnetic labelling and microfluidic sorting

M Peca^{1,2}, D Gothard¹, H Morgan², ROC Oreffo¹

¹ Bone and Joint Research Group, Human Development and Health, Faculty of Medicine; ²Hybrid Biodevices, Institute of Life Sciences, Electronic and Computer Science, University of Southampton, UK

INTRODUCTION: Osteoarthritis is prevalent within an increasingly aged population¹. Skeletal stem cells (SSCs) derived from human bone marrow (HBM) provide a unique cell source for the regeneration of bone, muscle, ligament, tendon and stroma². However, clinical efficacy is dependent on cell population purity, thus effective and efficient SSC sorting from BM is essential. Traditional immunological sorting methods such as fluorescence/magnetic activated (FACS/MACS) have a number of limitations with regards to purity of sorted cells (~70%), cell viability (20-25% post sorting), running cost, mechanical complexity and the need for trained dedicated technicians, especially with FACS. The aim of this study was develop a microfluidic device to isolate and sort SSCs, which resolves most of these issues.

METHODS: In the interest of developing a fast and simple continuous process of cell separation a quadrupole magnetic cell separation system (QMS) was utilized. QMS consists of a cylinder and a concentric rod where the working principle is to create a stream carrying the mixed sample near the central rod, surrounded by a sheath flow. Immunomagnetically labelled cells experience a drag force toward the outer stream due to a magnetic field generated by four permanent neodymium magnets. Preliminary experiments were performed using polystyrene beads labelled with magnetic nanobeads to simulate target cell isolation.

RESULTS: Green polystyrene beads ($10\mu m$) were labelled with magnetic nanobeads ($\approx 30 nm$) using streptavidin-biotin binding. Orange polystyrene beads ($10\mu m$) were mixed with the labelled beads to create the ORIGINAL sample. The two outputs (positive selection – TARGET; negative selection – NON-TARGET) of the device were analysed using a FACS machine. The device enriched more than 40% of the target particles population (Fig 1), demonstrating the efficacy of the sorting strategy in development. Current studies are focussed on further enrichment of collected target populations.

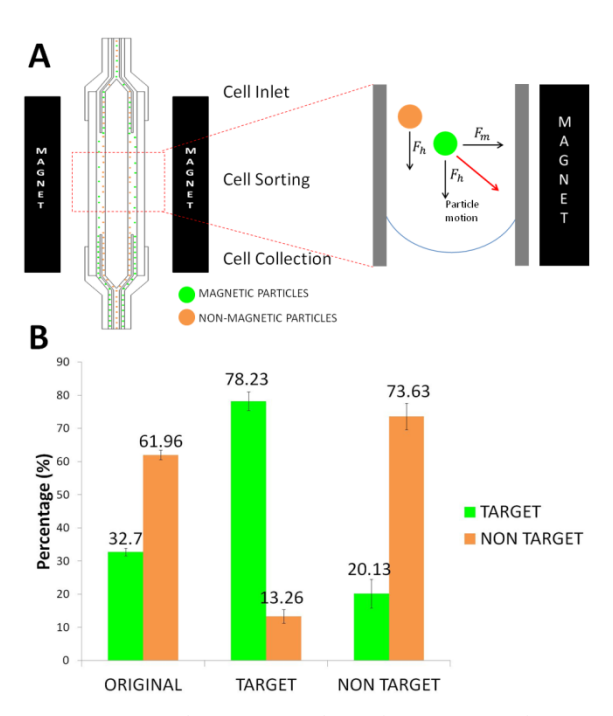


Fig. 1: Device diagram and working principle (A). Percentage recovery of beads from original mixture at the TARGET and NON-TARGET outlets (B).

DISCUSSION & CONCLUSIONS: Here we have shown the potential of a novel microfluidic device sorting different populations of immunomagnetically labelled beads. The main advantage presently is effective bulk separation of samples however, enrichment efficiency will require further improvement before clinical application. The ultimate goal would be sorting SSCs from HBM according to STRO-1expression (an accepted bone stem cell marker).

REFERENCES: ¹M. J. Dalby, *et al.*, "The control of human mesenchymal cell differentiation using nanoscale symmetry and disorder," *Nat Mater*, vol. 6, pp. 997-1003, 2007. ² M. F. Pittenger, *et al.*, "Multilineage potential of adult human mesenchymal stem cells," *Science*, vol. 284, pp. 143-147, Apr 2 1999.

ACKNOWLEDGEMENTS: funding from University of Southampton PhD scholarship is gratefully acknowledged.



Nanomechanotransduction of human mesenchymal stem cell

H Nikukar^{1, 3}, S Reid², M Riehle^{1,} A S Curtis¹, M J Dalby¹

¹ Centre for Cell Engineering, College of Medical, Veterinary and Life Sciences, University of Glasgow. ² Physics and Astronomy, University of Glasgow. ³ Shahid Sadoughi University of Medical Sciences, Yazd, Iran

INTRODUCTION: Mechanical stimulation of human mesenchymal stem cells has demonstrated changes in many cell behaviours through mechanotransductive pathways. These include experiments on effect of nanotopography ¹, shear stress, stiffness of extracellular matrix ², strain, stress and acoustic wave energy ³ on cells. In this research we are looking for mesenchymal stem cell responses to nanoscale mechanical vibrations in Z-axis. The changes in cell number and shape, differentiation and genetic changes were compared after stimulation with static control groups.

METHODS: A simple protocol for stimulation of cells in nanoscale Z-axis has been developed for this project (Figure 1). Piezo actuator (type: P-010.00H by PI Ceramic®) connected to the cell culture dish moves the entire surface up and down. The amount of displacement is dependent on the voltage applied. Attaching an aluminium disk to the base of the Petri dish ensures faithful transfer of the vibration to the cells. Human mesenchymal stem cells from bone marrow (PromoCell®) were seeded with 10⁴ cells/dish. After 4 hours seeding and cell settlement, the cells were stimulated for 24 hours. 1 week, and 2 weeks. Experiments were performed in an incubator with optimal temperature 37°C and 5% CO₂ concentration. The Petri dish was 60 mm x 15mm standard tissue culture treated polystyrene (52mm base diameter) from Corning Incorporated and cell culture media used was MEM alpha modification with L-Glutamine and nucleosides from PAA laboratories (Austria) supplemented with 10% FBS and antibiotics (penicillin and streptomycin).

RESULTS: We observed significant responses after 1 and 2-week stimulations in cell number, cell shapes and phenotypical markers. Microarray was performed for all groups and data is currently being analysed. Cell count shows normal cell growth with stimulation. However, cell surface area, cell perimeter, and arboration after 1-week stimulation showed significant increases. Immunofluorescent studies have showed significant increase in osteocalcin production after stimulation (Figure 2).

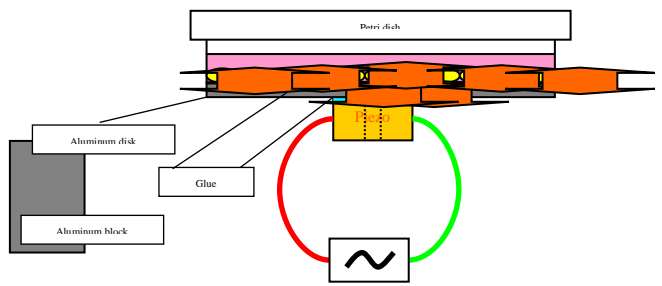


Fig. 1: Schematic picture of piezoactuator setup that shows a piezo device connected to an aluminum disk and attached to the Petri dish's base to vibrate overlying cells up and down.

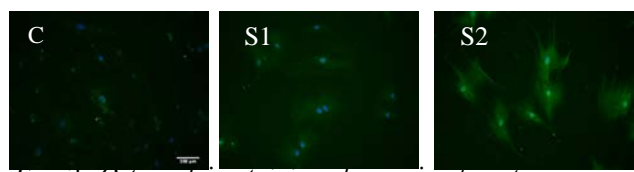


Fig. 2: Osteocalcin staining shows significant increase in two stimulated groups with various frequencies [S1 (500Hz), S2 (1000Hz)] compare to control group (C). Cells were displaced by 10-15 nm by application of 10 volts.

DISCUSSION & CONCLUSIONS: Nanoscale mechanical vibration showed significant changes in human mesenchymal stem cell behaviours. Cell morphology changed to become more polygonal and increased expression of the osteoblast marker osteocalcin was noted suggesting nanoscale mechanostimulation may be used to stimulate osteogenesis.

REFERENCES: ¹ Dalby, M.J. et al., The control of human mesenchymal cell differentiation using nanoscale symmetry and disorder. Nat Mater (2007). ² Engler, A.J., Sen, S., Sweeney, H.L. & Discher, D.E. Matrix elasticity directs stem cell lineage specification. Cell 126, 677-689 (2006). ³ Anders Fridberger, et al. An In Vitro Model for Acoustic Overstimulation. Acta Otolaryngol (Stockh) 118: 352–361 (1998).

ACKNOWLEDGEMENTS: My supervisors, all the CCE members in University of Glasgow, and the Iranian Ministry of Health for funding the research.



Characterisation of peptide biomaterials & innate metabolites that direct stem cell differentiation *in vitro*

E.V. Alakpa¹, V. Jayawarna², K Burgess³, R. Ulijn² & M. Dalby¹

¹Centre for Cell engineering, University of Glasgow, UK. ²Pure & Applied Chemistry, University of Strathclyde, UK ³Scottish Metabolomics Facility, University of Glasgow, UK.

INTRODUCTION: The innate physical characteristic of the cell niche is known to play an important role in lineage commitment of mesenchymal stem cells as they undergo differentiation. An understanding of how to mimic physical traits of the extracellular matrix is a valuable tool in being able to achieve targeted stem cell differentiation in vitro. The study aims to elucidate changes in the cell activity as it undergoes early stage differentiation

METHODS: Biomaterials used for directing stem cell differentiation were made by converting short chain peptide solution of diphenylalanine and serine into hydrogel substrates. The rigidity of these hydrogel substrates were tuned accordingly to mimic those of naturally occurring cell niches using pH alteration. Resultant Young's modulus for hydrogels were 2kPa (soft), 6kPa and 36kPa mimicking that of adipose, muscle and osteoid (demineralised bone) tissue types.

Cells were cultured on these substrates for up to one week after which samples were assessed for differentiation biomarkers using polymerase chain reaction (PCR) analysis and immunofluorescent labelling. Samples were then assessed using liquid chromatography coupled to mass spectrometry (LC-MS) for metabolite identification and subsequent profiling study

RESULTS: Cells were found to metabolically quiescent when maintained in culture and distinctly active on the hydrogel substrates. Cultured cells on the soft 2kPa hydrogels supported differentiation to towards soft tissue types while cells cultured on the 6 and 36kPa hydrogels showed a strong tendency toward cartilage and bone formation (harder tissue types). These differences in cellular behaviour could also be ascertained from examination of the cellular metabolome.

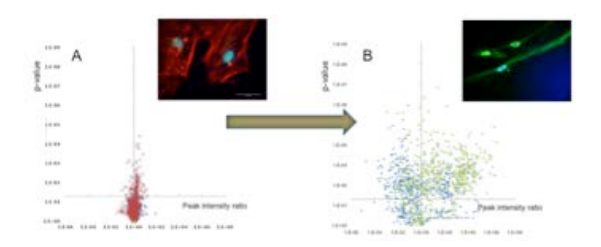


Figure 1 Visual representation of the metabolome of mesenchymal stem cells that have been A) maintained in cell culture and cells that are B) undergoing differentiation. Each individual point on the graph represents a metabolite.

DISCUSSION & CONCLUSIONS: Being able to track and profile distinct changes in cell activity over time as they respond to a number of external stimuli allows stem cell behaviour to be subject to detailed scrutiny. The plethora of information obtained from a metabolomics approach toward studying stem cell behaviour *in vitro* opens up the possibility of identifying small molecules that can play a key role in stem cell differentiation. This also possesses value with regards to the manner in which future biomaterials for cell culture is developed.

ACKNOWLEDGEMENTS: E. Alakpa is supported by the EPSRC DTC in Proteomic and Cell Technologies.

.



Establishment of a bioprocess step to enhance cell-based bone regeneration

Z Nie¹, H-Y Lee² H-W Kim², M Hoare¹, IB Wall^{1,2}

¹<u>Dept. Biochemical Engineering</u>, UCL, London, UK. ²WCU Dept. Nanobiomedicine, Dankook University, Cheonan, Korea

INTRODUCTION: Reducing cell loss, whilst maintaining cell integrity and function during processing are important challenges for cell therapy production. Cells are exposed to hydrodynamic forces during passaging that might affect cell function and viability¹. We previously showed that exposing muscle-derived precursor cells to high levels of shear stress enhanced their osteogenic capacity whilst having only minimal impact on their recovery². This project aims to assess the effect of shear stress on mammalian cells and ultimately whether this can be used as a positive regulator of differentiation for bone regeneration therapies.

METHODS: Bone marrow-derived mesenchymal stromal cells (MSCs) were obtained from 8-week old Sprague-Dawley rats and expanded in culture (Fig 1A). At passage 4 they were exposed to shear stress by passing through a capillary of known diameter (25G, 26G or 27G) at a constant flow rate of 13 ml/min for 10 passes (Fig 1B). Shear stress is proportional to capillary internal diameter³, which ranges from 0.254mm (25G and 26G) to 0.203mm (27G). Non-capillary exposed cells were used as a control. Cell recovery was measured immediately after shear and cell viability after 24 and 72 hrs of cell culture was determined using the CCK-8 dye reduction assay. Alizarin red S was used to quantitate mineralization in a preliminary study of osteogenic differentiation after 30 passes through a larger capillary of 0.308mm internal diameter.

RESULTS: MSC cultures were established and subjected to 10 passes through a capillary between luer lock syringes (Fig 1).

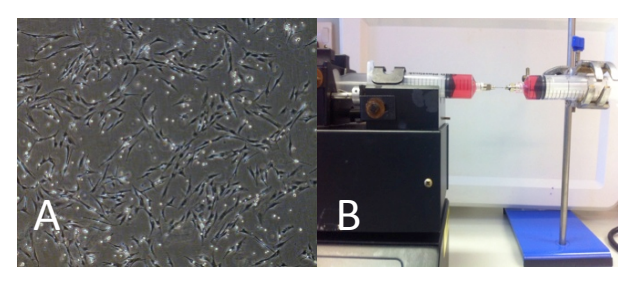


Fig. 1: (A) Passage 1 rat MSCs cultured in T25 flask (4×). (B) Shear system: Harvard PHD 2000 infuse/withdraw apparatus and interposing syringe/capillary setup.

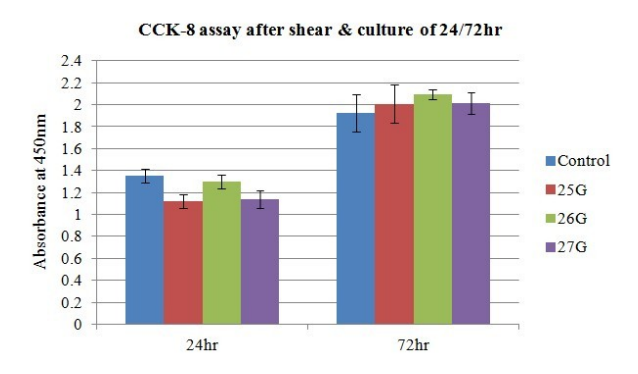


Fig. 2: Effect of different capillary diameters (25/26/27 gauge) on cell viability of p4 MSCs.

A small decline in viability was evident for MSCs passed through capillaries at 24h compared to controls (Fig. 2).

Preliminary investigations of the effect of shear stress on osteogenic differentiation using a larger diameter capillary revealed that production of calcified matrix is enhanced after exposure to capillary-induced shear stress (Fig. 3).

Alizarin Red S 14d



Fig. 3: Alizarin red S staining of calcified matrix after 14 days culture in osteogenic medium. MSCs passed through the capillary 30 times (right) stained more intensely than control cells (left).

DISCUSSION & CONCLUSIONS: Using the capillary diameters and flow rates we reported here, cell growth is permissible in spite of an early reduction in viable cell growth. Appropriate capillary wall shear stress also has potential to induce osteogenic differentiation.

REFERENCES: ¹Brindley et al (2011) J Tissue Eng online ID:620247. ²Mulhall et al (2011) J Tiss Eng Regen Med 5:629-635. ³Acosta-Martinez et al (2010) Biotech Bioeng 107:953-963.

ACKNOWLEDGEMENTS: Kind thanks to the WCU Program, funded by the National Research Foundation of Korea (No. R31-10069).



An investigation of the stiffness moduli of artificial bone materials

A Dunham¹, X T Yan², M H Grant¹

¹ <u>Bioengineering Unit</u>, University of Strathclyde, Glasgow. ² <u>Department of Design, Manufacture</u> <u>and Engineering Management</u>, University of Strathclyde, Glasgow

INTRODUCTION: The human face is highly individualised enabling us to distinguish one human being from another. Consequently, if disfigured the patient often suffers from severe psychosocial effects and strongly desires a functional and aesthetic restoration. However, current practice of facial reconstruction is frequently below the patients expectations [1]. This could be improved by 3D printing of artificial bone scaffolds personalised to the patient. This process requires a liquid binder to stick together ceramic powder one layer at a time. In this study the mechanical properties of hydroxyapatite (HA) discs using sodium trisilicate solution (STS) and malic acid with chitosan (MAC) as binders are investigated.

METHODS: HA powder was mixed with binders of various concentrations and poured into a mould to make discs of approximately 15mm diameter and 10mm height and set overnight in an oven at 37°C before sintering. The ratio of binder to HA is 1.2ml/g for all samples made with STS. For samples made with MAC, chitosan was mixed with various concentrations of malic acid (MA) at a concentration of 0.027g of chitosan per ml of acid. The ratio of binder to HA for all samples made with MAC was 1.8ml/g. Green bodies and sintered samples were tested in compression at a strain rate of 720μms-1. A stiffness modulus was determined by measuring the gradient of stress strain plots. Data is presented as Mean ± SEM, n=5.

RESULTS:

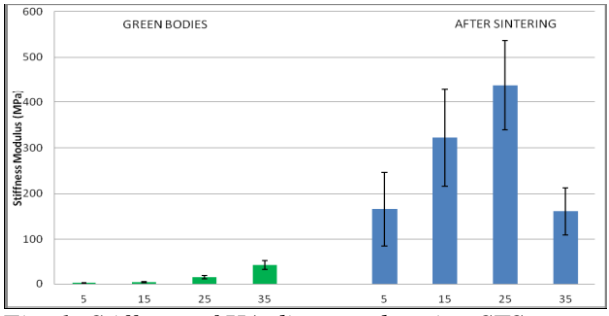


Fig. 1: Stiffness of HA discs made using STS at concentrations of 5,15, 25 and 35%v/v before and after sintering. *significantly less than 35%v/v STS pre sintering. †significantly less than 25% v/v

STS pre sintering. ‡significantly less than 25%v/v STS after sintering, p<0.05 by Mann-Whitney U test.

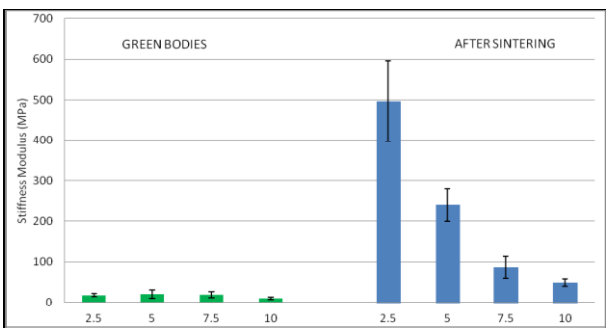


Fig. 2: Stiffness of HA discs made using MAC at concentrations of MA of 2.5, 5, 7.5 and 10wt% before and after sintering. *significantly less than 2.5% MA after sintering. †significantly less than 5% MA after sintering. p<0.05 by Mann-Whitney U test.

DISCUSSION & CONCLUSIONS: Samples made with both binders at all concentrations showed a significant increase in stiffness after sintering.

The increase of stiffness with increased binder seen for the green bodies and sintered samples made with STS was expected. However the drop in stiffness seen at 35% v/v STS and the decrease in stiffness with increased concentration of binder seen for all the discs made using MAC may be due to the presence of too high a concentration of binder damaging the samples due to binder burning during the sintering process. Another reason for this occurring in the discs made with MAC, could be due to the higher concentrations being more viscous thus causing reduced wetting of the HA powder leading to weaker binding.

The stiffnesses measured for post sintered samples made with 25% v/v STS of 0.438GPa and with 2.5wt% MA of 0.497GPa are dramatically less than the compressive stiffness of cortical bone (10-16GPa) [2]. However, these could still be suitable for non load bearing applications.

REFERENCES: ¹J.J. Mao et al (2010) *Tissue Eng B Rev* **16**(2): 257-62. ²J.R. Woodard et al (2007) *Biomaterials* **28**:45-54

CELLS MATERIALS

Design of functional octa-peptide to direct bone formation.

LA Castillo¹ A Saiani², JE Gough², AF Miller¹

¹ <u>Manchester Interdisciplinary Biocentre</u> & The School of Chemical Engineering and Analytical Science ² <u>The School of Materials</u>. <u>The University of Manchester</u>.

INTRODUCTION: The octa-peptide FEFEFKFK is an ionic-complementary peptide, where F is phenylalanine, E glutamic acid and K lysine. It has been shown that this peptide is capable of self-assembling into a beta-sheet rich fibrous network, that supports the culture of human fibroblasts and bovine chondrocytes¹.

Bone metabolism is regulated by a wide variety of molecules, including the RANK/RANKL/OPG system, which participates in the differentiation and activation of osteoclasts. Diseases such as the periodontitis may up-regulate the RANK-RANKL interaction, which will exacerbate alveolar bone loss².

In this paper, the ability of FEFEFKFK-peptide hydrogels to support the attachment and viability of skeletal cells is explored..

METHODS: FEFEFKFK peptide powder was purchased from Cambridge Research Biochemicals, UK and gels from FEFEFKFK peptide 30 mg ml⁻¹ were prepared. Saos-2 cells from human primary osteogenic sarcoma were purchased from ECACC. Bovine chondrocytes were isolated from animals from Higginshaw Abattoir, Oldham. For live/dead assay and collagen staining, 10⁵ cells resuspended in 100μL of cell culture medium were used.

RESULTS: Live dead assay images show a stable density of living chondrocytes inside the gels for up to 7 days. However the osteoblast density started to decrease from day 3 and it continued to day 7 (Figure 1).

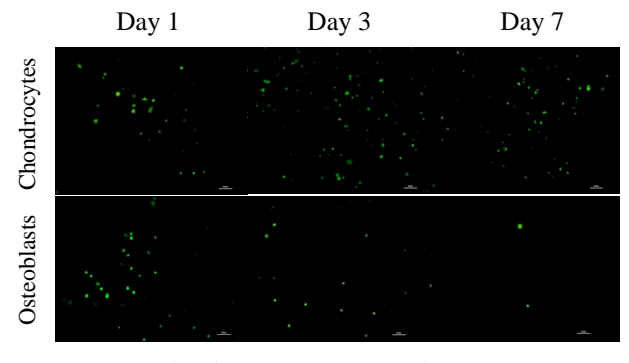


Fig. 1: Live/dead assay images of human chondrocytes and osteoblasts over 7 days. Scale bars represents 50 µm.

Figure 2 shows both chondrocytes and osteoblasts producing few collagen II and I respectively at day 7. Collagen expression in both cell types is increased at day 14, in both the control (glass) and in the peptide hydrogel (Figure 2).

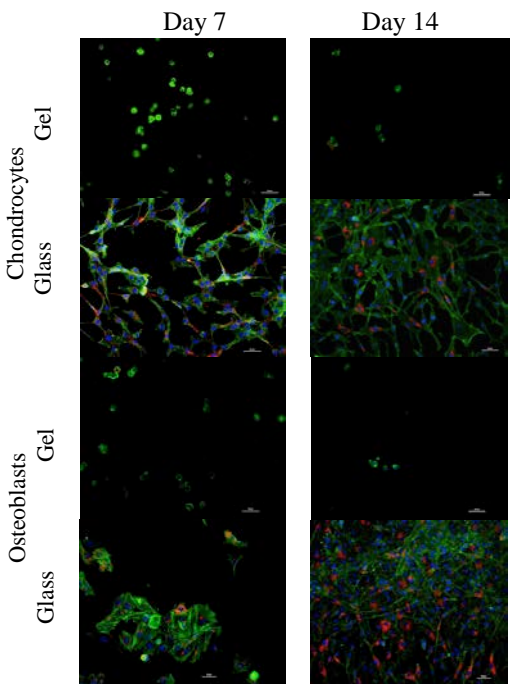


Fig. 2: Collagen I and II staining of human chondrocytes and osteoblasts over 14 days. Scale bars represent 50 µm.

DISCUSSION & CONCLUSIONS: The viability of chondrocytes inside the FEFEFKFK gels is stable for 7 days of culture. It seems that Saos-2 cells viability decreases at day 7. The expression of collagen I and II by osteoblasts and chondrocytes respectively tends to increase over a time period of 14 days in cells cultured both in gels and in the control glass. Thus, gels from the FEFEFKFK peptide might be functionalized with natural proteins from ECM, in order to direct the activity of skeletal cells for regenerative applications.

REFERENCES: ¹ A. Saiani, A. Mohammed, H. Frielinghaus, R. Collins, N. Hodson, C.M. Kietly, M.J. Sherratt, and A.F. Miller (2009) *Soft Matter*. **5**:193-2002. ² D.T. Graves, T. Oates and G. P. Garlet (2011) *Journal of oral microbiology*. **3**:5304-DOI 10.3402/jom.v310.5304.

ACKNOWLEDGEMENTS: This research was funded by CONACYT, Mexico.



Astrocytes expressing GFP in 3D collagen gels provide an effective model for screening the glial response to potential CNS cell therapies

N Johns¹, E East¹, JP Golding¹, AJ Loughlin¹, JB Phillips¹

The Open University, Milton Keynes, UK.

INTRODUCTION: Cell therapies hold promise for use in many CNS repair scenarios. A critical consideration in selecting cells suitable for implantation into the CNS is the extent of the host glial cell response. In particular, astrocytes can become reactive in response to the presence of non-CNS cells, undergoing proliferation and hypertrophy and contributing to the 'glial scar' and inhibition of neuronal regeneration [1,2]. Here we have developed a 3D culture system for screening the effect of potential therapeutic cells on astrocyte reactivity. This builds on previous work that developed 3D cultures to model reactive gliosis as assessed by immunodetection of astrocyte reactivity markers (such as glial fibrillary acidic protein, GFAP) over 15 days [3]. Here we use changes in astrocyte green fluorescent protein (GFP) volume as an early indicator of astrocyte hypertrophy, a key feature of reactive gliosis.

METHODS: Primary cortical astrocytes from rats expressing GFP were seeded at 2 x 10⁶ cells/ml within 1.5 ml (~4 mm deep) type I collagen gels in 24-well culture plates. Schwann cells, PNS glia that induce astrocyte reactivity, were seeded onto the surface of the gels (20k cells/gel). After 5 days in culture, gels were fixed and analysed using confocal microscopy and 3D image analysis. Within each individual gel, three regions at the top of each gel (in contact with the cells under test) and three control regions at the bottom of each gel were analysed for GFP volume per cell. Gels were also immunostained for GFAP as previously [3]. For each gel, the volume of GFP and GFAP staining per cell at the top was expressed as a ratio over the equivalent control volume at the bottom.

RESULTS: Astrocyte morphology was detectable using GFP fluorescence and GFAP immunostaining (Fig 1). Astrocytes in the 'top' regions adjacent to the Schwann cells showed a ~5-fold greater cytoplasmic volume (hypertrophy) as determined by GFP volume analysis than control cells near the bottom of the gels. There was a corresponding increase in the volume of GFAP immunoreactivity, although this was less marked (~2-fold greater than control cells; Fig 2).

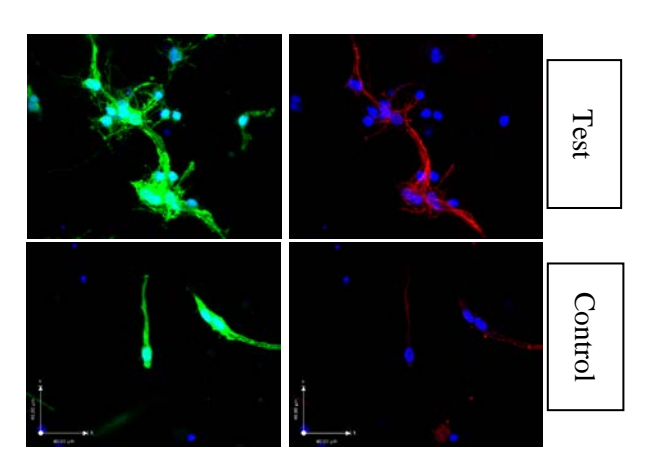


Fig. 1: Typical micrographs of GFP (green) and GFAP (red) in test (top) and control (bottom) regions of 3D astrocyte gels after 5 days.

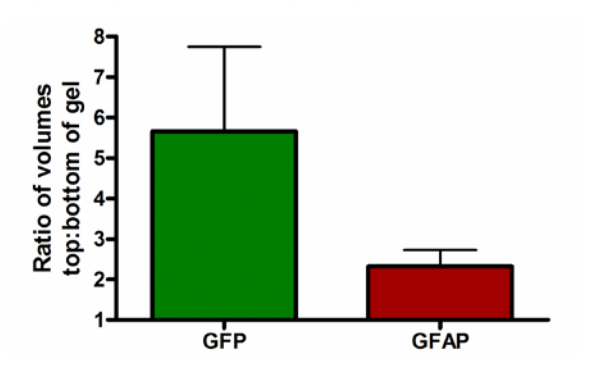


Fig 2: Astrocyte reactivity in response to Schwann cells. Data are means \pm SEM of the ratio of GFP or GFAP volume per cell compared to control regions in the same gel.

DISCUSSION & CONCLUSIONS: Astrocyte GFP volume in 3D culture provided an effective readout for detecting hypertrophy related to reactive gliosis in response to adjacent Schwann cells after 5 days. An added advantage of using GFP astrocytes is that it allows them to be distinguished from test cells, some of which might also express astrocyte reactivity markers. This approach provides a rapid and effective new tool for screening potential therapeutic cells *in vitro* in terms of their ability to elicit reactive gliosis.

REFERENCES: ¹ K.H. Adcock et al (2004) *Eur J Neurosci* **20**: 1425-35. ² A. Lakatos et al., (2003) *Exp Neurol* **184**: 237-46. ³ E. East et al (2009) *J Tiss Eng Regen Med* **3**: 634-46.



Defining glial cell self-alignment parameters for 3D CNS tissue models.

C M O'Rourke¹, A J Loughlin¹, R Drake², J B Phillips¹

¹ Open University, Milton Keynes, UK. ² TAP Biosystems, Royston, Hertfordshire, UK.

INTRODUCTION: Recreating the 3D spatial environment of the CNS allows neural cells *in vitro* to behave more like their counterparts *in vivo*, providing robust and controllable model systems that mimic key aspects of the cell biology of the nervous system ¹. The overall aim is to develop engineered neural tissue models to resemble functional CNS tissue, with anisotropic tracts of neurons and glia arranged within a robust collagen hydrogel, at a scale suitable for drug screening. To establish viable production technology for the manufacture of CNS tissue models, the parameters, cell density and contraction, that govern glial cell self-alignment have been optimised.

METHODS To achieve consistent predictable glial cell alignment, an assay system was developed for determining optimal glial cell seeding density. 24-well and 96-well plate contraction profiles were conducted using C6 glioma cells in free-floating round collagen gels at 0.1 to 6 million cells/ml. Specific seeding densities were then used in alignment assays using tethered rectangular collagen gels ². Tethered gels were fixed and stained using Haematoxylin and Eosin and micrographs were analyzed to assess cellular alignment in 2 regions with characteristic alignment patterns (side and middle) and a control region, in which cells are randomly oriented ².

RESULTS: The two contraction profiles (Fig 1) follow a similar pattern, illustrating that a satisfactory profile can be constructed in either a 96-well or a 24-well plate. Contraction reached a plateau at 3×10^6 cells/ml.

A significant degree of alignment was measured using cell densities of 2, 3 and 4 x 10^6 cells/ml in both middle and side regions, whereas 0.5 and 1 x 10^6 cells/ml only produced significant alignment in the side region (Table 1).

DISCUSSION & CONCLUSIONS: A two-stage approach was developed to determine the optimal glial cell seeding density to achieve consistent, predictable alignment. The establishment of the relationship between contraction and alignment will allow the optimal seeding density for alignment to be predicted using a small number of cells, regardless of the cell source.

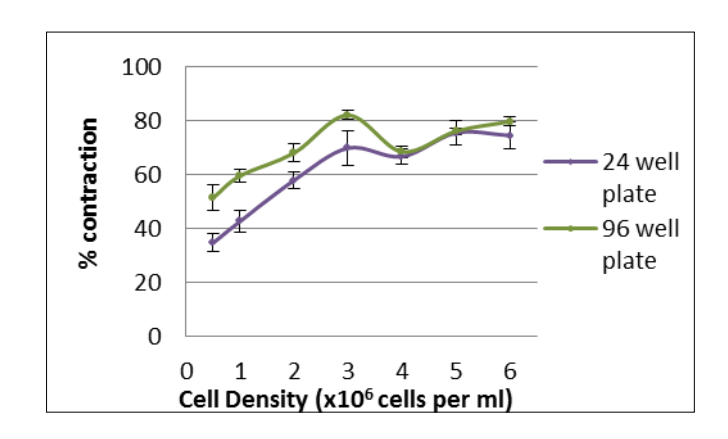


Fig. 1: Contraction Profiles show the extent of gel contraction after 24 h.

Seeding density (cells/ml gel)	Control v Mid	Control v Side
0.5 x10 ⁶	ns	***
1 x10 ⁶	ns	***
2 x10 ⁶	***	***
3 x10 ⁶	***	***
4 x10 ⁶	***	***

Table. 1. Table shows whether statistically significant alignment was present in test (middle and side) vs. control zones of tethered gels. (ANOVA with Dunnett's post test to compare each test zone to the unaligned control zone, ns = no significance, ***P < 0.001.

This is important for the development of viable production technology to generate anisotropic CNS tissue models; since the contraction profile of a small sample of cells can now be used to indicate the optimal seeding density required to give alignment throughout the collagen hydrogel. Thereby, the optimal cell density, regardless of type and source of cell, which will produce reliable alignment is one that achieves between 60 and 80% contraction, information which can be easily calculated using a simple 96- well-plate assay

REFERENCES:

¹E. East, J.P. Golding, et al (2012) *Tissue Eng Part C Methods*. ² E. East, D B De Oliveira, et al (2010) *Tissue Eng Part A* **16**(10): 3173-84



Impact of cell seeding density on early neuronal differentiation of human pluripotent cells

JW Thwaites^{1,2}, N Habib², P Dalby¹, I Wall^{1,3}

¹ Dept. Biochemical Engineering, UCL London, UK. ² Division of Surgery and Cancer, Hammersmith Hospital, London, UK, ³ WCU Dept. Nanobiomedicine, Dankook University, Korea

INTRODUCTION: Derivation of neurons from pluripotent stem cells could lead to a treatment for debilitating neurologic disorders such as Parkinson's disease. Differentiation efficiency, yield and purity remain sub-optimal regardless of the protocol used. Our aim was to determine the impact of initial cell seeding density (ICSD) on pluripotency and differentiation markers during early neuronal differentiation.

METHODS: hESC and hiPSC cells were cultured under feeder-free conditions using a standard protocol. An established neuronal differentiation protocol¹ was followed from day 4 for a further 8 days at different ICSD. Confluence analysis was undertaken daily. Markers of pluripotency and neuronal differentiation were examined at day 8 and 11 using qPCR. Genes studied were pluripotency markers – *nanog* & *oct4*, and neuronal markers - *pax6* & *sox1*. Gene expression in undifferentiated cells was used as a control.

RESULTS: Pluripotency was maintained during expansion of both cell lines (data not shown). When culturing cells only in expansion medium, ICSD had an impact on confluence early in culture (up to day 4) but by day 7 all plates were confluent regardless of ICSD (Fig 1).

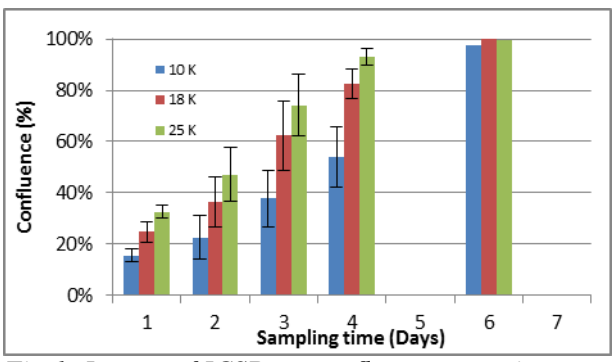


Fig 1: Impact of ICSD on confluence over time.

In subsequent experiments, day 4 was chosen as the point to commence differentiation as that time point provided a reproducible range of confluence to investigate from <50% confluence to >90%. Analysis of pluripotency genes revealed a consistent down regulation in *nanog* and *oct4* that became more prominent with increased differentiation time (Fig 2).

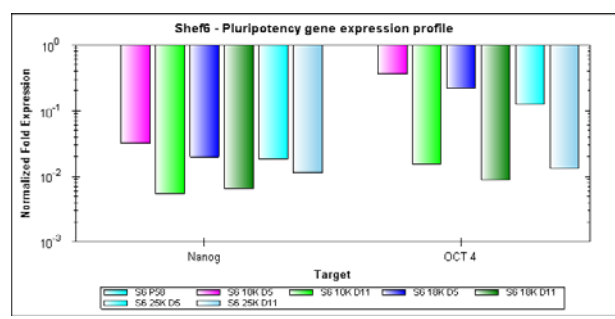


Fig 2: Relative gene expression for pluripotency genes during the differentiation protocol using Shef6.

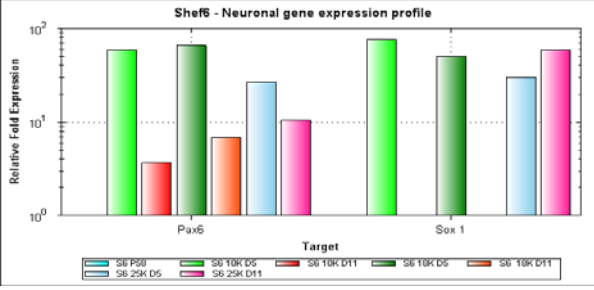


Fig 3: Relative gene expression for neuronal genes during the differentiation protocol using Shef6.

Analysis of neuronal gene expression revealed upregulation of both *sox1* and *pax6* at day 5. The degree of expression was greatest at low ICSDs (10k and 18k cells/cm²) and by day 11, levels of these early neuronal markers had substantially declined. In contrast, at the highest ICSD, levels of *pax6* and *sox1* seemed subdued, experiencing a delay in expression.

DISCUSSION & CONCLUSIONS: In these preliminary experiments, ICSD can influence gene expression in differentiating neuronal progenitors. Over the culture period there was a uniform decrease in pluripotent gene expression but increased neuronal gene expression was seen at low ICSD. Optimising ICSD could improve the yield and purity of neurons for cell therapy.

REFERENCES: ¹S.M. Chambers, C.A. Fasano, E.P. Papapetrou, M. Tomishima, M. Sadelain, L. Studer (2009) *Nature Biotechnology*. 27(3), 275-280.

ACKNOWLEDGEMENTS: Funding from the UK Stem Cell Foundation and EPSRC. Ludmila Ruban, UCL for technical assistance and expertise.



Engineered neural tissue with aligned Schwann cells supports neuronal regeneration *in vivo* and can be assembled using differentiated adipose-derived stem cells.

M. Georgiou¹, J. Loughlin¹, J. P. Golding¹, P. J Kingham² & J. B. Phillips¹

Department of Life, Health and Chemical Sciences, The Open University, Milton Keynes, MK7 6AA.

Department of Integrative Medical Biology, Umeå University, Sweden, SE 901 87

INTRODUCTION: There are many limitations associated with the current gold standard treatment for peripheral nerve injury, the nerve autograft. Another option is to use nerve guidance conduits (NGCs) to bridge the gap in injured nerves. However these are limited to repairs up to ~3cm due to their lack of neurotrophic support in long gaps. We have developed Engineered Neural Tissue (ENT) - a living biomaterial with aligned neural cell architecture that can function as the 'core' of a repair device. In this study we aimed to optimise the assembly of this material in a nerve repair device, and then to produce a construct with clinically relevant cells (adipose-derived stem cells differentiated into Schwann cells (dADSCs)).

METHODS: The rat F7 Schwann cell line was used for device optimisation. For production of ENT, cells were mixed with neutralised type I rat tail collagen (2 mg/ml) and cast into the tethering/stabilisation system^{1,2}, Fig 1. ENT was

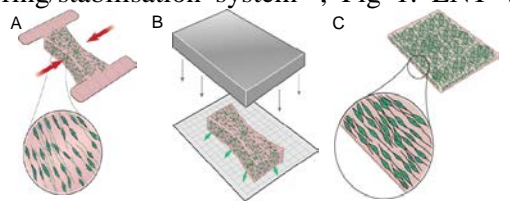


Fig. 1. Production of ENT. A Cell activity contracts the gel, cells become elongated and form chains along the longitudinal axis. B Stabilisation of aligned cellular gel by removal of some of the interstitial fluid. C ENT: a tissue-like robust hydrogel with highly aligned cells.

assembled to form the nerve core of repair devices, Fig 2. Various column formats were tested in the rat sciatic nerve model (5mm gap). Regeneration was assessed by immunostaining with antineurofilament (axons) and anti-S100 (Schwann cells (SC)) antibodies, using confocal microscopy. To investigate neuronal growth on an ENT containing dADSCs, primary adult rat neurons were cultured on the ENT surface for 3 days. Deviation of neurite growth from the direction of cell alignment was quantified in confocal micrographs following immunostaining of cultures with anti-S100 and anti-βIII tubulin (neurites).

RESULTS: *In vivo* experiments suggested regenerating axons grew preferentially between

layers of cellular ENT in close contact with the aligned SCs, compared to unaligned or acellular controls (Fig 3). dADSCs maintained their alignment during preparation of ENT & over 3 days in culture. Neurons growing on ENT-dADSC were guided by the aligned cells (Fig 4).

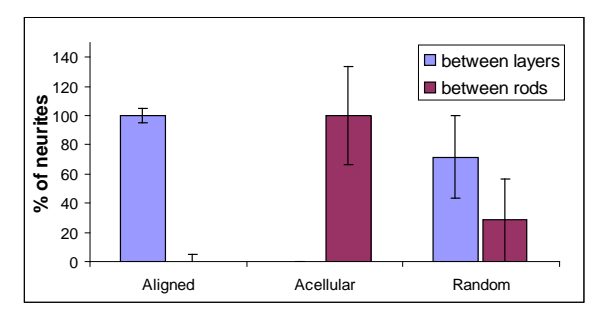


Fig. 3. Device optimisation in 5mm rat sciatic nerve model. Aligned cellular ENT promotes growth of neurites between layers (means \pm SEM).

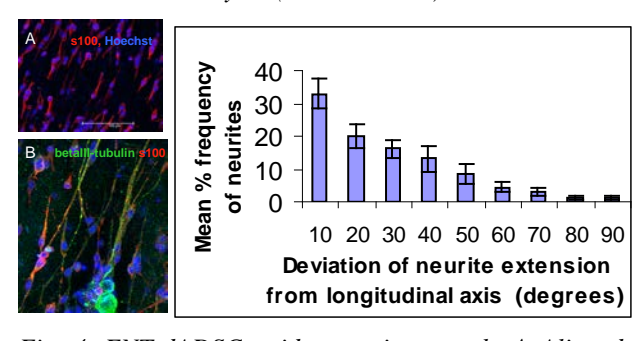


Fig. 4. ENT-dADSC guides neurite growth. A Aligned dADSCs in ENT \boldsymbol{B} Confocal micrograph showing neuronal growth (green) on the surface of the aligned dADSC (red) biomaterial. \boldsymbol{C} Deviation between angle of neurite growth and dADSC alignment (means \pm SEM).

experiments showed that ENT supports axon regeneration and that this is greatest between the layers of ENT when aligned SCs are present. As a potential clinical source of SCs for development of ENT, we showed that dADSCs survive and maintain their alignment following the stabilisation process to form sheets of ENT. Neurons growing on the surface of ENT extended neurites that were guided by the orientation of the aligned dADSCs.

REFERENCES: ¹ Phillips J.B. *et al.* (2005) *Tiss Eng* **11** 1611-7. ² Brown R.A. *et al.* (2005) *Adv Funct Mater* **15** 1762-70.



Quantifying spatial and temporal variation in cell function in collagen constructs for tissue engineering applications

A Ardakani¹, RJ Shipley^{1,2}, K Stamati¹ U Cheema¹ & RA Brown¹

¹University College London, Tissue Repair and Engineering Centre, Institute of Orthopaedics and Musculoskeletal Sciences, Stanmore and ²Mathematical Institute, University of Oxford

INTRODUCTION: Tissue Engineering was described by Robert Langer and Joseph P Vacanti as the process of biologically engineering a substitute for damaged tissues, which would eventually overcome the limitations of transplants and biomaterial implants. The successful design of any tissue engineered construct requires: (i) biocompatibility, (ii) integration once implanted in vivo, (iii) material support of the cell population, (iv) mechanical integrity and (v) ability to mimic features of native tissue architecture. Meeting these design criteria presents a significant challenge that is being gradationally addressed through the use of plastic compression to produce dense collagen scaffolds that can mimic the fibril density found in native tissues. An extensive amount of information has been gathered with regards to sustenance and support of growing cells via mass transport of nutrients and waste materials in and out of the construct; however, the connection between these features and ultimate cell fate remains to be quantified. This study seeks to address this by monitoring cell fate at different spatial positions throughout such scaffolds.

METHODS: Plastic compression allows for a controlled removal of fluid from the collagen scaffolds resulting in collagen densities of 11.6% after just a single compression. The increase in density results in a mechanically stronger scaffold. This density is representative of the fibril densities in vivo native collagen type I tissues which provides a more accurate studying model of 3D tissue. Three segments of compressed collagen matrix core, middle and outer, (where the outer segment is exposed to the highest oxygen concentration and the inner the least), were quantifying cell analysed by death proliferation, using a live/dead and proliferation assay. Histology and SEM was used to analyse the structural changes of these constructs.

RESULTS: The study design and approach provides quantitative information on cell fate within a 3D construct under a known oxygen gradient. The results indicate that changes in cell

behavior do not occur immediately and take at least 72hrs to manifest. The outer segment showed an increase in both proliferative cell number (37% p<0.01) and viability (3.8% p<0.01)) when compared to the middle and core segment. Cell Viability decreased in the core (7% p<0.01) and middle (3.7% p<0.01) segments but proliferative cell number increased in these segments (9% and 9.7% respectively p<0.01).

DISCUSSION æ **CONCLUSIONS:** The approach in this study informs of cell fate within a 3D construct with varying oxygen gradients. Through combining this information with oxygen tension data through the 3D construct, quantitative information on the relationship between cell fate and oxygen tension is obtained. Moreover these results parameterise and test a mathematical model, which allows the extraction of continuous data on cell fate in time and space. This model will allow for better prediction of cell fate within a collagen construct and can be re-tuned to accommodate for different cell types and scaffold parameters. The current study enlightens us of the process that occurs within the core of the 3D construct that were amid concerns of rapid cell death through oxygen and nutrient depletion This data can be used to develop the collagen construct design to make it more accommodating in the core and allow better cell support within the construct. For example this may be achieved by introducing vascular structure and channels to penetrate into the core to aid with cell support in the core.



Gummetal – a new implantable metal with chemical and mechanical biocompatibility

W. Chrzanowski¹, S. Yamaguchi³, N. Mordan², V Salih², T. Kokubo³

¹ The Faculty of Pharmacy, The University of Sydney, Australia; ² BTE, UCL Eastman Dental Institute, UK; Chubu University, The Faculty of Health Sciences, Japan

INTRODUCTION: Despite significant advances in biomaterial sciences and the introduction of several polymers, glass, composite and hybrid materials, metals still play an important role in biomedical engineering. Metallic implants are indispensable in many applications where new materials failed to replace them. At the same time metals have suboptimal biological and mechanical biocompatibility. Recently, we have investigated a new class of titanium alloy - 'gummetal' - that presents unique mechanical properties: ultra-low Young's modulus, ultra high strength and nonlinear elastic behaviour. Such material is very well suited for many applications: stents, hip implants, plates and many more. The aim of this work was to investigate cellular responses on gummetal developed by Saito et al., before and after bioactivation.

METHODS: Gummetal alloys (Ti-36Nb-2Ta-3Zr-0.3O) were used. Sample surfaces (10x10mm) were ground and samples incubated in 1M NaOH (60° C) for 24 h, then 100mM CaCl₂ (40° C) for 24h, heat treated at 700° C for 1h, and finally incubated in hot deionised water (80° C) for 24h. Treated samples were coded as BioGum. Topography of the surface was analysed using atomic force microscopy. To assess cell responses, human mesenchymal stem cells (1×10^{4}) were seeded on samples. Cell metabolic activity was evaluated using AlamarBlue assay up to 14 days. Cell membranes and actin filaments were stained at day 1 and 3 post seeding.

RESULTS: AFM analysis showed changes in surface morphology after chemo-thermal treatment. Sharp edges and grooves that appeared after grinding were softened by the treatment. Roughness (R_{a)} of the samples dropped from 140 nm to 100 nm after the treatment. AlamarBlue showed that cell growth on treated samples was similar up to day 7 on both samples. At day 14 the growth increased on treated samples (BioGum) while on untreated samples it remained the same. Actin network of cells on BioGum samples was very well developed with clearly visible and stretched actin filaments. Cells on untreated samples showed also well-developed actin network

but they were organised and directed along the

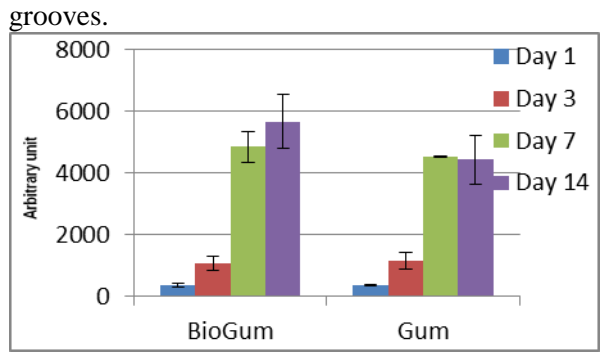


Fig. 1 Cell proliferation on BioGum and Gum metal as measured by Alamar Blue

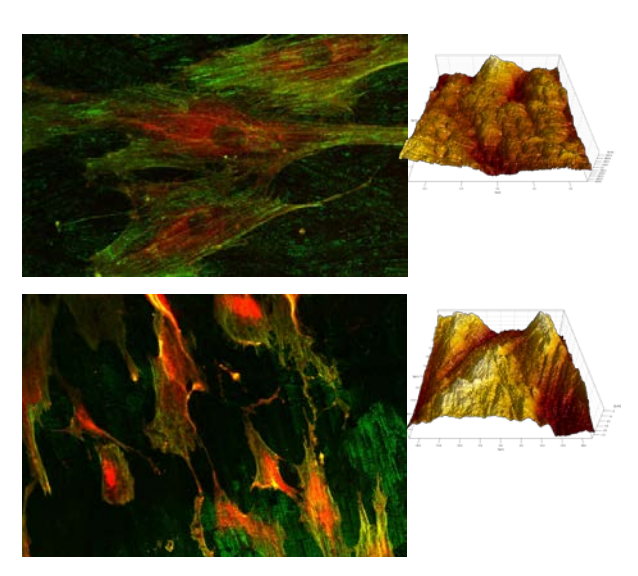


Fig. 2: Cells spreading on the surface of BioGum & Gummetal and AFM morphology profiles

DISCUSSION & CONCLUSION: Gummetal is a very attractive material for implants from a mechanical point of view. This study demonstrated positive responses of cells on bare gummetal and the possibility of further improvement of bioactivity of the alloy by chemo-thermal treatment.

REFERENCE:

T. Kokubo and S. Yamaguchi (2010) "Bioactive Ti metal and its alloys prepared by chemical treatments: state of the art and future trends" *Advanced Engineering Materials*, 12: 579-591.



Development of microfibrous and nanofibrous PLGA electrospun scaffolds: Strategies in corneal tissue engineering

<u>S Dunphy</u>^{1,2,3}, H Dua², A El Haj³, A Hopkinson², F Rose⁴

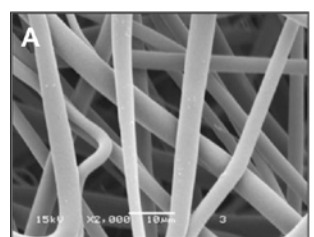
¹EPSRC DTC for Regenerative Medicine, School of Pharmacy, University of Nottingham, UK. ²Division of Opthalmology and Visual Sciences, University of Nottingham, UK. ³ISTM, Keele University, UK. ⁴Wolfson Centre for Stem Cells, Tissue Engineering and Modelling (STEM), School of Pharmacy, University of Nottingham, UK.

INTRODUCTION: Corneal trauma and ulceration is a leading cause of blindness worldwide (WHO)¹. The cornea is composed of five layers: epithelium, Bowman's layer, stroma, Descemet's membrane and endothelium. outermost epithelium strongly adheres to a basement membrane (BM) while the highly organised collagen network of the stroma is interspersed with keratocytes. Toward a novel synthetic cell-biomaterial scaffold for ocular surface reconstruction, preliminary work explored electrospun Poly (lactide-co-glycolide) (PLGA) as a possible growth substrate for corneal cells. The effect of electrospun fibre diameter on cell behaviour was investigated with the aim of mimicking structural characteristics of the BM and stroma.

METHODS: Scaffolds with fibre diameters in the nanometer range were manufactured by electrospinning 11 wt% solution of PLGA (75:25) in 1,1,1,3,3,3, hexafluoro-iso-propanol. Microfibres were produced from 25 wt% solution in dichloromethane. Primary human corneal fibroblasts or SV40-immortalised human corneal epithelial cells (HCECs) were seeded onto microfibrous and nanofibrous scaffolds.

Proliferation and viability was assessed using PrestoBlueTM. Immunofluorescence staining was performed to study cytoskeletal arrangement and phenotypic expression. Cell morphology was examined using scanning electron microscopy.

RESULTS:



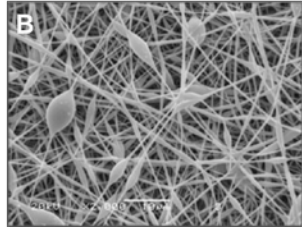


Fig. 1 Scanning electron micrographs of microfibrous (A) and nanofibrous (B) PLGA electrospun scaffolds without cells.

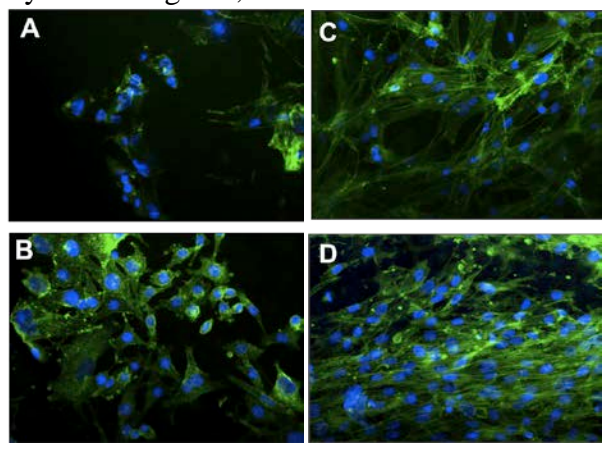


Fig. 2 Immunofluorescence staining for actin structure of HCECs (A-B) adhered on microfibrous (A) and nanofibrous (B) scaffolds and corneal fibroblasts (C-D) adhered on microfibrous (C) and nanofibrous (D) scaffolds after 5 days in culture.

DISCUSSION & **CONCLUSIONS:** adhered to and proliferated on both nanofibrous and microfibrous PLGA scaffolds. Fibroblasts readily penetrated microfibres, whereas, nanofibres showed greater resistance to cell infiltration. suggest that microfibrous Results electrospun scaffolds are better suited supporting fibroblasts. Nanofibrous membranes may be an appropriate substrate for growth of corneal epithelial cells, as they better mimic the basement membrane microenvironment. Future work will explore a dual construct to recreate the anterior layers of the cornea toward a possible clinically relevant corneal replacement.

REFERENCES: ¹ J.P. Whitcher, M. Srinivasan, and M.P. Upadhyay (2001) Corneal blindness: a global perspective, *Bulletin of the World Health Organization* **79**: 214-21.M.

ACKNOWLEDGEMENTS: This work was funded by the EPSRC Doctoral Training Centre for Regenerative Medicine. Thank you to all the members of the Tissue Engineering Group and Division of Opthalmology and Visual Sciences at the University of Nottingham.



Abdominal wall reconstruction using novel PLLA-collagen scaffolds

FR Pu¹, NP Rhodes¹, Y Bayon², R Chen¹, O Lefranc², P Gravagna², G Brans³, R Benne³, JA Hunt¹

¹UKCTE, Clinical Engineering, University of Liverpool, Liverpool, UK. ²Sofradim Production, 01600 Trevoux, France. ³Applikon Biotechnology BV, PO box 101, 3100 AC Schiedam, The Netherlands

INTRODUCTION: The repair of large abdominal wall defects remains a clinical challenge. In attempting to develop clinically feasible TE biomaterials for use in abdominal wall replacement reconstruction, we have generated highly cellularised 3D-tissue constructs using novel PLLA-collagen scaffolds in a perfusion bioreactor system to increase cell densities. The constructs were studied *in vitro* and *in vivo*. It is anticipated that this approach could eventually be introduced to repair human hernias.

METHODS: The PLLA-collagen composite scaffolds used had a unique structure with a collagen sponge formed within a mechanically stable knitted mesh of PLLA (Fig. 1a, b). Scaffolds 5cm in diameter were seeded with human dermal fibroblasts at a density of 10⁶/cm². Cell-loaded scaffolds were cultured in vitro in a perfusion bioreactor (Applikon) for 7 days prior to implantation. For the *in vivo* model, both acellular and cell-loaded constructs (1cm²) were implanted subcutaneously in Wistar rats. The implants were removed at day 2 and 7 and histopathology performed using both tinctural and immunohistochemical staining.

RESULTS: The *in vitro* studies demonstrated that the PLLA-collagen scaffolds supported cell proliferation, confirmed by cell viability assay and SEM observation (Fig. 1c, d). The flow perfusion system, increased cell proliferation and the homogeneous distribution of cells throughout the PLLA-collagen scaffolds (Fig. 2). A highly cellularised 3D-tissue construct was formed by 7 days in perfusion culture in vitro. The in vivo model demonstrated that the constructs with the increased high cellularity resulted in greater host cell infiltration (Fig. 3c) compared to the acellular constructs (Fig. 3a), with cells produced their own extracellular matrix in the cells nearby compared to the controls. More mature blood vessels were observed on the scaffold seeded with fibroblasts (Fig. 3b, d), demonstrated by immunostaining for the blood vessel marker, smooth muscle actin.

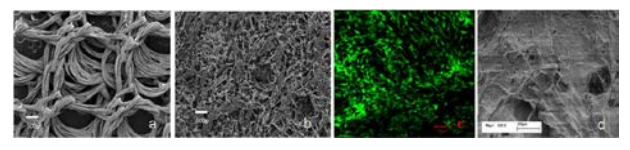


Fig. 1: SEM observation of (a) PLLA knitted mesh with coated collagen, (b) mesh with the collagen sponge. (c) Confocal images of cell viability and (d) SEM view of cell seeded on PLLA-collagen scaffolds up to 7 days.

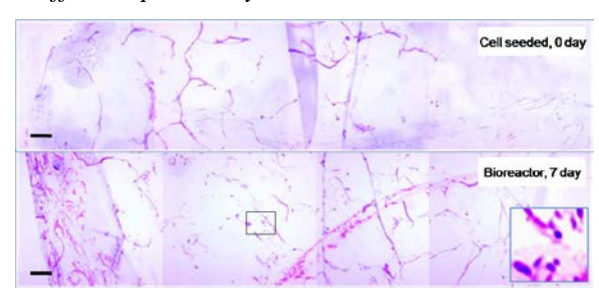


Fig. 2: Histological evaluation of cell distribution and proliferation in the scaffold constructs. Cross sections of cell-loaded scaffolds cultured for 0 and 7 days.

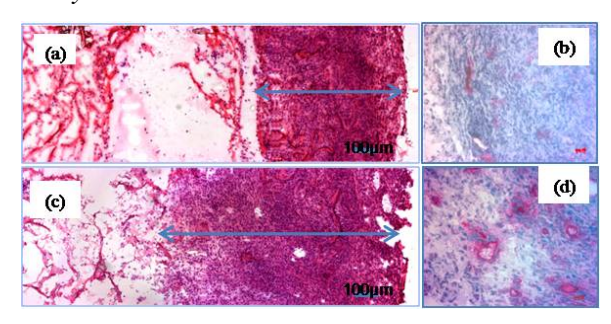


Fig. 3: H&E staining and immunohistochemistry for α SMA on (a, b) acellular and (c, d) fibroblasts-loaded constructs.

three-dimensional biodegradable PLLA-collagen scaffolds loaded with dermal fibroblasts are an excellent candidate for abdominal wall tissue engineering that facilitates cell proliferation and differentiation when matured using a perfusion bioreactor system. It is promising for them to be used in abdominal wall replacement in the future.

ACKNOWLEDGEMENTS: Funding from the European Commission contract number FP6-500465 is gratefully acknowledged.



Supercritical fluid foaming: a novel route to polymeric allografts?

MS Purcell¹, E Tayton², RO. Oreffo², KM Shakesheff³, SM Howdle¹

¹School of Chemistry, University of Nottingham, UK, ²Human Development and Health, University of Southampton, UK, ³School of Pharmacy, University of Nottingham, UK

INTRODUCTION: The number of total hip replacement operations is increasing, with over 85,000 hip operations being carried out in the U.K. in 2009, over 10% of which were revision procedures. A large proportion of the revision procedures require bone augmentation for which morselised allograft is the current 'gold standard'. The acute shortage of morselised allograft in addition to the associated issues of expense, rejection, and risk of disease transmission creates a need for a synthetic alternative.

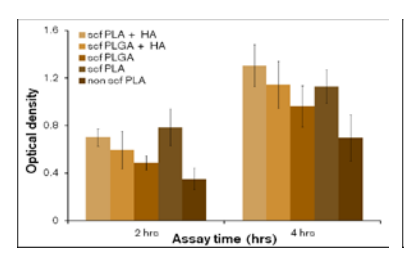
Biodegradable polymers are widely used in tissue engineering and it has been demonstrated that by using supercritical carbon dioxide (scCO₂) highly porous polymeric scaffolds can be produced.² Previous work by the authors identified scCO₂ foamed high molecular weight (M_w) poly (D, L-lactide) (P_{DL}LA) and poly (D, L-lactide-co-glycolide) (P_{DL}LGA) as promising polymeric scaffolds for mesenchymal stem cells (MSCs)³ with potential application in impaction bone grafting (IBG).

METHODS: High M_w $P_{DL}LA$ and $P_{DL}LGA$ have been foamed using $scCO_2$, both with and without hydroxyapatite (10% w/w), and the resulting porous scaffolds were ground using a bone mill, seeded with MSCs, and impacted in a process that mimics IBG. Two week *in vitro* experiments were carried out followed by five week *in vivo* (murine) to determine the most suitable scaffold composition for application in IBG.

The scaffolds were assessed in terms of cellular compatibility, osteogenic differentiation, and vascularisation through cellular assays (WST-1, ALP) (n=3) and fluorostaining (live/dead, collagen-1, osteocalcin, bone sialoprotein, and Von Willebrand factor). Additionally micro computer tomography (μ CT) was used to determine evidence of bony matrix formation and vascularisation. One way ANOVA was used to assess significance.

RESULTS: All scaffolds showed good evidence of viability and proliferation of cells with no significant difference between samples (Fig. 1). Cells seeded on $P_{DL}LA$ scaffolds showed significant evidence of increased levels of osteoblastic differentiaton in comparison to those seeded on $P_{DL}LGA$ scaffolds (Fig. 2). μCT

imaging of scaffolds subcutaneously implanted in mice showed evidence of bony like matrix formation and vascularisation around the scaffolds. The results presented suggests $scCO_2$ foamed $P_{DL}LA$ scaffolds outperform $P_{DL}LGA$ and the presence of hydroxyapatite within the scaffolds improves osteoblastic differentiation.



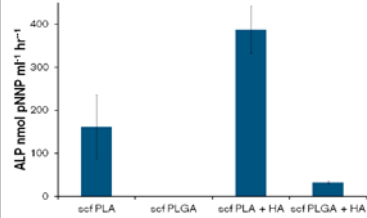


Figure 1: WST-1 assay mean optical density values (minus controls) with standard deviations at 2 and 4 hour time points following scaffold submersion. No significant differences between scf scaffolds observed (one way ANOVA, n=3)

Figure 2: Mean alkaline phosphatise (ALP) activity values (minus controls) are presented with standard deviations. One way ANOVA results included (* P<0.05, ** P<0.01, n=3).

foamed, high M_w, P_{DL}LA and P_{DL}LGA form porous scaffolds suitable for MSC culture. MSCs seeded on these porous scaffolds survive remain viable post-impaction. MSCs seeded on P_{DL}LA scaffolds gave positive results for osteoblastic differentiation and in terms of ALP specific activity and collagen-1 show greater expression than MSCs seeded on P_{DL}LGA scaffolds. The use of hydroxyapatite has also been shown to improve levels of osteoblastic differentiation. P_{DL}LA with hydroxyapatite showed the greatest promise and a larger *in vivo* model (ovine) is suggested.

REFERENCES: ¹ The National Joint Registry (2010), *National Joint Registry for England and Wales 7th Annual Report.* ² R.A. Quirk, R.M. France, K.M. Shakesheff, and S.M. Howdle (2004) *Curr. Opin. Solid St. M.* **8**: 313-321. ³ E Tayton, M. Purcell, A. Aarvold, J. Smith, S. Kalra, A. Briscoe, K. Shakesheff, S.M. Howdle, D. Dunlop, and R. Oreffo (2012) *Acta Biomateria.* **8**: 1918-1927.

ACKNOWLEDGEMENTS: The authors would like to thank the MRC and EPSRC for providing financial support to this project.



Characterisation of ceramic - filled fibrous polylactide membranes for cell engineering applications

W. Chrzanowski¹, Izabela Raizer³, N. Mordan², JC Knowles² and <u>V Salih²</u>

¹ The Faculty of Pharmacy, The University of Sydney, Australia; ² BTE, UCL Eastman Dental Institute, UK

³ATH – University of Bielsko-Biala; Institute of Textile Engineering and Polymer Materials, PL

INTRODUCTION: Polylactic acid (PLA) is widely used in biodegradable materials in the form of fibres obtained by pulling or electrospinning. Electrospinning is mainly concentrated on formation of non-woven mats of polymer and other compounds with therapeutic function. Pure polymer scaffolds have suboptimal biological properties; hence the use of various fillers is required. Thus, incorporation of fillers such as tricalcium phosphate (TCP) and hydroxyapatite (HAp) is used to improve clinical performance (mimicking mineral extracellular matrix and optimising chemical conditions during polymer degradation. Our previous work has demonstrated a significant improvement of cell responses to polymer implants filled with titanium doped phosphate glass. In this study glass particles were incorporated into PLA fibres and compared with commercially available TCP and HAp fillers.

METHODS: Fibrous membranes were prepared by electrospinning from PLDL/filler solution. Nano-hydroxyapatite (n-HAp), TCP (Plasma Biotal) and phosphate glass were used as fillers. The solutions (10% of filler) were spun at a working distance of 20 cm with a driving force of 30 kV. Materials were characterized using SEM and EDX (elemental mapping). Fibre diameter, pore size distribution as well as FTIR spectra for modified and unmodified fibres were also determined. To test cell responses to the materials human osteosarcoma cells were seeded on the scaffolds (2x10³ cells) per sample (10x10 mm). Cell growth was assessed using Alamar Blue up to day 7 in culture. Cell morphology was investigated using SEM.

RESULTS: SEM and EDX mapping evidenced the presence of fillers in the fibres structure (Fig. 1). The average fibre diameter of the electrospun composites was 1μm and membranes had uniform structure in all three materials. Phosphate glass and TCP particulates were 12 μm and EDX maps showed non-uniform distribution of the particles in the scaffold structure. AlamarBlue assay showed that cell growth on TCP and glass filled samples was similar to that

observed for control Thermanox surfaces. The growth rate was seemingly reduced on nanoHAp filled samples. SEM observations confirmed these results and at day 7 layers of well- developed and spreading cells were observed on all materials. Small differences in cell morphology between cells were observed; typically cells presented with a flattened morphology (as observed for Thermanox control surface – Fig. 2).

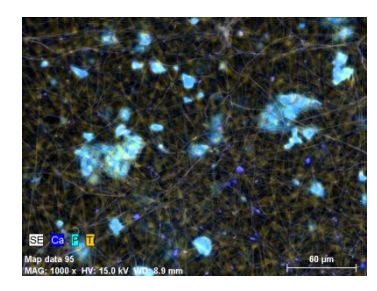


Fig. 1 Elemental map depicting distribution of the titanium doped phosphate glass filler in the PLDL scaffold

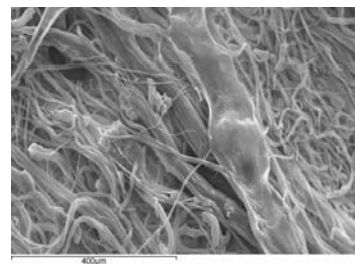


Fig. 2: Cells spreading on the surface of glass polymer scaffold.

DISCUSSION & CONCLUSION: Our previous studies demonstrated beneficial effects of phosphate glass filled polymers on cell responses. These results were not fully confirmed in this study. Similar cell responses were observed for glass and TCP filled materials. We anticipate that non-uniform distribution of glass particles in the three-dimensional substrate hindered expected positive effects of the glass. It was concluded that size of the glass particles distribution in the scaffold structure played a major role on cell responses.

REFERENCE:

Chrzanowski W., Abou Neel E.A., Lee K.-Y., Bismarck A., Young A.M., Hart A.D., Dalby M.J. and Knowles J.C.: Tailoring cell behaviour of polymers by the incorporation of titanium doped phosphate Glass Filler. Advanced Engineering Materials: Advanced Biomaterials 2010;12(7):B298-B308



Influence of varying HMDI crosslinking parameters on porcine dermis

<u>Helen Ashwin</u>*^{1,2}, John Hunt², Emilie Mausy¹, Jo Migliozzi³, David Beers³, and Stephen Wohlert¹

Covidien, 116 Avenue du Formans – BP132, F-01600 Trevoux, France. ²Clinical Engineering (UKCTE), The Institute of Ageing and Chronic Disease, University of Liverpool, Liverpool, L69 3GA, United Kingdom. ³Covidien, 60 Middletown Avenue, North Haven, CT 06473, USA.

INTRODUCTION: Collagen based surgical implants are used in a wide range of tissue repair applications. They can either be sourced from human donors (allograft) or animals (xenograft), with harvest locations including dermis, small intestine submucosa and pericardium. To help reduce antigenicity and provide the desired characteristics of the implant, all these materials are processed. In this study the effects of using 1,6 hexamethylene diisocyanate (HMDI) as a crosslinking reagent on acellular porcine dermal collagen was assessed. HMDI is incorporated into the amino acid structure of collagen by reacting with the amine groups, found on lysine and hydroxylysine side chains. To establish the degree of crosslinking achieved the lysine and hydroxylysine residues were measured by HPLC analysis after digestion. Any changes to the behavioural characteristics of the material were then assessed by subjecting them to differential scanning calorimetery (DSC) and enzyme digestion.

METHODS: Sample preparation: Porcine dermis was harvested and then prepared using the proprietary Permacol process, with the exception of the HMDI crosslinking step. 25 variants were produced varying the exposure duration and HMDI concentrations used.

Amino acid analysis: The samples were hydrolysed in constant boiling HCl. Following hydrolysis the samples were subjected to high performance liquid chromatography (HPLC) attached to a uv/vis detector and the amino acid levels quantified. Analysis performed by Alta Bioscience (Birmingham)

DSC: TA Q100 DSC, MT DSC822e and TA were used to determine the denaturation temperature (Td) of the samples. 10mg samples were placed in sealed sample pans, isocratic ramp was used starting at 20°C rising to 85°C at 3°/minute.

Enzyme analysis: 0.5g samples were exposed to collagenase type IV from *e.coli* at 37° for 20 hours, the remaining collagen weight was measured.

RESULTS: As the level of exposure to HMDI was increased either by exposure duration or the concentration, the levels of lysine and hydroxylysine measured reduced. A reduction in the lysine levels was observed as the HMDI concentration increased (Fig. 1) Indicating that

the HMDI had been incorporated in the collagen structure. As the amino acid concentrations reduced an increase in the Td temperatures was observed (figures 2).

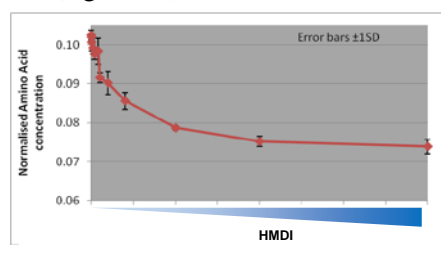


Fig. 1. Normalised lysine concentrations of porcine dermis exposed to various concentrations of HMDI for 20 hours.

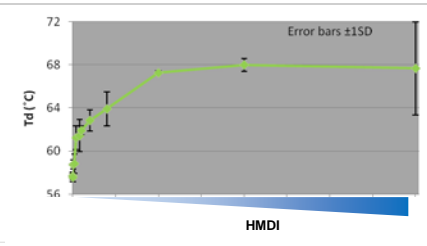


Fig. 2. Td temperatures of porcine dermis exposed to various concentrations of HMDI for 20 hours.

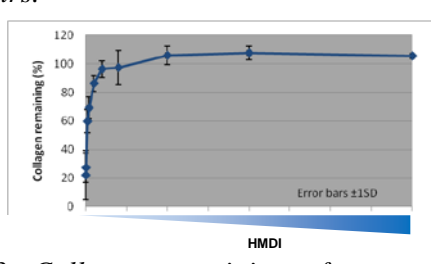


Fig. 3. Collagen remaining after exposure to collagenase enzyme for porcine dermis exposed to various concentrations of HMDI for 20 hours.

be used to add crosslinks into porcine dermis attached to the lysine and hydroxylysine side chains. The amount of HMDI crosslinking can be controlled by either altering the duration of exposure or the concentration of HMDI added to the reaction vessel. Adding HMDI crosslinks to the porcine dermis alters some of its characteristics, there is a shift in the denaturation temperature and increased enzyme resistance.



In Vivo and In Vitro assessment of foreign body reaction to HMDI crosslinked porcine dermis

Helen Ashwin*^{1,2}, Nick Bryan², Stephen Wohlert¹ and John Hunt²

¹Covidien, 116 Avenue du Formans – BP132, F-01600 Trevoux, France. ²Clinical Engineering (UKCTE), The Institute of Ageing and Chronic Disease, University of Liverpool, Liverpool, L69 3GA, United Kingdom.

INTRODUCTION: Biological implants manufactured from collagen can be used in a wide range of tissue repair applications. Upon implantation these materials can illicit a foreign body reaction. This is a critical part of the healing process, though an excessive reaction to the implant material can be detrimental to the patient and implant functionality. One of the first major cells of interest in this cascade is neutrophils. To help control the antigenicity and provide the desired characteristics biological implants are processed. Various processes are used to achieve this including, harvest location, decellularisation, crosslinking and sterilisation.

In this study the *in vitro* and *in vivo* inflammatory response of acellular porcine dermal collagen crosslinked with varying concentrations of 1,6 hexamethylene diisocyanate (HMDI) was assed.

METHODS: Sample preparation: Porcine dermis was harvested and then prepared using the proprietary Permacol process, with the exception of the HMDI crosslinking step. 25 variants were produced for the *in vitro* testing. 3 variants were selected for *in vivo* testing, non crosslinked, Permacol and highly crosslinked (100 times the HMDI concentration used in Permacol).

In vitro characterisation: Reactive oxygen species (ROS) mediated neutrophil activation assay. Discs of each material were placed in the bottom of a 96 well plate. The Able® cell activation test with Pholasin® reagents were used. The luminescence expressed by each material was read continuously for 200 minutes.

In vivo characterisation: Sub Cutaneious implants were performed on 6 week old male Wistar rats. 4 1cm² implants were positioned adjacent to the dorso-lumbar musculature. Sacrifices were performed on days 2, 7, 14 and 28. Tictoral histology was used to asses the foreign body reaction.

RESULTS: The *in vitro* assessment of the materials in the ROS assay did not show any significant differences between the non crosslinked sample and the crosslinking variants (see figure 1).

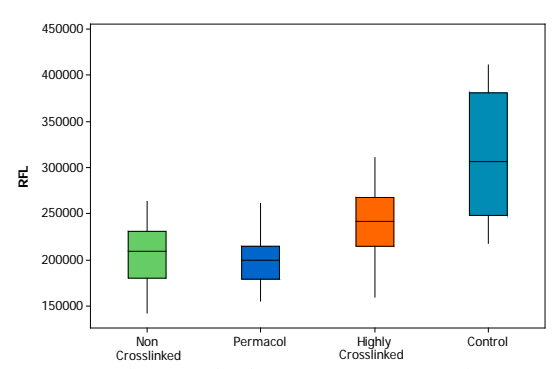


Fig. 1. Observed fluorescence results for the ROS assay of porcine dermis exposed to various concentrations of HMDI.

The histological analysis of the *in vivo* sections backed up the *in vitro* ROS results. With no differences being observed in the inflammatory response to non crosslinked and crosslinked material implanted, see figure 2.

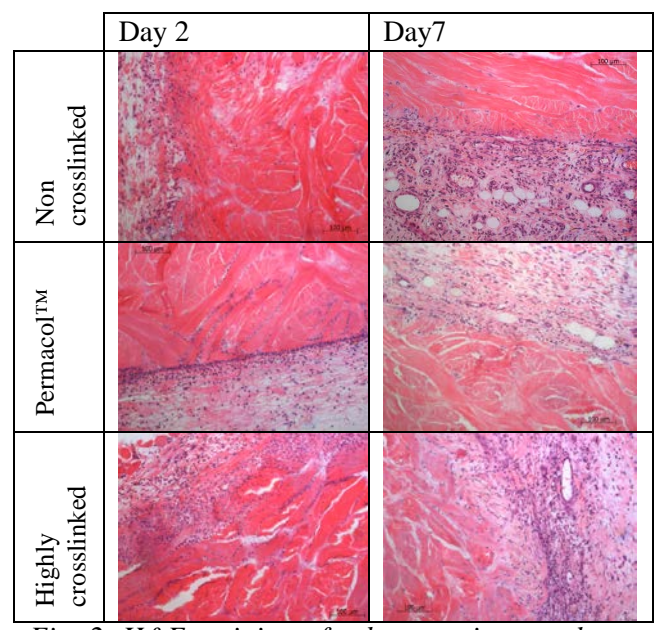


Fig. 2. H&E staining of sub cutaneious explants for days 2 and 7.

DISCUSSION & CONCLUSIONS: HMDI can be used to add crosslinks into porcine dermis. The addition of these crosslinks does not affect the *in vitro* and *in vivo* response to these materials.



Defining in vitro co-culture systems for human liver tissue engineering

M.Navarro1, L. Nelson1, O. Tura2, K.Samuel2, P.Hayes1, J. Plevris1

<u>1 Laboratory Department of Hepatology</u>, University of Edinburgh, Edinburgh, <u>2 CRM/Scottish Centre for Regenerative Medicine</u>, University of Edinburgh, 49 Little France Crescent Edinburgh, EH16 4SB, United Kingdom

INTRODUCTION: Development of new *in vitro* human hepatoxicity models, for pre-clinical drug development and cell therapeutics including bioartificial liver support systems, is challenging.

Fabrication of organotypic structures which mimic aspects of the complex structure of the liver require overcoming tissue engineering challenges, such as vascularisation to improve oxygen and nutrient supply. Co-culture of parenchymal cells with nonparenchymal cells on different extracellular matrix (ECM) scaffolds show evidence of improvement in hepatic cell functionality. growth Furthermore, the interactions morphology[1]. between cell-cell adhesions and signalling-pathways regulate cell phenotype and genotype expression during organogenesis, and in cancer[2].

In this preliminary study, we aimed to assess hepatic functionality in 2D co-cultures; and morphology in 3D co-cultures of Human Umbilical Vein Endothelial Cells (HUVECs) with hepatic C3A cells, using appropriate ECM scaffolds.

METHODS: HUVECs and C3As were seeded at the same concentration 1:1 and at a more physiological ratio, 3:1 (C3As: HUVECs). Timelapse fluorescence microscopy was used for 24 hours with appropriate immunostaining in both mono and co-culture systems. Cellular phenotype in either Matrigel or MaxGel were tested as candidate bio matrices, and compared with standard 2D cultures of each cell line on plastic and collagen-1 substrates as controls. Albumin Blue 580 Fluorescence Assay was used for testing hepatic-specific functionality.

RESULTS: Albumin synthesis increased in the co-culture with a parallel increase of C3A cell number by day 3, at a ratio of 3:1 (C3As: HUVECs). This ratio was optimal for phenotype and for integrin expression using endothelial culture medium (Lonza EGM-2 medium, UK). Tissue-specific phenotype in Matrigel was maintained for 48 hours in co-culture in ECM. Using time-lapse, C3A cells migrate toward

HUVECs promoting the formation of an interconnected vascular network with defined geometry (Fig 1). By contrast, 3D MaxGel sandwich culture promoted differentiation and proliferation of C3As, but no vascular structures were observed.

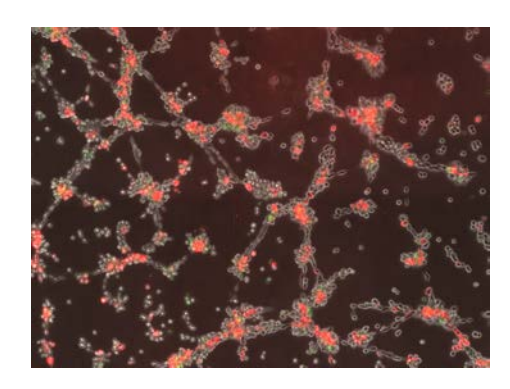


Fig. 1: Time-lapse fluorescence microscopy. Coculture of HUVEC (Red) and C3A (Green) cells in Matrigel after 24 hours in co-culture.

DISCUSSION & CONCLUSIONS: Optimisation of cell phenotype is a critical factor in developing a successful hepatic co-culture system. This study provides a preliminary step in the understanding of cellular responses in different micro-environments for future development of a vascularised liver tissue for downstream pharmaceutical applications. On-going studies: 3D co-culture studies with hyaluronic acid-based hydrogels into a sponge as an ECM scaffolding structure, drug metabolism (CYP450) assays, metabolomics and defining cell-cell/ cell-matrix mechanical properties using Atomic Force Microscopy.

REFERENCES:

1. A. Soto-gutierrez, N. Navarro-alvarez, H. Yagi, M. L. Yarmush, and N. Kobayashi, "Engineering of an Hepatic Organoid to Develop Liver Assist Devices," *October*, vol. 19, no. 6, pp. 815-822, 2010 2. K. Matsumoto, H. Yoshitomi, J. Rossant, and K. S. Zaret, "Liver organogenesis promoted by endothelial cells prior to vascular function.," *Science (New York, N.Y.)*, vol. 294, no. 5542, pp. 559-63, Oct. 2001.



Developing electrospun scaffolds with tailored geometries

C M Rogers¹, S Toumpaniari¹, R Bail², J Segal², K M Shakesheff¹, F R A J Rose¹

1 Tissue Engineering, School of Pharmacy, University of Nottingham, England. 2 Manufacturing Research Division, School of Pharmacy, University of Nottingham, England.

INTRODUCTION: Electrospinning technique widely used to fabricate fibrous scaffolds for tissue engineering. Experimental parameters such as flow rate and applied voltage can be adjusted to influence the morphological aspects of the scaffold. More recently the ability of the collector plate design to influence the morphology of the fibrous scaffolds has been investigated. In this study, we show the ability of patterned collectors produced by rapid prototyping, to produce electrospun scaffolds with tailored The three-dimensional scaffold geometries. geometries generated were shown to influence both cell adherence and growth.

METHODS: Patterned collectors composed of acrylic oligomer were manufactured on a rapid prototyping system. Collector geometries (including hexagonal and sinusoidal) designed and manufactured. Poly(lactide-coglycolide) was electrospun onto the patterned collectors for 3 hours. The generated fibrous scaffold geometries were visualized by scanning electron microscopy. Electrospun PLGA disks (0.5mm) were cut from the scaffolds and seeded with 3T3 fibroblast cells. The constructs were cultured for up to 4 days and imaged using both fluorescence stereomicroscopy and microscopy.

RESULTS: Resin based collectors with sawtooth, sine wave and hexagonal geometries were successfully fabricated using rapid-prototyping on the Envisontec PerfactoryTM. Patterned electrospun scaffolds resembling the geometries of the collectors were produced. 3T3 fibroblast cells were found to preferentially adhere to the patterns of the scaffolds.

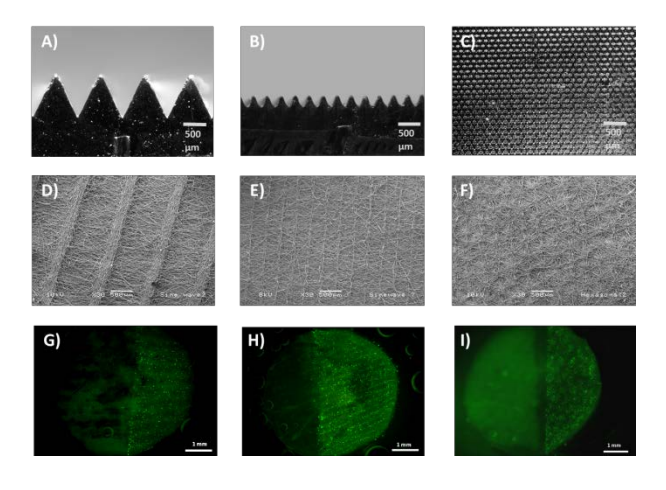


Fig. 1: Images of A,B,C) Resin based collectors with sawtooth, sinusoidal and hexagonal geometries, D,E,F) Electrospun scaffolds with patterns resembling the collectors and G,H,I) 3T3 fibroblasts seeded onto scaffolds preferentially adhered to the fibre patterns.

DISCUSSION & CONCLUSIONS: A novel method for developing patterned electrospun scaffolds has been illustrated. The patterning of the fibres has been shown to directly influence mammalian cell adhesion. This scaffold fabrication method can therefore be used to fibrous scaffolds with directional cues to influence cellular behavior.

REFERENCES: ¹ Bhardwaj et al (2010), *Biotechnology Advances*, **28**(3):325-47. ² Li et al (2005) *Nano Letters* 5:913-6. ³ Zhang et al (2007) *Advanced Materials* **19**:3664-7.

ACKNOWLEDGEMENTS: The authors would like to thank the EPSRC Centre for Innovative Manufacturing in Regenerative Medicine.



Production of dipentaerythritol-poly(ethylene glycol) acrylate based constructs via microsteriolithography for cell-based tissue engineering

HT Gilbert¹, IA Barker², S Leigh³, JA Covington³, AP Dove², JA Hoyland¹, SM Richardson¹

¹ Regenerative Medicine, Faculty of Medical and Human Sciences, University of Manchester, Manchester, M13 9PT. ² Department of Chemistry, University of Warwick, Coventry, CV4 7AL;

³ School of Engineering, University of Warwick, Coventry, CV4 7AL.

INTRODUCTION: Tissue engineering often requires the use of cell scaffolds in ordered to provide cells with an adherent surface and help direct tissue formation and function. In addition to biocompatibility, the reproducibility and accuracy of scaffold fabrication is important, becoming more challenging with increasing complexity of the modelled tissue. Here we present a novel. solvent free "off the shelf" resin formulation based on acrylate end-capped low molecular weight linear PEG, in which crosslinking is brought about by the use of dipentaerythritol penta-/hexaacrylate, for fabrication of complex cell scaffolds through the use of UV light microsteriolithography (µSL). We demonstrate, as a proof of principle, the biocompatibility of the scaffolds and propose this technique for the fabrication of complex cellular scaffolds.

METHODS: The liquid resin (poly(ethylene glycol) diacrylate and dipentaerythritol penta-/hexa-acrylate) (Sigma) was photopolymerised using µSL to form a disc with a surface area of 0.5cm². Human mesenchymal stromal cells (MSCs) were isolated from the bone marrow aspirates of 4 patients following hip replacement surgery, expanded in culture and seeded onto cell scaffolds at a density of 5x10³ cells/cm². Following culture for 1, 3 and 7 days, cell viability and adherence/proliferation were assessed Live/Dead staining (2µM calcein AM and 4µM ethidium homodimer-1) (Invitrogen) quantification of cellular DNA using Picogreen assay (Invitrogen), respectively.

RESULTS: All MSCs remained viable at all 3 time points studied (Figure 1 A-C,E-G). The density of adhered cells increased with culture duration, suggesting cells were able to proliferate on the surface of the scaffolds (Figure 1 A-C,E-G), also supported by the Picogreen proliferation data (Figure 2).

The number of MSCs adhered to scaffolds and tissue culture plastic (TCP) increased with increasing culture duration, with cell numbers significantly greater at days 3 and 7 compared to day 1 ($p \le 0.05$) (Figure 2). There was no significant

difference in adherent cell number between MSCs seeded on scaffolds or TCP at any of the three time points analysed (Figure 2).

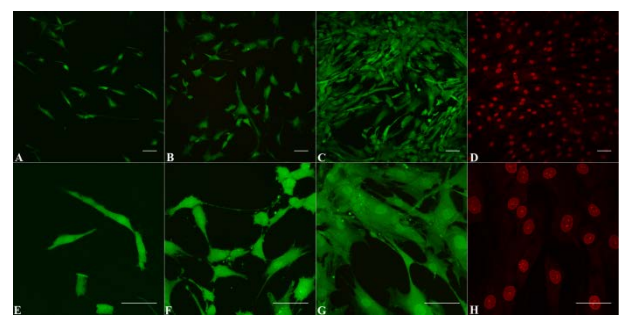


Fig. 1: Live/dead images of MSCs cultured for A+E: 1 day, B+F: 3 days and C+G: 7 days. D+H: methanol treated dead cells control. Scale bars = $50\mu m$.

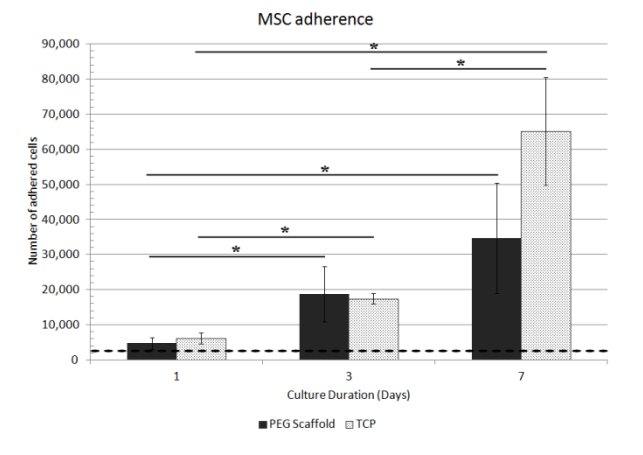


Fig. 2: Number of adhered MSCs on scaffolds and TCP following 1, 3 and 7 days of culture. Dotted line indicates number of seeded cells (2500) and * denotes significance $p \le 0.05$.

DISCUSSION & CONCLUSIONS: Scaffolds were biocompatible, with MSCs not only adhering to the scaffolds but proliferating in a similar manner to that observed with TCP. We propose the use of μ SL as a means to fabricate complex cell scaffolds for use in tissue engineering.

ACKNOWLEDGEMENTS: The authors would like to acknowledge the BBSRC and EPSRC for funding.



Self-assembling peptide gels for intervertebral disc tissue engineering

S Wan¹, A Saiani¹, S Richardson², J Gough¹

¹School of Materials, The University of Manchester, Manchester, M13 9PL. ²School of Biomedicine, The University of Manchester, Manchester, M13 9PT.

INTRODUCTION: Back pain affects 80% of people in their lifetime and costs the UK economy £12 billion annually [1]. While aetiology varies, degeneration of the intervertebral discs (IVDs) is strongly associated with back pain in over 40% of cases [2].

IVDs are found in between the vertebrae of the spine where they act as shock absorbers and allow movement of the spine. Each disc consists of the tough fibrous annulus fibrosus (AF) which surrounds the gel-like nucleus pulposus (NP). With age, the NP dehydrates and deteriorates which accelerates disc degeneration and can cause back pain. Current treatments are symptomatic however a cell-based therapy has the potential to be curative.

While adult stem cells have been shown to be suitable cell source for IVD tissue engineering, appropriate biomaterials are required [3].

A self-assembling octapeptide (FEFEFKFK F-phenylalanine, E-glutamic acid, K-lysine) was chosen as the scaffold material due to its biodegradability, ease of modification and bioactivity. In solution, the peptide self-assembles and forms β -sheet rich nanofibres which entangle to form self-supporting hydrogels [4]. The nanofibres are of similar scale to various extracellular matrix components.

METHODS: 30mgml⁻¹ peptide hydrogels were prepared. Bovine nucleus pulposus cells (bNPCs) were used to assess the biocompatibility of the hydrogels. Live/dead staining was used to assess cell viability and lactate dehydrogenase (LDH) assay was used to measure cell number.

RESULTS:

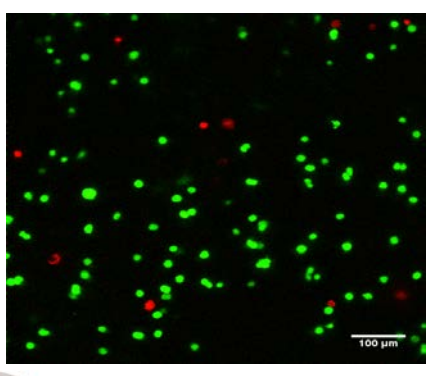
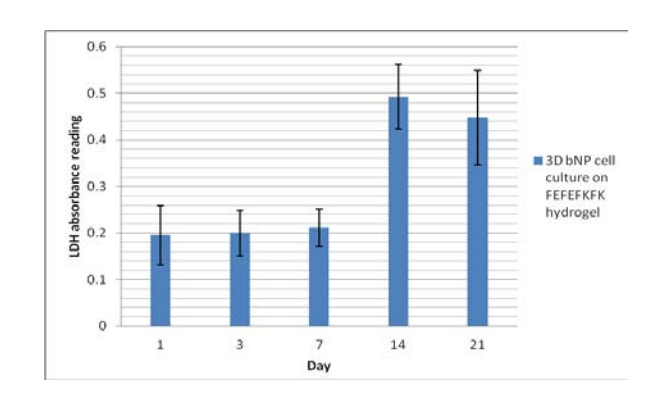


Fig. 1: Cell viability of bNPCs encapsulated in FEFEFKFK hydrogel after 1 day of culture. Live cells have green fluorescence whilst dead cells have red fluorescence.



Graph.1: Graph showing LDH absorbance readings for 3D cell culture of bNPCs on FEFEFKFK hydrogels.

bave never been cultured with octapeptide hydrogels. 3D cell culture was carried out as it better replicated the natural NP environment. The fluorescence imaging showed the distinctive rounded morphology of NPCs and 93% of cells were viable (stained green) after 1 day of cell culture. The LDH assay showed evidence of cell proliferation with increasing time.

In conclusion, the nanofibrous self-assembling hydrogels could sustain the 3D cell culture of bNPCs for up to 21 days. The gels successfully mimicked the NP and allowed cells to maintain their characteristic rounded morphology which is crucial in maintaining their phenotype.

REFERENCES: [1] Maniadakis N *et al*, *Pain*, 2000, **84** 95-103. [2] Cheung K *et al*, *Spine*, 1976, **34** 934-940. [3] Richardson S *et al*, *Biomaterials*, 2008 **29** 85-93 [4] Collier J *et al*, *J Am Chem Soc*, 2001, **123** 9463-9464.

ACKNOWLEDGEMENTS: Biomaterials & Tissue Engineering Group; Polymers & Peptides Research Group.



Processing silk-based naturally derived materials for three-dimensional cell culture and tissue engineering applications

K Luetchford¹, J Chaudhuri², P De Bank¹

¹ Department of Pharmacy and Pharmacology, University of Bath, UK. ² Department of Chemical Engineering, University of Bath, UK.

INTRODUCTION: The extracellular matrix (ECM) acts as a scaffold for cells, providing physical support for cell attachment as well as influencing cell migration, proliferation. differentiation and cell-cell communication. In order to engineer viable tissues, cells must be provided with a three-dimensional scaffold to mimic or recreate the in vivo ECM. This study explores the use of silk fibroin (SF), blended with other naturally derived proteins, as a scaffold material for two- and three-dimensional cell culture. Processing the material blends into microparticles, or cell carriers, provides the potential to assemble the particles into a macroscopic tissue construct.

METHODS: SF was collected from the cocoons of Bombyx mori [1]. Briefly, the cocoons were boiled in 0.02 M Na₂CO₃ before rinsing in distilled water. The dried silk was dissolved in 9 M LiBr before dialysis against distilled water for two to three days. Type A gelatin was dissolved in water at 60°C, and maintained at 37°C before use. 3T3 fibroblasts were maintained in DMEM with 10% (v/v) fetal bovine serum, 100 U/mL penicillin and 100 µg/mL streptomycin, at 37°C in a 5% CO₂ atmosphere. To assess cell adhesion and viability on the material surface, 3T3 cells were seeded in 48 well plates coated with the relevant matrix. Cell viability was assessed using an MTS assay. A microfluidic flow-focussing device was used to process SF and SF-gelatin blends into spherical microparticles (figure 1).

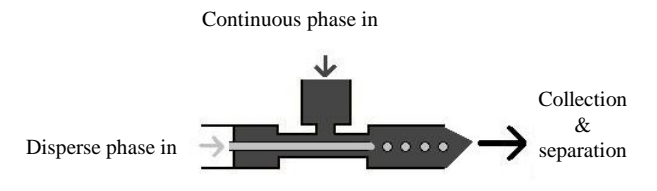


Figure 1: Schematic of the microfluidic flow-focussing device used to generate microparticles. The continuous phase (oleic acid/methanol/Span 80 (74:25:1)) is shown in dark grey, while the disperse phase (aqueous SF/gelatin) is in light grey. Both inputs are controlled by syringe pumps. The output was collected into methanol.

RESULTS: In 2D, 3T3 cells were viable on SF coatings though cell adhesion was improved by including a proportion of gelatin. SF hardens on exposure to methanol (the protein converts to a β -sheet dominated structure) providing structural strength within the microcarriers. SF-gelatin blended at a ratio of 70:30 (dry weight) produced spherical microparticles that were easily collected from solution, and supported 3T3 cell growth (figure 2). The size of the particles could be altered by varying the ratio between the inner and outer flow rates.

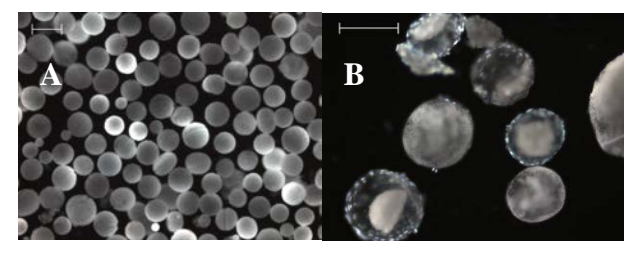


Figure 2: Fluorescent image of SF-gelatin microparticles (A) without cells, and (B) with adherent Hoechst 33342-stained 3T3 cells. Scale bars represent 200 µm.

DISCUSSION & CONCLUSIONS: Using blended materials allows the creation of final products with tailored properties, for ease of handling and production as well as improved cell viability. With SF providing the bulk of the scaffold, other proteins such as gelatin or collagen can be incorporated into the microparticles. The microparticles produced in this study have the potential to be used as building blocks for three-dimensional tissues. Approaching tissue design in this way allows architecture to be developed from the bottom up, combining different cell types or cell carriers with different properties to direct cell differentiation.

REFERENCES: ¹ X Wang, E Wenk, A Matsumoto, et al (2007). *Journal of controlled release* **117(3)**:360-370.

ACKNOWLEDGEMENTS: The authors would like to thank to the Medical Research Council for funding this project.



Evaluation of electrospun gelatin/ polycaprolactone as a potential artificial corneal stroma

JB Rose¹, DJ Williams², A. El Haj³, H. Dua⁴, A. Hopkinson⁴, FRAJ Rose¹

¹School of Pharmacy, University of Nottingham, UK. ²Healthcare Engineering Group, Loughborough Universty, UK. ³Institute for Science and Technology in Medicine, Keele University, UK. ⁴School of Clinical Sciences, University of Nottingham, UK.

INTRODUCTION: Corneal transplant recipients who have experienced more than one rejection episode currently have very little clinical option. Keratoprostheses typically have low success rates and are associated with multiple complications on failure¹. There is currently a clinical need for a synthetic, artificial corneal substrate capable of reducing inflammation, inhibiting vascularisation and stabilising the hostile ocular surface environment in these patients.

Herein the authors evaluate *in vitro*, the suitability of electrospun gelatin/polycaprolactone (PCL) sheets seeded with human corneal keratocytes (HCK) as a potential candidate for clinical development.

METHODS: All scaffolds were electrospun from blends of gelatin and PCL at various ratios to form nonwoven fibrous mats. The fibre diameter and mat thickness was measured in 4 different blend ratios (100:0, 50:50, 25:75, 0:100 – gelatin: PCL) was measured using scanning electron microscopy (SEM) and histological cross sectioning.

Crosslinking was required in the case of the pure gelatin scaffold, which was achieved through treatment with gluteraldehyde vapour. Residual aldehyde was blocked with a glycine solution post cross-linking.²

Proliferation of HCKs on the scaffolds was quantitatively assessed through the AlamarBlue® assay, measuring metabolic activity of the cells cultured on the scaffolds after 1, 3, 6 and 12 days. SEM was used to investigate cell growth patterns over the scaffolds.

RESULTS: The four blends of gelatin:PCL were electrospun with a range of fibre morphologies and in turn significant variation in fibre diameter (Fig. 1). The mat thickness was relatively well controlled and fell within the 60–80µm range.

HCK cells could be successfully cultured on all of the scaffolds after UV sterilisation. Whilst each blend showed varied rates of proliferation after 6 days of culture there were no significant differences between the scaffolds after 12 days (Fig 2).

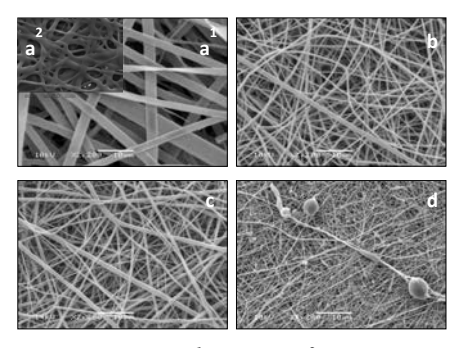


Fig.1 SEM images of a^1)100:0; a^2) 100:0 crosslinked with gluteraldehyde; b)50:50; c) 25:75; d) 0:100 blends of electrospun gelatin:PCL.

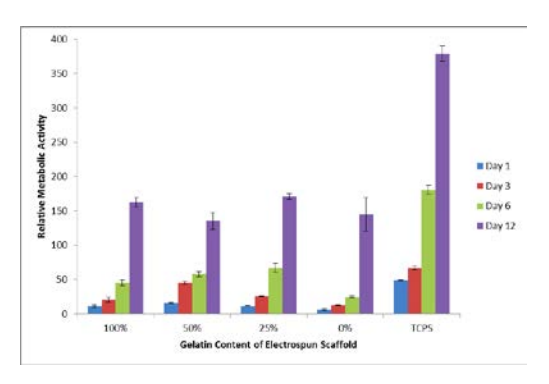


Fig.2 Representative data showing comparison of cell proliferation of HCKs on gelatin: PCL scaffolds at 1,3,6 and 12 days. Mean \pm SEM (n=2)

demonstrates that gelatin:PCL blends can be electrospun with modest control and that the electrospun sheets possess good cell compatibility. Whilst increased gelatin content may offer better initial cell adhesion, cells proliferate to confluence over 12 days even its absence. Control of the blend ratio will offer a level of control over both degradation rate and mechanical strength. To the authors knowledge this is the first demonstration of culturing this cell type upon electrospun gelatin:PCL blends. Although early on in the process, this work represents a good starting point, and a lead into the next phase of development.

REFERENCES: ¹ F. Chang Lam, et al.(2011) Br. J. Ophthalmology. ²S. Eun Kim, et al.(2009) Biomaterials



Developing an autologous engineered connective tissue using a biodegradable scaffold for the treatment of stress urinary incontinence and pelvic organ prolapse

S Roman¹, N Osman^{1,2}, A Mangera^{1,2}, AJ Bullock¹, CR Chapple², S MacNeil¹

Kroto Research Institute, Department of Materials Science and Engineering, University of Sheffield, UK. ² Royal Hallamshire Hospital, Sheffield, UK.

INTRODUCTION: Stress urinary incontinence (SUI) and pelvic organ prolapse (POP) are very bothersome diseases with a huge and rising prevalence in women from all ages [1]. Currently there is no recommended material for use in the surgical management of these disorders. These materials are all used as cell free prosthesis and are often degraded and their biomechanical properties deteriorate with time producing worrying failure and erosion rates.

Our aim is to develop a cell impregnated scaffold which will achieve long lasting repair by good integration into the native tissues maintaining the biomechanical properties with time by renewal of extracellular matrix (ECM) components.

METHODS: Th PLA (Thermoannealed poly-(L)-lactic acid) was chosen as our candidate scaffold, being a biodegradable material which was made via electrospinning technique in a clean room.

Tissue engineered prosthesis were developed under free, static and dynamic conditions from comparing oral mucosa fibroblasts (OFs) and adipose-derived stem cells (ADSCs) for: 1. Cell attachment using Alamar Blue (vital stain) and DAPI (nuclear stain). 2. Collagen production using Sirius red staining. 3. Biomechanical properties using BOSE electroforce tensiometer. 4. Scaffold contraction using serial photographs. 5. Immunostaining for collagen I, III and elastin.

RESULTS: Both cell types, OFs and ADSCs, showed good cell attachment and proliferation on PLA scaffolds. However, while ADSCs produced higher amount of total collagen under free condition, OFs produce more ECM under dynamic condition. Same is revealed from biomechanical properties where ADSCs under free condition achieved the strongest tissue engineered prosthesis with closest properties to the native tissues [2].

Immunostaining showed very good ECM distribution for ADSCs were cultured under free condition; and, interestingly, higher elastin production for OFs under dynamic condition.

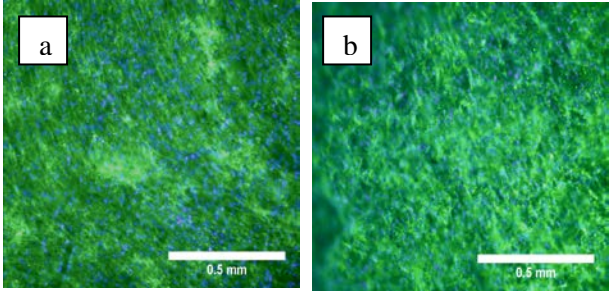


Fig. 1: Distribution for collagen I (a) and III (b) (green color) with cell nucleus (blue color) when ADSCs were cultured under free condition using immunostaining and DAPI respectively.

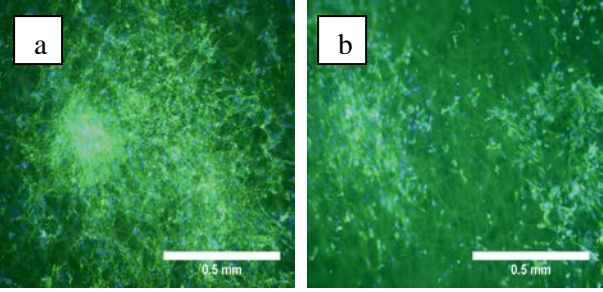


Fig. 2: Distribution for collagen I (a) and elastin (b) (green color) with cell nucleus (blue color) when OFs were cultured under dynamic condition using immunostaining and DAPI respectively.

DISCUSSION & CONCLUSIONS: In summary we seek to have tissue engineered prosthesis with good biomechanical properties at time of implantation. However, now we are considering issues of implantation in ongoing work. This is looking at tissue integration, immune response, neovascularisation and the production of new ECM *in vivo* for lasting repair of SUI and POP.

REFERENCES: ¹ L.D Cardozo and S.L Stanton (1980) Genuine stress incontinence and detrusor instability--a review of 200 patients. *Br J Obstet Gynaecol* **87**(3):184-90. ² L. Lei, Y. Song, R. Chen (2007) Biomechanical properties of prolapsed vaginal tissue in pre- and postmenopausal women. *Int Urogynecol J Pelvic Floor Dysfunct* **18**:603-7.

ACKNOWLEDGEMENTS: The Urology Foundation and Robert Luff foundation and the TRUST European Marie Curie Network.



Development and Characterisation of Biodegradable PLGA Scaffolds for Delivering Corneal Limbal Stem Cells to Damaged Corneas

<u>F Sefat¹</u>, P Deshpande¹, C Ramachandran², I Mariappan², D Balasubramanian², G Vemuganti³, AJ Ryan⁴, VS Sangwan², S MacNeil¹

¹Department of Material Sciences & Engineering, Kroto Research Institute, University of Sheffield, Sheffield, United Kingdom, ²Sudhakar and Sreekant Ravi Stem Cell Lab, LV Prasad Eye Institute, Kallam Anji Reddy Campus, L V Prasad Marg, Hyderabad, India, ³School of Medical Sciences, University of Hyderabad, Hyderabad, India, ⁴Department of Chemistry, University of Sheffield, Sheffield, United Kingdom.

INTRODUCTION: There are a range of conditions which affect the stem cell population that maintains the avascular transparent surface of the cornea. When these cells are lost it is possible to culture them from an adjacent eye or donor eye and transplant them to the damaged eye. This is most commonly done by culturing the cells on donor human amniotic membrane and then transplanting this to the eye (cells uppermost) where this membrane degrades over several weeks leaving cells in place. However access to this donor tissue can be difficult and results with it are variable and all human donor tissue carries some risk of disease transmission. The aim of this research is to make a synthetic biodegradable alternative membrane to replace the use of human amniotic membrane for this purpose. We selected PLGA as it has been used for many years in dissolvable sutures, it is biodegradable and biocompatible.

METHODS: We used biodegradable Poly DL-lactic-co-glycolic (PLGA (44 kg/mol); Sigma Aldrich, with a 50:50 ratio of PLA and PGA). The scaffolds were electrospun to produce fiber diameters of 3-5μm. Rabbit limbal epithelial cells were isolated from the limbus and cultured on these scaffolds for up to 6 weeks. The rate of degradation of the scaffolds was investigated with and without cells *in vitro* and examined by SEM. Image J software was used to measure fiber diameters. Scaffold handling was assessed by picking up scaffolds with a pair of forceps. Scaffolds storage was examined at temperatures -80°C to +50°C, assessing fiber diameter and integrity over periods of up to 16 weeks.

RESULTS: The results of *in vitro* degradation of PLGA scaffolds with an initial fiber diameter of 3-5µm showed that degradation was clearly evident within 3 weeks and this was slightly faster in the

presence of cells (Figure 1.a shows results with cells). Handling results showed that these scaffolds could be handled for up to 3 weeks but there was clear evidence of breakdown beyond this.

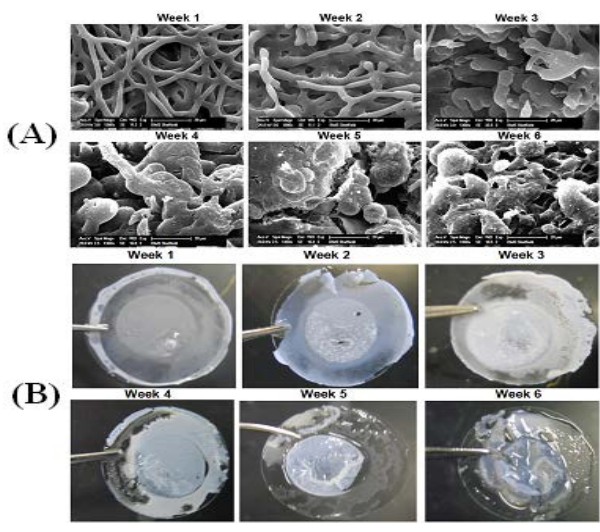


Fig 1. In vitro degradation (by SEM) (A) and scaffold handling (B) of electrospun PLGA (50/50) scaffolds in the presence of rabbit limbal epithelial cells over 6 weeks at 37°C.

Storage results showed that scaffolds at 4°C were stable for only 6 weeks with a clear swelling in scaffold fibers after this point. For longer term storage scaffolds could be stored at lower temperatures (-20°C or -80°C) for at least 16 weeks without any change in fiber diameter.

CONCLUSIONS: We suggest that this carrier may be used as an alternative to the amniotic membrane.

REFERENCES: Blackwood KA et al. (2008) *Biomaterials* 2008 29:3091-104, Deshpande P et al. (2010) *Regen Med.* 5:395-401.

ACKNOWLEDGEMENTS: This work is funded by a Wellcome Trust, Affordable Healthcare for India award.



Development of a simple 3D melanoma skin model incorporating Pt (II) labels and two photon / time-resolved emission imaging microscopy for detection

Ahtasham Raza¹, Elizabeth Baggaley², Julia A. Weinstein², Sheila MacNeil¹ and John W. Haycock¹

**Ikroto Research Institute, Materials Science & Engineering and ²Department of Chemistry, University of Sheffield

INTRODUCTION: Previously, small robust platinum (II) complexes (PtLnCl) have been developed [1,2], which subsequently we used in vitro for live cell imaging by confocal and time resolved emission-imaging microscopy (TREM) [3]. Results showed that complexes had long (microsecond) lifetimes. Furthermore, they are photo stable, have a high emission quantum yield (70%) and low cytotoxicity. Lifetime is related to oxygen tension in solution. Therefore this study is a step towards a novel non-invasive imaging method combining Pt (II) complexes and TREM for melanoma cell detection, based on a hypothesis of differential oxygen regulation between melanoma cells and normal skin keratinocytes (and fibroblasts). To test this we are developing a simple 3D human in vitro melanoma skin model and labeling the total cell population with Pt (II) complexes. Characterization by 3D confocal microscopy and 2-photon microscopy is being used initially to develop the model, leading towards TREM lifetime fluorescence for differential detection

METHODS: A an in vitro melanoma skin model using a 12-well plate containing human HBL melanoma cells and HaCat keratinocytes was constructed. HBL cells were labeled (with or without) Cell Tracker® Red for 48 hours at a low density, followed by HaCat keratinocytes on top thereafter (with and without) Cell Tracker® Green. Samples were cultured for a further 2 days submerged and for 4 days at an air-liquid interface. Samples were then labeled with Pt (II) complexes for 15 minutes. A Zeiss LSM510 confocal microscope was used for excitation at 488nm (green emission) and at 543nm (red emission). Two-photon excitation at 800nm was used for Pt (II) complexes.

RESULTS:



Figure 1: Confocal z-stack of melanoma skin construct showing HBL melanoma cells (Cell Tracker Red) and HaCat keratinocytes (Cell

Tracker Green). Left to right – bottom to top of construct (z stack slice shown at every 8μm, total depth of construct - 68μm).

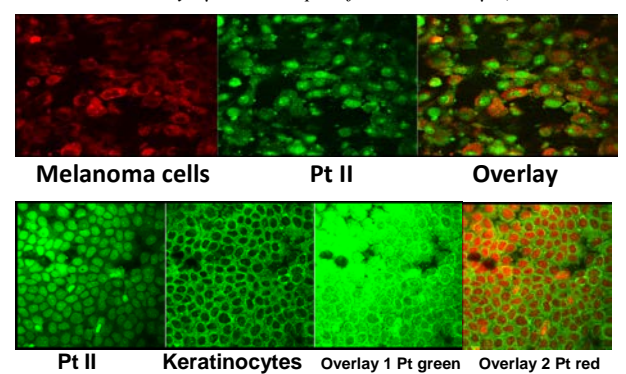


Figure 2: Top) Melanoma cells alone labeled with Cell Tracker Red and Pt (II). Bottom) Keratinocytes cells alone labeled with Cell Tracker Green and Pt (II).

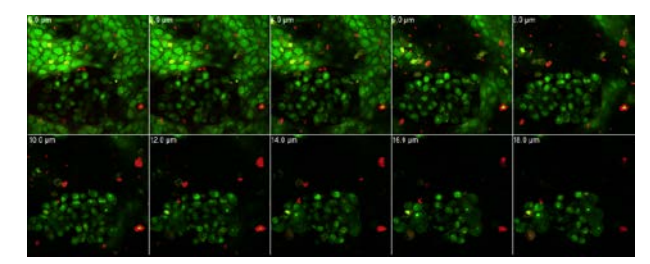


Figure 3: 2-photon z-stack of melanoma skin construct. After 6 days in culture Pt (II) only label present identifying melanoma cell and keratinocytes at 800nm excitation. Scan interval 2um.

DISCUSSION

We have developed a simple in vitro melanoma model in which a multilayer of keratinocytes forms an uppermost epithelium physically above the melanoma cells. Basic 3D imaging reveals the respective location of these cells using Cell Trackers and the ability to visualise the model additionally using Pt(II) labels by confocal and 2-photon excitation. 3D model conditions will now be used to ascertain the potential difference in lifetime for Pt(II) labelled cells for discrimination between keratinocytes and melanoma cells, with a forward plan to extend the model in to the use of fibroblasts.

REFERENCES:

¹ J. Williams, A. Beeby, J. Weinstein *et al* (2003) *Inorg Chem* 42:8609-11. ² S. Farley, D. Rochester, J. Williams *et al* (2005) *Inorg Chem* 44:9690-03. ³ SW. Botchway, M. Charnley, JW.Haycock, AW Parker, DL Rochester, JA Weinstein, JAG Williams (2008) *Proc Natl Acad Sci* 105:42 16071-76.

ACKNOWLEDGEMENTS: We thank the BBSRC for funding AR with a PhD studentship.



Continual propagation of cells in three-dimensional culture

A Chhatwal^{1, 2}, R Mold², S Przyborski^{1, 2}

¹ Department of Bioactive Chemistry, Durham University, United Kingdom. ² Reinnervate Ltd., NETPark Incubator, Sedgefield, United Kingdom.

INTRODUCTION: Traditionally, cell culture has been undertaken in two dimensions, with cells being grown in monolayers. Presenting cells with a two dimensional growth substrate causes them to aberrantly flatten out, and lose their characteristic shape¹. Cell shape is fundamental to cell function, and thus the artificiality of 2D cell culture may produce inaccurate and physiologically irrelevant observations of cell behaviour². Alvetex® is an inert porous polystyrene scaffold engineered into discs that are compatible with existing cell culture plastic-ware. In this way, the technology enables routine cell culture in 3D, in a simple, straightforward and cost-effective manner. Being able to maintain cells in 3D long term would allow more insight into the impact cell shape has on cell function, as well as enabling cell biology research to be conducted in more representative culture systems

METHODS: Alvetex® 6 well inserts were placed in a standard 6 well culture plate and sterilised with 70% EtOH. HepG2 cells were harvested from T75 culture flasks and seeded at a cell density of 1 x10⁶ cells per Alvetex® disc in a concentrated 150µl droplet. Cultures were maintained at 37°C with 5% CO₂ for 3-4 days, with media changes every other day. After incubation, cells were retrieved. 3ml Trypsin-EDTA solution was added to each disc and the plates were placed on a shaking platform at 37°C for 15 minutes. The trypsin solution was pipetted up and down over the surface of each disc several times, and transferred to a 15ml tube. A further 3ml fresh media was also pipetted over each disc before being added to the Cells were collected by trypsin solution. centrifugation and assessed for viability. Samples were also collected for histology. Cells were then re-seeded using the same protocol as for the first generation. Cells at P13 were retrieved and cryopreserved in DMSO.

RESULTS: As the graph in Figure 1A shows, HepG2 cells can be retrieved from a 3D scaffold, and re-passaged onto fresh scaffold discs, allowing the long term culture of cells in 3D. Trypan Blue counts indicate that cell viability remains above 98% between P1 and P13, and that cell yield remains constantly high.

Histology data similarly shows successful cell retrieval and cells appear viable throughout the experimental period (Fig. 1B) Cells at P13 were successfully frozen down, and brought up straight into 3D culture with no significant loss in viability.

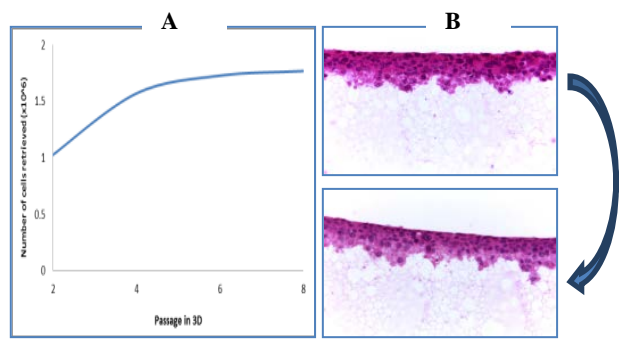


Fig. 1: A) Shows the average cell yield per Alvetex® disc between P1 and P8. B) Shows H&E stained cells at P2and P12, with no visible change in viability or cell density. Magnification: 40x

DISCUSSION & CONCLUSIONS: The results indicate that a successful protocol has been established for the long term maintenance and cryopreservation of hepatocytes in their native three-dimensional state, using the polystyrene scaffold Alvetex®. This will allow further research into how cell morphology is determined by cellular environment, and how morphology in turn determines cell function. It also has implications for pharmacology and preclinical drug testing. The protocol designed here will be used to investigate whether primary liver explants can be maintained in culture for extended periods of time, allowing functional assays for potential drugs to be carried out in vitro, with a higher degree of physiological relevance than those currently achievable using existing models.

REFERENCES: ¹ M. Schutte, B. Fox, M.O. Baradez, et al (2011) *Assay & Drug Dev. Tech.* **9(5)**:475-486. ² C.S. Chen, X. Jiang, & G.M. Whitesides (2005) *MRS Bulletin* **30(3)**: 194-201

ACKNOWLEDGEMENTS: This work was funded by a CASE studentship from BBSRC, with industrial support from Reinnervate Ltd.



Development of tissue engineered skeletal muscle constructs for nutritional supplement testing

DJ Player^{1,2}, S. Passey¹, V. Mudera³, MP Lewis^{1,2,4}

¹Musculoskeletal Biology Research Group, School of Sport, Exercise and Health Sciences, Loughborough University, ²Institute for Sport and Physical Activity Research, University of Bedfordshire, ³UCL School of Orthopaedics and Musculoskeletal Science, ⁴UCL School of Life and Medical Sciences

INTRODUCTION: Nutritional therapies are used in the treatment and prevention of many skeletal pathologies. Ethical muscle (SkM) methodological limitations prevent controlled in vivo experiments being conducted to investigate a effect, reducing the supplements empirical data for patients and clinicians alike. Utilising an in vitro-based 3D model would many of issues. these investigations using a representative extracellular matrix (type 1 collagen), have shown in vivo-like characteristics with respect to the macroscopic morphology, histology and gene expression [1-2]. These experiments have utilised 5 ml and 3 ml collagen gels which require large cell numbers, reducing culture efficiency for generating replicates. Reducing gel volume and developing a model whereby multiple constructs can be cultured in a single culture chamber, will increase productivity and reduce variability samples. To this end, the aim of the current study was to characterise the use of collagen gels with reduced volume for engineering SkM in vitro.

METHODS: 3D collagen constructs were seeded with C2C12's at 4 x10⁶ cells/ ml. 3 ml constructs (n = 3) were engineered as previously described [2], whilst 2 ml (n = 3) and 0.75 ml (n = 2) constructs were prepared by equally reducing all constituents. Following 4 days in growth medium (DMEM, 20% FBS and 1% penicillin/ streptomycin), media was changed to differentiation media (DMEM, 2% FBS, 1% penicillin/ streptomycin and 10ng/ml IGF-I) for a further 10 day maturation period. Constructs were sampled at 14 days for histological analysis. Statistical analysis was performed using SPSS.

RESULTS: Evaluation of the macroscopic contraction of 3 ml and 2 ml constructs revealed no statistical difference (p> .05) at any time-points. This suggests that reducing the construct volume does not affect or enhance the ability of the cells to attach and remodel the matrix (Fig. 1).

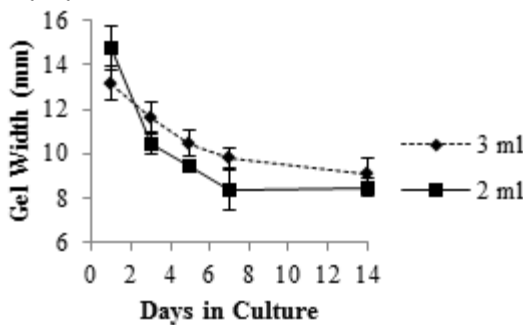


Fig 1. Macroscopic construct contraction of 3 ml and 2 ml collagen gels of same original dimensions over 14 days in culture. N = 3, Mean \pm SD.

Preliminary histological analysis demonstrated the high degree of longitudinal orientation of the cells within the constructs, analogous to *in vivo* skeletal muscle. Phase contrast images revealed that the ability of the cells to fuse to form multinucleated myotubes was enhanced in the 2 ml compared to 3 ml constructs. The 0.75 ml constructs displayed macroscopic contraction with increased cell attachment to the matrix compared to 2 ml and 3 ml constructs, as evident with phase contrast microscopy.

DISCUSSION & **CONCLUSIONS:** presented here provides evidence that reducing the volume of the constructs maintains characteristics of the previously published model. Furthermore, reducing gel volume has been shown to increase the potential of the cells to fuse to form myotubes, increasing the bio-mimicity of the model. Reducing required cell number along with the facility to culture multiple constructs per chamber will increase productivity especially for primary cell cultures and provide a sound model for the testing of nutritional therapies. The use of such models will facilitate the investigation of the cellular and molecular consequences of many commercially available nutritional supplements.

REFERENCES: ¹Mudera V, Smith AS, Brady MA, Lewis MP, (2010). *J Cell Physiol*. Vol. 225(3):646-53. ²Smith AS, Passey S, Greensmith L, Mudera V, Lewis MP, (2012), *J Cell Biochem*. Vol. 113(3):1044-53.

ACKNOWLEDGEMENTS: DJP is funded by UoB



The production and characterisation of primary calvarial cell-secreted decellularised matrices

AJ Taylor¹, MR Alexander², LDK Buttery¹

¹ Division of Drug Delivery & Tissue Engineering, School of Pharmacy, The University of Nottingham, Nottingham, UK. ² Laboratory of Biophysics & Surface Analysis, School of Pharmacy, The University of Nottingham, Nottingham, UK

INTRODUCTION: In developing bio-inspired materials for tissue engineering interventions it is important to understand how relevant cell types interact with a range of extracellular environs. *In vitro* cell-secreted decellularised matrices (DMs) provide a useful model system over simple protein coats as they closer reflect the complex native microenvironment found in *vivo*. Here we describe the production and characterization of primary calvarial cell-secreted DMs, showing the removal of cellular material, retention of relevant ECM proteins, and reattachment of relevant cell types.

METHODS: Murine primary calvarial (mPC) cells, extracted from neonatal CD-1 mice, are cultured on tissue culture plastic for 7 to 14 days in osteogenic media. They express a characteristic extracellular matrix that may decellularised and isolated through treatment with 20 mM ammonium hydroxide solution (15 min, room temperature); followed by DNase treatment (50-200 U/ml, 1 hr, 37°C) to remove residual nuclear material.

RESULTS: The resulting DM sheets are characterised using a range of imaging, histological, immunohistochemical and materials analysis techniques. DMs exhibit retention of bone-relevant ECM proteins including Collagen I and Fibronectin; and removal of key cellular components including DNA fragments and the Factin cytoskeleton.

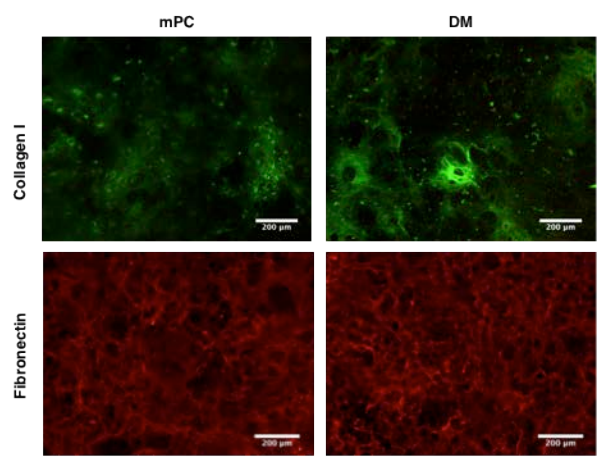


Fig. 1: Immunohistochemistry shows retention of Collagen I and Fibronectin in DM

CELLS& MATERIALS

Live/Dead staining of reseeded mPC cells on the DM before and after DNase treatment demonstrates the importance of complete nuclear material removal for subsequent cell adhesion. The adherence, viability and proliferation of mPC and mES cells on the DM demonstrated, indicating that the surface is viable as a tool to interrogate cell-matrix interactions.

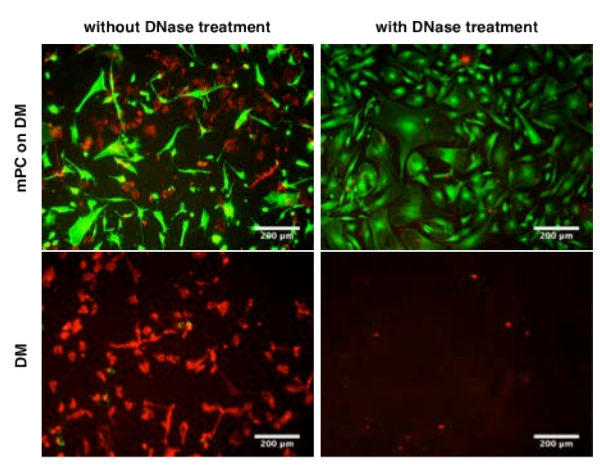


Fig. 2: Live/Dead staining shows that DNA fragments in DM (Bottom left) which is removed following DNase treatment. (Bottom right). On reseeding with mPC cells, confluence is only achieved when the DM has undergone DNase treatment (top).

DISCUSSION & CONCLUSIONS: We have produced intact decellularised matrices secreted by mPC cells. DMs are cell free and retain relevant ECM proteins and structure. The DM may be reseeded with a range of cell types to examine the influence of native ECM on their behaviour and differentiation. In particular we are interested to explore the behaviour of murine embryonic stem (mES) cells on the DM in an osteogenic environment. In vitro cell-secreted DMs provide a platform to understand cell-matrix interactions, and may inform the future development of bio-inspired synthetic substrates.

ACKNOWLEDGEMENTS: The authors would like to thank the EPSRC Doctoral Training Centre in Regenerative Medicine for providing financial support to this project.

Biologically active copolymer hydrogels

A.C. Harvey¹, S.P. Armes¹, C.W.I. Douglas² and S. MacNeil³
I- Department of Chemistry, Dainton Building, University of Sheffield, Brook Hill, Sheffield

2-Department of Oral Pathology, School of Clinical Dentistry, University of Sheffield, Claremont Crescent , Sheffield

3- The Kroto Research Institute, Department of Engineering Materials, University of Sheffield, Broad Lane, Sheffield

INTRODUCTION: The aim of the current study is to explore the relationship between polymer composition and architecture, and how this effects antibacterial actions. This work continues and investigates the anti-bacterial activity towards *Staphylococcus aureus* [SA] of various different thermo responsive copolymers based on 2-(meth acryloyloxy)ethylphosphorylcholine [MPC] and 2-hydroxy propyl methacrylate [PHPMA].^[1,2]

METHODS: Polymers were synthesized using either atom transfer radical polymerization [ATRP] or reversible addition-fragmentation [RAFT] polymerization and characterized via ¹H NMR, GPC and rheology.

Anti-bacterial activity was assessed using several well-known assays, including direct contact, adhesion, minimum inhibitory concentration [MIC] and minimal bactericidal concentration [MBC]. Fluorescently-labeled copolymers were prepared to view their interactions with human dermal fibroblasts [HDF] and bacteria.

RESULTS:

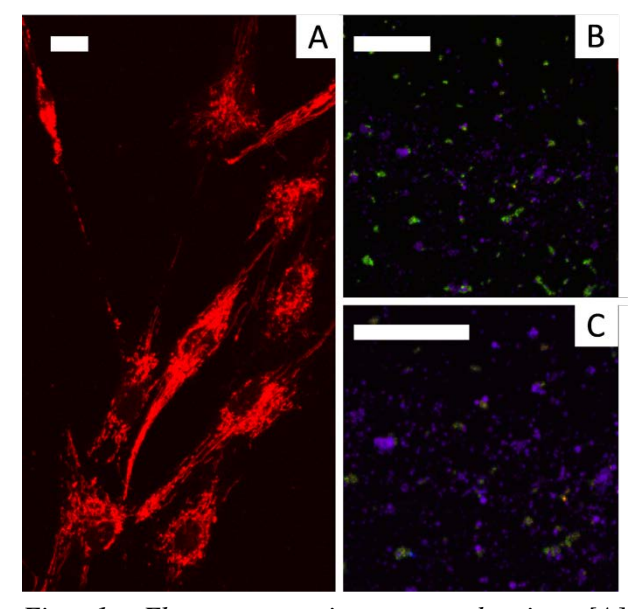


Fig. 1: Fluorescent microscopy showing [A] polymer interaction (red) with HDF cells [B & C] live/dead viability of SA after treatment with polymer gels (green is live, purple is dead). All scale bars represent 20µm.

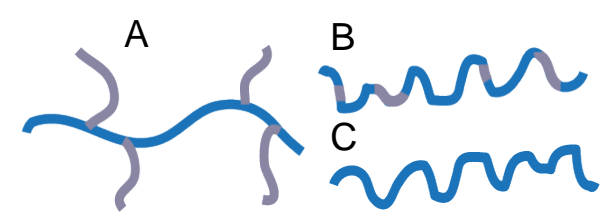


Fig. 2: Polymer architectures investigated [A]graft copolymer (-g-) [B] statistical copolymer (-s-) [C] homopolymer.

Table 1. Polymers antimicrobial activity against SA, and biocompatibility towards HDF

Polymer	Activity Biocompatible Gel		
PHPMA _{30,50}	-	-	X
200PMPC	X	Y	X
200MPC-s-120PHPMA	. X	Y	X
200MPC-g-4PHPMA ₃₀	Y	Y	Y
300MPC -g- 4PHPMA ₅₀	Y	Y	Y
80-400-80 MPC-HPMA	Y	Y	Y

physicochemical properties of the copolymer gel play an important part in the antimicrobial activity; the PHPMA 'chains' are thought to be a key component. It is possible that the MPC is dragging the PHPMA blocks into solution, or rather gel form. This is due to MPC's highly hydrophilic nature. The weakly hydrophobic properties of the PHPMA seem to be responsible for the thermo responsiveness, and possibly the antimicrobial activity of these copolymers.

The composition of PMC and PHPMA alone does not predict gelation or antimicrobial activity. Architecture and concentration of the polymers has an effect on the overall activity which is very sensitive. The combination of antimicrobial activity with mammalian cell biocompatibility is unexpected for these polymers though the mechanisms of action are not currently know. Nonetheless, these properties suggest potential biomedical applications for these materials.

REFERENCES: 1. Madsen, J., et al. Journal of Materials Science, 2009. 44(23): p. 6233-6246
2. Bertal, K., et al, Biomacromolecules, 2008. 9(8): p. 2265-75.

ACKNOWLEDGEMENTS: BBSRC; Dr J. Madsen, Dr J. Rosselgong, Dr N. Warren, Dr A. Blanazs, Dr A. Bullock & Mr J Heath.



Development of a porous polymer scaffold for mastoid bone regeneration

<u>Toby W.A. Gould</u>^{1*}, Ali S. Mallick¹, John P. Birchall², Larry R. Lustig³, Kevin M. Shakesheff¹, Cheryl V. Rahman¹

^{1*}Division of Drug Delivery and Tissue Engineering, University of Nottingham, ²Faculty of Medicine & Health Sciences, University of Nottingham, ³Department of Otolaryngology, UCSF, San Fransisco

INTRODUCTION: In the case of severe infection or the presence of invasive growths in the mastoid bone a mastoidectomy is performed and a portion of the bone is removed. A common problem associated with this type of procedure is further tissue morbidity at the site of the resulting bone cavity. Problems include hearing impairment or loss and continuous discharge. Cavity obliteration usually performed to avoid these problems does not restore the vital functions of the mucosa-lined mastoid air cells. Mastoid air cells serve vital functions as part of the mastoid bone including sound conduction, maintaining pressure regulation, gas exchange, material secretion, waste excretion and middle ear cavity aeration. We have previously reported the development of scaffolds based poly(lactic-*co*-glycolic) (ethylene (PLGA)/polv glycol) (PEG) microparticles¹. Here we describe the development of a highly porous, biodegradable polymer scaffold mastoid bone regeneration based PLGA/PEG microparticles blended with alginate beads.

METHODS: PLGA/PEG particles were fabricated by high temperature blending of PLGA (85:15 53kDa) and PEG 400 polymers. Polymer pieces were ground into particles in a bench-top mill and sieved to obtain the 100-200µm size fraction. Alginate beads were obtained by dropping a 2% sodium alginate solution from a 25G needle into a 5% calcium carbonate solution. These two materials were mixed in an aqueous carrier and sintered at 37°C to form the scaffolds. Mechanical strength and Young's modulus of scaffolds (n=3) of varying sintering time was assessed by compression using a Texture Analyser (Stable Microsystems). Bone marrow derived human mesenchymal stem cells were cultured on the scaffolds. Viability assessed using live/dead stain and imaged using a Leica confocal macroscope.

RESULTS: When the PLGA/PEG particles and alginate beads are mixed with liquid a paste which can be injected to fit a cavity and solidifies at 37°C

is created. The alginate beads degrade rapidly resulting in a highly porous PLGA/PEG scaffold structure. An in vitro model of mucosa-lined scaffolds with drug release is currently being developed to demonstrate the potential for regeneration of mastoid bone containing mucosa-lined air cells using this system.

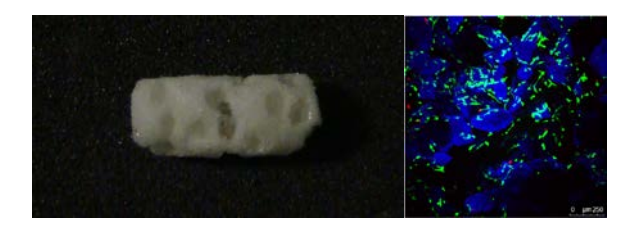


Fig. 1: 12mm Scaffold with 60% (w/w) alginate bead content (left) and (right) seeded with $2x10^5$ hMSCs and cultured for 3 days (live = green, dead = red)

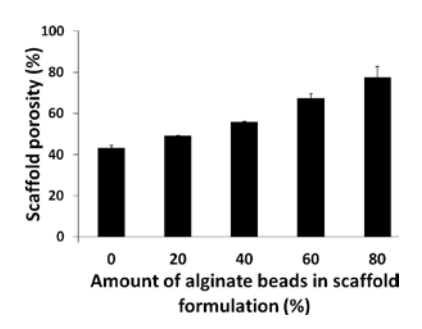


Fig. 2: Scaffold porosity increases with increase of alginate bead percentage in the formulation

DISCUSSION & CONCLUSIONS: A novel scaffold which becomes mechanically strong with increased porosity is reported. It is capable of supporting cell growth which is beneficial in the proposed regeneration of lost mastoid bone.

REFERENCES: ¹Hamilton L. *et al.*, J. Pharm. Pharmacol. 58:A52-A53, 2006

ACKNOWLEDGEMENTS: The authors would like to thank the EPSRC and University of Nottingham for funding.



Engineering anisotropy in mechanical properties by orientated collagen crosslinking

J Wong¹, AJ MacRobert² U Cheema¹, RA Brown¹

¹ UCL, Institute of Orthopaedics, Stanmore Campus, London UK. ² UCL, UCL Medical School, National Medical Laser Centre, Division of Surgery & Interventional Science, London, UK.

INTRODUCTION: Plastic compressed (PC) collagen gels (1) provide a biocompatible, biomimetic extra cellular matrix. Orientated focal cross-linking can be used to generate surface anisotropy, improve material stiffness and layer integration for the production of a stable 3D construct.

METHODS: Riboflavin (0.25mM) mediated photodynamic cross-linking of PC collagen gel was first assessed by measuring the diffusion depth of riboflavin with time, to ensure riboflavin diffusion was limited to the material surface. A peal test (fig.1) was performed using the dynamic mechanical analysis (DMA) to investigate the effect of increasing illumination time (cross-linking) on collagen layer integration. The DMA was also used to test material stiffness in perpendicular axis after orientated/topical cross-linking.

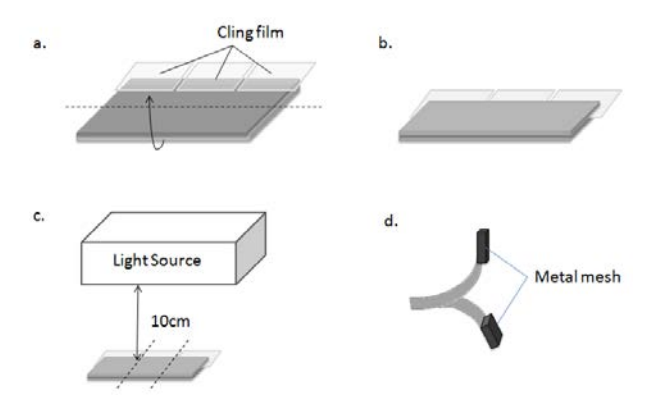


Fig.1: Preparation of samples for DMA peal testing. a,b) The collagen gel was cut lengthways and folded with riboflavin containing surfaces in contact. Cling film was used to separate part of the two layers. c,d) The samples were crosslinked between 4 to 15 minutes (one minute intervals) and were prepared for DMA testing.

RESULTS: One minute riboflavin diffusion time on either surface will saturate >12% of the collagen gel. Bonding strength doubled between PC collagen gel layers with a 5 minute increase in cross-linking time, and break stress was increased significantly after cross-linking. Importantly, mechanical anisotropy was introduced in the break

stress using orientated stripes of riboflavin in cross-linking, almost doubling the break stress parallel to the stripes (fig.2).

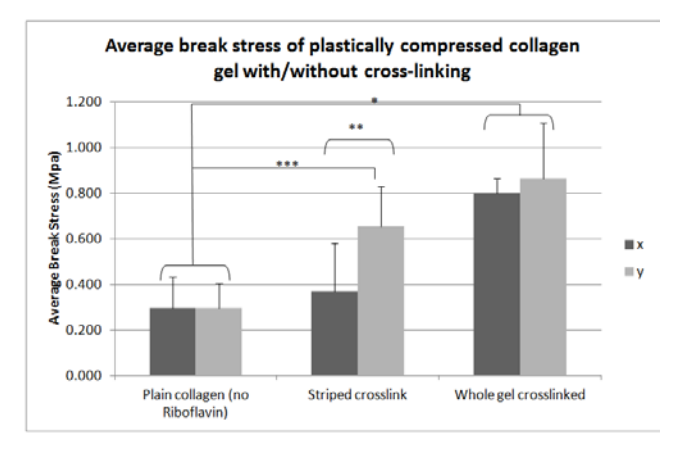


Fig.2: The mechanical strength of the PC collagen gel was tested along the vertical (y) and horizontal axis (x) on the dynamic mechanical analyzer. Stripes of riboflavin were printed parallel to the y-axis. Plain compressed collagen gels and completely cross-linked gels were used as controls.

DISCUSSION & CONCLUSIONS: Limited riboflavin penetration in one minute means that surface photodynamic cross-linking will enhance deep cell survival within the gel which is advantageous for tissue engineering purposes. Riboflavin mediated focal/orientated cross-linking generated new predictable anisotropy at the construct. This graded surface stiffness may then impact on cellular/mechanical properties of compressed gels. The increase in bonding strength between layers after cross-linking enhances layer integration which may help increase the stability of 3-dimentional constructs.

REFERENCES: ¹ Brown R.A. et al. (2005) *Adv. Funct. Mater.* **15(11).** 1762-1770.

ACKNOWLEDGEMENTS: We thank Ms. Rebecca Porter and Dr. Tijna Alekseeva for their technical assistance and Mr. George Georgiou for his assistance on the DMA.



The development of functional peptide scaffolds for cell culture.

L.Szkolar¹, J.E.Gough¹, A.Saiani¹

¹ Materials Science Centre, <u>School of Materials</u>, The University of Manchester, UK.

INTRODUCTION: Degenerative diseases of cartilage affect a high proportion of the population. The focus of current research is to produce ways of culturing chondrocytes on a large scale [1] or producing replacement cartilage [2].

Self-assembly has emerged as a powerful tool for materials fabrication. In recent years the self-assembly of peptide materials has allowed scope for cell culture scaffolds and has proven successful for a range of cell types [3,4]. It has been shown that peptide materials can allow for the culture and proliferation of chondrocytes [4], where cartilage-like ECM was produced.

This work looked at the effect of peptide sequence upon the mechanical properties of hydrogels and the resulting effect on proliferation and morphology of bovine chondrocytes (BC's). From previous group work, the peptide FEFKFEFK (F-8) has been shown to be suitable for cell culture. The natural ECM exhibits a net positive charge due to the attraction of sodium ions by proteoglycans. For this reason a nonapeptide analog to F-8 comprising an additional positive charge (F-9) was chosen for comparison.

METHODS: Cells were cultured in 5 % CO₂ atmosphere at 37 °C. BC's were maintained in Dulbecco's modified Eagle's medium (DMEM) supplemented with 10 % fetal bovine serum (FBS) and 1 % antibiotic. Peptide solutions were prepared at 30 mg mL⁻¹ and c.a. 40µL of 1M NaOH. Cells were suspended in media at 5x10⁵ cells per 300µL and cultured in 3D. Rheometry was performed on a TA AR-G2 rheometer, with fixed strain and frequency of 1% and 1HZ respectively. Cell counts were performed in triplicate by dissolving the gel in excess media and then counting using a haemocytometer. Cell morphology was assessed using light microscopy. Image analysis was performed to compare the change in cell area compared to an average round cell.

RESULTS:

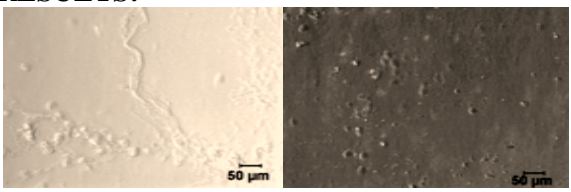


Fig. 1: Images of bovine chondrocytes after 3 days culture on a) F-8 and b) F-9.

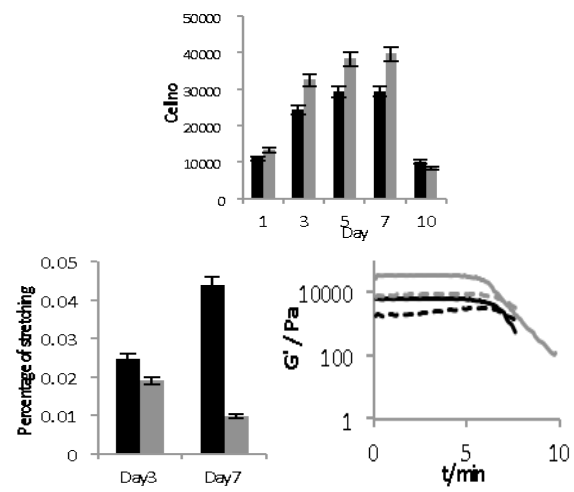


Fig. 2:a) Cell numbers over 10 days on F-8[Black] and F-9[Grey] b) Percentage of stretching of F-8 and F-9 and c) Rheology of F-8and F-9 before [Solid line] and after [dashed line] seeding with BC's

DISCUSSION & CONCLUSIONS: Cells seeded on F-8 and F-9 initially declined due to environmental shock. After day 3 numbers increased on both gels, with F-9 exhibiting higher numbers. Both systems plateaued until day 10, when numbers declined due to gel breakage.

An increase in the strength of both systems was seen after 7 days of culture suggesting the cells are laying down matrix. The increased strength of the F-9 gel may partially be due to more matrix production. The cells seeded on F-9 also exhibited a more rounded morphology.

REFERENCES: ¹ Tae-Jin Lee et al (2011) *Biotechnol Lett* 33:829–836. ² Benjamin D. Elder et al (2010) *Neurosurgery* 12:722-727, 201. ³ Holmes TC et al (2000) *proceedings Nat acad sci* 97:6728-6733. ⁴ J. Kisiday (2002) *Proceedings Nat acad sci* 15: 9996-10001

ACKNOWLEDGEMENTS:

Peptisyntha (a member of the Solvay Group), Belgium (http://www.peptisyntha.com)



Sustained delivery of active BMP-2 from PLGA microspheres for bone regeneration applications

HC Cox, LJ White, Y Reinwald, GTS Kirby, FRAJ Rose and KM Shakesheff

School of Pharmacy, University of Nottingham, CBS Building, University Park, Nottingham, UK NG7 2RD.

INTRODUCTION: This project aimed to create biodegradable bone morphogenetic-2 (BMP-2) loaded microspheres with control over both their size and *in-vitro* release profile. The goal was to show that BMP-2 was active at the point of delivery.

To this end, poly (D, L lactic co-glycolic acid) (PLGA) microparticles were specially formulated to incorporate a PLGA-polyethylene glycol-PLGA triblock copolymer to achieve sustained release thus overcoming the much reported and clinically unsatisfactory tri-phasic release profile [1]. The osteogenic effect of BMP-2 on C2C12 myoblast cells was used as the marker to determine BMP-2 activity [2].

METHODS: Microspheres were fabricated from PLGA (L:G ratio 50:50) formulated with 10% PLGA-PEG-PLGA triblock in a controlled double emulsion solvent evaporation process. BMP-2 with human serum albumin (HSA) as a carrier was loaded at 1% (w/w) (HSA:BMP-2 ratio 95:5). Microspheres were sized using laser diffraction and imaged by scanning electron microscopy. Release was monitored by suspending microparticles in phosphate buffered saline, incubating at 37°C on a rocker and regularly sampling and replacing the media. The pH and total protein (bicinchoninic acid assay) in the supernatants was determined. Release was monitored over 30 days.

Supernatants were diluted 1:1 in Dulbecco's modification of Eagles medium containing 10% foetal calf serum. This media was used to culture C2C12 cells where any active BMP-2 would be detected by the dephosphorylation of paranitrophenylphosphate by alkaline phosphatase. The colorimetric change is directly related to BMP-2 concentration. Microparticles were also co-cultured with C2C12 cells to determine a direct response on the cells.

RESULTS: The PLGA microspheres were sized at 20-30 micron in diameter. Entrapment efficiencies were in the order of 51-76%. The addition of PLGA-PEG-PEG triblock copolymer ensured sustained release of total protein over 30 days (Figure 1) which equated to a clinically

relevant dose of BMP-2. BMP-2 activity could be detected in the supernatants up to day 13. Beyond this, the degradation products lowered the pH rendering the *in-vitro* assay ineffective. Direct co-culture resulted in a linear dose response of microparticle mass with BMP-2 activity and there were associated changes in cell morphology.

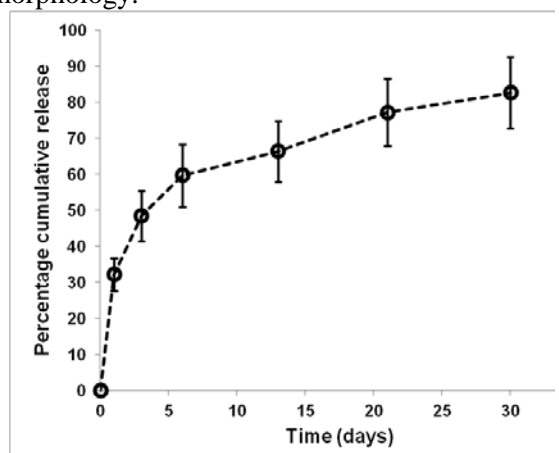


Figure 1 Cumulative release of total protein from PLGA microspheres formulated with 10% PLGA-PEG-PLGA triblock and loaded with 1% $_{(w/w)}$ total protein (HSA: BMP-2 ratio 95: 5) (n=3)

DISCUSSION & CONCLUSIONS: This work has shown that PLGA microparticles can deliver active BMP-2 at a sustained rate. These microparticles will be tested in an *ex-vivo* embryonic chick femur model to investigate their effect on bone development and defect repair.

REFERENCES: ¹M Ye, S Kim. and K Park (2010) *Issues in long-term protein delivery using biodegradable microparticles* Journal of Controlled Release **146**, 241-260 ²T Katagiri, A Yamaguchi, M Komaki, E Abe, N Takahashi, T Ikeda, V Rose, JM Wozney, A Fujisawa-Sehara, and T Suda (1994) *Bone morphogenetic protein* – 2 *converts the differentiation patway of C2C12 myblasts into the osteoblast lineage* Journal of Cell Biology Vol. **127** No Part 1 1755-1766

ACKNOWLEDGEMENTS: This work is funded by a BBSRC LoLa grant No BB/G010617/1



Assessment of TiO₂-doped bioactive glass microcarriers for expansion of adherent mammalian cells

JC Guedes^{1,2}, Nilay Lakhkar³, JC Knowles^{3,4}, I Wall^{1,4}

¹<u>Dept. Biochemical Engineering</u>, UCL, UK. ²<u>Dept. Bioengineering</u>, IST, Lisboa, Portugal, ³<u>Biomaterials & Tissue Engineering</u>, Eastman Dental Institute, UCL, UK. ⁴WCU Dept. Nanobiomedicine, Dankook University, Korea

INTRODUCTION: Current limitations to cell therapy include expanding cells to the desired number for clinical use. Several different types of microcarrier have been explored as a substrate for cell attachment and expansion with varying degrees of success ^[1]. In this study, bioactive glass microspheres doped with 5% titanium dioxide (TiO₂) were seeded with mouse embryonic fibroblasts (MEFs) or rat mesenchymal stromal cells (MSCs) in order to evaluate the capacity of the microspheres to support attachment and growth.

METHODS: Using ultra low attachment 96-well plates, MEF and rat MSCs were seeded onto microcarriers doped with 5% TiO₂. Their survival and expansion were determined using staining procedures and cell proliferation assays (CCK). Also, during time in culture, glucose and lactate concentrations were determined to confirm cell metabolism. In addition, immunofluorescence microscopy provided a visual assessment of cells.

RESULTS: Cell seeding in low adhesion plates revealed clear cell attachment and interactions with the Ti-doped microcarriers (Fig. 1). Higher magnification confocal microscopy after 72h revealed established cell attachment and growth (Fig. 2). In the cell proliferation assays, MEFs seeded on TiO₂ glasses showed a significant increase in cell number over several days of culture correlating with glucose consumption and lactate production (Fig. 3).

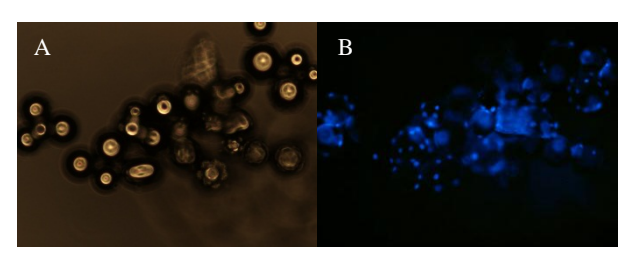


Fig. 1: Adhesion of p5 MEFs to Ti-doped microcarriers in ultra low attachment plates, pictures of (A) phase contrast image and (B) labelling with DAPI staining (both 10x magnification).

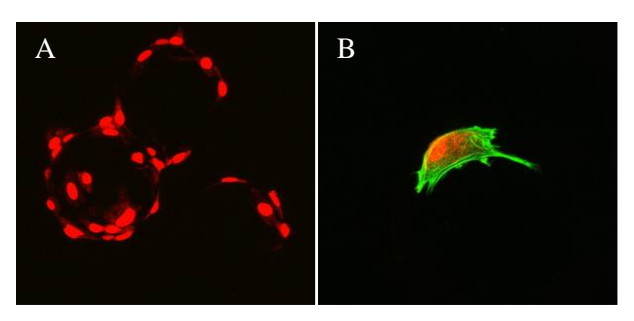


Fig. 2: Labelling of (A) p5 MEF with PI staining and (B) p2 MSCs with Phalloidin and PI staining 72 h after cell seeding using high magnification confocal laser scanning microscopy (both 40x magnification).

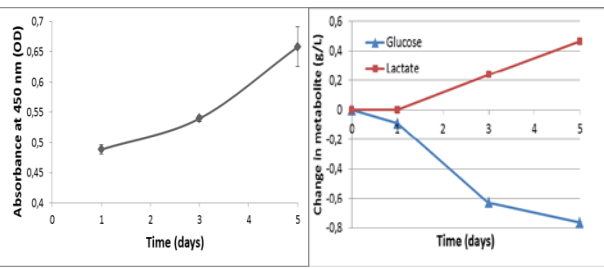


Fig. 3: Proliferation of p3 MEF on the TiO_2 doped microcarriers and corresponding metabolic analysis.

DISCUSSION & **CONCLUSIONS:** Cell attachment and proliferation was supported on the microcarriers doped with 5% TiO₂. This is attributable to the known biocompatibility of TiO₂ [2]. Current investigations in our lab focus on stem cell growth and differentiation on Ti-doped beads for regenerative cell therapy.

REFERENCES: ¹ F. dos Santos, P. Z. Andrade, M. M. Abecasis et al (2011) *Tissue Engineering: Part C* Volume **17**, Number 12 ² E.A. Abou Neel, T. Mizoguchi, M. Ito et al (2007) *Biomaterials* **28**:2967-2977

ACKNOWLEDGEMENTS: Kind thanks to the WCU Program, funded by the National Research Foundation of Korea (No. R31-10069).



Cell manipulation using an acoustic tweezing device – Application in cell patterning and adhesion testing

F Gesellchen¹, AL Bernassau², DRS Cumming², MO Riehle¹

¹ <u>Centre for Cell Engineering</u>, University of Glasgow, Glasgow, UK. ² <u>Electronics & Nanoscale</u> <u>Engineering</u>, University of Glasgow, Glasgow, UK.

INTRODUCTION: We have developed an acoustic tweezing device (sonotweezer) for non-invasive manipulation of particles in the micrometer size-range. While it has been shown that this device is very efficient in acoustic trapping of polystyrene beads and lipid droplets [1], our aim was to extend the application to mammalian cells and prove the usefulness of the device for cell culture experiments.

METHODS: The heptagon-shaped sonotweezer has been described elsewhere [1]. For the experiments in this study, two non-adjacent piezoelectric transducers were operated at 4MHz, 8Vpp for acoustic trapping of cells in a linear pattern. The experimental setup included an agar layer (1.5 ml, 1.5% in PBS) in the device (to reduce acoustic streaming) with a glass cover slip on top and 500 ul of complete growth medium. After setting up the device on a microscope stage and activating the transducers 100 µl of a cell suspension (C2C12 or HUVEC at 5x10⁵ cells/ml) were added. A 180° phase shift of the acoustic wave was performed to shift the position of the acoustic pressure nodes, after the cells were sufficiently adhered (usually 30 min).

RESULTS: Figure 1A shows the initial trapping of C2C12 mouse myoblast cells added to the device. Cells are trapped at nodes of minimal acoustic pressure, which are arranged in lines spaced 240 µm apart.

After letting the C2C12 cells adhere for 30 min the position of the pressure nodes was adjusted ~120 μ m laterally by shifting the phase of one of the transducers by 180°. After adding 100 μ l of a HUVEC cell suspension, the newly added cells were trapped in between the lines formed by the initially patterned C2C12 cells (*Fig. 1B*).

DISCUSSION & **CONCLUSIONS:** By extending the application of the sonotweezer device to cultured cells we have shown the general usefulness of the device for tissue culture experiments. Cells are trapped in linear patterns determined by the transducer configuration. Moreover, shifting the phase of the acoustic wave

after a first round of patterning allows a second set of cells to be deposited between the first set. This is potentially very useful for tissue engineering where the precise positioning of different cell types is needed for controlled tissue formation. Other possible applications include adhesion testing of cells to surfaces – after letting the cells adhere for a short time only, a phase shift can then be used to move cells out of their position, depending on the adhesiveness of the substrate.

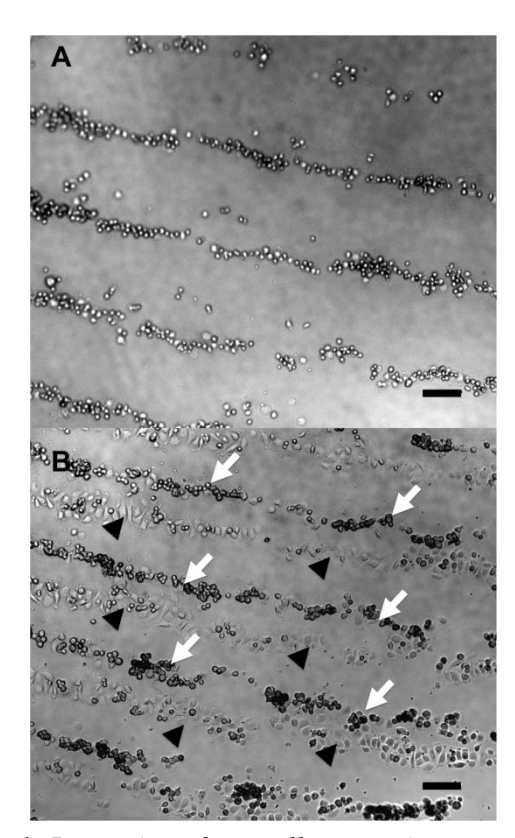


Fig. 1: Patterning of two cell types using an acoustic tweezer. (A) Initial acoustic trapping of C2C12 cells in linear pattern (prior to phase shift). (B) Trapping of HUVEC cells in between lines of C2C12 after a phase shift. Arrowheads indicate adherent C2C12 cells, white arrows point to still rounded HUVEC cells. Scale bars 100 µm

REFERENCES: ¹ Bernassau, A., Ong, C.-K., Ma, Y., et al (2011), *IEEE Trans. Ultrason.*, *Ferroelect.*, *Freq. Contr.* **58**, 2132–2138.



using functionisled gold nanoparticles for the delivery of siRNA to bone cancer cells in vitro

M.McCully¹, H.Child¹, M.J.Dalby¹, C.C.Berry¹

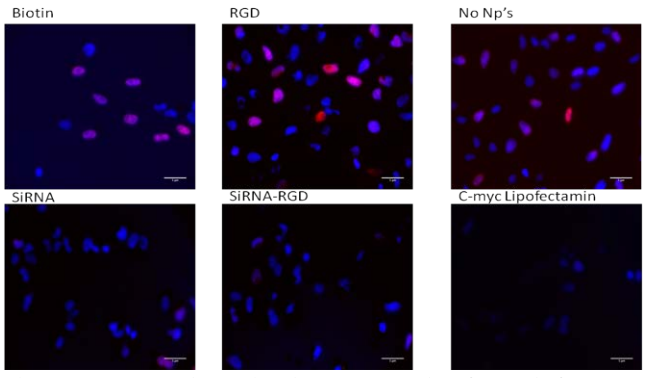
¹ <u>Centre for Cell Engineering</u>, College of Medical Veterinary and Life Sciences, University of Glasgow, Scotland

INTRODUCTION: RNA interference is a promising method of gene silencing that can be used to reduce over expression of oncogenes as a novel form of cancer treatment. The main barrier facing therapeutic RNAi is the successful delivery of the necessary small interfering RNA (siRNA) molecules into cancer cells within the body¹. This study aimed to overcome this barrier by using gold nanoparticles (AuNPs) to deliver siRNA into bone cancer cells (MG63) in order to knockdown the cmyc oncogene by RNAi. siRNA against c-myc was conjugated covalently to the gold nanoparticle, which was further functionalised with RGD (to enhance cell interaction) and biotin (for imaging purposes). Nanoparticle toxicity was assessed by MTT assay; cellular uptake was visualized by TEM and quantified via ICP-MS, whilst c-myc knockdown was assessed by quantitative Real-Time PCR (qRT-PCR) and corresponding Western blots, and the effect of knockdown on the cell cycle was investigated by BrdU staining. Results indicated successful delivery of the AuNPs into the cells. In addition, some knockdown is evident with the siRNA and a parallel reduction in the cells entering S phase was noted.

METHODS:Brdu Immuno Staining. Cells seeded for 24 hours at 1x10⁴ cells/ml in Dulbecco's modified Eagle's medium (DMEM with 10% Foetal Bovine Serum, 2% Penicillin, Streptomycin and L-glutamine. After 24 hours AuNPs were added or siRNA in Lipofectamine (Invitrogen, UK) .After 42 hours 1mM Brdu (Sigma Aldrich, UK) was added for 6 hours. Cells were fixed and permealised before treatment with 1% BSA-PBS at 37°C for 10 minutes. The primary antibody BrdU (GE healthcare, Buckinghamshire, UK) was diluted in DNase I and added for 2.5 hours at 37°C Samples were PBS-tween washed [0.5%V/V]. Cells were stained with Anti-mouse texas red (Vector Laboratories, UK) in 1% BSA-PBS for 1 hour, before co-staining with DAPI mounting oil (Vector Laboratories, UK)

RESULTS: Our results indicate that the siRNA conjugated nanoparticles are up taken and retain their functionality, by arresting the cell cycle.

Comparing populations of MG63's that have been treated with biotin- or RGD- conjugated cells have similar proportions of cells in S-Phase comparable to cells treated with no AuNPs. In comparison cells treated with siRNA conjugated AuNPs have a noticeable decrease in the proportion of cells in S-phase, with comparable levels to the highly efficient lipofectamine transfection system of siRNA's (Fig1).Fig. 1:Brdu staining of MG63cells in S-Phase — From top left to right, we can see biotin treated, RGD treated and cells with no nanoparticles have a greater number of cells in S-



phase compared to the lower panels, from left to right of siRNA, siRNA-RGD and C-Myc siRNA transfected with lipofectamine. Scale bar= $5\mu m$

DISCUSSION & CONCLUSIONS: The Brdu stain indicates the functionality of the siRNA – AuNp system. Further work has shown that some knockdown is evident at the RNA and protein level.

REFERENCES: ¹ R.Lévy(2010) Gold nanoparticles delivery in mammalian live cells: a critical review, Nano Reviews 1, 1-18.

ACKNOWLEDGEMENTS: Carol-Ann Smith



Improving the elasticity of an autologous tissue engineered prosthesis (TEP) for pelvic floor repair by the use of mechanical stimulation

NI Osman ¹², S Roman ¹, AJ Bullock ¹, CR Chapple ², S MacNeil ¹ *Kroto Research Institute, University of Sheffield.* ²Sheffield teaching Hospitals NHS trust, Sheffield.

INTRODUCTION: Stress urinary incontinence and pelvic organ prolapse are bothersome conditions that have a deleteriously impact on quality of life. They affect 40% of the female population and women have an 11% lifetime risk of requiring surgical intervention. Current synthetic repair materials are non-absorbable and too stiff, resulting in high erosion rates. Previously we have developed a tissue-engineered prosthesis (TEP) for this application cultured under static conditions¹. However the material was not sufficiently stiff (below the "ideal" range of elasticity of healthy native tissue). We sought to assess the effect of mechanical stimulation on the final stiffness of the TEP.

METHODS: Human oral fibroblasts (OF) were obtained from oral biopsies taken after informed consent and ethical approval. After expansion in culture, 500,000 cells were seeded onto 2x1cm sheets of heat annealed electrospun poly-lactic acid scaffolds. Cells were then cultured for 14 days in 10% DMEM at 37°C. Two days after seeding, cells were mechanically stimulated with fluid shear forces for a period of 1 hour on a rocking platform (6 well plate,2ml media, tilt angle 6°, 40 rpm) along the longitudinal axis of the scaffolds. This was repeated daily for 5 days, followed by 2 rest days then a further 5 days of rocking. Using Alamar Blue (vital stain) we observed the cell metabolic activity, and Dapi (nuclear stain) we observed cell attachment to the scaffold. Additionally we assessed the final biomechanical properties of the TEP using a BOSE electroforce tensiometer. Total collagen production by Sirius red (stain per gram) was also measured.

RESULTS: We observed an increase in metabolic activity throughout the 14-day period and good cell attachment. There was no difference between the static controls and exercised cells in total collagen production (figure 1). However the final elasticity (Young's Modulus) of the construct was just above the range of healthy native tissue (Figure 2).

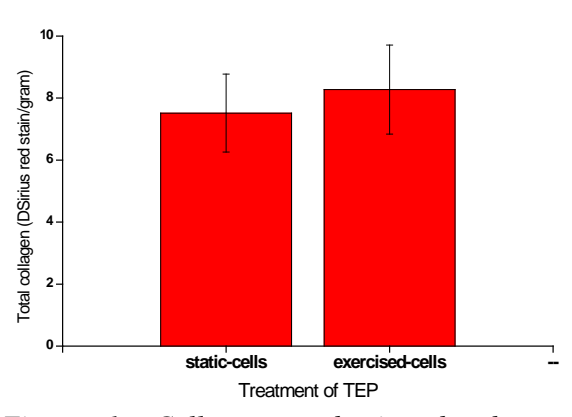


Figure 1: Collagen production-absorbance of Sirius red stain per gram of scaffold $(n=9\pm SEM)$

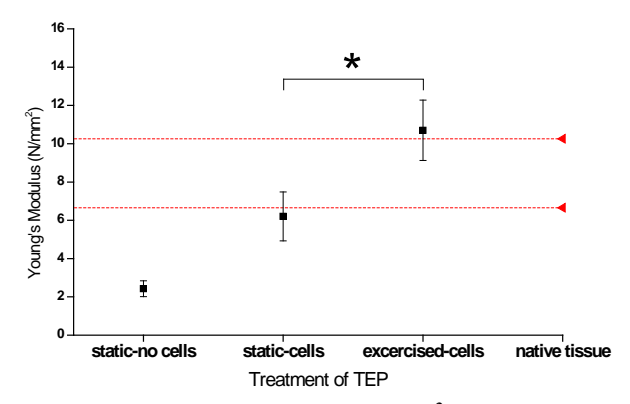


Figure 2: Young's Modulus (N/mm^2) of scaffolds. $(n=9\pm SEM)$, *P<0.05

DISCUSSION & CONCLUSIONS:

We have demonstrated that through mechanical stimulation of TEP's by fluid shear forces, stiffness can be improved. Additionally, cell attachment is not adversely affected by fluid shear force stimulation and the metabolic activity of cells increases. The improvement in stiffness is not explained by total collagen production but we postulate may be due to collagen fibre organisation and alignment. Further work will attempt to further characterise collagen morphology, collagen type, elastin production and optimise the conditioning protocol to obtain stiffness akin to native tissue.

REFERENCES: ¹Mangera A, Bullock AJ, Chapple CR, MacNeil S. Creating a tissue engineered autologous prosthesis for use in stress urinary incontinence and pelvic organ prolapse repair. European Cells and Materials Vol. 22. Suppl. 2, 2011 (Page 65).



Elucidating skeletal development to inform bone tissue regeneration – lessons from *ex vivo* chick femur cultures

EL Smith, CA Roberts, JM Kanczler, ROC Oreffo

Bone & Joint Research Group, Centre for Human Development, Stem Cells and Regeneration, Human Development and Health, University of Southampton.

INTRODUCTION: Enhancement and application of our understanding of skeletal developmental biology offers innovative strategies to bone tissue regeneration. We propose that use of a model of-bone development (fetal femur) to understand skeletal stem cell differentiation, skeletogenesis, and the effects of key differentiation agents, will aid our understanding of the developing bone niche, providing a unique regenerative medicine paradigm. Thus we have recently developed a 3D ex vivo culture system of embryonic chick femora¹, used in this study to investigate effects of key growth factors on skeletogenesis. Microinjection of distinct skeletal cell populations into the femurs, transfection of whole femurs with silencing siRNA, or combination with a chick chorioallantoic membrane (CAM) system, further widens the potential of the model.

METHODS: Isolated embryonic day 11 chick femurs were placed in organotypic cultures for 10 days in basal media, alone or supplemented with 100ng/ml PTH or 100ng/ml PTHrP. In addition, selected femurs were microinjected with chick preosteoclasts to assess bone remodelling. Effects were silenced with Accell siRNA against the PTH receptor. Organotypic cultures were analysed by micro-computed tomography (μ CT), and further assessed histologically for proteoglycan (Alcian blue) and collagen production (Sirius red) as well as proliferation (PCNA), osteoclast activity (TRAP) and the presence of skeletal stem cells (STRO-1) and endothelial cells (CD31).

RESULTS: Stimulation of E11 chick femur cultures with either PTH or PTHrP initiated osteogenesis. Bone formation was enhanced, with increased collagen I and STRO-1 expression, accompanied by a reduction in cartilage, as observed by decreased chondrocyte proliferation, collagen II expression glycosaminoglycan levels. Increased CD31 expression in areas of bone formation indicated an increase in endothelial cell number. Cultured chick femurs were successfully transfected with Accell PTH1R siRNA, and transfection blocked the osteogenic effects of PTH and PTHrP. Addition of microinjected preosteoclasts into the chick femurs induced catabolic, rather than anabolic, bone effects after PTH and PTHrP stimulation, diminishing collagen I, STRO-1 and CD31 expression.

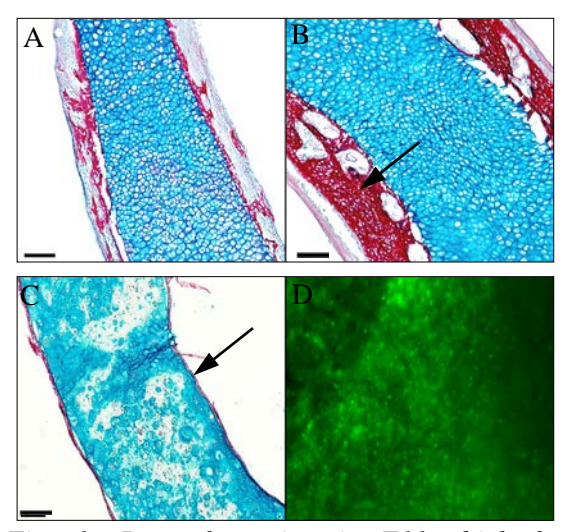


Fig. 1: Bone formation in E11 chick femurs cultured in basal media (A), enhanced bone formation following stimulation with PTH or PTHrP (B). Addition of preosteoclasts diminished the osteogenic effects (C). Cells of whole chick femurs were successfully transfected with Accell siRNA (D).

DISCUSSION & CONCLUSIONS: This study demonstrates the successful use of organotypic chick femur cultures as a model system for bone development, evidenced by the effects of exogenous PTH / PTHrP to modulate bone formation. The *ex vivo* model, in combination with microinjection, siRNA and CAM techniques, provides a tool for analyzing key temporal stages of skeletal development, and offers significant potential as a test bed for scaffold / cell / growth factor therapies for regenerative medicine.

REFERENCES: ¹ J.M. Kanczler, E.L. Smith, C.A. Roberts & R.O.C. Oreffo (2012, In Press) *Tissue Engineering Part C: Methods*.

ACKNOWLEDGEMENTS: This work was supported by the strategic longer and larger grant (LOLA) from the BBSRC, UK-grant number BB/G010579/1.



Optimizing cell sources and materials for cleft palate repair

S. Puwanun¹, F. Bye¹, R.M. Delaine-Smith¹, J. Yates², S.MacNeil¹ & G.C. Reilly¹

¹Kroto Research Institute, Department of Materials Sciences and Engineering, University of Sheffield, UK.

²School of Dentistry, University of Manchester, UK.

INTRODUCTION:

In major defects of the cleft palate there is a need for a suitable bone forming cell to form the hard part of the upper palate. One option is to use human jaw periosteal cells (HJPs), which can be obtained from the patient using an oral biopsy. Biodegradable electrospun polymers such as polycarpolactone (PCL) and polylactic acid (PLA) can be used as a scaffold to support the cells and fill the specific tissue defect.

AIM:

Our aim was to establish scaffold and media conditions for tissue engineering of cleft palate using HJP cells. Two biodegradable electrospun polymer scaffolds of PCL and PLA were compared for their ability to support the osteogenic differentiation of HJPs.

METHODS:

Human jaw periosteum tissue biopsies were received from 2 donors. These were isolated using collagenase II and then cultured in α -MEM. The cells (HJPs-1 and HJPs-2) were seeded on PCL and PLA scaffolds. The samples in each scaffold were divided into 2 different media conditions; all supplemented with 50µg/mL ascorbic acid-2phosphate (AA) and 5mM beta-glycerolphosphate but only samples from one group supplemented with 10nM dexamethasone (Dex). proliferation was assessed by a resazurin reduction assay at days 7, 14, 21, and 28. Calcium deposition was assessed as an indicator of osteogenic differentiation by alizarin red staining on days 21 and 28.

RESULTS:

The resazurin reduction assay showed an increase in cell proliferation in cells from both donors over time (days 7, 14, 21, and 28) (Fig.1A and D). The addition of Dex slightly increased proliferation for cells seeded in PCL and PLA scaffolds. Cells seeded on PCL scaffolds proliferated more than the cells seeded on PLA scaffold. Quantitative analysis by alizarin red staining of HJPs-1 and HJPs-2 indicated an increase in calcium deposition over time (from days 21 to 28 for HJPs-1 (Fig.1B) and HJPs-2 (Fig.1E)). The pictures showed alizarin red staining on HJPs-1 (Fig.1C) and HJPs-2 (Fig.1F) showed that the cells seeded on PCL scaffold were slightly darker than the cells seeded on the PLA scaffold.

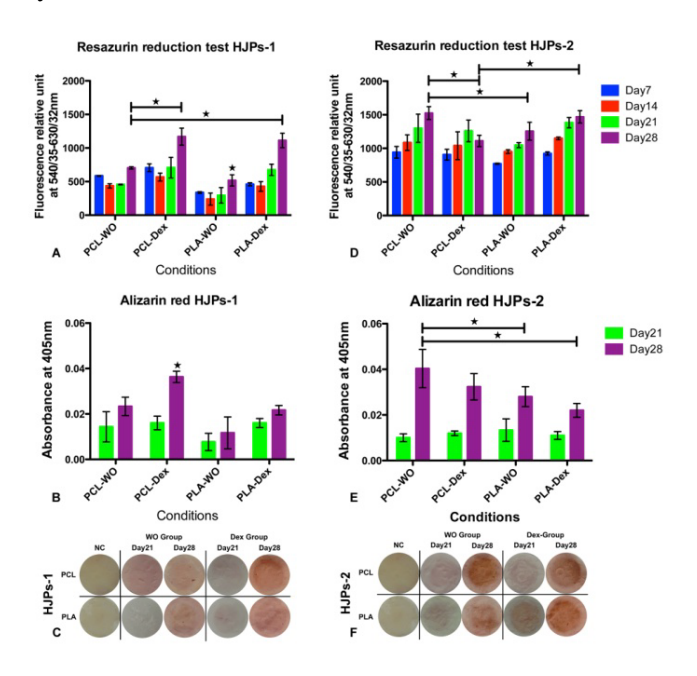


Fig.1: Cell proliferation assessed by resazurin reduction of HJPs-1 (A) and HJPs-2 (D) in different media and on PCL and PLA scaffolds. Alizarin red staining showed calcium deposition of HJPs-1 (B) and HJPs-2 (E). The pictures show alizarin red staining of the cell seeded scaffolds; HJPs-1 (C) and HJPs-2 (F).

DISCUSSION & CONCLUSION:

Both biodegradable electrospun polymer (PCL and PLA) scaffolds can support proliferation and differentiation of human jaw periosteal cells. The cell proliferation and calcium mineralization of HJPs-2 was slightly greater than with HJPs-1 cells on both types of scaffolds. We conclude that while there is patient variability between cells (and more work is required to test HJPs from more patients) the results support the use of these cells and a PCL scaffold for cleft palate repair.

ACKNOWLEDGEMENTS: This project was supported by Naresuan University Scholarship, Thailand.



In vivo evaluation of the influence of processing variables in the down-stream inflammation elicited by xenogeneic soft tissue repair biomaterials

N Bryan¹, H Ashwin², R Chen¹, Y Bayon², S Wohlert², N Smart³, JA Hunt¹

¹Clinical Engineering (UKCTE), University of Liverpool Institute of Ageing and Chronic Disease, Duncan Building, Daulby Street, Liverpool, UK. ²Covidien – Sofradim Production, 116 Avenue du Formans – BP132, F-01600 Trevoux, France. ³Exeter Health Science Research Unit, Royal Devon and Exeter Hospital, Barrack Road, Exeter, UK.

INTRODUCTION: In order to maximise the potential of successful biomaterial mediated surgical intervention it is paramount to understand the interaction between the material and the host inflammatory physiology. Following implantation any material will be interrogated by a plethora of leukocyte classes and stromal cells as part of the host defence, which together orchestrate material stabilisation, integration and in-growth appropriate wound healing cells. It is well documented that biomaterials have the potential to modify the host response in both constructive and destructive manners. In this study we considered synthetic and tissue-based materials commonly in soft tissue repair, particular hernia Using controlled manufacturing variables the goal of the study was to elucidate the influence of various processing stages on the ultimate bulk inflammatory properties of the materials. In the instance of tissue-based prosthetics these variables may include source tissue species and anatomical and origin, delipidation decellularisation procedures and cross-linking to resist degradation by bacterial collagenase, favouring their indication in contaminated areas. In this study materials of interest were implanted subcutaneously in a nonimmunosuppressed rat model to characterise their inflammatory properties.

METHODS: Synthetic meshes; polypropylene terephthalate polyester (PET) polyglycolic acid (PGA) varied in polymer composition & fibre conformation. Tissue-based implants consisted of human & porcine materials from dermal and small intestinal submucosal (SIS) tissues varying decellularisation and cross-linking chemistries. Implants were delivered into 6 week old, male wistar rats. In the SC model each animal received 4 implants above each shoulder and hip adjacent to the dorso-lumbar musculature. Implants were delivered through a single 1cm dorsal incision into SC channels created using blunt dissection. Explants were characterised tinctural histology immunohistochemistry after fixation using PLP fixative and infiltration with GMA resin,

n=6/material/time point. Tissue response was evaluated using pathological indexing and quantitative image analysis. Procedures conformed to UK home office use of animals in scientific procedures guidelines. Statistics were performed using Waller-Duncan post hoc ranking and chi squared analysis.

RESULTS: Subcutaneous delivery of tissue-based prostheses demonstrated a number of material specific inflammatory characteristics. Classical histopathology allowed clear demonstration of the extent of cellular infiltration, neo-vascularisation, interface thickness and composition. SIS elicited the most intense acute like inflammation reaction with the recruitment of abundant neutrophils compared to equivalent dermal matrices. The processing of different dermal materials from controlled variations showed that i) Sodium dodecyl sulphate (SDS) was the most proinflammatory decellularisation reagent and ii) cross-linking using had no effect on host response. All materials remained entirely recoverable after 28 days with the exception of SIS which had partially resorbed. In the instance of synthetics it was much more difficult to elucidate material specific differences in cellular response in vivo. Overall, material weave and polymer combination were the predominant factors dictating the inflammatory properties of the material compared to underlying polymer chemistry

DISCUSSION: In vivo implantation of a large of soft tissue repair prostheses panel demonstrated key differences in their interaction physiology induced with host fabrication. SDS and SIS were particularly proinflammatory manufacturing elements. Crosslinking tissue- based materials using HDMI did not induce any significant differences in host response vs a non-cross-linked equivalent. Synthetic meshes allowed for the interesting demonstration that polymer weave topography plays a greater consequence in cellular response than intrinsic polymer chemistry.

ACKNOWLEDGEMENTS: The authors would like to thank Covidien for funding this research.



THE APPEARANCE AND DISTRIBUTION OF OCHRONOSIS IN THE CALCIFIED CARTILAGE OF A MURINE MODEL OF ALKAPTONURIA

<u>CM Keenan¹</u>, C Equus Edwards¹, AJ Preston¹, H Sutherland¹, B Wlodarski¹, AM Taylor¹, D Williams², LR Ranganath^{1,3}, JA Gallagher¹, JC Jarvis¹

¹ University of Liverpool, Department of Musculoskeletal Biology, Institute of Ageing and Chronic Disease, Sherrington Building, Ashton Street, Liverpool, L69 3GE, UK. ² Department of Molecular and Clinical Pharmacology, Institute of Translational Medicine, Sherrington Building, Ashton Street, Liverpool, L69 3GE, UK. ³ Royal Liverpool University Hospital, Prescot Street, Liverpool, L7 8XP, UK.

INTRODUCTION: Alkaptonuria (AKU) is a rare disorder characterized by loss of function of the homogentisate 1, 2- dioxygenase (Hgd) enzyme, leading to a high concentration from birth of homogentisic acid (HGA) in plasma and urine. HGA polymerizes as pigment in collagenous tissues, principally in the cartilage of loaded joints (ochronosis). Previous studies suggested AKU mice do not develop ochronosis. We made a comprehensive survey of AKU mice, identified whether signs of ochronosis were present and investigated whether nitisinone, a potential therapy for AKU, prevents initiation and progression of ochronosis.

METHODS: BALBc Hgd-/- mice were culled between 6 and 65 weeks for whole of life studies. For the nitisinone study, 4mg/L nitisinone was added to the drinking water of 15 out of a group of 30 mice. 3D analysis was performed using imageJ and OriginPro.

We **RESULTS:** report the detection of BALB/c ochronosis in AKU mice. Pigmentation, when seen at 15 weeks, was confined to the pericellular matrix in the calcified articular cartilage. By 40 weeks, pigmentation cellular of material observed, and by 65 weeks there was extensive pigmentation throughout the femoral and tibial calcified articular cartilage of the whole joint. Pigmentation of chondrons was identified using Schmorl's reagent, a modified stain for melanin-like pigment. 3D image analysis of the tibial plateau from a 25 week old AKU mouse shows that pigmented chondrons are distributed throughout the joint, and not in a defined area of mechanical stress (Figure 1). Histological analysis showed that nitisinone prevented pigmentation of chondrons. The appearance of pigmented chondrocytes, both pyknotic and viable and often in the same isogenous group of cells, suggested that pigmentation follows localized changes in the composition or organization of the matrix. Sections of the tibio-femoral joint from untreated animals contained on average 227±23 pigmented chondrocytes. Sections from treated animals contained none.

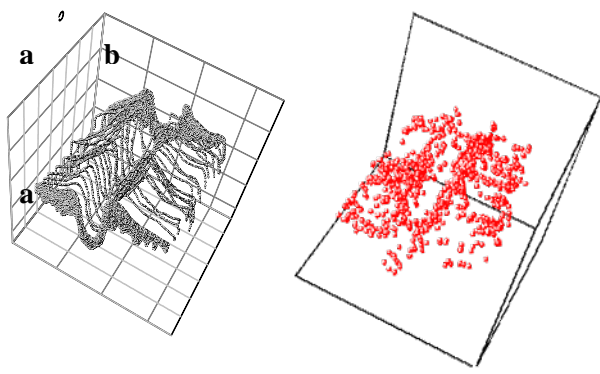


Figure 1 (a) Tibial articular cartilage through 23 serial sections, posterior to anterior. (b) Location of pigmented chondrocytes in the tibial articular cartilage through same sections as in (a).

DISCUSSION&CONCLUSIONS: Observation of ochronosis in AKU mice establishes a to investigate early pathological changes associated with AKU that, in humans, progress to joint degeneration. Furthermore, AKU mice provide a new model to investigate initiating events in osteoarthritis. appearance of pigmented chondrocytes, both pyknotic and viable and often in the same isogenous group of cells, suggests that pigmentation follows localized changes in the composition or organization of the matrix. We also show that nitisinone given for the whole of the life-span prevents ochronosis in AKU mice.



Is "Frostian" bone remodelling the dominant mechanism of altering bone microarchitecture in ageing human bone?

C Platt¹, AM Taylor², JC Jarvis¹, LR Ranaganth¹, A Boyde³, JA Gallagher¹

¹Bone and Joint Research Group, University of Liverpool. ²Faculty of Health and Medicine, Lancaster University. ³Institute of Dentistry, Queen Mary University of London.

INTRODUCTION: The Frostian concept of bone remodelling, in which there is a coupled process between initial osteoclastic bone resorption and subsequent osteoblastic bone formation, has been the widely accepted model for the past half a century. In this study a histological examination of cadaveric bone tissue was undertaken, to determine whether trabecular excrescences are present in Trabecular healthy ageing bone tissue. excrescences are novel microanatomical structures previously identified in grossly pathological tissues of weight bearing joints in patients with osteoarthritis and ochronotic arthropathy, a result of the autosomal recessive enzyme deficiency disorder Alkaptonuria (AKU).[1,2] identification of these excrescences, representing areas of bone formation with no evidence of prior osteoclastic resorption, questions whether the Frostian model constitutes the sole mechanism of bone remodelling or whether there also exists additional processes occurring at focal sites in the trabecular bone domain.

METHODS: Coronal slices of proximal tibia were obtained from three cadavers with no clinical history of bone or joint pathology. Following decalcification, slices were mapped and divided into anatomically discrete areas before subsequently processing for histology. Sections were stained using haematoxylin and eosin (H&E) staining. Histological examination took place using bright field microscopy in addition to polarised light and autofluorescence observation.

RESULTS: Trabecular excrescences were identified in all three cadaveric samples, their existence not restricted to any particular area of the bone domain. Excrescences appeared as basophilic structures of varying morphology, often displaying close relation to adipocyte cell contours. In general, they exhibited poor adherence at the interface with trabecular bone and an absence of discernible lamellar structure under polarised light. Rarely, excrescences comprised a central area of eosinophilic mature bone displaying lamellar structure and an autofluorescence intensity comparable to that of the oldest bone of the adjoining trabecula.

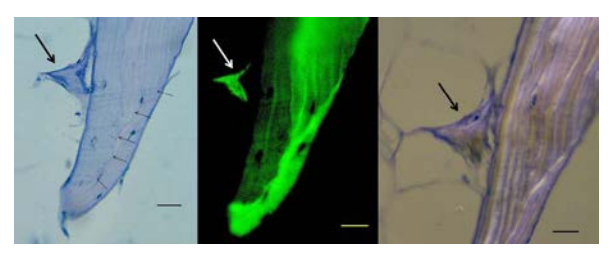


Fig. 1: Trabecular excrescence denoted by large arrow in an H&E section of ageing bone. A. Bright field. Thin arrows highlight a reversal line. B. Autofluorescence with UV light source. The three different ages of bone are clearly visible with the most mature bone displaying the greatest degree of autofluorescence. The excrescence appears to display the same degree of autofluorescence as the oldest bone present. C. Polarised light. Bar=20µm.

DISCUSSION & CONCLUSIONS: This study revealed the presence of trabecular excrescences in weight bearing joint tissues free from overt pathology. The absence of evidence of osteoclastic resorption prior to excrescence formation questions whether the traditional Frostian model of coupled bone remodelling is the only mechanism responsible for bone architectural change. Close interaction between adipocytes and excrescences in the absence of osteoblast activity implies a potential adipocyte-mediated osteogenic process via bone templating or the deposition of a preliminary bone matrix. Further investigation is required to determine the prevalence of these excrescences in the healthy population, at what age they arise and whether they are present in nonweight bearing tissues.

REFERENCES: ¹ A.M. Taylor, A. Boyde, P.J. Wilson, J.C. Jarvis, et al (2011) *Arthritis Rheum* **63**:3887-96. ² A.M. Taylor, A. Boyde, J.S. Davidson, J.C. Jarvis, et al (2012) *Eur Cell Mater* **23**:300-9.

ACKNOWLEDGEMENTS: The study was supported by the AKU Society and the Rosetrees Trust. The authors would like to extend their gratitude to the patients who donated their bodies to research.



Developing a novel 3D migration model to study colon cancer cell invasion.

RL Adams^{1,2}, SA Przyborski^{1,2}

¹ School of Biological Sciences, Durham University, South Road, Durham, DH1 3LE, UK

INTRODUCTION: Colon cancer is the fourth most diagnosed in England, with ~100,000 cases identified during 2001-2006 with a five-year survival rate of 50.4% ¹. The initial tumour adopts an invasive phenotype via the epithelial-mesenchymal transition (EMT) and cells begin to invade the local tissue before forming distant metastases, causing a decline in patient survival, from 90% for early stages down to 8% for tumours with distant metastases ².

Previous literature has highlighted the limitations of two-dimensional (2D) cancer cell migration assays³. These include alterations in gene expression and the provision of a migration substrate which does not closely reflect that of the *in vivo* environment.

This project aims to develop a three-dimensional (3D) model which mimics the *in vivo* situation to investigate factors which affect cancer cell invasion; these include the expression of EMT markers and signals found within the system.

METHODS: This project utilises commercial scaffold known as Alvetex[®] placed in a standard well insert (Fig 1A and B)⁴. Two colon cancer cell lines (SW480 and SW620) were used to look at the differences between pre- and post-metastatic colon cancer respectively. Both cell lines were cultured prior to analysis using various biochemical assays and histological processing.

RESULTS:

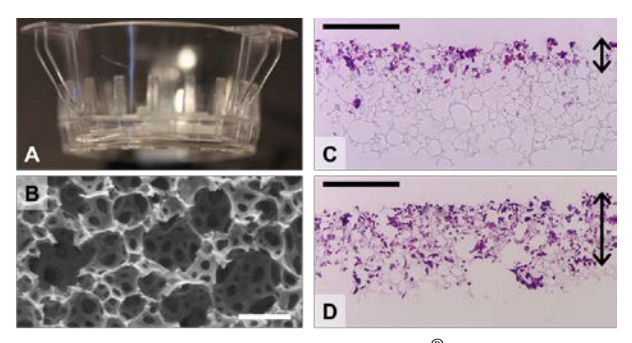


Fig 1A: Well insert for Alvetex[®] Scaffold; B: electron micrograph image of Alvetex[®] Scaffold (scale bar = 50μ m) and histology images for C: SW480 and D: SW620 cells grown on Alvetex[®] Scaffold (scale bars = 200μ m).

Our data show a difference in cell penetration between the two cell lines. The later stage SW620 cells, which have a more motile phenotype in 2D, migrate and penetrate the scaffold to a greater extent than the earlier stage, less invasive, SW480 cells. This reflects a known difference in the level of EMT markers between the two cell lines, as a result of the Wnt signalling pathway.

This novel 3D cell invasion model also allows for the use of the known chemoattractant Insulin-like Growth Factor (IGF) to encourage cell penetration. IGF has been shown to play an important role in cancer cell migration. The use of IGF results in a 54% increase in cell penetration by the SW480 cell line, but not the SW620 cell line (Fig 2). This may be due to increased activation of the Wnt signalling pathway.

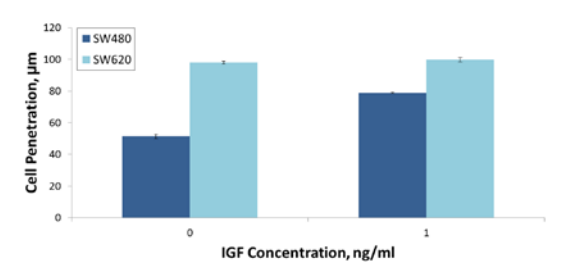


Fig. 2: Average cell penetration into scaffolds for each cell type in the presence and absence of chemoattractant IGF. n=3, $\pm SEM$

DISCUSSION & CONCLUSIONS: Our data shows great potential for further development of a 3D cancer invasion model using these scaffolds. This model provides a more realistic 3D environment and will be a tool for chemoattractant and co-culture studies to determine the mechanism of invasion utilised by these cells.

REFERENCES: ¹ Walters et al (2009) cancersurvival-Eng-2001-2006. ² Hollande et al (2010) *Drug Resist Updat* **13**:44-56. ³ Decaestecker et al (2007) *Med Res Rev* **27**:149-76 ⁴Bokhari et al (2007) *Biochem Biophys Res Commun* **354:**1095-100.

ACKNOWLEDGEMENTS: This work was carried out with funding from the Grevillea Trust, Reinnervate Limited and BBSRC.



² Reinnervate Limited, NETPark Incubator, Thomas Wright Way, Sedgefield, TS21 3FD, UK

The influence of surface chemistry on ECM production by retinal pigment epithelial (hRPE) cells on expanded polytetrafluoroethylene (ePTFE) substrates

V.R.Kearns¹, K.Vasilev², C.M.Sheridan¹ & R.L.Williams¹

¹ Eye and Vision Science, University of Liverpool, Liverpool, UK. ² Mawson Institute, University of South Australia, Adelaide, Australia

INTRODUCTION: Subretinal transplantation of functioning RPE cells grown on a synthetic substrate is a potential treatment for age-related macular degeneration. We have previously reported two surface modifications of ePTFE (ammonia plasma-treated, NH₃-ePTFE and n-heptylamine-coated, HA-ePTFE) that support a functional monolayer RPE cells¹. We hypothesise that the surface chemistry of the substrate will influence extracellular matrix production by cells, which will, in turn, affect the long-term success of the implant. The aim of this work was to investigate extracellular matrix production on NH³-and HA PTFE at the protein and gene expression level.

METHODS: RPE were isolated from human cadaver eyes, grown for several passages and used before passage 10. RPE were cultured on NH₃- and HA-ePTFE and tissue culture plastic (TCP) control substrates as previously described¹. For gene expression studies, total RNA was isolated at 1, 7 and 14d, converted to cDNA and analysed using an extracellular matrix and adhesion molecules PCR array (Qiagen). The expression profile 84 genes from cells grown on surface-modified was compared to that on TCP at each time point; only 3-fold or greater changes were considered. For protein distribution studies, substrates were fixed at 7, 14 and 28d with methanol and stained for collagen I (col-I), collagen IV (col-IV), and fibronectin (Fn) and laminin (Lam) using immunofluorescence. Nuclei were counterstained with DAPI.

RESULTS: In gene expression studies, no difference was noted between cells grown on either of the modified ePTFE substrates at 1d or at 7d on NH₃-ePTFE. On HA-ePTFE at 7d, a down-regulation was recorded for 7 genes, including 3 integrin subunits. At 14d on HA-ePTFE, 4 genes were down-regulated, including 2 integrin subunits and collagen I. At the same time point on NH₃-ePTFE, 28 genes were down-regulated, including 9 integrin subunits, 5 collagens including type I and IV, fibronectin 1 and laminin β1.

Fn (Fig 1), col-I and col-IV formed a fibrillar network on TCP substrates at 7d where cell density

was high. Lam formed a network, but was more localised to cells. At 28d, a more fibrillar Lam network was observed, and the other ECM components formed thicker fibrils than at 7d. In contrast, on modified ePTFE substrates Fn (Fig 1) and Col-IV distribution was generally globular, with isolated areas of fibrillar structure observed in some areas at 14 and 28d. Col-I networks were found in some areas from 7d, whereas Lam staining was not observed at 28d. Qualitatively, more ECM appeared to be secreted on TCP substrates.

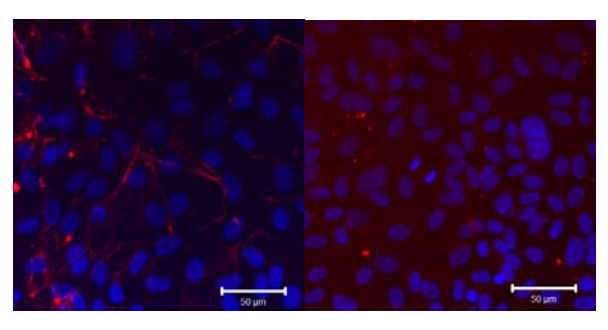


Figure 1 – Fn secreted by RPE on TCP (left) and NH_x -ePTFE (right). Scalebar 50 μ m.

DISCUSSION & CONCLUSIONS:

Although a functioning monolayer was observed on all substrates, some differences in the gene expression profile of RPE cells grown on TCP and surface-modified ePTFE were identified, in particular in the expression of genes related to and some extracellular integrins components. These data may be supported by the apparent lack of structured ECM on ePTFE compared with the control TCP. Further investigation is required to quantify protein production and examine expression of certain genes at different time points. This should aid optimisation of substrate surface chemistry for long-term survival of transplanted RPE.

REFERENCES: ¹ Kearns VR, Vasilev K, Sheridan C and Williams R L (2009) Surface Modification of ePTFE Substrates for Retinal Pigment Epithelial Growth and Function. ESB annual conference, Lausanne, CH

ACKNOWLEDGEMENTS: The authors would like to thank a private local charity for their financial support.



System for expressing high quantities of growth factors in E.Coli in soluble form

H. Peto¹, L. Buttery¹, K. Shakesheff¹

¹ STEM, Division of Drug Delivery and Tissue Engineering, CBS, School of Pharmacy, University of Nottingham, NG7 2RD, UK

INTRODUCTION: BMP2 and other human growth factors are extracellular proteins, often rich in disulphide bonds, which are expressed and folded in the Golgi apparatus. Attempts thus far to express BMP in E.coli have lead to the formation of unfolded protein in inclusion bodies [1]. BMP2 and other growth factors are sparingly soluble in the pH range required to form disulphide bonds pH 7-9. Refolding to active protein with disulphide bonds requires expensive chaotropic agents and separation of misfolded protein [2]. chaotropic agents interfere with labeling of BMP2 with potentially useful tags such as Fluorescein. We have designed a propriety system, Fold, a solubility tag to growth factors, which can be removed with enterokinase to leave native protein.

METHODS:

Fold has been cloned into pET24d with a multiple cloning site (MCS) for the insertion of the gene of interest. The BMP2 gene was cloned with restriction sites and inserted into the MCS. The pET24d (Fold-BMP2) is transformed into BL21 pLysS and grown at 37°C in 2YT with antibiotic selection. At OD600 0.6 the temperature is reduced to 25°C and expression of Fold-BMP2 induced with 1mM Isopropyl- β -D-thio-galactoside (IPTG). The cells are grown overnight and harvested the following morning.

The cells are lysed and the lysate applied to a Nickel column as the first round of purification. The elutant is then applied to a Q sepharose column at pH 8.5 and separated with a salt gradient, figure 1. The tag is then removed by applying enterokinase in a ratio of 1:1000 for 4hr.

RESULTS: At 25°C Fold-BMP2 is expressed as a soluble protein in the *E.coli* cytosol. It remains soluble when the *E.coli* are lysed and can be purified in a two step procedure: (i) Nickel affinity, (ii) Ion exchange on Q-sepharose column, figure 1.

Fold-BMP2 remains soluble indefinitely in Borate buffer pH 8.5, 300mM salt, figure 2, enabling disulphide formation in the presence of oxidised glutathione. Cleavage with enterokinase liberates native BMP2 which remain soluble, figure 2. Yields of 20mg of BMP2 are obtained from a 2.5L culture.

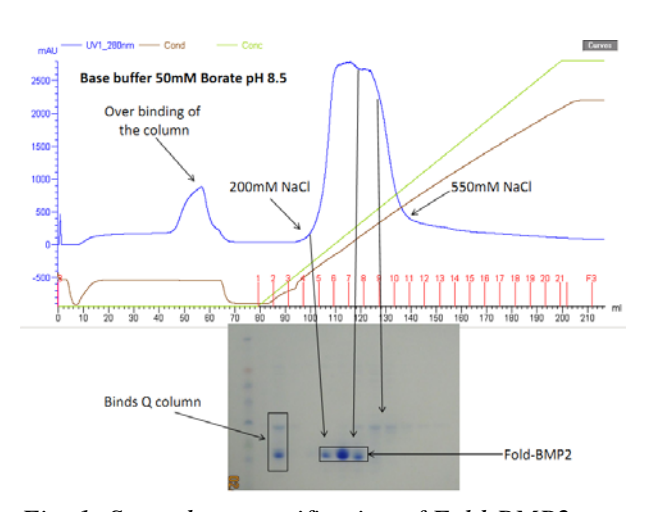


Fig. 1: Second step purification of Fold-BMP2 using a salt gradient on a Q sepharose column. Protein gel analysis shows 100% purification.

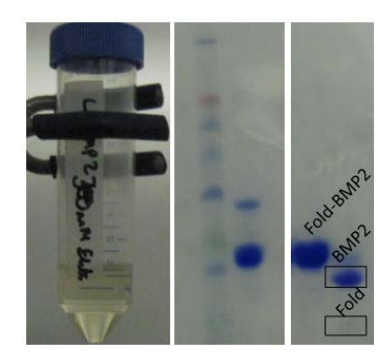


Fig. 2: Left, native BMP2 remains soluble. Centre & right, protein gel of Fold-BMP2 treated with enterokinase to liberate soluble native BMP2.

DISCUSSION & CONCLUSIONS: The Fold-tag expression system enables high yield production of disulphide containing growth factors in *E.coli*, with a two step purification. This reduces the cost of growth factor production and enables labeling and mutagenesis studies of growth factors.

REFERENCES: ¹ K. Yano, M. Hoshino, W. Sebald, K. Takaoka (2009) *J. Bone Miner Metab* 27: 355-63. ² N. Cerletti, G. McMasters, D. Cox, B. Meyhack (1991) *European Patent Application* 0433 225 A1. Biomedical Research Papers, McGraw-Hill, Inc.

ACKNOWLEDGEMENTS: This work was generously funded by the European Research Council.



A NOVEL CAGED CARBONYL FOR BIOMATERAL MODIFICATION AND CELL PATTERNING

L. O' Donovan & P. De Bank

Department of Pharmacy and Pharmacology & <u>Centre for Regenerative Medicine</u>, University of Bath, BA2 7AY, UK.

INTRODUCTION: The ability to turn material properties "on" or "off" with external stimuli in order to control biological responses is gaining considerable interest. In particular, the controlled patterning of cells to mimic the arrangements found in vivo would be highly desirable. Photolabile protecting groups (PPGs) have been used to "cage" functional groups such as carboxylic acids and amines on biomaterial surfaces.^{1,2} "Uncaging" specific areas by masked exposure to UV light allows cell-adhesive biomolecules to be ligated to the free groups, enabling cell patterning. However, cells are rich in these groups, so sequential patterning of different species is not possible without modification of both the scaffold and existing biomolecules.

METHODS: A novel bi-functional linker, which possesses a "caged" carbonyl at one end and a free amine for facile attachment to natural and synthetic cell scaffolds was synthesized.³ This molecule was subsequently attached to collagen. Attachment and subsequent PPG loss following UVA exposure was confirmed by UV/vis spectroscopy, HPLC and mass spectrometry. Cell adhesion and viability on modified biomaterials was investigated. Collagen coated circular coverslips were modified with PPG and photolysed. The resultant free carbonyl was treated with a cell adhesive protein (gelatin) modified to incorporate hydrazide functionality. As a control it was attempted to ligate unmodified gelatin to the photolysed surfaces. Patterned surfaces were generated using photo-resistant masks during photolysis.

RESULTS: Attachment of the caged carbonyl to collagen and loss of PPG after 10 min UV exposure proceeded smoothly. The presence of PPG on the collagen surface prevented cell adhesion (Fig. 1 (A) (edge of coverslips indicated by dotted line)). However, the selective ligation of hydrazide functionalised gelatin led to the reintroduction of cell adhesion (Fig 1 (C)). Ligation with non-hydrazide containing gelatin did not result in cell adhesion on the modified surfaces (Fig 1 (D)). UVA exposure of collagen using photo-resistant masks resulted in the creation of patterns. Patterns were visualized *via* treatment

with fluorescein-5-thiosemicarbazide (FTSC) (Fig 2).

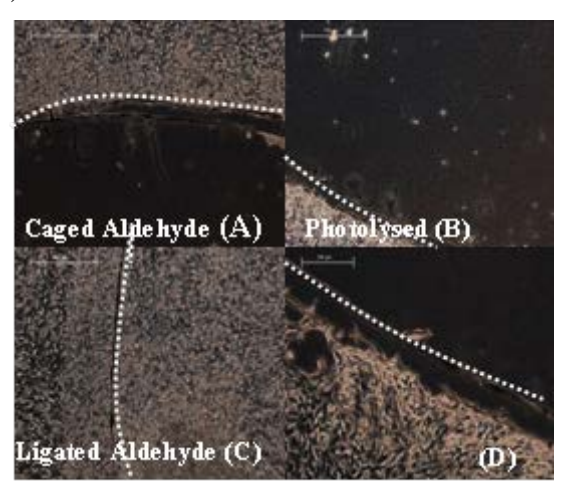
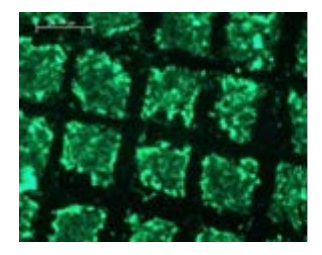


Fig. 1: Collagen coated coverslips modified with PPG (A), photolysed (B), photolysed and ligated with modified gelatin (C), photolysed and ligated with unmodified gelatin (D) seeded with C2C12 cells for 72 hr.



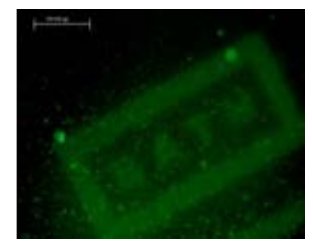


Fig. 2: Patterning of collagen film (left) and gel (right) following photolysis of PPG and treatment with FTSC.

DISCUSSION & CONCLUSIONS The ability to control cell adhesion and create patterns on modified biomaterials using a novel caged carbonyl has been demonstrated. This approach has great potential for recapitulating natural microenvironments and guiding 3D cell growth with patterned molecular cues.

REFERENCES: ¹ J. Nakanishi et al (2008) Anal Sci 24:67-72. ² D. Falconnet et al (2006) Biomaterials 27:3044-63. ³ L. O'Donovan, P. A. De Bank manuscript in preparation.

ACKNOWLEDGEMENTS: We would like to thank the EPSRC for funding (EP/G049572/1)



Adhesion strength of the MG63 cell line and its applicability to a fluidised bed bioreactor

I Benzeval¹, IG Turner², MJ Ellis¹

¹ University of Bath, Chemical Engineering, Bath, UK ² University of Bath, Mechanical Engineering, Bath, UK

INTRODUCTION: The shear strength of attachment of the osteosarcoma cell line, MG63, has been investigated using a tailor made convergent flow chamber. The decreasing crosssectional area for flow, incorporated in the design of the chamber, increases the linear velocity and thus the shear stress applied to cells in the chamber. Furukawa *et al*¹. have altered a rheometer to allow shear to be applied to cells, and measured. However, their approach only allows one shear stress to be applied per experiment. In the current study the flow chamber geometry allows a range of shear stresses to be tested simultaneously. The aim of the study was therefore to measure the adhesion strength of an MG63 cell line in response to the application of two different volumetric flow rates. This work will contribute to the development of an experimental system and computational fluid dynamics (CFD) model of a fluidised bed bioreactor for the proliferation of MG63s in a porous hydroxyapatite scaffold.

METHODS: MG63 cells were seeded at 20,000 cells/cm² on to the tissue culture plastic base of the chamber and allowed to attach under static conditions. After 24 hours, media was pumped through the chamber at 80 ml/min for ten minutes. This first flow removed any unattached cells as well as applying shear stress to the attached cells. The media flowrate was then increased to 150 ml/min for a further ten minutes. To quantify the attached cells, images were recorded after each of the two flow regimes using an inverted microscope at 10x magnification. Images were taken at 5mm intervals along the length of the chamber; ten positions were assessed with three micrographs recorded at each position.

RESULTS: The variation of cell number with shear stress for the two different flow rates of 80 ml/min and 150 ml/min is shown in Figure 1. At 80 ml/min the cell number decreased exponentially from a shear stress of 30 to 120 mPa. At 150 ml/min there was negligible variation in cell number between a shear stress of 60 and 230 mPa, once the standard deviation is considered. However the data from 140 mPa onwards suggest a continuation of the exponential decrease in cell number. Where the two sets of data overlap, in the

range 60 - 125 mPa, the second, higher, flowrate resulted in a greater removal of cells at those shear stresses.

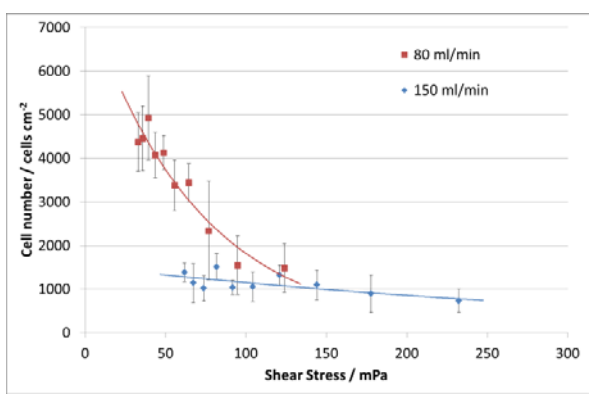


Fig 1: Cell number post shearing at two volumetric flowrates. Error bars are ± 1 s.d., n = 3.

DISCUSSION & CONCLUSIONS: Initially, at 80 ml/min, there is a graduation of cell detachment in the range 25 – 125 mPa with the number attached at 100 mPa only 30% of the number seen at 40 mPa. At 150 ml/min the number of cells remaining is similar across the range of shear stresses. The over-lapping data occurred at the downstream end of the chamber at 80 ml/min and upstream at 150 ml/min. Cell number at a given shear stress was expected to be comparable, so the differences suggest also time-dependency, or entrance effects in the chamber.

An innovative convergent flow chamber has been developed which allows a range of shear stresses to be applied simultaneously to a cell population, allowing investigation of attachment and detachment kinetics. These results show that there was not a critical shear stress which resulted in the loss of all cells, in the range tested. The studies also suggest there is both shear rate and time dependency, and possible entrance effects.

The next steps are to examine the rate- and timedependencies of cell removal experimentally and using FLUENT. The experiments will then be repeated on a hydroxyapatite surface.

REFERENCES: ¹ K.S. Furukawa *et al* (2003) *Int. J. Artif. Organs* **26**: 436-441.

ACKNOWLEDGEMENTS: This work was funded by EPSRC Grant EP/I015922/1.



Titanium phosphate glass microspheres: novel microcarriers for bioreactormediated bone cell scale-up and differentiation

NJ Lakhkar¹, JH Park², V Salih¹, JC Knowles^{1,2}

INTRODUCTION: Titanium phosphate glasses have attracted great interest for many potential applications in the orthopaedic, dental and maxillofacial fields because of their highly tunable material properties and considerably favourable bone cell response [1-2]. This study explores a novel application of glasses which involves processing to form microspheres that can be used as microcarriers in bioreactors for bone cell scale up and possibly for guided differentiation as well.

METHODS: Titanium phosphate microspheres of sizes 50-100 µm and having the following compositions were prepared by meltquenching and subsequent flame spheroidisation: $0.5P_2O_5-0.4CaO-(0.1 - x)Na_2O-xTiO_2$; x = 0.03, 0.05 and 0.07 mol. fr. (denoted as Ti3, Ti5 and Ti7 respectively). Degradation in deionised water at 37.5°C was studied over a 3-day period using a novel time-lapse imaging method. Cell culture studies such as confocal laser scanning microscopy (CLSM) and AlamarBlueTM cell proliferation assay (control: cell-cultured transwell mesh) were carried out with MG63 cells in transwell plates over 1, 4 and 7 days.

RESULTS:

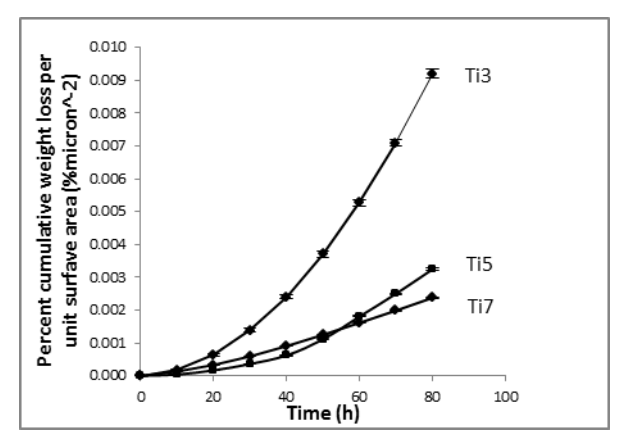


Fig. 1: Cumulative weight loss per unit surface area of Ti3-Ti7 microspheres as a function of time.

Microspheres were successfully obtained for all the investigated compositions. The microspheres underwent nonlinear degradation, with Ti3 showing significantly greater weight loss than Ti5 and Ti7 (Fig. 1).

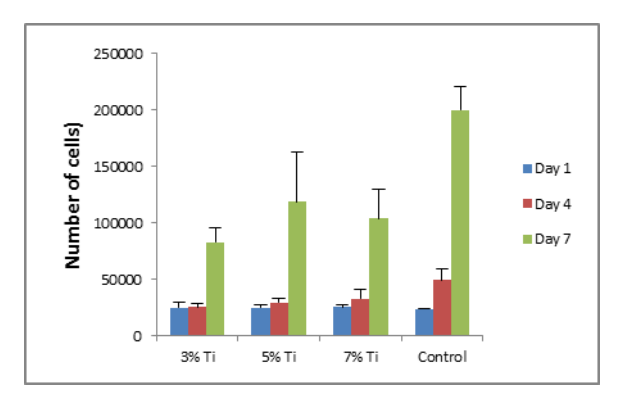
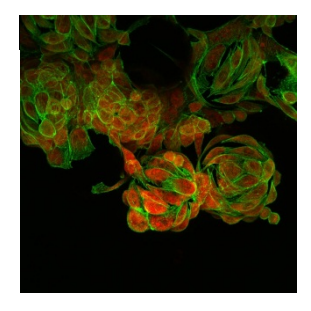


Fig. 2: Results of AlamarBlueTM assay carried out for MG63 cells cultured on Ti3 and Ti5 glass microspheres over time points of 1, 4 and 7 days.

The cell culture results revealed significant cell growth and proliferation. By day 7, a considerable increase in cell numbers in comparison with days 1 and 4 was observed in the assay results (Fig. 2), while CLSM images revealed a confluent cell layer on microspheres of all the investigated compositions (Fig. 3).



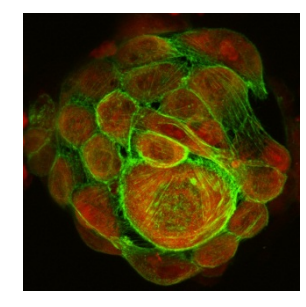


Fig. 3: CLSM images obtained for Ti5 glass microspheres cultured with MG63 cells at 7 days (magnification: 40x).

DISCUSSION & CONCLUSIONS: For the first time, it is reported that titanium phosphate glass microspheres having variable Ti contents show considerable promise as cell microcarriers. Further studies will focus on dynamic 3D cell culture of these microspheres in bioreactors.

REFERENCES: ¹ M. Navarro, M.P. Ginebra, J. Clement et al. (2003) *J Am Ceram Soc* **86**:1345-52. ² A. Kiani, N.J. Lakhkar, V. Salih et al. (2012) *Phil Trans R Soc* **370**:1352-75.



¹ Division of Biomaterials and Tissue Engineering, UCL Eastman Dental Institute, London, UK ²Department of Nanobiomedical Science and WCU Research Center, Dankook University, South Korea

Regulation of SOX9 in human chondrocytes by the RNA binding protein tristetraprolin

SR Tew, McDermott B, Clegg PD

¹ Department of Musculoskeletal Biology, Institute of Ageing and Chronic Disease, University of Liverpool, Leahurst Campus, Neston, CH649RQ, UK

INTRODUCTION: Expression of the transcription factor SOX9 by chondrocytes is essential for their function and leads to the regulation of critically important extracellular matrix (ECM) genes. Regulating the expression of SOX9 is highly relevant to cartilage tissue engineering as high SOX9 levels strongly promote the ECM formation by human chondrocytes in vitro¹ We have previously shown that SOX9 is regulated at the post transcriptional level in human articular chondrocytes (HAC) following exposure to hyperosmolarity and other stress stimuli^{2,3}. We decided to investigate whether the turnover of SOX9 mRNA was also controlled by chondrocyte phenotype and to identify mechanisms regulating this process.

METHODS: Passage 2 HAC or human bone marrow derived stem cells (BMSCs) were cultured in standard 14 day chondrogenic pellet conditions containing TGFβ1+/- BMP7. Pellets were assessed for their chondrocytic characteristics and the half-life (t_{1/2}) of SOX9 mRNA was determined following actinomycin D chase. siRNAs targeting RNA binding proteins (RNBPs) were transfected into SW1353 chondrosarcoma cells or passage 2 HAC and protein knockdown assessed by western blotting before SOX9 mRNA and protein levels were measured. Levels of RNBP mRNA expression were also measured in the chondrogenic pellet cultures. All mRNA quantification was performed using qRT-PCR.

RESULTS: During dedifferentiation **HAC** exhibited a decrease in levels but an increase in t_{1/2} of SOX9 mRNA. Both HAC and BMSC produced chondrocytic pellet cultures, which were optimised by BMP7 addition. Total SOX9 mRNA levels were increased by pellet culture but average SOX9 mRNA t_{1/2} was not changed regardless of cell type or growth factor treatment. Interestingly however, when data from all pellet cultures were pooled together a negative correlation was observed between SOX9 mRNA levels and t_{1/2} of SOX9 mRNA. A similar correlation existed between the SOX9 mRNA t1/2 and the levels of the RNA-BP tristetraprolin (TTP). siRNA knockdown of TTP in

both SW1353 cells and HAC caused SOX9 mRNA and protein levels to increase. Furthermore TTP knockdown led to the stabilisation of SOX9 mRNA in SW1353 cells.

DISCUSSION **CONCLUSIONS:** & We demonstrate a relationship between SOX9 mRNA expression and its $t_{1/2}$ in HAC and BMSC. We also have evidence that the control of SOX9 t_{1/2} can be controlled by the RNBP TTP in both a chondrocytic cell line and articular chondrocytes derived from osteoarthritic knee cartilage. SOX9 has eight AU rich elements within its 3'UTR and we have some preliminary evidence suggesting that TTP is present in human chondrocytes and can interact with one of these AREs (not described here). These findings may represent a novel means of chondrocyte ECM regulation via posttranscriptional control of SOX9. The potential for controlling the levels of this master transcription factor by influencing its mRNA decay as a strategy to improve cartilage tissue engineering now requires investigation.

REFERENCES: ¹Tew et al (2005) Osteoarthritis Cartilage **13**:80-9 ²Tew et al Am J Physiol Cell Physiol (2009) **297**:C898-906 ³Tew & Hardingham (2006) J Biol Chem **281**:39471-9

ACKNOWLEDGEMENTS: Arthritis Research UK funded this work.



Modelling fluid and nutrient transport to determine the influence of cell seeding on the growth of cell aggregates on a permeable membrane

L A C Chapman^{1,3}, S L Waters¹, R J Shipley², H M Byrne¹, J P Whiteley³, M J Ellis⁴

¹Mathematical Institute, University of Oxford. ² Department of Mechanical Engineering, Faculty of Engineering Science, UCL. ³ Department of Computer Science, University of Oxford. ⁴Department of Chemical Engineering, University of Bath

INTRODUCTION: We consider a simple 2D model of the growth of cell aggregates attached to a permeable membrane past and through which a culture medium containing nutrient flows. The physical set-up of the problem is motivated by the set-up inside a hollow fibre membrane bioreactor (HFMB)¹. The process by which cells are seeded onto the outer surface of the fibre in a HFMB does not yield a uniform distribution of cells. Rather cells tend to attach unevenly over the surface and form single-layer aggregates of varying densities¹. Although more work is required to improve the precision and reproducibility of the cell seeding process, there is also a need for experimental and theoretical investigations to determine how the seeding influences the growth of the cells. In our model we consider how the growth of the cell aggregates affects the local fluid flow and nutrient distribution, and thus are able to assess the effect of the initial distribution of the cell aggregates on their subsequent growth.

METHODS: The model set-up consists of two regions of fluid separated by a permeable membrane, on top of which are a number cell aggregates (Fig. 1). The cell aggregates are treated as line sinks in the nutrient field (as the cells are much smaller in diameter than the depth of the membrane and fluid regions), and assumed to grow at either end at a rate proportional to the excess in the local nutrient concentration over a critical threshold for growth. Lubrication theory is used to simplify the equations governing the fluid flow and nutrient transport in the membrane and fluid regions. The reduced system is then solved numerically for a given cell aggregate distribution and the result used to evolve the aggregate distribution. The model is used to investigate the effect of changing the initial distribution and density of cell aggregates on the time taken to reach confluence (i.e. for the aggregates to cover the entire membrane).

RESULTS: As expected, the time taken to reach confluence decreases as the initial density of cell aggregates increases and is inversely proportional to the growth rate of the aggregates. Increasing the

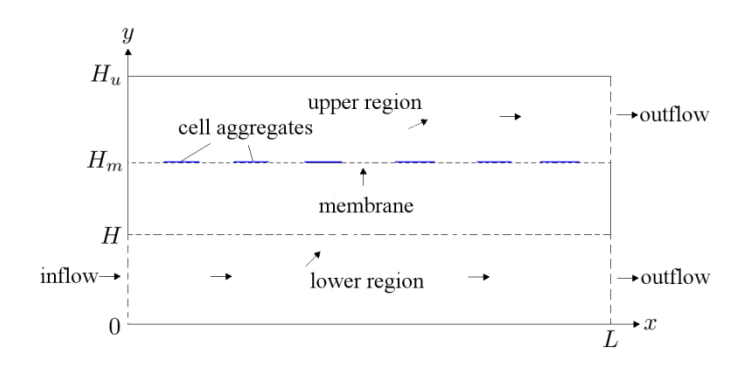


Fig. 1: Schematic of the model set-up. Solid lines indicate impermeable boundaries; dotted lines indicate permeable/open boundaries. Arrows show the direction of fluid flow. H, H_m , and H_u are the respective heights of the bottom and top of the membrane, and the top of the upper region above the bottom of the lower region. L is the length of the model domain.

nutrient uptake rate of the cell aggregates leads to an increase in the time taken to reach confluence since the aggregates cannot grow as quickly when there is less nutrient available. In nutrient-limited conditions, in which the concentration does not exceed the critical threshold for growth at all points along the membrane at all times, the initial distribution of cell aggregates can significantly affect the confluence time. For instance, if the concentration is initially lower than the threshold at only the right-hand end of the membrane a distribution of aggregates skewed towards the left-hand end will reach confluence more quickly than one skewed to the right.

DISCUSSION & CONCLUSIONS: The model developed here has the potential to aid in the optimisation of cell seeding in a HFMB and other similar bioreactor systems. Future work will involve collaboration with experimentalists to parameterise and validate the model.

REFERENCES: ¹ M. J. Ellis and J. B. Chaudhuri (2007) *Biotechnology and Bioengineering*

ACKNOWLEDGEMENTS: The authors would like to thank EPSRC for funding this work.



The effect of an inflammatory environment on the response and differentiation of osteogenic embryonic stem cells.

L. E. Sidney, G. R. Kirkham, L. D. K. Buttery

Drug Delivery and Tissue Engineering, Department of Pharmacy, University of Nottingham, UK.

INTRODUCTION: Non-union fractures and inflammatory diseases are significant targets for osteochondral tissue engineering strategies. The inflammatory environment present in these conditions may have great consequence on the success or failure of a tissue engineering strategy or cell therapy. Therefore, studying the effect of inflammation on cells with potential for bone regeneration, such as osteogenically differentiated embryonic stem cells is of great importance. To investigate the possible effect of inflammation on cells, proinflammatory cytokines can provide a simple in vitro model when added to the media. Proinflammatory cytokines such as interleukin-1β (IL-1 β), tumour necrosis factor- α (TNF- α) and interferon-y (IFN-y), are associated with the innate inflammatory response during tissue healing; are critical for control of bone tissue remodelling and play a large role in inflammatory diseases, such as rheumatoid arthritis^{1,2}.

METHODS: Mouse primary calvarial cells (mPCs) were extracted from neonatal CD1 mice by sequential trypsin and collagenase digestion. Mouse embryonic stem cells (mESCs) were osteogenically differentiated via formation of embryoid bodies (EBs) and subsequent dissociation to single cell monolayer (osteomESCs). mPCs and osteo-mESCs were seeded separately in osteogenic media containing 50 μg/mL ascorbate-2-phosphate and 50 mM βglycerophosphate. IL-1β, TNF-α, IFN-γ were added to the culture media for 48 hours at various time points of osteogenic culture, subsequently cells were changed back to osteogenic culture and continued up to 14 days (alkaline phosphatase activity assay) or 28 days (alizarin red staining). Response to proinflammatory cytokines was also determined by nitrite production, PGE₂ production and cell viability. Differences in osteogenic markers were measured by immunocytochemistry and RT-PCR.

RESULTS: Treatment with the proinflammatory cytokines IL-1 β , TNF- α , IFN- γ in early culture caused inhibition of later differentiation of the mPCs, in both bone nodule formation and calcium deposition (fig. 1) and alkaline phosphatase activity (fig. 2). This inhibition of differentiation was not seen when adding proinflammatory

cytokines at the start of osteo-mESC culture. The osteo-mESCs went on to form bone nodules and there was no difference seen in alkaline phosphatase activity. This trend was also seen with osteocalcin, osteopontin and collagen-1 expression (data not shown).

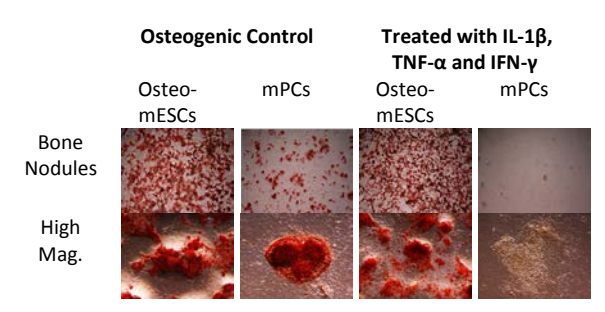


Fig. 1: Alizarin red staining of calcium deposits in cells treated with proinflammatory cytokines for 48 hours at day 0 of culture, before continued osteogenic culture for 28 days.

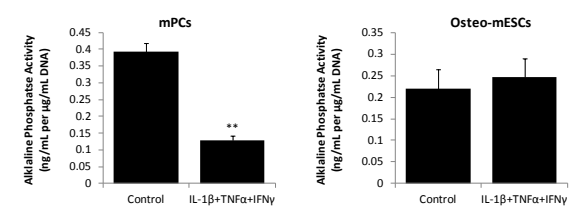


Fig. 2: Alkaline phosphatase activity of mPCs (left) and osteo-mESCs (right) treated with proinflammatory cytokines for 48 hours at day 0 of culture, before continued osteogenic culture for 14 days.

DISCUSSION & CONCLUSIONS: In comparison to primary calvarial cells, the differentiation and response of osteo-mESCs is not inhibited by the presence of proinflammatory cytokines. This may have an impact when considering the use of embryonic stem cells as osteochondral cell therapies, due to an increased tolerance to the presence of an inflammatory environment.

REFERENCES: ¹T.Skerry, (1994) *Eur. J. Clin. Nutr.* **48**, S190-S198. ²F. J. Hughes et al., (1999) *J. Biol. Chem.* **274** 1776-1782.

ACKNOWLEDGEMENTS: The authors would like to acknowledge the help of Adam Taylor and the EPSRC Doctoral Training Centre in Regenerative Medicine for funding.

